

KINETICS AND INTERACTIONS OF THE SIMULTANEOUS CATALYTIC
HYDRODENITROGENATION OF PYRIDINE AND
HYDRODESULFURIZATION OF THIOPHENE

by

JOHN A. WILKENS

B.S., Cornell University (1969)

Master of Engineering (Chemical), Cornell University (1971)

Submitted in Partial Fulfillment
of the Requirements for the
Degree of Doctor of Philosophy

at the

MASSACHUSETTS INSTITUTE OF TECHNOLOGY

August, 1977

Signature of Author:

Department of Chemical Engineering

Certified by:

Professor C. N. Satterfield
Thesis Supervisor

Professor M. Modell
Thesis Supervisor

Accepted by:

Chairman, Departmental Committee
on Graduate Theses



Abstract

KINETICS AND INTERACTIONS OF THE SIMULTANEOUS CATALYTIC HYDRODENITROGENATION OF PYRIDINE AND HYDRODESULFURIZATION OF THIOPHENE

by

JOHN A. WILKENS

Submitted to the Department of Chemical Engineering in August, 1977, in partial fulfillment of the requirements for the degree of Doctor of Philosophy

Interactions between the simultaneous catalytic hydrodenitrogenation (HDN) of pyridine and hydrodesulfurization (HDS) of thiophene were investigated in a continuous-flow, packed-bed microreactor using a sulfided NiMo/Al₂O₃ catalyst. The reactions were carried out in the vapor phase at total pressures from 150 to 1000 psig (1.1 to 7.0 MPa), and temperatures from 150 to 410°C. Pyridine and thiophene partial pressures ranged from 93 to 186 torr (12 to 25 kPa).

Thiophene HDS was severely inhibited by the presence of pyridine under all reaction conditions studied. Butylamine caused the same degree of inhibition as did pyridine. A Langmuir-Hinshelwood kinetic analysis showed a pyridine adsorption strength greater than that of thiophene on active catalytic sites. Hydrogen sulfide, present as a product of thiophene hydrogenolysis, appeared to be more weakly adsorbed than thiophene.

At temperatures above 350°C, thermodynamic equilibrium was established between pyridine and its saturated reaction intermediate, piperidine, at all pressures studied. Higher hydrogen partial pressures shift the equilibrium composition

toward piperidine. Complete conversion of pyridine to piperidine was achieved at the higher pressures.

The presence of thiophene inhibited the hydrogenation of pyridine at temperatures below 350°C. Above 350°C, thiophene enhanced the pyridine hydrogenation, giving conversions greater than those of the pure-pyridine feed reactions.

The concentration of piperidine decreased greatly with the addition of thiophene, caused by both the inhibition of pyridine hydrogenation and the enhancement of piperidine hydrogenolysis. This enhancement was most likely due to increased catalytic activity caused by the sulfiding action and acidity of hydrogen sulfide, a product of thiophene HDS. In the presence of thiophene, piperidine did not reach its equilibrium concentration under any reaction conditions studied. The overall conversion of pyridine to products beyond piperidine was enhanced by the presence of thiophene for temperatures greater than 300°C at the higher pressures.

Kinetic analysis showed piperidine to compete with pyridine for catalytic sites with an adsorption strength equal to or slightly greater than that of pyridine. Ammonia adsorption was equal to or weaker than that of pyridine.

The activity of the sulfided NiMo/Al₂O₃ was strongly dependent upon the state of sulfiding of the catalyst. The addition of thiophene to the reactor feed maintained the catalyst activity in the presence of pyridine, a basic nitrogen compound.

Thesis Supervisors: C. N. Satterfield
Professor of Chemical
Engineering
M. Modell
Professor of Chemical
Engineering

Department of Chemical Engineering
Massachusetts Institute of Technology
Cambridge, Massachusetts 02139

August, 1977

Professor Irving Kaplan
Secretary of the Faculty
Massachusetts Institute of Technology
Cambridge, Massachusetts 02139

Dear Professor Kaplan:

In accordance with the regulations of the Faculty, I herewith submit a thesis, entitled "Kinetics and Interactions of the Simultaneous Catalytic Hydrodenitrogenation of Pyridine and Hydrodesulfurization of Thiophene", in partial fulfillment of the requirements for the degree of Doctor of Philosophy in Chemical Engineering at the Massachusetts Institute of Technology.

Respectfully submitted,

^u
John A. Wilkens

This Thesis is Dedicated to my Family

ACKNOWLEDGEMENTS

First, I am grateful to my thesis advisors, Professor Charles N. Satterfield and Professor Michael Modell, for their support, guidance, and enhancement of my professional development.

I wish to acknowledge the U.S. Environmental Protection Agency for providing financial support for part of my M.I.T. career, and to thank Prof. Glenn Williams for arranging Departmental support for some of the remaining times.

Monsieur Claude Declerck deserves special thanks for his excellent advice on gas chromatographic separations; and for providing, through the Solvay Company of Brussels, Belgium, the catalyst analyses presented in this thesis. His uplifting spirits were also greatly appreciated.

The mass spectrometric analysis was carried out by Mr. Robert Laflamme and Prof. Ronald Hites.

I wish to thank many people who have contributed to the success of my M.I.T. career in various ways, particularly Mrs. Johanna Bond, Mr. Arthur Clifford, Prof. Richard Donnelly, Mr. Charles Foshey, Mr. John Fresina, Mr. Kent Griffis, Mr. Paul Halloran, Prof. Jack Howard, Mrs. Elenore Kehoe, Dr. Jerry Mayer, Mr. Richard McKay, Mr. Stanley Mitchell, Mr. Hank Prichard, and Prof. John Vivian.

It was the close association of fellow students from

many parts of the world which made life during these M.I.T. years interesting and enjoyable. Of particular significance, through nearly all of my days in Cambridge, were the friendships of Michael van Eek and Fahri Özel.

Of special importance throughout the last several years has been the encouraging and comforting presence of my wife, Lucie. Her contributions to my work have ranged from scholarly advice to the typing of many parts of this thesis.

Finally, I wish to thank my parents, grandfather, and brother for nearly three decades of continual development, encouragement, stimulation, and support of my interest in science and technology. It has been their love, patience, and understanding which have helped make this long educational process both possible and enjoyable.

John A. Wilkens
Cambridge, Massachusetts
August, 1977

Table of Contents

I.	Summary	21
I.A.	Introduction	21
I.B.	Objectives	22
I.C.	Literature Review	22
I.D.	Experimental Apparatus and Procedure	29
I.E.	Results	31
I.E.1.	Catalyst Activity	32
I.E.2.	Pure Thiophene Hydrodesulfurization	33
I.E.3.	Thiophene HDS in the Presence of Nitrogen Compounds	34
I.E.4.	Pure Pyridine Hydrodenitrogenation	35
I.E.5.	Pyridine HDN in the Presence of Sulfur Compounds	37
I.F.	Discussion of Results	39
I.F.1.	Catalyst Activity	39
I.F.2.	Pure Thiophene Hydrodesulfurization	40
I.F.3.	Thiophene HDS in the Presence of Nitrogen Compounds	41
I.F.4.	Thiophene HDS: Kinetic Analysis	42
I.F.5.	Pure Pyridine Hydrodenitrogenation	45
I.F.6.	Pyridine HDN: Equilibrium Analysis	47
I.F.7.	Pyridine HDN in the Presence of Sulfur Compounds	49
I.F.8.	Pyridine HDN: Kinetic Analysis	50
I.F.9.	Relative Rates of Thiophene HDS and Pyridine HDN	53
I.G.	Conclusions	54
I.G.1.	Catalyst Activity	54
I.G.2.	Thiophene Hydrodesulfurization	54
I.G.3.	Pyridine Hydrodenitrogenation	55
II.	Introduction	69
II.A.	General Background	69

II.B. Literature Review	73
II.B.1. Desulfurization and Denitrogenation Catalysts	73
II.B.2. Thiophene Hydrodesulfurization	74
II.B.2.a. Thiophene Adsorption	75
II.B.2.b. Hydrogen Adsorption	77
II.B.2.c. Hydrogen Sulfide Adsorption	79
II.B.2.d. Hydrocarbon Adsorption	81
II.B.2.e. Adsorption of Basic Nitrogen Compounds	84
II.B.2.f. Reaction Products of Thiophene HDS	86
II.B.2.g. Thiophene HDS Reaction Mechanism	87
II.B.3. Pyridine Hydrodenitrogenation	92
II.B.3.a. Pyridine HDN: Mechanism, Kinetics, and Compound Adsorptions	92
II.B.3.b. Pyridine HDN: Equilibrium Limitation	96
II.B.3.c. Pyridine Hydrogenation: Constant Determination	97
II.B.3.d. Pyridine HDN: Effects of Sulfur Compounds	99
II.C. Thermodynamics of Thiophene HDS and Pyridine HDN	101
II.D. Objectives	104
III. Apparatus and Procedure	106
III.A. Reactor Design Considerations	114
III.B. Reactor System	116
III.C. The Catalyst Used, and Catalyst Sulfiding Procedures	121
III.D. Reactant Feed Systems	123
III.E. Reactant Stream Composition Analysis	126
III.F. Safety Considerations	133
III.G. Experimental Procedure	136
IV. Results	140
IV.A. Catalyst Activity	142
IV.B. Thiophene Hydrodesulfurization	149

IV.B.1.	Pure Thiophene HDS	150
IV.B.2.	Thiophene HDS in the Presence of Nitrogen Compounds	152
IV.B.3.	Effect of Methyl Substitution on Thiophene HDS	153
IV.C.	Pyridine Hydrodenitrogenation	160
IV.C.1.	Pure Pyridine HDN	161
IV.C.2.	Pyridine HDN in the Presence of Sulfur Compounds	173
V.	Discussion of Results	186
V.A.	Catalyst Activity	187
V.B.	Thiophene Hydrodesulfurization	190
V.B.1.	Pure Thiophene HDS	190
V.B.2.	Thiophene HDS in the Presence of Nitrogen Compounds	191
V.B.3.	Effect of Methyl Substitution on Thiophene HDS	193
V.B.4.	Thiophene HDS: Kinetic Analysis	196
V.C.	Pyridine Hydrodenitrogenation	213
V.C.1.	Pure Pyridine HDN	213
V.C.2.	Pyridine HDN: Equilibrium Analysis	219
V.C.3.	Pyridine HDN in the Presence of Sulfur Compounds	233
V.C.4.	Pyridine HDN: Kinetic Analysis	241
V.D.	Relative Rates of Thiophene HDS and Pyridine HDN	255
V.E.	Quality of the Experimental Data	260
VI.	Conclusions	266
VI.A.	Catalyst Activity	266
VI.B.	Thiophene Hydrodesulfurization	266
VI.C.	Pyridine Hydrodenitrogenation	267
VII.	Recommendations	269

VIII.	Appendix	271
VIII.A.	Apparatus - Further Details	271
VIII.B.	Physical Property Data	278
VIII.C.	Run Data Summaries	282
VIII.D.	Derivation of Equations and Supporting Principles	310
VIII.D.1.	Plug Flow Reactor Parameters	310
VIII.D.2.	Conversion of Reactants	312
VIII.D.3.	Data Quality - Statistical Determination	316
VIII.D.4.	Pyridine-Piperidine Equilibrium - Principles of calculation	319
VIII.E.	Sample Calculations	326
VIII.E.1.	Sample Calculations - Reduction of Experimental Data	326
a.	Calculations for Each GC Sample	329
1.	Total Reactor Flow Rate at Standard T and P	329
2.	Normalized Chromatogram Peak Area	329
3.	Standardized Area-Flow Rate Product	330
b.	Calculations for Each Set of Samples, at one Reaction Temperature	331
1.	Average Conditions for Set	331
a.	Mean Values	331
b.	Absolute Reactor Pressure	331
2.	Conversion of Reactants for Thiophene and/or Pyridine	332
3.	Confidence Limits for Conversion Values	333

	a. Variance, Standard Deviation, and Relative Standard Deviation	333
	b. Confidence Limits	334
	4. Relative Molar Quantities	335
	5. Reactor Performance Parameters	336
	a. Residence Time	336
	b. Space Time and Space Velocity	337
	c. Liquid Hourly Space Velocity	338
	c. Calculations for Overall Run	338
	1. Run Average Reactor Conditions	338
	2. Hydrogen Feed Values	339
	3. Mole Fractions, Partial Pressures, Feed Ratios	339
VIII.E.2.	Sample Calculations for Pyridine-Piperidine Equilibrium	339
	a. Change in Free Energy for Reaction	339
	b. Equilibrium Constant	340
	c. Equilibrium Pyridine-Piperidine Ratio Values	341
	d. Experimental Pyridine-Piperidine Ratio Values	342
	e. Experimental Values of Equilibrium Constant Expression	343
VIII.F.	Assessment of Possible Heat and Mass Transfer Limitations	350
VIII.F.1.	Heat Transfer	354
	a. Interparticle Heat Transfer Criterion	354
	b. Interphase Heat Transfer Criterion	357

c. Intraparticle Heat Transfer Criterion	358
d. Subsidiary Calculations	359
1. Fluid Parameters	359
a. Viscosity	359
b. Prandtl Number	360
2. Reynolds Number for Reaction Stream	360
3. Heat Transfer Coefficient Between Gas and Particle	361
4. Wall Heat Transfer Coefficient	362
VIII.F.2. Mass Transfer	362
a. Effectiveness Factor for Catalyst Pellets	362
b. Subsidiary Calculations	364
1. Binary Diffusion Coefficient	364
2. Knudsen Diffusion Coefficient	365
3. Total Effective Diffusivity	366
VIII.G. Langmuir-Hinshelwood Kinetic Models	367
VIII.H. Pyridine-Piperidine Equilibrium Results	373
VIII.I. Location of Original Data	377
Bibliography	378
Biographical Sketch	386

List of Figures

1-1	Reactor System: Main Components and Primary Flows	57
1-2	Thiophene HDS for Pure Thiophene and Mixed Thiophene-Pyridine Feeds at Total Pressures of 150, 500, and 1000 psig	58
1-3	Comparison of the Effects of Pyridine and Combined Butylamine plus Ammonia on the Conversion of Thiophene at a Total Pressure of 1000 psig	59
1-4	Pyridine HDN for Pure Pyridine and Mixed Pyridine-Thiophene Feeds at Total Pressures of 150, 500, and 1000 psig	60
1-5	Piperidine Presence in the Product Stream For Pure Pyridine and Mixed Pyridine-Thiophene Feeds at Total Pressures of 150 and 1000 psig	61
1-6	Product Distributions for Pyridine HDN for Pure Pyridine and Mixed Pyridine-Thiophene Feeds at a Total Pressure of 1000 psig	62
1-7	Product Distributions for Pyridine HDN for Pure Pyridine and Mixed Pyridine-Thiophene Feeds at a Total Pressure of 500 psig	63
1-8	Product Distributions for Pyridine HDN for Pure Pyridine and Mixed Pyridine-Thiophene Feeds at a Total Pressure of 150 psig	64
1-9	Comparison of the Effects of Hydrogen Sulfide and Thiophene on Pyridine Conversion at a Total Pressure of 1000 psig, using Propanethiol in Feed for Hydrogen Sulfide Generation	65
1-10	Comparison of the Experimental Values of The Equilibrium Constant Expression for Pyridine Hydrogenation with the Equilibrium Constant, for Pure-Pyridine and Pyridine-Thiophene Feeds at a Total Pressure of 1000 psig	66

1-11	Comparison of the Experimental Values of The Equilibrium Constant Expression for Pyridine Hydrogenation with the Equilibrium Constant, for Pure-Pyridine and Pyridine-Thiophene Feeds at a Total Pressure of 500 psig	67
1-12	Comparison of the Experimental Values of The Equilibrium Constant Expression for Pyridine Hydrogenation with the Equilibrium Constant, for Pure-Pyridine and Pyridine-Thiophene Feeds at a Total Pressure of 150 psig	68
2-1	Thermodynamics of Thiophene HDS	102
2-2	Thermodynamics of Pyridine HDN	103
3-1	Reactor System: Main Components and Primary Flows	107
3-2	Gas Sampling, Gas Chromatograph, and Flow Measurement Systems	108
3-3	Key to Apparatus Figures	109
3-4	Thermocouple Temperature Measurement Systems	110
3-5	Reactor Facility, Overall Exterior View	111
3-6	Reactor Assembly: Reactor, Preheat Coil, and Thermocouple; On Support Frame	112
3-7	Fluidized Sand Bed Heater and Immersed Reactor Assembly	112
3-8	Liquid Reactant Feed System: Pump, Rupture Disk, and Liquid Feed Preheater	113
3-9	Measurement and Control Systems for Fluid Flow and Temperature	113
3-10	Separation of Products of Pure Thiophene HDS	131
3-11	Separation of Products of Pure Pyridine HDN	131

3-12	Separation of Products of Simultaneous Pyridine HDN and Thiophene HDS	132
4-1	The Effects of Time on Stream and Sulfiding on the Activity of Sulfided NiMo/Al ₂ O ₃ Catalyst	146
4-2	Pore Size Distributions for New and Used Sulfided NiMo/Al ₂ O ₃ Catalysts	147
4-3	Thiophene HDS for Pure Thiophene Feeds at Total Pressures of 150, 500, and 1000 psig	155
4-4	Thiophene HDS: Effect of the Partial Pressure of Thiophene on Thiophene Conversion at Total Pressures of 150 and 1000 psig	156
4-5	Thiophene HDS for Pure Thiophene and Mixed Thiophene-Pyridine Feeds at Total Pressures of 150, 500, and 1000 psig	157
4-6	Comparison of the Effects of Pyridine and Combined Butylamine plus Ammonia on the Conversion of Thiophene at a Total Pressure of 1000 psig	158
4-7	Thiophene HDS: Effect of Methyl Substitution of Thiophene on Reactant Conversion at a Total Pressure of 500 psig	159
4-8	Pyridine HDN for Pure Pyridine Feeds at Total Pressures of 150, 500, and 1000 psig	168
4-9	Piperidine Presence in the Product Stream for Pure Pyridine Feeds at Total Pressures of 150, 500, and 1000 psig	169
4-10	Product Distribution for Pyridine HDN for Pure Pyridine Feed at a Total Pressure of 1000 psig	170
4-11	Pyridine HDN: Effect of the Partial Pressure of Pyridine on Pyridine Conversion at Total Pressures of 150 and 1000 psig	171

4-12	Pyridine HDN: Effect of the Partial Pressure of Pyridine on the Amount of Piperidine Present in the Product Stream at Total Pressures of 150 and 1000 psig	172
4-13	Pyridine HDN for Pure Pyridine and Mixed Pyridine-Thiophene Feeds at Total Pressures of 150, 500, and 1000 psig	178
4-14	Comparison of the Effects of Hydrogen Sulfide and Thiophene on Pyridine Conversion at a Total Pressure of 1000 psig, using Propanethiol in Feed for Hydrogen Sulfide Generation	179
4-15	Piperidine Presence in the Product Stream for Pure Pyridine and Mixed Pyridine-Thiophene Feeds at Total Pressures of 150 and 1000 psig	180
4-16	Product Distributions for Pyridine HDN for Pure Pyridine and Mixed Pyridine-Thiophene Feeds at a Total Pressure of 1000 psig	182
4-17	Product Distributions for Pyridine HDN for Pure Pyridine and Mixed Pyridine-Thiophene Feeds at a Total Pressure of 5000 psig	183
4-18	Product Distributions for Pyridine HDN for Pure Pyridine and Mixed Pyridine-Thiophene Feeds at a Total Pressure of 150 psig	184
4-19	Conversion of Pyridine and Piperidine for Pure-Pyridine and Pyridine-Thiophene Feeds at Total Pressures of 150, 500, and 1000 psig	185
5-1	The Inhibition of Thiophene Conversion by Pyridine at Total Pressures of 150, 500, and 1000 psig	194
5-2	Performance of Langmuir-Hinshelwood Kinetic Models in Correlating Thiophene HDS Reaction Data	209

5-3	Equilibrium Compositions for Pyridine Saturation to Piperidine at Total Pressures of 150, 500, and 1000 psig	227
5-4	Comparison of Pyridine HDN Product Composition with Calculated Equilibrium Values for Pure-Pyridine and Pyridine-Thiophene Feeds at Total Pressures of 150, 500, and 1000 psig	228
5-5	Comparison of Pyridine HDN Product Composition with Calculated Equilibrium Values for Pure-Pyridine and Pyridine-Thiophene Feeds at Total Pressures of 150, 500, and 1000 psig	229
5-6	Comparison of the Experimental Values of The Equilibrium Constant Expression for Pyridine Hydrogenation with the Equilibrium Constant, for Pure-Pyridine and Pyridine-Thiophene Feeds at a Total Pressure of 1000 psig	230
5-7	Comparison of the Experimental Values of The Equilibrium Constant Expression for Pyridine Hydrogenation with the Equilibrium Constant, for Pure-Pyridine and Pyridine-Thiophene Feeds at a Total Pressure of 500 psig	231
5-8	Comparison of the Experimental Values of The Equilibrium Constant Expression for Pyridine Hydrogenation with the Equilibrium Constant, for Pure-Pyridine and Pyridine-Thiophene Feeds at a Total Pressure of 150 psig	232
5-9	Percentage of Converted Pyridine Remaining as Piperidine in the Product Stream for Pure-Pyridine and Pyridine-Thiophene Feeds at 500 and 1000 psig	236
5-10	Comparison of the Effects of Thiophene on the Conversion of Pyridine with the Effects of Thiophene on Conversion of Pyridine and Piperidine at Total Pressures of 150, 500 and 1000 psig	240

5-11	The Relative Performance of Six Langmuir-Hinshelwood Models for Correlating Pyridine Hydrogenation Data at a Total Pressure of 1000 psig for $K_{Pip}/K_{Pyr} = 1.0$	253
5-12	The Ratio of Thiophene Conversion to Pyridine Conversion for Pure and Mixed Feeds at Total Pressures of 150, 500, and 1000 psig	257
5-13	The Ratio of the Conversion of Thiophene to the Conversion of Pyridine and Piperidine for Pure and Mixed Feeds at Total Pressures of 150, 500, and 1000 psig	259
5-14	95 Percent Confidence Limits for Pyridine Conversion Data	263
8-1	Heating Circuits	272
8-2	Automatic Safety System - Basic Component Interactions	273
8-3	Automatic Shutdown System - Control Circuit	274
8-4	Key for Automatic Shutdown Control Circuit Diagram	275
8-5	Mass Flow Meter Output Signal Buffer Circuit	276
8-6	High-Pressure Metering Pump Calibration	277
8-7	Performance of Langmuir-Hinshelwood Kinetic Models in Correlating Thiophene HDS Reaction Data	370
8-8	Performance of Langmuir-Hinshelwood Kinetic Models in Correlating Thiophene HDS Reaction Data	371
8-9	The Relative Performance of Four Langmuir-Hinshelwood Models for Correlating Pyridine Hydrogenation Data at a Total Pressure of 1000 psig for $K_{Pip}/K_{Pyr} = 2.0$	372

List of Tables

3-1	Key to Figures for the Chromatographic Product Separations on 10% SP-2310 on 100/120 Mesh Supelcoport	130
4-1	Analysis of New and Used Sulfided NiMo/Al ₂ O ₃ Catalysts	148
4-2	Key for Thiophene HDS Figures: 4-3, 4-4, 4-5, 4-6, 4-7	154
4-3	Key for Pure-Pyridine Feed HDN Figures: 4-8, 4-9, 4-10, 4-11, 4-12	167
4-4	Key for Pyridine-Thiophene Feed HDN Figures: 4-13, 4-14, 4-15, 5-6, 5-7, 5-8	177
4-5	Key for Pure-Pyridine and Pyridine-Thiophene Feed HDN Product Distribution Figures: 4-16, 4-17, 4-18	181
8-1	Properties of Chemicals Used	279
8-2	Free Energies and Heats of Formation for Compounds Relevant to this Study	281
8-3	Catalyst History - Final Catalyst Loading	282
8-4	Data Summaries for Individual Runs	283
8-5	Catalyst Activity Run Data	305
8-6	Pyridine HDN Conversion Curve Values	306
8-7	Thiophene HDS Conversion Curve Values	307
8-8	Pyridine HDN Product Distribution - Pure Pyridine Feed Data	308
8-9	Pyridine HDN Product Distribution - Simultaneous Pyridine-Thiophene Feed Data	309

8-10 Values of Piperidine-Pyridine Ratio at Total Pressure = 1000 psig	374
8-11 Values of Piperidine-Pyridine Ratio at Total Pressure = 500 psig	375
8-12 Values of Piperidine-Pyridine Ratio at Total Pressure = 150 psig	376

Chapter I - Summary

I.A. Introduction

Liquid fuels derived from unconventional sources such as oil shale and coal contain significant amounts of organic nitrogen compounds in addition to the organic sulfur compounds commonly found in many petroleum feedstocks. The concentrations of these compounds must be reduced before refining in order to prevent catalyst degradation, and before use to meet air pollution standards.

The overall objective of this long-term research program is to examine the interactions which result from the presence of both organic nitrogen and sulfur compounds in such petroleum feedstocks, and to determine the implications which these interactions might have for industrial operations. Earlier work in this program, as covered later, studied the interactions between model organic sulfur and nitrogen compounds thiophene and pyridine at pressures from 50 to 150 psig (4 to 11 bars). Several interactions were found between the simultaneous desulfurization and denitrogenation reactions, and an equilibrium limitation on the conversion of pure pyridine was observed.

As industrial fuel processing is carried out at significantly higher pressures than those originally studied, it was desired to investigate the interactions in more detail and at pressures more representative of those in actual use.

I.B. Objectives

This particular study focused on the interactions between the model compounds thiophene and pyridine in hydrogenolysis reactions at pressures up to 1000 psig (70 bars). It was desired to determine the inhibitions, enhancements, and changes in product distributions which might occur under temperature and pressure conditions similar to those of commercial processes. This would be accomplished by comparing the results of the hydrodenitrogenation (HDN) of pure pyridine and the hydrodesulfurization (HDS) of pure thiophene with the results of these reactions carried out using mixed pyridine-thiophene feeds.

Of particular importance was the examination of the potential equilibrium limitation on the reaction of pyridine. Specifically, if the reaction did reach equilibrium, then increasing the hydrogen partial pressure should help overcome the constraint by shifting the composition of the equilibrium mixture toward completion. The effect which the presence of thiophene would have on such a thermodynamic limitation was of great significance.

I.C. Literature Review

This review of thiophene and pyridine hydrogenolysis literature focuses on areas of significance to this experi-

mental study: the mechanisms by which thiophene is desulfurized and pyridine denitrogenated on catalysts such as sulfided CoMo/Al₂O₃ and NiMo/Al₂O₃; the specific competitive adsorptions which are important in the formulation of kinetic rate expressions for the two reactions; and the pyridine-piperidine equilibrium properties which may affect the HDN of pyridine.

Three basic modes for the adsorption of the thiophene molecule onto an active catalytic site have been proposed: single-point, through the sulfur atom; two-point; or four-point. Nicholson (1962) identified two- and four-point adsorptions using infrared spectrometry. Lipsch and Schuit (1969c), however, examined Nicholson's data and concluded that it supported single-site adsorption through the sulfur atom. G.W. Roberts (Roberts, 1965; Satterfield and Roberts, 1968) found two-point adsorption to give much better kinetic correlations than did single-point adsorption. The significance of this study was that its results were determined under actual reaction conditions.

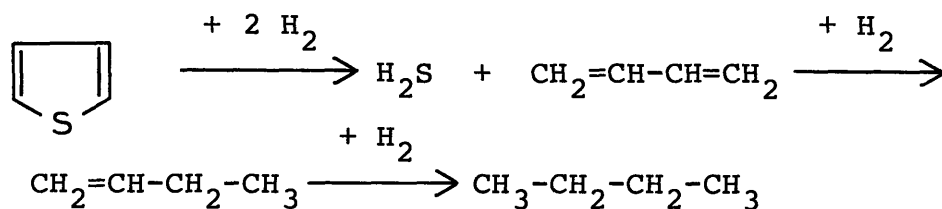
The adsorption of reactant hydrogen was determined by Lipsch and Schuit (1969c) to occur on sites adjacent to, but distinctly different from, those for thiophene adsorption. A second, stronger type of hydrogen adsorption was proposed (Owens and Amberg, 1961, 1962b) to compete with thiophene for active sites, but this is disputed by Lipsch and Schuit (1969c).

Hydrogen sulfide is known to adsorb competitively with thiophene. Desikan and Amberg (1964) and Owens and Amberg (1961) found that H₂S generated by the decomposition of thiophene could not compete equally with thiophene for active sites. Roberts (1965), however, found the two adsorptions to be approximately equal in strength.

Hydrocarbons do not appear to compete strongly for catalytic sites when in small quantities such as would be produced by the decomposition of pure thiophene (Owens and Amberg, 1961, 1962b). However, in petroleum feedstocks, where the ratio of hydrocarbons to thiophene is high, significant competitive effects were observed (Kirsch, Heinemann, and Stevenson, 1957; Phillipson, 1971; Frye and Mosby, 1967).

Basic nitrogen compounds, notably pyridine, have been identified as having strong competitive effects on thiophene adsorption and reaction (Mayer, 1974; Satterfield et al., 1975 ; Desikan and Amberg, 1964; Dirsch, Shalit, and Heinemann, 1959).

Butadiene, a potential reaction intermediate in thiophene HDS, was identified over several hydrodesulfurization catalysts (Kolboe and Amberg, 1966). Tetrahydrothiophene was generally not found as a reaction product (Owens and Amberg, 1961, 1962b). These two findings led to a proposed reaction mechanism for thiophene desulfurization which first desulfurized thiophene, producing butadiene and H₂S; and subsequently hydrogenated the butadiene to butane:

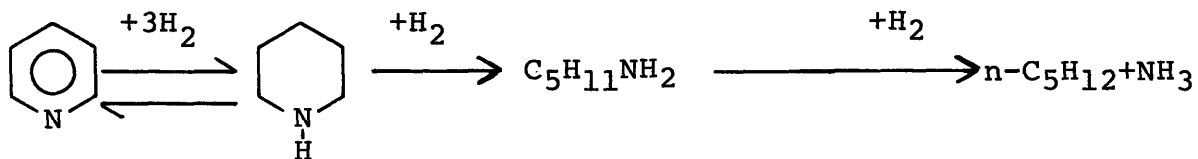


For carrying out this mechanism, two types of sites were proposed. Type I sites, strongly acidic and easily poisoned by basic nitrogen compounds, are responsible for butene hydrogenation and a small amount of desulfurization. Type II sites, slightly acidic, are responsible for most of the thiophene desulfurization, but no hydrogenation beyond butene, and are less susceptible to poisoning (Desikan and Amberg, 1964).

Other two-site mechanisms have been proposed. Mayer (Satterfield et al., 1975) suggested strong active desulfurization sites which are easily poisoned by nitrogen bases; and weaker, less active sites which maintain desulfurization activity under these conditions.

Lipsch and Schuit (1969c) and Ben-Yaacov and Richardson (1975) proposed two-site adsorption models where only one site, either molybdenum or molybdenum sulfide, was responsible for catalyst activity; and the other, the catalyst support, displayed a generally-unreactive adsorption.

A stepwise mechanism for the hydrodenitrogenation of pyridine proposed by McIlvried (1971) begins with the saturation of pyridine to piperidine. The hydrogenolysis of the saturated ring to n-pentylamine is followed by the subsequent hydrogenolysis of the alkyl amine to n-pentane and ammonia:



Subsequent researchers have found supporting evidence for this mechanism (Sonnemans, 1973; Meyer, 1974; Goudriaan, 1974)

Goudriaan (1974) proposed a two-site model for pyridine HDN, with one type of site active in the ring hydrogenation of pyridine, and the other in the hydrogenolysis steps. The similarity to the two-site model for thiophene HDS (one type primarily for desulfurization, the other primarily for butene hydrogenation) proposed by Desikan and Amberg (1964) is intriguing. However, the nearly complete poisoning of the thiophene model hydrogenation sites by pyridine, while confirming nothing about potential hydrogenation of pyridine on these sites, indicates that the hydrogenation sites of the two models may not be the same.

Several kinetic studies have focused on the application of a Langmuir-Hinshelwood rate expression to pyridine hydrodenitrogenation. The relative adsorption strengths of the reactant, pyridine; and products, piperidine and ammonia, are of significance in such formulations. However, difficulties in determining the relevant adsorption parameters have frequently led to the use of a common adsorption term for all nitrogen compounds (Sonnemans, 1973; McIlvried, 1971;

Goudriaan, 1974). In a study directed toward the determination of relative adsorption strengths on $\text{MoO}_3/\text{Al}_2\text{O}_3$ catalysts, Sonnemans (1973b) found piperidine to adsorb approximately six times as strongly as pyridine; and ammonia, about one-fourth as strongly as pyridine. However, from studies made on the alumina support alone, it was evident that the compounds indiscriminately adsorbed on both active sites and non-active support areas, precluding the determination of the relative adsorptions of compounds on the active sites alone.

McIlvried (1971) observed greater reaction inhibitions at higher pyridine conversions, and from this inferred a stronger adsorption of the reaction product ammonia than that of the reactant pyridine on the active catalytic sites.

From his study of the effects of specific components on reaction rates, Goudriaan (1974) determined that the adsorption of ammonia was five times stronger than that of pyridine on pyridine hydrogenation sites, but that on separate piperidine hydrogenolysis sites the adsorptions were of the same magnitude.

An equilibrium limitation on pyridine HDN was suggested by Mayer (Satterfield et al., 1975) as a possible explanation for an observed decrease in the conversion of pyridine with increases in temperature (at 150 psig total pressure and reaction temperatures above 350°C) over several sulfided catalysts. Cocchetto (Satterfield and Cocchetto, 1975)

confirmed that equilibrium was reached under those conditions. Goudriaan (1974) showed that at 80 bars and 400°C over sulfided and unsulfided CoMo/Al₂O₃ catalysts the reaction was thermodynamically limited.

The determination of equilibrium limitations on pyridine HDN requires a value for the equilibrium constant for the hydrogenation of pyridine to piperidine. Goudriaan made a careful empirical determination of the equilibrium constant, correcting for effects of consecutive reactions. His results agreed reasonably well with those calculated from the most recent free energy of formation data for pyridine and piperidine (McCullough et al., 1957; Scott, 1971).

Thiophene was shown to inhibit pyridine conversion under certain reaction conditions, while enhancing it under others (Mayer, 1974; Satterfield et al., 1975). These researchers attributed the inhibition to competition between pyridine and thiophene for active catalytic sites at temperatures where the hydrogenation step was proposed to be rate limiting; and the enhancements to the increase of the rate of piperidine hydrogenolysis under conditions where this latter step was assumed to be rate limiting. Goudriaan (1974), examining the effect of hydrogen sulfide on pyridine HDN, observed an enhancement of the hydrogenolysis capability of sulfided CoMo/Al₂O₃ and an inhibition of the hydrogenation capability.

I.D. Experimental Apparatus and Procedure

The reactions of this study were carried out in a packed-bed catalytic reactor at pressures up to 1000 psig (70 bars). A catalyst loading consisted of 1.5 grams of sulfided NiMo/Al₂O₃ ground and sieved to an average particle diameter of 0.77 mm. The continuous-flow integral reactor was run at constant space velocity, and data taken under steady-state isothermal conditions in the absence of heat or mass transfer limitations. Details of the reactor system are shown in Figure 1-1.

The reactor, a quarter-inch stainless-steel tube, contained a catalyst bed 13 cm deep and 4.6 mm in diameter, in a straight, vertical configuration. Isothermal reaction temperatures were maintained by immersing the reactor in a fluidized sand bed heater, and measured with a thermocouple at the entrance to the catalyst bed.

Liquid reactants were injected with a high-pressure metering pump, passed through a heated-capillary preheater, and vaporized into a stream of heated hydrogen. This vapor mixture was fed to the reactor through preheating coils, the final one immersed in the heated fluidized sand bed. Oxygen and water were removed from the reactant hydrogen by passing the stream first over a palladium catalyst, and then through a bed of 4A molecular sieves.

System pressures were maintained by the reactant hydrogen cylinder regulator, and flows by valves downstream of the

reactor. Flow rates through the system were measured with soap-film flowmeters after the reaction stream was reduced to atmospheric pressure. The heavy streamlines in Figure 1-1 indicate the primary flows through the reactor system during steady-state operation.

Safety aspects of construction included the use of a reactor barricade, an automatic pressure-activated shutdown system, and numerous other design considerations.

Reaction streams were analyzed by gas chromatography, utilizing a heated, on-line gas sample valve as an interface between the reactor and analysis systems. Reactant conversions were determined as the disappearance of the feed component, as measured by changes in the chromatographic peak area under different reactor conditions.

An experimental run consisted of determining the conversion characteristics of thiophene and/or pyridine at several reaction temperatures, maintaining all other parameters constant. A base-level reactant concentration was first determined by analyzing the product stream at low reactor temperatures, at which no reaction took place. The reactor temperature was then raised, and the reaction allowed to reach steady state. Samples of the product stream then showed the decreased concentrations of reactant on which conversions were based. Partial reaction product distributions were also determined at each reaction temperature.

Maintaining the catalyst in a standard state of activity was important for obtaining reproducible results under greatly differing reactor feed conditions. Three methods of sulfiding were developed and used to insure that the catalyst was properly activated at the start of each experimental run: I. Formal sulfiding, the manufacturer's recommended procedure for activating the catalyst, involved maintaining the catalyst under a flow of 10 percent H_2S in H_2 during a specific time-temperature program; II. Run sulfiding involved the inclusion of a sulfur compound in the reactor feed which would decompose, producing H_2S , and sulfide the catalyst during the run; and III. Shutdown sulfiding was carried out by cooling the reactor after a run, under a stream of H_2S in H_2 .

I.E. Results

The results presented here are based on data from the continuous plug-flow packed-bed catalytic reactor using 1.5 grams of sulfided $NiMo/Al_2O_3$. Quantitative results from this integral reactor are presented as the conversion (disappearance) of reactant as a function of reactor temperature at constant space velocity. For pyridine runs, product distributions are presented as the normalized concentrations of components in the product stream, expressed as the moles of a component in the product stream per mole

of pyridine fed to the reactor. Total reactor pressures were set to nominal values of 150, 500, or 1000 psig, and the partial pressures of the sulfur and nitrogen reactants to either 93 or 186 torr. For clarity of presentation, these nominal values will be used in textual material.

I.E.1. Catalyst Activity

Three sulfiding methods were used to maintain a constant level of activity of the sulfided NiMo/Al₂O₃ catalyst during this work. The techniques were developed because early experiments showed that in the absence of further sulfur exposure, a fresh, sulfided catalyst gradually lost half of its initial activity after 100 to 150 hours on stream. Although the high activity of the fresh catalyst was never regained, each of the three sulfiding procedures was able to consistently restore activity to three-quarters of the initial level. This reproducible state was then used as the standard state of catalyst activity.

After 280 hours on stream with pyridine and thiophene, the catalyst was used for 240 hours with quinoline feeds. Following the quinoline runs, only about half of the previously-restorable pyridine conversion activity was achieved. Two factors could have accounted for this: quinoline was likely to produce more heavy substances which could form carbon deposits; and quinoline runs were made at slightly

higher reaction temperatures, at the catalyst limit.

After resulfiding, this used catalyst was compared with a fresh, sulfided sample. The B.E.T. surface areas of the used and new sulfided catalysts were the same. However, the used catalyst had ten percent less total pore volume and a slight shift in the pore size distribution to larger pore diameters. The ability of the catalyst to retain sulfur decreased 12 percent. While the fresh catalyst contained no detectable carbon deposits, the use loading contained 37g/Kg carbon.

I.E.2. Pure Thiophene Hydrodesulfurization

The influence of hydrogen partial pressure on the conversion of pure thiophene at total pressures of 150, 500, and 1000 psig for a thiophene feed partial pressure of 93 torr is shown in Figure 1-2 (open symbols). The conversion of thiophene was rapidly effected over the sulfided NiMo/Al₂O₃ catalyst at pressures as low as 150 psig. Increasing the total pressure by increasing the hydrogen partial pressure caused significant increases in conversion.

The effect on thiophene conversion of doubling the partial pressure of thiophene was to decrease the conversion at any given reaction temperature.

Tetrahydrothiophene was detected in the product streams under conditions which yielded thiophene conversions between

five and 50 percent. The maximum amount observed at 150 psig, using 186 torr feed partial pressure, was approximately 0.3 percent of the amount of thiophene fed, at a thiophene conversion of seven percent. At 1000 psig and 186 torr feed partial pressure, a maximum of five percent of the amount of thiophene fed was observed as tetrahydrothiophene, at a thiophene conversion of 25 percent.

I.E.3. Thiophene HDS in the Presence of Nitrogen Compounds

The effect of the presence of pyridine on thiophene HDS in runs using mixed thiophene-pyridine feeds, with equal component partial pressures of 93 torr, is also shown in Figure 1-2 for the same three total pressures (solid symbols). For each pressure studied there was a strong inhibition, resulting in similar shifts of all three curves to higher temperature ranges. The qualitative behavior of the mixed-feed curves was similar to that of the pure-thiophene feed curves.

To compare the effect of ammonia with that of pyridine on thiophene HDS, n-butylamine was added in equimolar amounts to a 93 torr thiophene feed at 1000 psig, intending that the decomposition of the amine would produce ammonia of the same partial pressure. Although the butylamine did not react as rapidly as had been expected, and actually decomposed at a rate closer to that of pyridine, Figure 1-3

shows that the inhibition was nearly identical to that of pyridine.

Tetrahydrothiophene was not present in the product streams of the mixed thiophene-pyridine feed runs. Its qualitative presence could have been detected at levels as low as one-tenth of one percent of the amount of thiophene fed.

I.E.4. Pure Pyridine Hydrodenitrogenation

The influence of hydrogen partial pressure on the HDN of pyridine was studied at total reactor pressures of 150, 500 and 1000 psig. The effects on the conversion of pyridine for a feed partial pressure of 93 torr are shown in Figure 1-4 (open symbols). Pyridine conversion was strongly influenced by pressure. Data at 150 psig showed increasing conversion until a maximum of 29 percent was reached at 370°C, after which it decreased to 20 percent at 410°C. In contrast, at 1000 psig conversion increased rapidly with temperature, achieving complete conversion at 390°C. Results at 500 psig showed characteristics closer to those at 1000 psig.

The normalized concentration of the reaction intermediate piperidine is shown in Figure 1-5 (open symbols) as a function of reaction temperature. Expressed as the moles of piperidine in the product stream per mole of pyridine in

the reactant stream, the concentration reached a maximum at approximately 315°C at each reaction pressure, the higher pressures greatly increasing the amounts present. By 400°C, piperidine had essentially disappeared from the product stream.

For the pyridine runs, three components were identified in the product stream: pyridine, piperidine, and n-pentylamine. Figures 1-5, 1-6, and 1-7 show the relationships of these three components in the product stream as their normalized concentrations as a function of reaction temperature for total reactor pressures of 1000, 500, and 150 psig, respectively (open symbols). N-pentylamine was present in the product stream, but only in amounts less than one mole percent of the amount of pyridine fed at 1000psig, and on the order of 0.1 mole percent at the lower pressures.

The relationship between the pyridine and piperidine curves should be noted. At 1000 psig, whereas pyridine was rapidly converted to only four percent of its feed concentration at 330°C, the piperidine concentration increased as pyridine disappeared, and was still present at 40 percent of the molar pyridine feed at 350°C. Similar results were obtained at 500 psig. At 150 psig, piperidine was always a small fraction of the amount of pyridine present, due to the very low pyridine conversions and piperidine levels.

Doubling the partial pressure of pyridine decreased the pyridine conversions for the higher partial pressures,

indicating a reaction order less than one in pyridine.

An attempt was made to identify a few small product peaks, totaling approximately 0.5 mole percent of the amount of pyridine fed, using mass spectrometric analysis. Low-boiling compounds were mainly unsaturated hydrocarbons. High boilers consisted of substituted unsaturated ring compounds and possibly unsaturated rings linked by alkyl side chains.

I.E.5 Pyridine HDN in the Presence of Sulfur Compounds

The effect of the presence of thiophene on pyridine HDN was investigated using a mixed feed containing equal pyridine and thiophene partial pressures of 93 torr. Figure 1-4 shows the effect of using the mixed feeds on the conversion of pyridine (solid symbols). At 150 and 500 psig a large inhibition at lower reaction temperatures was maintained until the pure-feed curves decreased their slopes, at which point an enhancement began. At 150 psig the previously observed downturn was eliminated, and at 500 psig complete conversion was achieved by 390°C. At 1000 psig a mild inhibition was observed above 280°C, until at 350°C the same type of enhancement was seen as at the lower pressures.

The effect of hydrogen sulfide on pyridine HDN was studied by adding 1-propanethiol to the reactor feed in equimolar amounts with pyridine; the propanethiol was com-

pletely converted to H_2S at temperatures above $250^{\circ}C$. Figure 1-9 shows the H_2S to have a stronger inhibiting effect than thiophene over the entire temperature range, except where enhancement at higher temperatures led to the same $360^{\circ}C$ point for complete conversion.

The addition of thiophene to the reactor feed caused the amount of piperidine formed at all temperatures to decrease significantly, as shown in Figure 1-5 (solid symbols). The maximum amounts of piperidine in the product stream were only 20 to 60 percent of those for the pure-pyridine feeds.

The effects of thiophene on the product distribution for pyridine HDN are shown in Figures 1-6, 1-7, and 1-8. At 1000 psig there was little change in the pyridine disappearance due to thiophene addition, but great decreases occurred in the amounts of piperidine present. The 500 psig product distribution displayed characteristics similar to those at 1000 psig. The 150 psig product distribution was different because of its much lower pyridine conversion. The addition of thiophene at the low pressure produced the greatest percentage decreases in the piperidine output of all three pressures. Data on n-pentylamine were not available for pyridine-thiophene feed runs, as the amine peak in the chromatographic analysis was obscured by that of thiophene.

The conversion of the combined quantities of pyridine and piperidine was much higher at 500 and 1000 psig for the

pyridine-thiophene feedstocks than for the pure-pyridine feeds.

I.F. Discussion of Results

I.F.1 Catalyst Activity

The use of the three types of catalyst sulfiding procedures previously described overcame long-term catalyst deactivation tendencies. By carrying out one of the three sulfiding procedures, the catalyst was returned to a standard state of activity for the start of each run. A new catalyst loading was installed and used for approximately 200 hours before the final set of quantitative runs was made, overcoming the initial high-activity effects shown by the fresh catalyst.

The deactivation of the catalyst after 550 hours on stream appeared to result primarily from the quinoline runs. As the NiMo/Al₂O₃ catalyst was sensitive to overheating, the higher temperatures used for the quinoline runs may have been enough to affect the catalyst by sintering, altering the pore structure, or enhancing the deposition of carbon. The presence of carbon deposits was a significant difference between the new and used catalyst samples. While no sample was tested after use with only pyridine, qualitative observations indicated that much of this deposit may have been

due to the quinoline usage.

The pore structure should not have been altered significantly by heat at the temperatures studied, as the alumina was specified to be completely stable to at least 550°C (American Cyanamid, 1969). Of the factors studied, however, small differences in pore structure would probably be due to either the thermal treatment or carbon deposition.

A significant difference between the catalysts was the amount of sulfur retained after the formal sulfiding procedures. The ten percent lower sulfur level of the used catalyst could represent a significant loss of active catalytic sites. This was the only test performed which had a degree of selectivity between the metallic sites and the alumina support, and thus could have been an important factor, as the sulfided metal provided much of the activity for the HDS and HDN reactions.

I.F.2. Pure Thiophene Hydrodesulfurization

The conversion of pure thiophene was easily carried out at reaction pressures as low as 150 psig over the sulfided NiMo/Al₂O₃ catalyst. Increases in pressure up to 1000 psig produced even more rapid desulfurization, while maintaining the same character of the conversion

curve. This indicates that the same reaction mechanisms were probably in effect over the pressure range studied.

The S-shaped curves conform to expectations for a reaction order greater than zero in thiophene. Doubling the thiophene partial pressure decreased the conversion at any given temperature; a first-order reaction would have shown identical curves for the two partial pressures. The results thus also indicate a reaction order less than one in thiophene.

The presence of tetrahydrothiophene in the product stream indicated that at some reaction conditions two parallel reaction mechanisms might be operating. Application of evidence from the analysis of the C₄ reaction products by Owens and Amberg (1961) suggests that the formation of tetrahydrothiophene is a secondary reaction mechanism appearing under a narrow range of reaction conditions.

I.F.3. Thiophene HDS in the Presence of Nitrogen Compounds

The inhibition of thiophene HDS by pyridine resulted in a nearly-direct shift of the three pure-thiophene curves to higher temperatures. This implies that one basic type of HDS mechanism was operating under both sets of conditions.

The inhibitions of thiophene conversion by the butyl-amine-ammonia combination and by pyridine were nearly identical; the actions of the aromatic pyridine and the aliphatic amine-ammonia combination affected the active sites in the same way, in spite of greatly different basicities. This could imply a type of threshold inhibition, where once a certain strength of adsorption on active sites is reached, the activity is decreased to a specific and constant level.

The complete disappearance of tetrahydrothiophene from the product stream in the presence of pyridine probably indicates a blocking of the particular mechanism by which it was formed. The remaining HDS occurred strictly by the sulfur-removal-then-saturation mechanism.

From these results it follows that proper combinations of high pressure and temperature will overcome the inhibition by pyridine. Complete conversion of thiophene is thus possible, even for mixed-feed streams.

I.F.4. Thiophene HDS: Kinetic Analysis

To determine a kinetic expression for describing the integral reactor data for thiophene HDS, it was necessary to assume specific models, integrate the associated rate expressions in the plug-flow reactor performance equation,

and compare the predictions of these integrated forms with the actual experimental results.

As was expected for a system with strong reactant and product adsorption characteristics, power-law kinetics was inadequate to describe the reaction data. A series of Langmuir-Hinshelwood models was then formulated to account for various assumptions of the relative adsorption strengths of thiophene and hydrogen sulfide, and the nature of the chemisorptive bond between thiophene and the active surface catalytic site; as covered in the literature review. The basic equation used was:

$$-r_{\text{Thi}} = \frac{k_{\text{Thi}} \gamma K_{\text{Thi}} P_{\text{Thi}}}{(1 + K_{\text{Thi}} P_{\text{Thi}} + K_{\text{H}_2\text{S}} P_{\text{H}_2\text{S}})^m}$$

where $-r$ represents the reaction rate of thiophene; k , the surface reaction rate constant; γ , the hydrogen functionality; K 's, adsorption constants; P 's, partial pressures; and m , the number of points through which thiophene adsorbs onto the surface.

The resulting rate expression was evaluated for $(K_{\text{H}_2\text{S}}/K_{\text{Thi}})$ ratios of 0.0, 0.25, and 1.0; and for both single- and dual-point adsorption of thiophene. This relation was substituted into the plug-flow catalytic

reactor performance equation, and the resulting expression integrated for each set of assumptions. After insertion of the reaction data, the quality of fit of the models was determined by the linearity of the logs of the adsorption constant and rate constant values with the inverse absolute temperature.

From examination of the results of the different parameter assumptions, two trends were apparent for the application of the models to this experimental data: first, the adsorption of hydrogen sulfide appeared to be weaker than that of thiophene; and second, two-point adsorption of thiophene showed a better correlation than did one-point adsorption. Further, an analysis of the hydrogen functionality indicated that hydrogen adsorption appeared to be atomic rather than molecular.

Using the best models from the pure-thiophene feed analysis, the data for the addition of pyridine to the thiophene feed were examined by adding a competitive adsorption term covering all nitrogen compounds. The data were roughly accounted for by a model in which the nitrogen compounds competed for thiophene HDS sites, and the average nitrogen adsorption strength was approximately five times that of thiophene.

I.F.5. Pure Pyridine Hydrodenitrogenation

The pure pyridine HDN data of Figure 1-4 shows bends in the conversion curves beginning about 340°C. At 500 and 1000 psig this was only a reduction in the slope of the curve, but at 150 psig it led to decreases in the conversion at temperatures above 370°C. It is important to determine whether kinetics or thermodynamics was responsible for this behavior.

Simple kinetics cannot account for the downturn as seen at 150 psig. More advanced kinetic models, accounting for strong competitive adsorption of products, could predict such behavior. However, if competitive adsorption of products were solely responsible for the downturn, then the most significant effects should have been observed at 1000 psig, where there was a much higher concentration of products. Instead, as the downturn was present only at 150 psig, it appears that another factor must be at least partially responsible.

If a thermodynamic limitation were to cause the downturn, the piperidine hydrogenolysis step must first become rate limiting, allowing piperidine accumulation. With relatively rapid forward and reverse hydrogenation reactions, equilibrium could be attained.

If an equilibrium situation did exist, then

LeChatelier's principle would apply. The reduction in the number of moles with the forward reaction should force the equilibrium composition to the right, increasing the amount of pyridine converted to piperidine. Figure 1-5 shows that when the pressure was increased from 150 to 1000 psig, the amount of piperidine present in the product stream increased sevenfold. Qualitatively, this was precisely the behavior expected for the equilibrium-limited case. This is covered quantitatively in a subsequent section.

The product distributions for pyridine HDN focus on pyridine and piperidine. N-pentylamine, always less than one mole percent of the amount of pyridine fed, was apparently converted at a rate much faster than it was formed. Those side reaction products analyzed by mass spectrometry indicated that a wide variety of side reactions took place. It is significant that both the lighter and heavier compounds formed remained predominantly unsaturated. This indicates that there may be a very low hydrogenation capability of the catalyst toward many olefins and aromatics in the presence of pyridine.

The effect on pyridine conversion of doubling its partial pressure indicated that the reaction was less than first order in pyridine. As the conversion curve shift was less than that for a zero-order reaction, the

observed order was between zero and one.

I.F.6. Pyridine HDN: Equilibrium Analysis

The equilibrium constant for pyridine hydrogenation as a function of temperature was determined in two independent ways: by calculation from thermodynamic free energy of formation data; and by utilization of an empirical expression developed by Goudriaan (1974). By estimating the activity coefficients of the components, Goudriaan determined that non-idealities of pyridine and piperidine mutually compensated in the equilibrium constant expression, and that as a result the component activities could be replaced by their partial pressures.

To assess the approach of the reactor product stream to its equilibrium concentration, an analysis compared experimental values of the equilibrium constant formulation with those from the calculated K_p -temperature relationships on a plot of the integrated van't Hoff equation, $\log_{10}(K_p)$ as a function of the inverse absolute temperature. To compare the experimental results of this study with these K_p lines, the quantity:

$$\log_{10} \left(\frac{P_{\text{Pip}}}{P_{\text{Pyr}} P_{\text{H}_2}^3} \right)$$

where P_{Pip} , P_{Pyr} , and P_{H_2} are the partial pressures of piperidine, pyridine, and hydrogen; was calculated from data at each experimental point. Figures 1-10, 1-11, and 1-12 present these values for total reaction pressures of 1000, 500, and 150 psig, respectively; each gives results for both pure-pyridine and pyridine-thiophene feed cases. Vertically-downward arrows indicate that, for mixed-feed cases, the piperidine concentrations were zero at those temperatures; the curves thus drop off precipitously as they approach these points. At all three pressures, the empirical equilibrium line was reached at approximately 350°C. Above this temperature the experimental curves followed the empirical equilibrium line very closely, demonstrating the attainment of equilibrium for pure-pyridine feeds.

For pyridine-thiophene feeds, the data were always farther from the equilibrium lines than the pure-feed points, and dropped off sharply well before reaching equilibrium. In reducing the amount of piperidine present, the addition of thiophene had removed a necessary criterion for the attainment of pyridine-piperidine equilibrium: the relatively slow hydrogenolysis step which permitted the piperidine concentration rise.

I.F.7. Pyridine HDN in the Presence of Sulfur Compounds

For the pyridine hydrogenation curves of Figure 1-4, the enhancement breakthroughs seen in the 500 and 1000 psig curves occurred at the same temperatures at which equilibrium was reached in Figures 1-10 and 1-11. It is thus likely that these pure-pyridine curves displayed decreasing slopes above these temperatures due not only to kinetic effects, but also very strongly to equilibrium limitations. The rates represented by the pyridine-thiophene feed curves at temperatures greater than breakthrough, then, were those of pyridine hydrogenation in the absence of a blocking piperidine concentration. Because this hydrogenation was once again rate limiting, as it was before piperidine hydrogenolysis became the rate limiting step, the competition for active sites was again significant.

Thiophene affected the amount of piperidine present in the product stream in at least two ways: by the inhibition of pyridine hydrogenation; and by the enhancement of the piperidine hydrogenolysis reaction. For the data of this study, the enhancement predominated at 1000 psig, and the inhibition at 150 psig. At 500 psig, the inhibition initially dominated, until at temperatures greater than 330°C the enhancement became the stronger factor.

Thiophene could enhance the hydrogenolysis of piperidine in several ways. First, the product H_2S could help maintain the catalyst in a more fully sulfided state. The acidity of H_2S is also likely to assist in the enhancement through either its ability to improve the acidity of the catalyst itself, or by helping to remove the basic nitrogen compounds from the catalyst surface.

The effects of thiophene on the relative reactions of pyridine and piperidine are important. For the conversion of pyridine there was an inhibition in mixed-feed runs relative to the pure-pyridine feed cases under most conditions. For the conversion beyond piperidine (disappearance of both pyridine and piperidine), however, there was a significant enhancement at intermediate temperatures for the two higher pressures, caused by the great decreases in the piperidine concentration. Thus at the higher reaction pressures of significance in commercial operations, whereas thiophene primarily caused an inhibition in pyridine hydrogenation, it effected an enhancement of the conversion beyond piperidine.

I.F.8. Pyridine HDN: Kinetic Analysis

Power-law kinetics was once again inadequate to describe the experimental data, probably due to the strong

adsorption of reactants and products. A Langmuir-Hinshelwood expression was thus written which could account for the competitive adsorption of all nitrogen species (based on the information presented in the literature review) and the approach to equilibrium which was shown to occur. It also accounted for potential losses of pyridine to heavy products which might form a tar, or in some other way not be involved in the competitive adsorption process. The basic equation used was:

$$-r_{\text{Pyr}} = \frac{k_{\text{Pyr}} K_{\text{Pyr}} \left(P_{\text{Pyr}} - \frac{P_{\text{Pip}}}{K_{\text{eq}} P_{\text{H}_2}^3} \right)}{1 + K_{\text{Pyr}} P_{\text{Pyr}} + K_{\text{Pip}} P_{\text{Pip}} + K_{\text{NH}_3} P_{\text{NH}_3}}$$

where the terms are analogous to those of the thiophene expression, with the addition of K_{eq} , the equilibrium constant for pyridine hydrogenation to piperidine. This rate relation was inserted into the plug-flow reactor performance equation, and the resulting expression integrated. The experimental data were then applied to each of 36 cases resulting from variations of the following parameters:

<u>Parameter</u>	<u>Cases Studied</u>
Pyridine-piperidine equilibrium accounted for (approach term included in concentration driving force) ?	(Yes) (No)
Ratio: $\frac{K_{NH_3}}{K_{Pyr}}$	(0.25) (1.00) (4.00)
Ratio: $\frac{K_{Pip}}{K_{Pyr}}$	(1.0) (2.0) (4.0)
Percentage of converted nitrogen lost as heavy products	(0.0) (15.0)

The techniques for evaluation of the models were similar to those described for the thiophene analysis. The best models for pyridine hydrogenation were those assuming the adsorption of ammonia to be less than or equal to, rather than greater than, that of pyridine. Also, the adsorption of piperidine correlated best when it was assumed to be equal to or twice that of pyridine, rather than four times as great. The equilibrium term contribution was small over the short temperature range where it took effect, and did not affect differentiation among the other model parameters. The loss as heavy products was significant only in the cases of strong ammonia adsorption, which were poorer models regardless of this parameter value. For the best models, the magni-

tude of the sum of the products $\sum K_{ads_i} P_i$ is of the order 1, implying that all terms of the denominator were significant.

I.F.9. Relative Rates of Thiophene HDS and Pyridine HDN

In pure-reactant form, the reactions of thiophene were faster than those of pyridine. The conversions of thiophene and pyridine were both inhibited in the presence of the other compound under most conditions, with the inhibition of thiophene by pyridine being the greater effect.

Accounting for the presence of piperidine, the relative rates are changed considerably. Here, with the unconverted piperidine included with the pyridine, the pure feeds exhibited a ratio of thiophene conversion to pyridine-plus-piperidine conversion up to five times the thiophene-to-pyridine conversion ratio noted above. The mixed-feed cases showed a great lowering of this ratio, as thiophene conversion was inhibited, while the conversion of the combined pyridine-plus-piperidine was enhanced.

At temperatures approaching 400°C, the high-pressure reactions for both thiophene and pyridine achieved or approached complete conversion, for both pure and mixed feeds. Thus the proper combinations of high temperatures

and high pressures were able to overcome the adverse effects of mixed thiophene and pyridine feed reactions.

I.G. Conclusions

I.G.1. Catalyst Activity

The activity of sulfided NiMo/Al₂O₃ catalysts is strongly dependent upon the state of sulfiding of the catalyst. The addition of easily-decomposed sulfur compounds to a reactor feed will maintain activity in the presence of basic nitrogen compounds such as pyridine.

I.G.2. Thiophene Hydrodesulfurization

Thiophene HDS is inhibited by the presence of the basic aromatic nitrogen compound pyridine at all temperatures and pressures from 150 to 1000 psig (11 to 70 bars). Aliphatic amines appear to cause the same degree of inhibition as does pyridine. Complete conversion is still possible under inhibited conditions, but at higher reaction temperatures than for the pure-thiophene reaction.

Pyridine competes strongly with thiophene for active catalytic sites, showing an adsorption strength greater than that of thiophene. Hydrogen sulfide is also competitive, but appears to have weaker adsorption than thiophene

when present as a product of thiophene hydrogenolysis. Two-point adsorption of thiophene gives better kinetic correlations for these data than does single-point adsorption.

I.G.3. Pyridine Hydrodenitrogenation

The HDN of pure pyridine is subject to a thermodynamic limitation above 350°C at pressures from 150 to 1000 psig, where pyridine reaches equilibrium with its saturated reaction intermediate piperidine. The higher hydrogen partial pressures, however, shift the equilibrium composition toward piperidine, and complete conversion of pyridine is then possible.

The presence of thiophene inhibits the hydrogenation of pyridine at temperatures below which the equilibrium limitation would be in effect for the pure feed reaction. At temperatures above which pure pyridine hydrogenation would be equilibrium-limited, thiophene enhances pyridine reaction, giving conversions greater than those observed for the pure-feed case.

The concentration of piperidine greatly decreases with the addition of thiophene, caused by both the inhibition of pyridine hydrogenation and the enhancement of piperidine hydrogenolysis. This reduction in the piper-

idine concentration removes a necessary criterion for equilibrium; there is no thermodynamic limitation on pyridine HDN in the presence of thiophene.

The conversion of pyridine to products beyond piperidine is enhanced by thiophene for temperatures greater than 300°C at pressures of 500 and 1000 psig. This is a better measure of the removal of the nitrogen atom from the liquid reactant stream than is the conversion of pyridine.

Piperidine competes with pyridine for active catalytic sites with an adsorption strength equal to or slightly greater than that of pyridine. Ammonia adsorption is equal to or weaker than pyridine on the active catalytic sites.

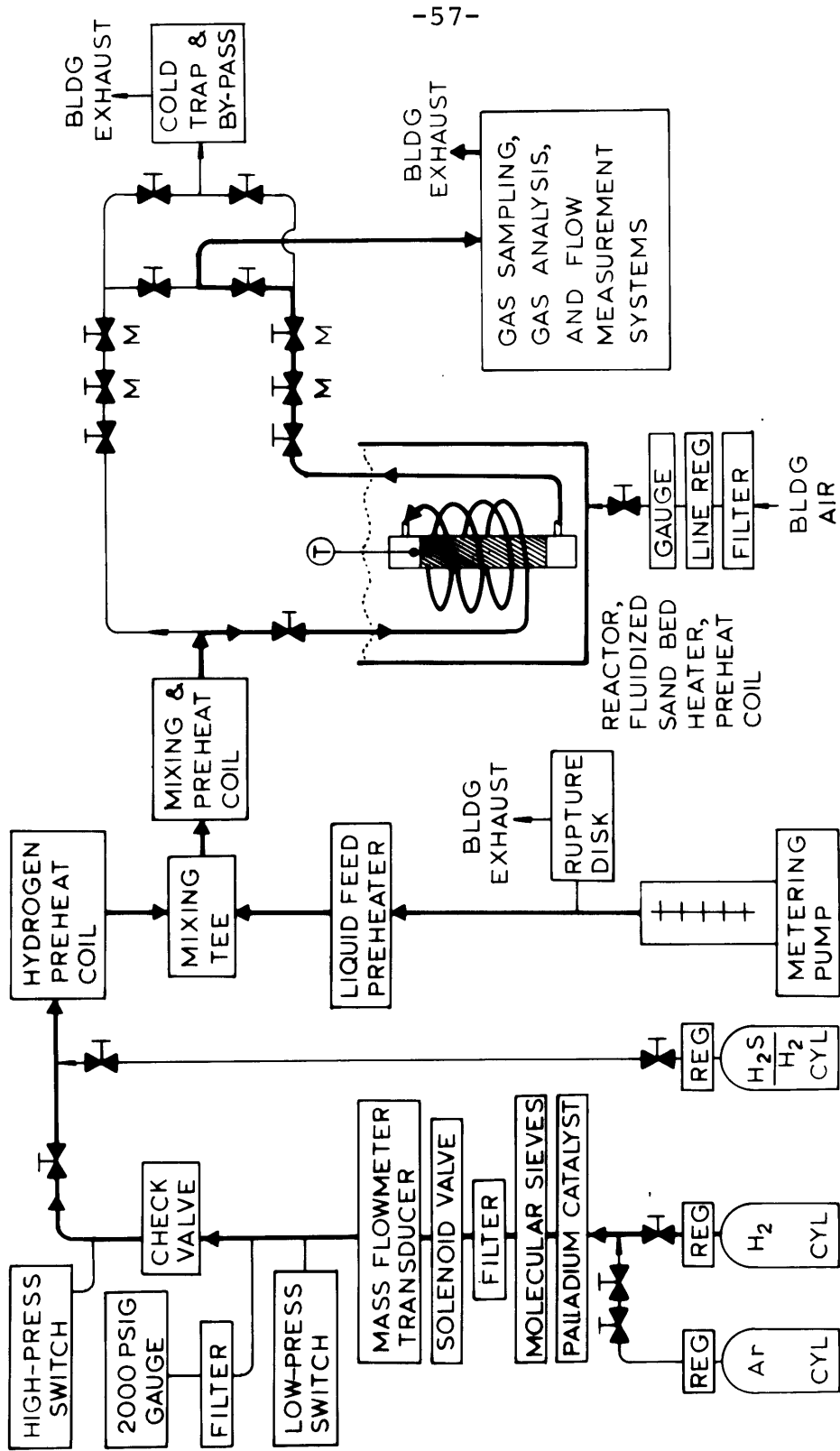


FIGURE 1-1: REACTOR SYSTEM: MAIN COMPONENTS AND PRIMARY FLOWS

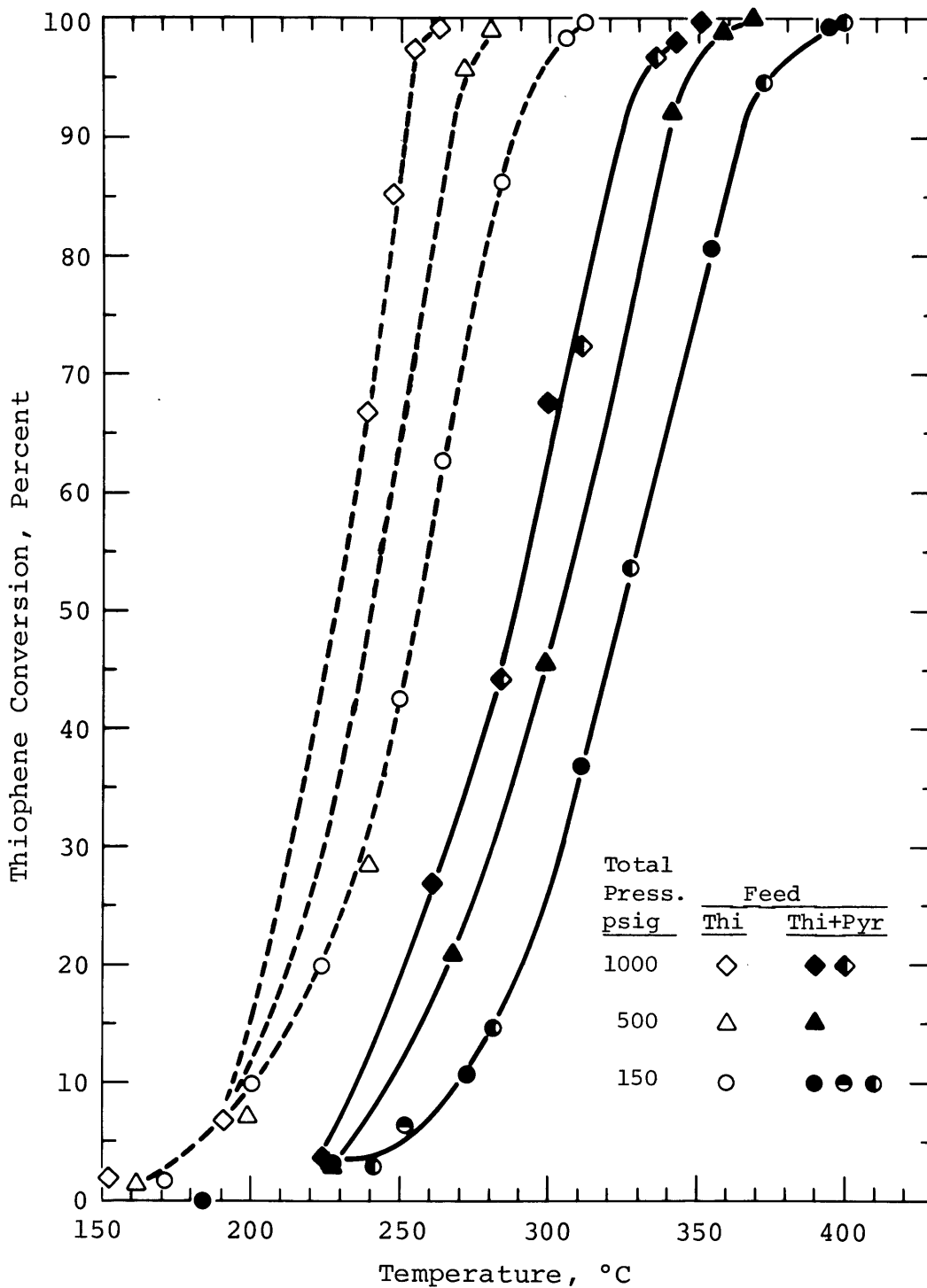


Figure 1-2: Thiophene HDS for Pure Thiophene (93 torr Partial Pressure) and Mixed Thiophene (93 torr)-Pyridine (93 torr) Feeds at Total Pressures of 150, 500, and 1000 psig.

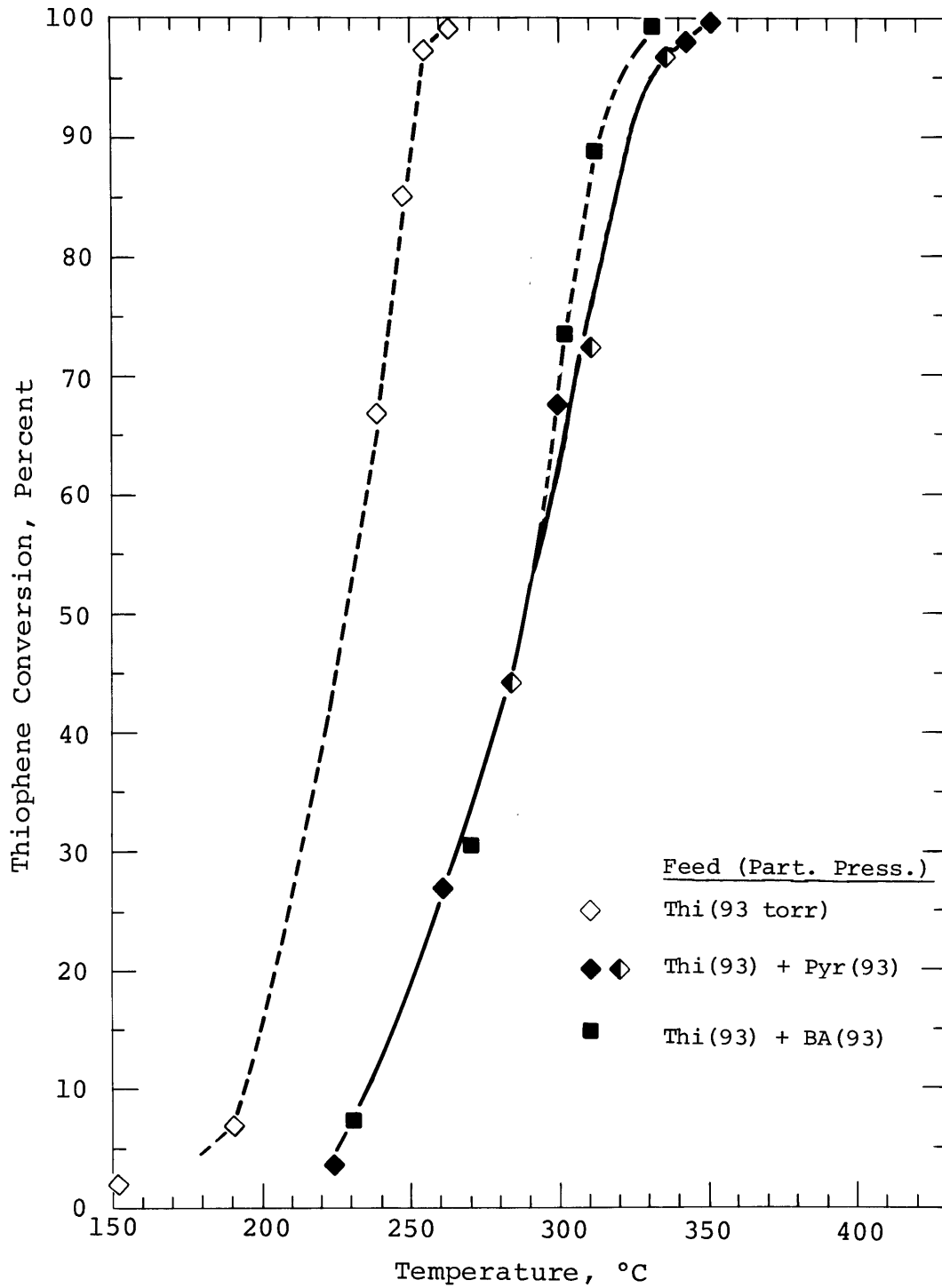


Figure 1-3: Comparison of the Effects of Pyridine and Combined Butylamine (BA) plus Ammonia on the Conversion of Thiophene at a Total Pressure of 1000 psig.

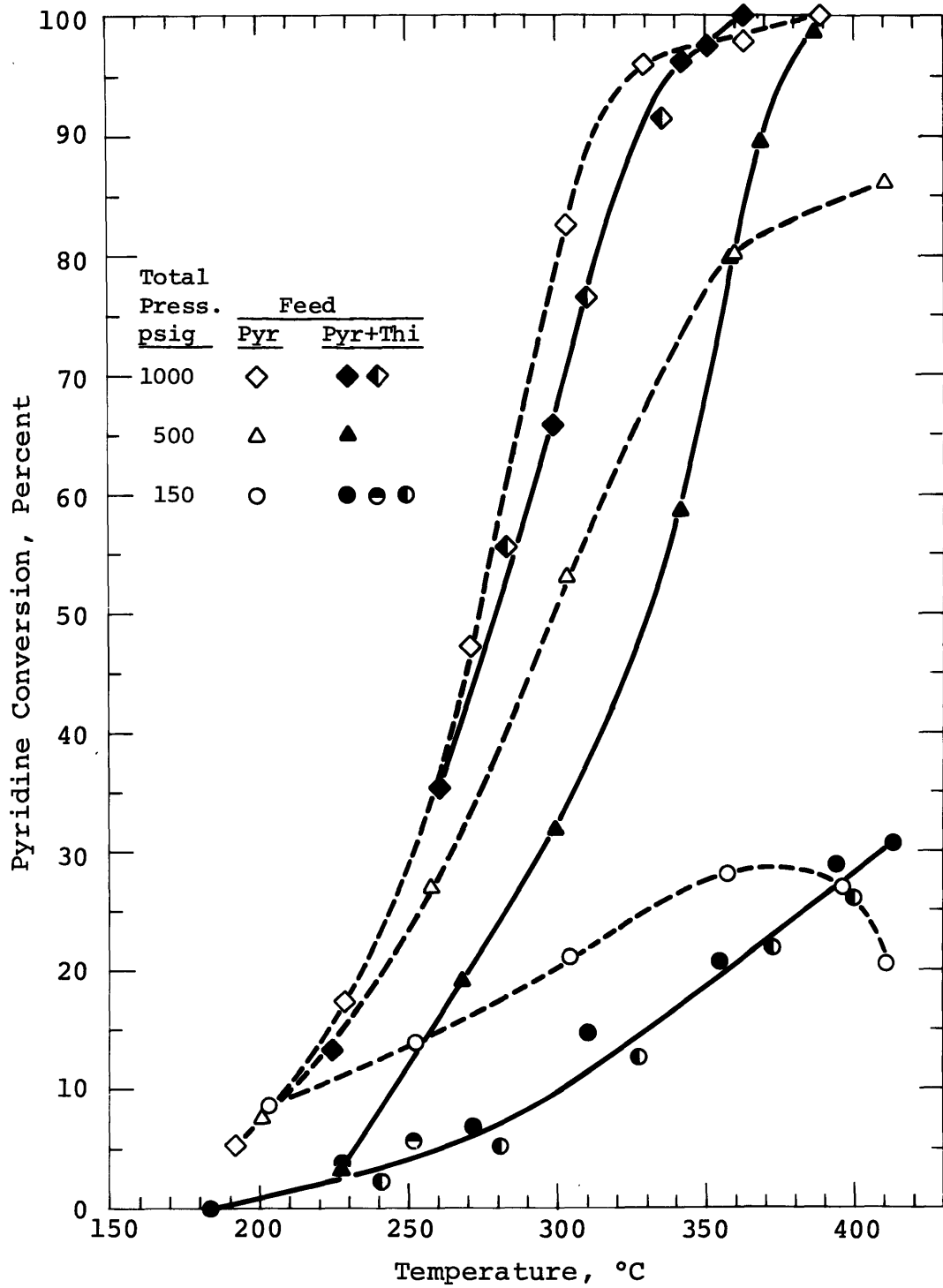


Figure 1-4: Pyridine HDN for Pure Pyridine (93 torr Partial Pressure) and Mixed Pyridine (93 torr)-Thiophene (93 torr) Feeds at Total Pressures of 150, 500, and 1000 psig.

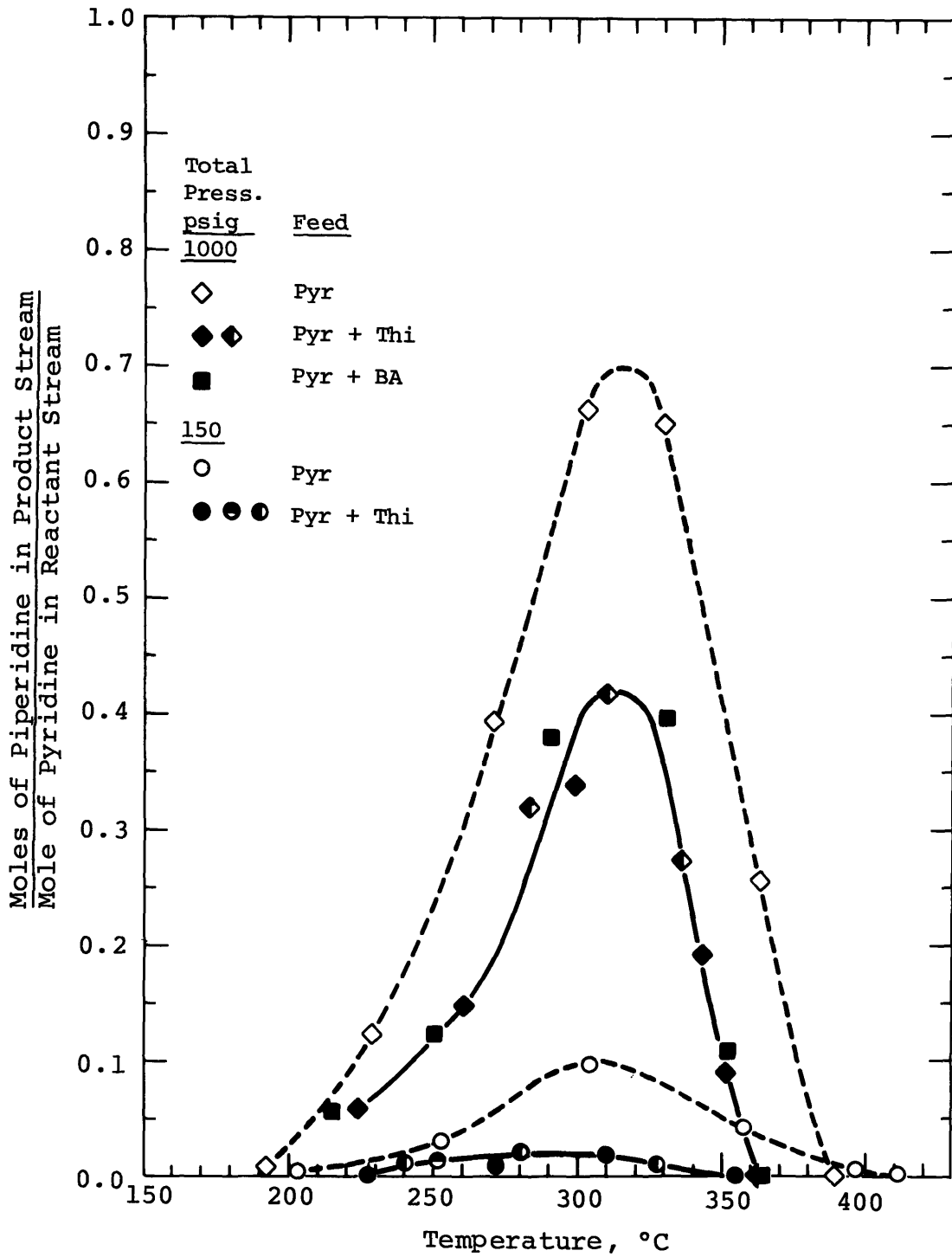


Figure 1-5: Piperidine Presence in the Product Stream For Pure Pyridine (93 torr partial press.) and Mixed Pyridine (93 torr)-Thiophene (93 torr) Feeds at Total Pressures of 150 and 1000 psig.

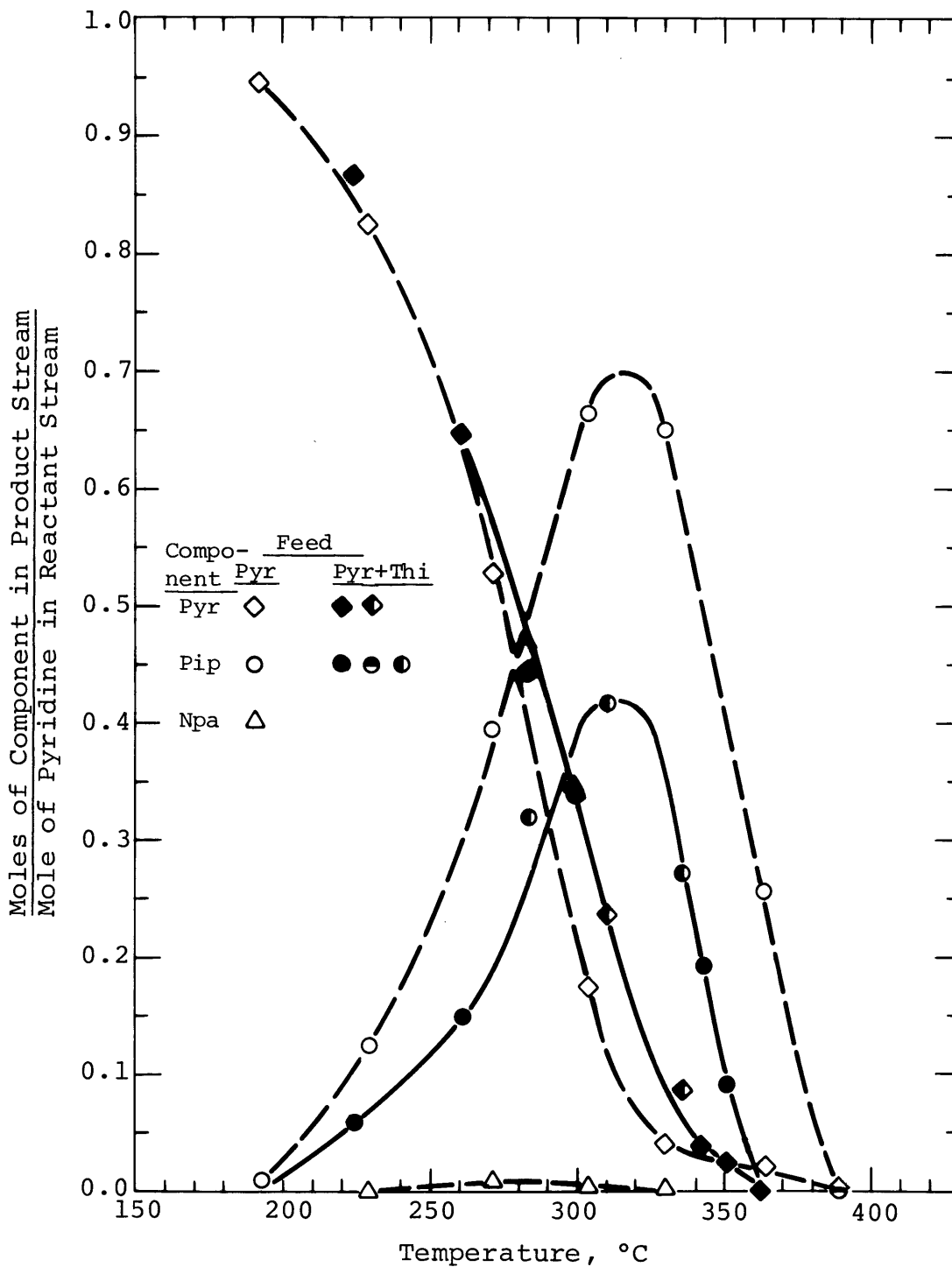


Figure 1-6: Product Distributions for Pyridine HDN For Pure Pyridine (93 torr partial press.) and Mixed Pyridine (93 torr)-Thiophene (93 torr) Feeds At a Total Pressure of 1000 psig. (Pip=piperidine, Npa=n-pentylamine)

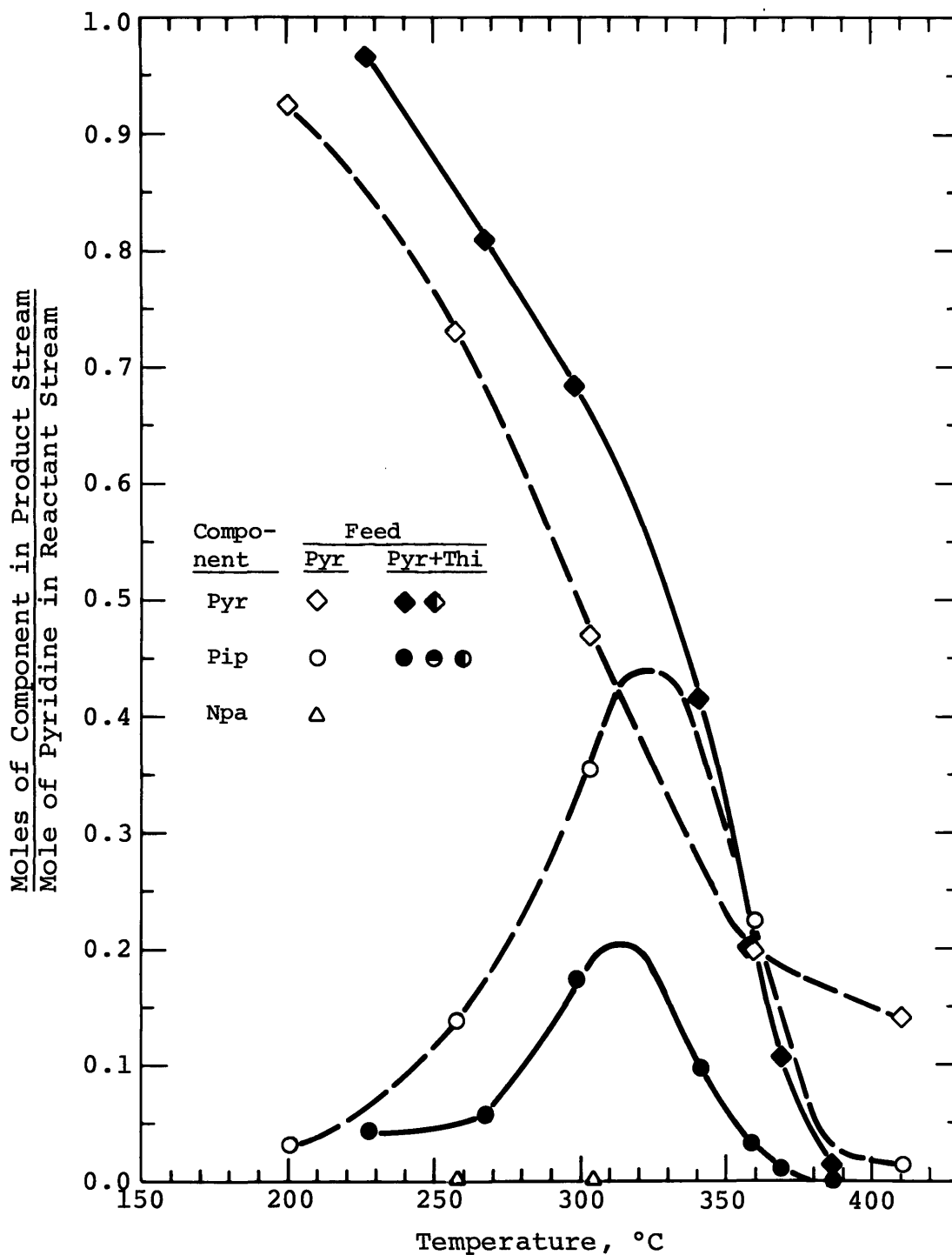


Figure 1-7: Product Distributions for Pyridine HDN For Pure Pyridine (93 torr partial press.) and Mixed Pyridine (93 torr)-Thiophene (93 torr) Feeds At a Total Pressure of 500 psig. (Pip=piperidine, Npa=n-pentylamine)

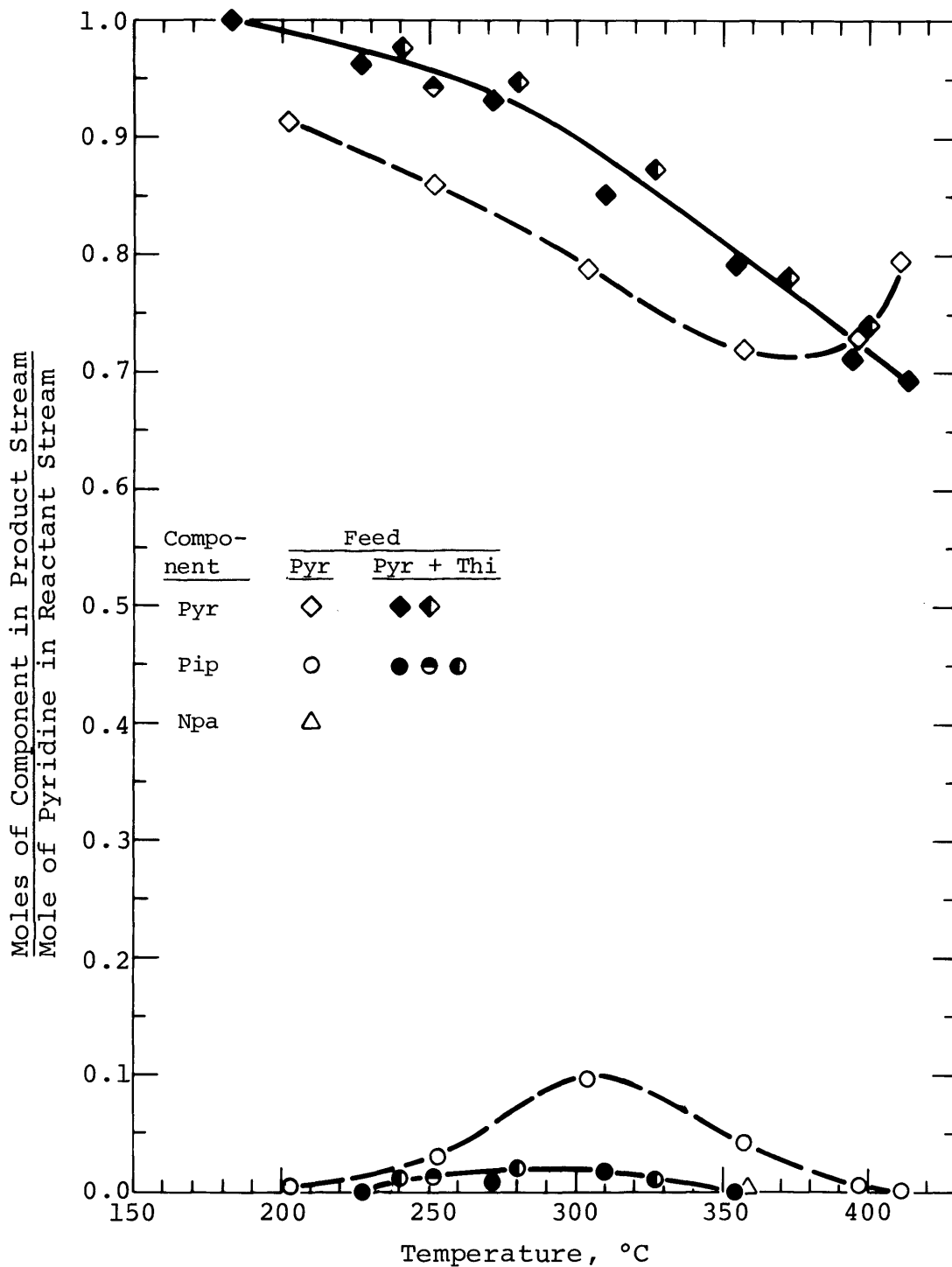


Figure 1-8 Product Distributions for Pyridine HDN For Pure Pyridine (93 torr partial press.) and Mixed Pyridine (93 torr)-Thiophene (93 torr) Feeds At a Total Pressure of 150 psig. (Pip=piperidine, Npa=n-pentylamine)

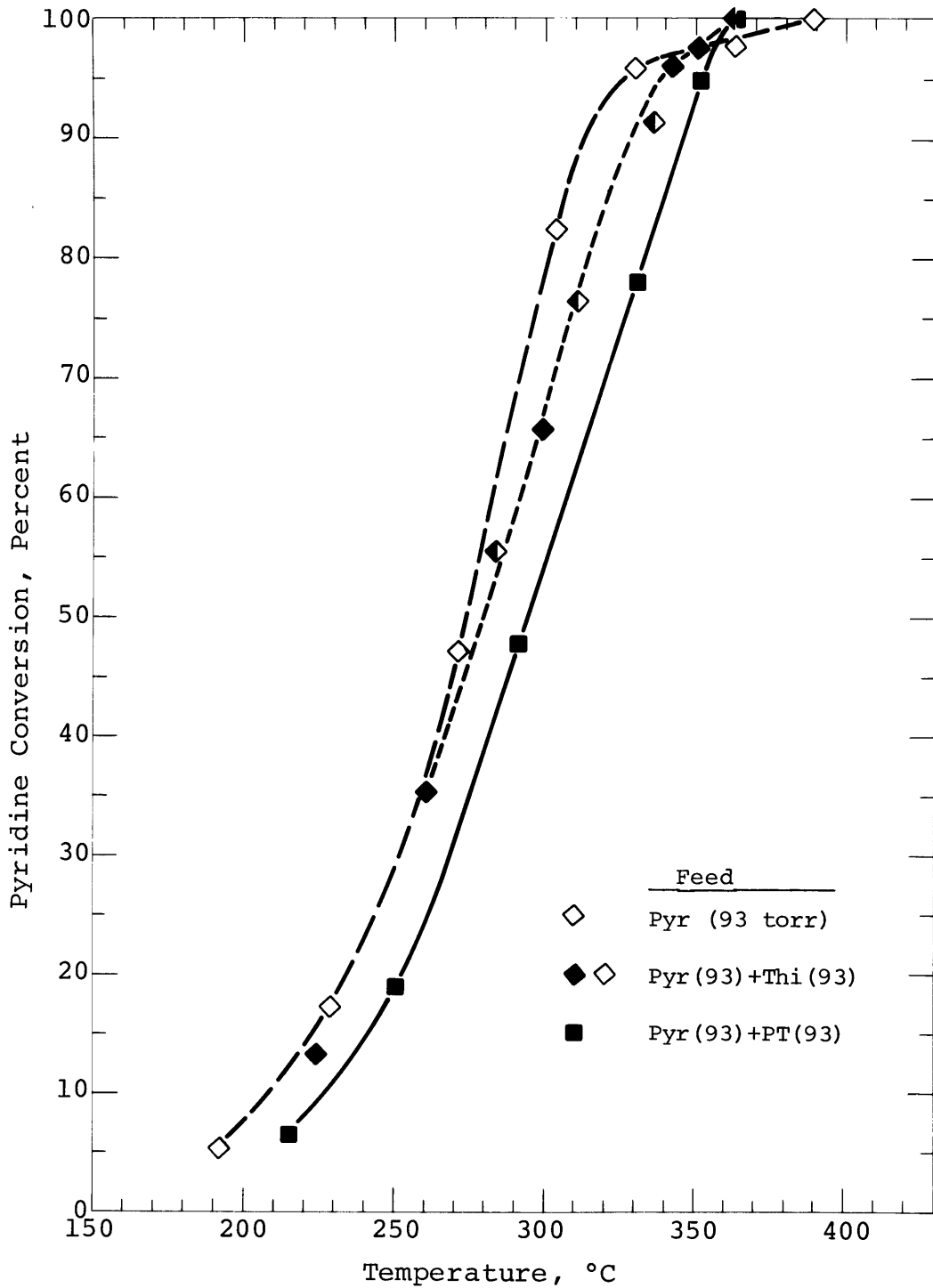


Figure 1-9: Comparison of the Effects of Hydrogen Sulfide and Thiophene on Pyridine Conversion at a Total Pressure of 1000 psig, using Propanethiol in Feed for Hydrogen Sulfide Generation.

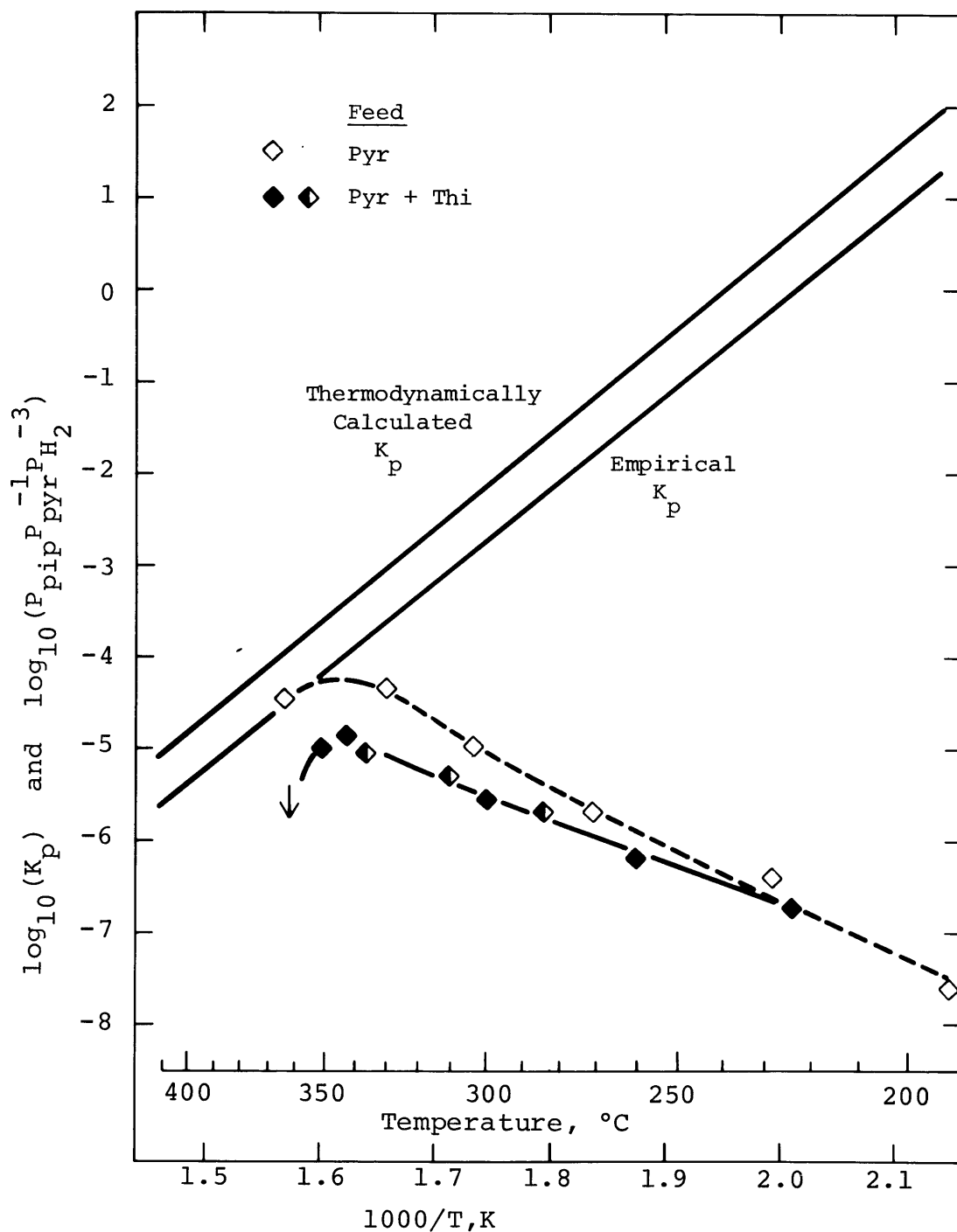


Figure 1-10: Comparison of the Experimental Values of The Equilibrium Constant Expression for Pyridine Hydrogenation with the Equilibrium Constant, for Pure-Pyridine and Pyridine-Thiophene Feeds at a Total Pressure of 1000 psig.

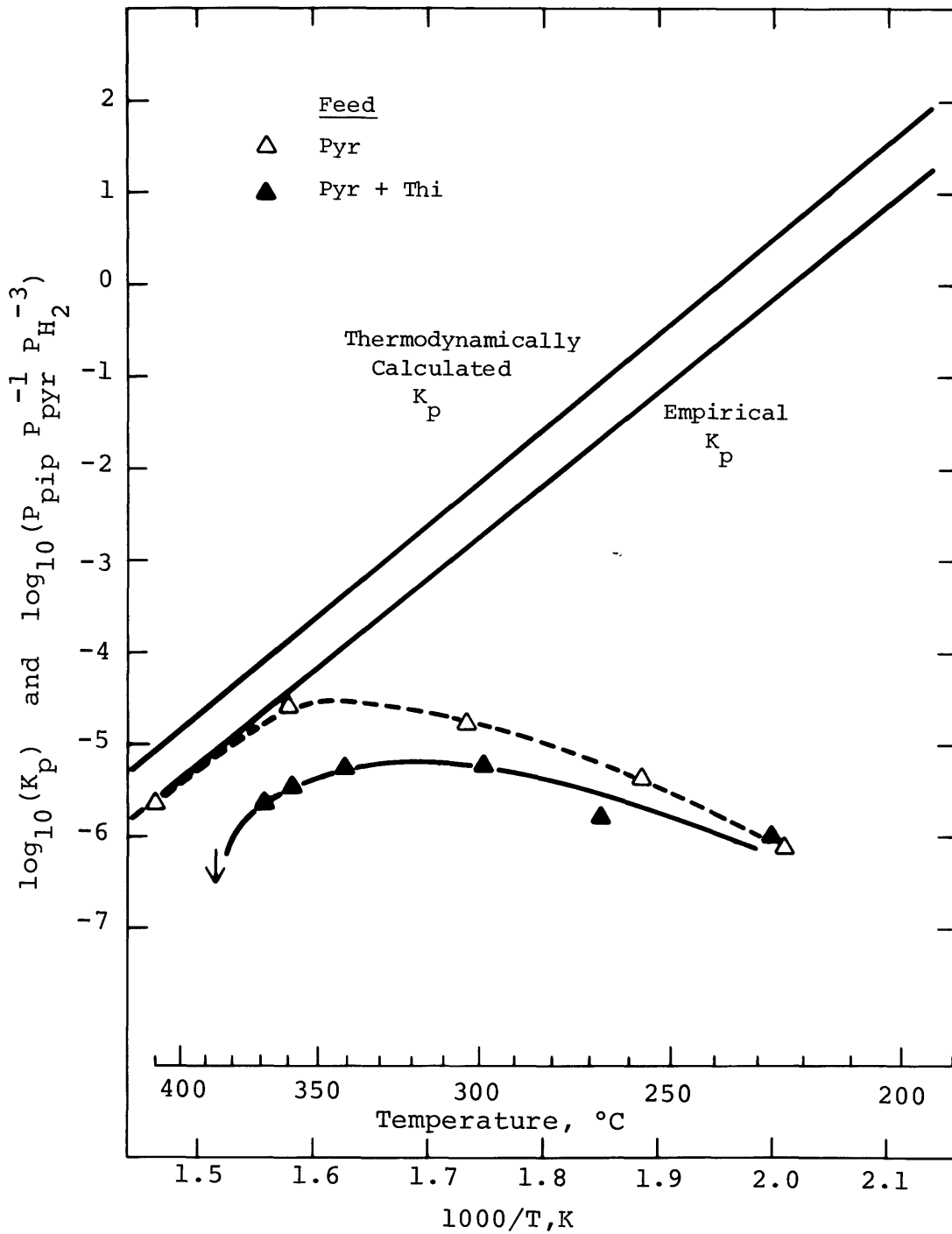


Figure 1-11: Comparison of the Experimental Values of The Equilibrium Constant Expression for Pyridine Hydrogenation with the Equilibrium Constant, for Pure-Pyridine and Pyridine-Thiophene Feeds at a Total Pressure of 500 psig.

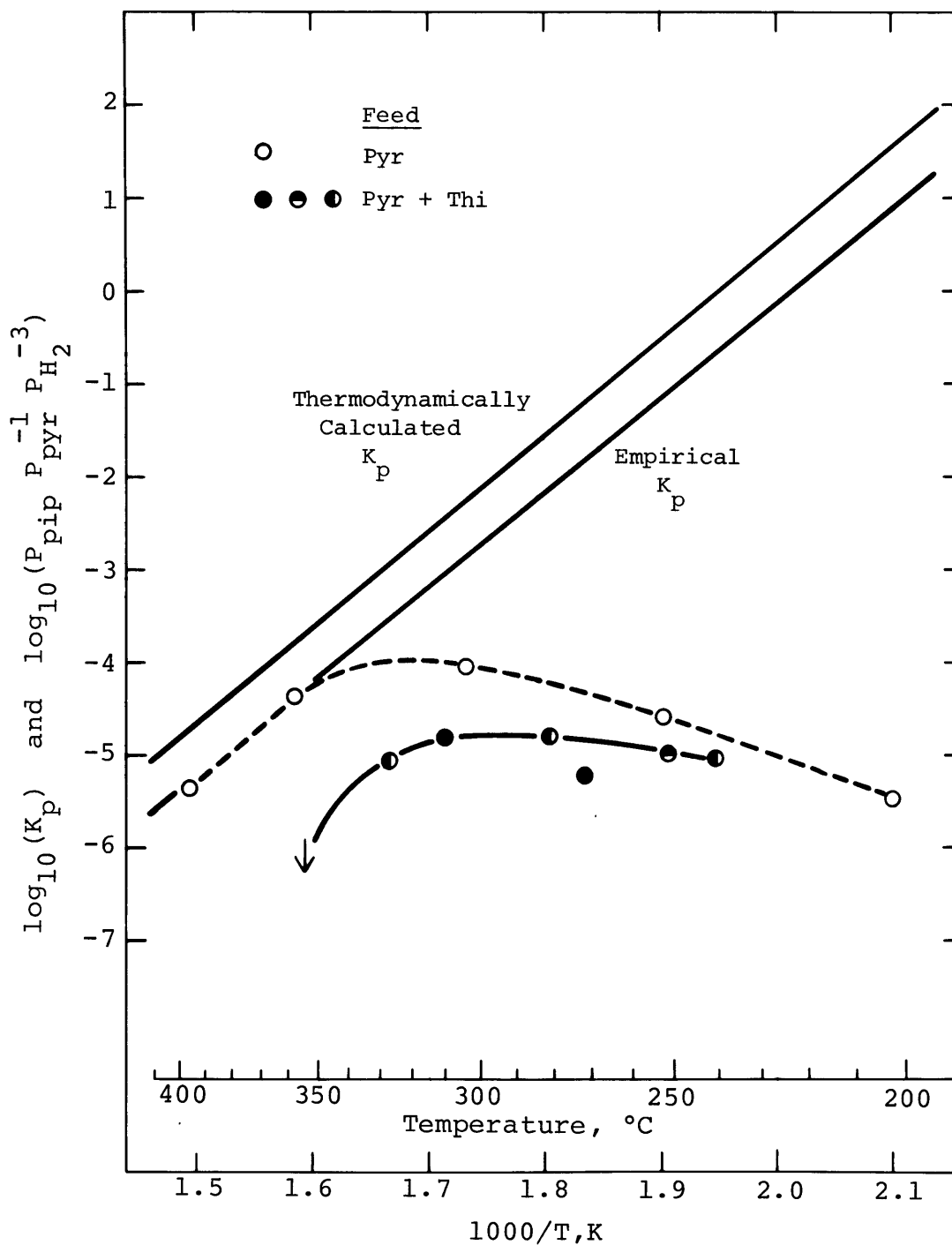


Figure 1-12: Comparison of the Experimental Values of The Equilibrium Constant Expression for Pyridine Hydrogenation with the Equilibrium Constant, for Pure-Pyridine and Pyridine-Thiophene Feeds at a Total Pressure of 150 psig.

Chapter II - Introduction

II.A. General Background

Conventional supplies of petroleum in the United States are decreasing, and in spite of the best efforts at energy conservation, the need for liquid hydrocarbon fuels will be substantial for a significant time into the future. Alternative sources of these fuels will be required to meet such needs as energy for transportation, where other forms of fuel have not yet proven feasible. Oil shale, coal, and tar sands may provide the needed energy, but the resulting liquid fuels will contain significant amounts of organic nitrogen compounds in addition to the organic sulfur compounds found in many current petroleum feedstocks.

The following table (Mezey et al., 1976) presents the total sulfur and nitrogen contents of several types of hydrocarbon-based fuels:

<u>Fuel</u>	<u>Total Sulfur, Weight percent</u>	<u>Total Nitrogen, Weight percent</u>
Petroleum Crude	0.1 - 5.	<<1.
Tar Sands Oil	0.2 - 6.3	<1.
Colorado Shale Oil	1.1	2.3
Coal Liquids, primary	<1.	>1.
Coal	0.4 - 13.	1. - 2.1

While there are variations among different sources of each type, it is clear that the presence of nitrogen in the

oils derived from oil shale and coal is significantly greater than that typically associated with conventional petroleum crudes. Thus the simultaneous removal of sulfur and nitrogen from a feedstock becomes of increasing importance as processes are developed to utilize these new energy sources.

In a recent review, Poulson (1975) puts nearly three decades of shale oil literature into perspective, citing evidence that some shale oils contain up to 61 percent by weight of heterocompounds, those containing nitrogen, sulfur, and oxygen. Thus it is generally not practical to clean such fuels by completely removing these compounds, as a significant amount of the fuel would not only be lost, but would also require some other type of disposal. In shale oils, whereas sulfur, mostly present as thiophenic compounds, is evenly distributed among the different boiling fractions of a shale oil, the nitrogen compounds concentrate in the heavier fractions. In one heavy shale-derived oil, this nitrogen was almost evenly divided between pyridines and pyrroles. The pyridinic-type molecules, in turn, consisted mostly (66 percent) of single-ring molecules, the rest being two-ring molecules of the same family. The thiophenic types of sulfur and pyridinic types of nitrogen are also found in the other liquid fuels

which have been studied to date (1976). There is thus great importance attached to the thiophenic types of sulfur and the pyridinic types of nitrogen in all types of liquid fuels.

Much of the current knowledge on the presence of sulfur and nitrogen compounds in the various fuels discussed here can be found in the review by Mezey (1976) and the papers of the American Chemical Society Symposium on Sulfur and Nitrogen in Coal and Oil Shale (1975).

One method for producing clean fuels from the organic nitrogen and sulfur molecules is through the hydrogenolysis of these heterocompounds. The hydrodenitrogenation and hydrodesulfurization reactions combine the partial or complete hydrogenation of the hydrocarbon portion of the molecules with the hydrogenation of the heteroatoms to ammonia and hydrogen sulfide. These latter two compounds are easily separated from the remaining hydrocarbon stream, leaving a clean fuel. Whereas hydrodesulfurization has been studied for many years due to the presence of sulfur in conventional petroleum sources, serious study of hydrodenitrogenation has only begun in the last decade, brought on by the recent significance of the alternative sources of hydrocarbon feedstocks.

The significance of the thiophenic and pyridinic

families of compounds has led to the use of thiophene and pyridine as model compounds in reaction studies. Their behavior can be considered representative of the lighter members of the families, and there are logical extensions of such studies to their more complex analogs.

II. B. Literature Review

II.B.1. Desulfurization and Denitrogenation Catalysts

Much research has been carried out recently on the structure and catalytic activity of desulfurization (and hence denitrogenation) catalysts, particularly CoMo/ Al₂O₃. Advanced instrumental techniques have been used to examine the roles of supports, usually alumina; the primary metallic component, such as molybdenum or tungsten; and the promoter, such as cobalt, nickel, zinc, or manganese. Prominent among these is a series of studies by Lipsch and Schuit (1969 a, b ;c). While most of the literature focuses on the desulfurization aspects of the catalysts, Sonnemans (1973a) examined the catalyst properties with a view toward hydrodenitrogenation.

Details of many of these studies were covered in a review by Schuit and Gates (1973), and were commented upon further by Richardson (Ben-Yaacov and Richardson, 1975). The sulfiding of the supported metal oxide catalysts is critical to the proper activation of these catalysts in actual use. A comprehensive review of the sulfided catalyst is the volume by Weisser and Landa (1973). Aspects of catalyst properties and performance directly related to the current study are included in the appropriate sections.

II.B.2. Thiophene Hydrodesulfurization

Hydrodesulfurization has been studied for many years, and a body of literature containing several thousand articles attests to the importance attached to this area of study. Two recent reviews, by Schuman and Shalit (1970) and Schuit and Gates (1973) together cover much of the latest chemical and engineering research, as well as industrial aspects, of hydrodesulfurization.

This review of thiophene hydrodesulfurization literature is focused on two major areas of consideration: first, the mechanism by which thiophene is desulfurized on sulfided catalysts such as $\text{CoMo}/\text{Al}_2\text{O}_3$ and $\text{NiMo}/\text{Al}_2\text{O}_3$; and second, the specific competitive adsorptions which are of significance in thiophene desulfurization, and thus in the formulation of a Langmuir-Hinshelwood kinetic rate expression.

One series of articles which addresses these questions in detail is by C.H. Amberg and co-workers. The adsorption and reaction characteristics of compounds involved in thiophene HDS were studied by Owens and Amberg (1961, 1962a) in pulse reactor studies on sulfided $\text{CoMo}/\text{Al}_2\text{O}_3$ and chromia catalysts. After sulfiding the catalyst, a flow of hydrogen over the bed was interrupted by pulses of compounds to be studied in various orders and combinations. The relative

retention times of the specific compounds and the changing distribution of reaction products with the various conditions gave good pictures of the relative strengths of adsorption and competitive reactivities of the compounds injected. Many aspects of the articles of this series will be covered here because of their applicability to this present work. Other viewpoints are also presented and compared.

II.B.2.a. Thiophene Adsorption

The way in which a thiophene molecule adsorbs onto the active site of a catalyst surface gives information about possible mechanisms for subsequent reaction. Three basic modes of thiophene adsorption have been proposed: single-point adsorption through the sulfur atom; two-point adsorption, either through the sulfur atom and an adjacent carbon atom, or through two carbon atoms; and flat adsorption of the thiophene ring, through four carbon atoms.

Nicholson (1962) studied thiophene adsorption on molybdenum sulfide, both unsupported and supported on gamma alumina; and on cobalt molybdate. From infrared spectrometric measurements of the adsorption bands produced by the adsorbed thiophene, he concluded that

the two-point (through two carbon atoms) and four-point adsorptions were present, under various conditions. Because none of the conditions were those of an active reaction, the most that one can conclude is that given Nicholson's interpretation of his spectra, these two forms were observed, and the single-point adsorption was not.

From an independent analysis of Nicholson's data, however, Lipsch and Schuit (1969c) concluded that the results supported the single-site adsorption of thiophene, rather than either of the other forms, particularly the four-point adsorption which Nicholson had proposed an active surface intermediate. They firmly assert that this adsorption is through the sulfur atom only, and continue to present a model where the thiophene is adsorbed through the sulfur atom onto an anion vacancy formed by the reduction of MoO_3 , with the sulfur atom bonded to the molybdenum atom. In a further refinement of this adsorption mechanism, for sulfided rather than unsulfided catalysts (Schuit and Gates, 1973), the same single-point adsorption was proposed to take place on an anion vacancy, again with the sulfur atom of the thiophene attached to the molybdenum atom.

Richardson (Ben-Yaacov and Richardson, 1975) arrived

at single-point adsorption for thiophene by assuming a molybdenum sulfide monolayer on the surface of the catalyst, and studying the amount of thiophene adsorbed. The adsorption here, however, was proposed to be between the sulfur atom of the thiophene and the sulfur atom of the molybdenum sulfide.

In a kinetic analysis of thiophene HDS, Roberts (1965) fitted a Langmuir-Hinshelwood rate expression to differential rate data. Models assuming two-point adsorption of the thiophene gave results far superior to those assuming single-point adsorption. Roberts' results represent the behavior of thiophene under actual reaction conditions, rather than under conditions which might permit instrumental analysis.

II.B.2.b. Hydrogen Adsorption

The competitive adsorption of hydrogen and thiophene has been proposed by Owens and Amberg (1961, 1962b). In studies near one atmosphere pressure, using both sulfided CoMo/Al₂O₃ and sulfided chromia, they found that the presence of hydrogen strongly affected the adsorption of thiophene. Much stronger adsorption of both thiophene and butene was observed using a nitrogen carrier gas than when using a hydrogen carrier. Further, thiophene adsorbed

under a nitrogen blanket could be partially removed by the injection of hydrogen.

Hydrogen itself also gave strong adsorption characteristics when adsorbed from a nitrogen stream. However, the presence of thiophene did not affect the hydrogen adsorption characteristics. In a reaction study, Owens and Amberg determined that the strongly-adsorbed hydrogen was unreactive for both thiophene desulfurization and butene hydrogenation.

From these studies, two types of hydrogen adsorption were proposed. First, a strong chemisorption of hydrogen competes with thiophene for catalytic desulfurization sites. This hydrogen is very strongly held, and is relatively inactive for both thiophene desulfurization and butene hydrogenation. A second type of adsorption is much weaker, and probably accounts for the hydrogen used in both types of reactions. As thiophene has no effect on this type of hydrogen adsorption, it would probably be on a type of site used exclusively for this hydrogen transfer from the gas phase to the adsorbed reactant state.

In direct contrast to the above results, Lipsch and Schuit (1969c), in a pulse reactor study using reduced Co-Mo/Al₂O₃ catalyst, found hydrogen adsorption to have no effect on the adsorption of thiophene. It is difficult to believe that the catalyst sulfiding alone could produce such divergent results, and the question must be left un-

resolved but not forgotten.

II.B.2.c. Hydrogen Sulfide Adsorption

The nature of the adsorption of hydrogen sulfide is extremely important in the analysis of thiophene HDS, as its ability to compete with thiophene for active catalytic sites, and its formation as a reaction product, combine to make desulfurization more difficult. The general inhibition by H_2S is well documented; nearly three decades ago Griffith et al. (1948) quantitatively described a reversible decrease in thiophene HDS by H_2S on nickel and molybdenum sulfides. Particularly-probing studies by Owens and Amberg (1961) and Desikan and Amberg (1964) determined greatly-differing levels of effects on thiophene desulfurization and butene hydrogenation. By studying these two reactions in a stream of hydrogen over a sulfided $CoMo/Al_2O_3$ catalyst, in some cases pretreating the catalyst with pulses of H_2S . The results of the H_2S pretreatment were an inhibition of thiophene desulfurization by a factor of approximately two, and an inhibition of butene hydrogenation ten times that of the thiophene reaction.

In spite of this large butene reaction hydrogenation, inhibition, however, there was no inhibition of butene cis-trans isomerization or double bond shift reactions; the reaction product mixtures reached thermodynamic equilib-

brium in all cases, whether or not H_2S was present. Further, the complete reaction of butadiene to butene was observed in all cases. These observations led the researchers to suggest the presence of two types of catalytic sites, which will be covered in the later mechanism discussion.

A further significant observation by the same group was a distinctly lower inhibition of the thiophene HDS when the H_2S present was a product of the HDS of thiophene, when contrasted with the situation where the H_2S had been preadsorbed on the catalyst before the injection of thiophene. This indicated that while H_2S does indeed adsorb strongly on the active sites, it could not preferentially adsorb on such sites in the presence of thiophene. It is this type of adsorption study, which places compounds in direct competition, that gives the best idea whether specific adsorptions would be of significance in the denominator inhibition terms of Langmuir-Hinshelwood kinetic expressions.

The competitive adsorption of hydrogen sulfide and thiophene during reaction over a $CoMo/Al_2O_3$ catalyst was studied by G.W. Roberts (Roberts, 1965; Satterfield and Roberts, 1968) in a continuous-flow differential reactor using thiophene, and thiophene- H_2S feeds. Roberts evaluated the resulting differential reaction data by fitting Langmuir-Hinshelwood kinetic rate expressions using re-

gression analysis. The constants determined for his best model gave adsorptions of thiophene and H_2S of the same general strength. This implied a strong competition for active sites by H_2S .

Another study which accounted for the competitive adsorption of hydrogen sulfide by using Langmuir-Hinshelwood kinetics was carried out by Metcalfe (1969). Using a CoMo catalyst supported on silica and focusing on the general reduction of the sulfur level of a petroleum feedstock, strong competitive effects were found to correlate well with a simplified model of this same kinetic form.

Using a sulfur-containing light cycle oil, Frye and Mosby (1967) carried the amount of H_2S fed with the mixed liquid-vapor feed for reaction over $CoMo/Al_2O_3$. Although the trickle-bed operation was significantly different from the previous gas-phase reactions discussed, it is interesting to note that in correlating the results with competitive-adsorption terms they found the term for H_2S to be much more significant than those for the sulfur compounds in the feed, even to the extent that the feed terms could be neglected.

II.B.2.d. Hydrocarbon Adsorption

The adsorption of alkanes and alkenes was studied by

Owens and Amberg (1961, 1962a), using the techniques previously described, for the purpose of determining the competitive effects of the C₄ hydrocarbon reaction products of the thiophene HDS. From comparisons of relative retention times, the adsorption of butene was found to be weaker by a factor of 10 to 15 than that of thiophene. By examining the inhibition of thiophene HDS by simultaneous injection of this compound and other hydrocarbons with thiophene several other conclusions were reached. Hexene and cyclohexene had very little effect, less than five percent, on the conversion of thiophene when present in equimolar quantities. Increasing the relative amount of hexene by a factor of three caused a 21 percent decrease in conversion. As the intent was to determine the effects of product butene on the adsorption of thiophene, the equimolar results are the most relevant, and indicate a very small effect. Further work by Owens and Amberg (1962b), on sulfided chromia showed similar results for hexene and cyclohexene.

While Kirsch, Shalit and Heinemann (1959) accepted olefin inhibition of desulfurization to be a solid basis for further assumptions, Owens and Amberg commented that the earlier work of Kirsch, Heinemann and Stevenson (57) on which this assumption was based required an eight-to-one molar ratio of heptene to thiophene in a heptane feed to

produce an 18 percent decrease in thiophene conversion on CoMo/Al₂O₃. A significant difference between the work of Kirsch and that of Amberg is that where Amberg used pulses of compounds in a microreactor, Kirsch used a heptane reactor feed to which was added a small percentage of thiophene.

Owens and Amberg(1961) carried out further studies on sulfided CoMo/Al₂O₃ using the saturated analogs of the alkenes mentioned above, allowing direct comparison between the olefins and paraffins. Whereas a slight inhibition was shown by hexene and cyclohexene, no effect on thiophene HDS was produced by hexane or cyclohexane. On sulfided chromia (Owens and Amberg, 1962b) there was again a negligible effect of the addition of equimolar amounts of cyclohexane. They suggested, however, that in the desulfurization of a petroleum feedstock with many light, cracked hydrocarbons, there might be significant inhibition.

In a study of the desulfurization of several sulfur compounds in a heptane feedstock, Phillipson (1971) found a significant inhibition by the large concentration of heptane, and proposed the addition of competitive adsorption terms for hydrocarbons in kinetic rate expressions.

From these studies one can conclude that in the case of pure model compounds, there would not be a large enough concentration of hydrocarbons, resulting only from thio-

hene desulfurization, for example, to cause a significant inhibition of the reaction. However, for models concerned with commercial feedstocks, where there is a small percentage of thiophene in a predominantly-hydrocarbon reaction mixture, competitive adsorption of hydrocarbons is indeed significant.

A similar relationship may hold for the presence of aromatics. Owens and Amberg (1961) reported that benzene had no effect on the rate of thiophene HDS, even though it was known to adsorb, while Frye and Mosby (1967) reported that for trickle-bed desulfurization of a light cycle oil, there was a significant competitive effect of aromatics on the removal of sulfur compounds.

II.B.2.e. Adsorption of Basic Nitrogen Compounds

The competitive adsorption of basic nitrogen compounds causes a serious inhibition of the desulfurization of thiophene. An examination of this effect was carried out by Desikan and Amberg (1964). Before attempting adsorption studies, a CoMo/Al₂O₃ catalyst was treated with a strong alkali, and was then found to have virtually no activity for either thiophene HDS or butene hydrogenation. This indicated the acidic nature the catalytic sites responsible for both types of reactions. By examining both the

shapes of pyridine desorption peaks from the catalyst and the effects of the presence of pyridine on thiophene HDS and butane hydrogenation, the researchers concluded that pyridine was more-strongly held on the butane reaction sites, although weaker adsorption on the thiophene sites also took place. That some desulfurization took place on the stronger sites was concluded from the rapid recovery of much of the thiophene reaction, followed by subsequent slow further increases, after poisoning by pyridine. Further details of their conclusions are covered with the mechanistic considerations.

Kirsch et al(1959) suggested the addition of pyridine to sulfur-containing feedstocks to selectively inhibit the saturation of oefins, while maintaining a significant percentage of the thiophene desulfurization activity on a sulfided CoMo catalyst. This proposition was based on an early two-site theory and laboratory tests using synthetic and natural petroleum feedstocks.

Lipsch and Schuit (1969c), using pulse techniques on reduced CoMo/Al₂O₃ catalysts found two types of pyridine adsorption. First, extremely strong, irreversible adsorption occurred on sites which apparently had no affinity for thiophene; thiophene and butene adsorption were not affected by this type of pyridine attachment. Second, a weak, reversible adsorption of pyridine was seen on a second

type of site on which thiophene and butene both adsorbed. This latter type of pyridine adsorption occurred only after the first class of sites was completely filled, and not until this second type began was there any effect on the adsorption of thiophene or butene. Further consideration of these two types of sites is covered in the mechanistic consideration discussion.

Mayer (Satterfield et al, 1975) found a significant decrease in the thiophene reaction in the presence of pyridine, and attributed this to competitive adsorption by the pyridine on the active catalytic sites.

II.B.2.f. Reaction Products of Thiophene HDS

The identification of reaction intermediates is critical in the determination of a complex reaction path. Amberg et al. have studied such products of thiophene desulfurization over sulfided CoMo/Al₂O₃ and sulfided chromia. Many details of these investigations are included in the series of articles, but two aspects are of particular significance in the determination of a reaction sequence: the searches for butadiene and tetrahydrothiophene.

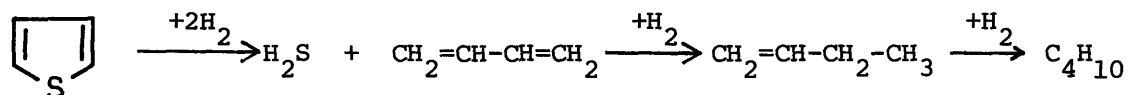
Butadiene was detected (Kolboe, 1969) in the gas phase over the sulfided chromia catalyst, as were the three butene isomers. Using the sulfided CoMo/Al₂O₃, however, small

amounts of butadiene were found with the butenes (Kolboe and Amberg, 1966); the rate of butadiene hydrogenation was separately determined to be very rapid on this catalyst. Its absence thus indicated a high conversion to butenes, as opposed to a distinctly different reaction path.

Tetrahydrothiophene and butylmercaptan were not detected as reaction products over either sulfided CoMo/Al₂O₃ or chromia (Owens and Amberg, 1961, 1962a). These and subsequent observations led Kolbe (1969) to decide that no organo-sulfur compounds were gas-phase intermediates in the reaction of thiophene. Neither did his proposed mechanism, discussed later, incorporate an adsorbed saturated sulfur compound.

II.B.2.g. Thiophene HDS Reaction Mechanism

From the examination of thiophene HDS reaction products, Amberg and his co-workers determined that thiophene was first desulfurized to butadiene and hydrogen sulfide, and the butadiene then saturated to butene and then butane:



While mechanistic considerations permeate the series of articles, a complete model is formulated in the paper by Desikan and Amberg (1964) with additional suggestions

by Kolboe (1969). They proposed a two-site model for desulfurization of thiophene, with one class of sites strongly acidic, and the other weakly acidic. The stronger sites, with a high affinity for electrons, will adsorb olefins, particularly butene for the case of thiophene HDS, and then saturate them. A small amount of thiophene desulfurization can also take place on this class of sites. These sites also strongly adsorb thiophene, hydrogen sulfide, and pyridine; and as a result are easily poisoned.

A second class of sites, weakly acidic, is responsible for most of the thiophene desulfurization and some of the butane hydrogenation. These sites, due to their lower affinity for electrons, are more resistant to poisoning by bases.

The reaction of a thiophene molecule would take place on the weaker sites, where it would be adsorbed and desulfurize, according to one of three probable paths. First, hydrogen could be added to the carbon-sulfur bonds, freeing H_2S . Second, by removing SH, an adsorbed carbonium ion would be formed. Third, as speculatively proposed in a later article in the series (Kolboe, 1969), H_2S could be removed as in the dehydration of an alcohol, and a diacetylene produced.

The butadiene (or butadiyne in the third case) is then almost completely hydrogenated on this desulfurization

site to butene. Butene requires the stronger sites for further saturation, and must migrate in the gas phase to a suitable site for readsorption and further hydrogenation.

For that small portion of the thiophene hydrodesulfurization which takes place on the stronger sites, the butadiene will saturate completely to butane on that site before desorption.

Another two-site theory was proposed by Lipsch and Schuit (1969c). Here type I sites are anion vacancies which adsorb and react both thiophene and butene. Hydrogen sulfide also adsorbs on these sites, and competes with both reactants, having a greater effect on the more weakly-held butene. Pyridine adsorption can take place on these sites, but only when all of the second type are filled. Type II sites appear similar to those of free alumina, based on the irreversible adsorption behavior of pyridine on these sites. The larger amount of pyridine which can adsorb on the type II sites would indicate a surface with much alumina uncovered by the metals. In the above reference and in a subsequent expansion of the model (Schuit and Gates, 1973), detailed crystallographic descriptions of the catalyst and its proposed active sites are given.

There is a significant difference between the two-site models of Amberg, and Lipsch and Schuit. The former model

has one type of sites on which thiophene desulfurization predominates, and a second type which is responsible for butene hydrogenation. While each reaction may take place to a limited extent on the other type of site, this distinction is quite clear. One piece of evidence in support of this dual nature is the greatly different effect of the addition of pyridine on the reactions of thiophene and butene. Lipsch and Schuit, on the other hand, postulated that thiophene desulfurization and butene hydrogenation take place on the same type of site, and as evidence show that pyridine affected the two reactions similarly. The second type of site of their model was not a reaction site, but a pyridine adsorption site. One major difference between the two studies was the use by Amberg of sulfided catalysts, and the use by Lipsch and Schuit of unsulfided catalysts prereduced in hydrogen. In later works, Schuit (deBeer et al, 1972, 1974) indicates that, contrary to some of their previous findings, sulfided catalysts did indeed have greater activities than unsulfided ones. Further refinement of the Lipsch and Schuit model, however (Schuit and Gates, 1973) indicates that the basic premise remains intact.

Richardson (Ben-Yaacov and Richardson, 1975) proposed a two-site model similar to that of Schuit. The active catalytic sites, however, were molybdenum sulfide. A

second type consisting of the alumina surface adsorbed thiophene but was not catalytically active.

In earlier work in this laboratory, J.F. Mayer (Mayer, 1974; Satterfield et al., 1975b) studied the hydrodesulfurization of thiophene over several sulfided catalysts in a continuous flow packed bed reactor at pressures up to 11 atmospheres. From comparison of experiments using pure-thiophene feeds with those using mixed thiophene-pyridine feeds, a model was proposed with two types of thiophene desulfurization sites. One type, strongly acidic and very active, was responsible for most of the desulfurization in the absence of a poison such as pyridine, but was quite susceptible to deactivation by strong bases. A second type of site was less acidic and less active, but more resistant to poisoning. In the presence of pyridine, this type of site was considered to be responsible for most of the desulfurization activity.

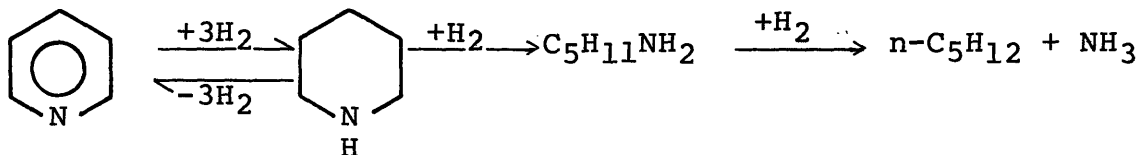
This model differed from that of Amberg in that in Mayer's work the thiophene desulfurization was proposed to take place primarily on the stronger, more-easily-poisoned sites, with a lesser amount of thiophene desulfurization being carried out on the weaker, more resistant sites. Amberg, on the other hand, proposed that most of the thiophene desulfurization took place on the less active, less-easily-poisoned sites, and that the

more active, more-easily-poisoned sites were primarily responsible for butene hydrogenation.

II.B.3. Pyridine Hydrodenitrogenation

II.B.3.a. Pyridine HDN: Mechanism, Kinetics, and Compound Adsorptions

McIlvried (1971) studied the HDN of pyridine on a sulfided NiCoMo/Al₂O₃ catalyst at pressures from 750 to 1500 psig, at a temperature of 315°C. He proposed a stepwise mechanism which first saturated pyridine to piperidine. The piperidine then underwent hydrogenolysis to n-pentylamine, followed by the hydrogenolysis of the alkyl amine to n-pentane and ammonia.



This mechanism differs significantly from that for thiophene HDS, in that whereas thiophene was first desulfurized to unsaturated hydrocarbons, the pyridine is first saturated, and then the nitrogen atom is removed in subsequent steps. At the single temperature studied, McIlvried observed the rapid hydrogenation of pyridine to piperidine followed by the slow hydrogenolysis of piperidine.

The hydrogenolysis of the pentylamine was also rapid relative to the piperidine disappearance step.

McIlvried used Langmuir-Hinshelwood kinetics to model his data, first assuming equal adsorption of the nitrogen compounds pyridine, piperidine, and ammonia. This did not adequately account for the increased inhibition of the reaction rate with higher conversions. A model with an adsorption term for only the ammonia gave better correlations with his experimental data. For piperidine hydrogenolysis, which he studied independently, a model assuming equal adsorption of ammonia and piperidine gave a good correlation of the data. From these results, McIlvried inferred that on sites where pyridine was hydrogenated, only ammonia caused serious adsorption competition. On separate sites for piperidine hydrogenolysis, he proposed equal adsorption of all nitrogen components.

Sonnemans accepted the McIlvried stepwise mechanism for pyridine HDN, and studied each step independently. Sonnemans et al (1973b) studied pyridine hydrogenation over an unsulfied CoMo/Al₂O₃ catalyst, and found the approximation of the equal adsorption of all nitrogen compounds on the catalytic sites to give a good correlation in a Langmuir-Hinshelwood kinetic model. The denominator adsorption terms were significantly greater than one, permitting dropping of the 1 term and incorporating the

lumped adsorption terms into a pseudo-first-order rate constant.

The investigation of the hydrogenolysis of piperidine (Sonnemans et al., 1974) showed that in addition to the reaction products n-pentane and ammonia, N-pentylpiperidine was formed. The reactions of n-pentylamine in hydrogen were complex (Sonnemans and Mars, 1974), yielding a wide variety of products. However, it appears that not all the types of products found in the reaction of the pure compound would be present in significant quantities in the product stream of a pyridine HDN reaction using sulfided catalysts at high-pressure reaction conditions.

Sonnemans (1973b) also studied the adsorption of pyridine, piperidine, and ammonia on $\text{MoO}_3/\text{Al}_2\text{O}_3$ catalysts and on the alumina support alone. On the supported metal oxide, he found piperidine to adsorb approximately six times as strongly as pyridine; and ammonia, about one-fourth as strongly as pyridine. However, from studies on the alumina support, it was evident that the compounds indiscriminately adsorbed on both active sites and non-active support areas, precluding the determination of the relative adsorptions of compounds on the active sites. It is interesting that in spite of reporting these detailed adsorption measurements, the final kinetic expression of Sonnemans contained the simplifying assumptions described

above. The adsorption of hydrogen was shown not to interfere at one atmosphere pressure with the adsorption of ammonia and pyridine. Also, the presence of nitrogen bases had negligible effects on the adsorption of hydrogen.

Goudriaan (1974) studied pyridine HDN over both sulfided and unsulfided $\text{CoMo/Al}_2\text{O}_3$ catalysts, and performed a detailed kinetic analysis. Inherent in Goudriaan's Langmuir-Hinshelwood model was the assumption of equal adsorption strengths for pyridine, piperidine, and ammonia; and the reduction to the same pseudo-first-order model of Sonnemans. By observing the different effects of the concentration of ammonia on the rates of pyridine hydrogenation and piperidine hydrogenolysis on the unsulfided catalyst, Goudriaan inferred that the two steps took place on different active sites. On the pyridine hydrogenation sites, ammonia adsorbed five times more strongly than pyridine or piperidine. On the sites for piperidine hydrogenolysis, however, all three compounds adsorbed about equally strongly.

The mode of adsorption of the pyridine molecule is proposed to be either vertical (Goudriaan, 1974; citing unpublished data); or flat (Aboul-Gheit and Abdou, 1973, citing the work of Balandin, 1964). The former mechanism is tacitly assumed in most publications, and from the nature of the acidic catalytic sites seems most probable.

II.B.3.b. Pyridine HDN: Equilibrium Limitation

An equilibrium limitation on pure-pyridine HDN was suggested by Mayer (Satterfield et al., 1975). In a study at a total pressure of 150 psig over sulfided NiMo/Al₂O₃, CoMo/Al₂O₃, and NiW/Al₂O₃ catalysts, pyridine conversion increased with increasing temperature, until above 350°C the rate of increase slowed, finally resulting in decreases in conversion as temperatures approached 400°C. To account for this, a thermodynamic limitation was proposed on the first step of the pyridine HDN reaction, the hydrogenation of pyridine to piperidine. If the hydrogenolysis of piperidine were to become rate limiting above 350°C, then piperidine could accumulate in the reaction stream. If the forward and reverse hydrogenation reactions were relatively rapid, then the pyridine and piperidine could reach equilibrium. Because the equilibrium for this reaction shifts to favor the reactant pyridine at these higher temperatures, this could effectively slow the rate of pyridine conversion.

In further work at total pressures of 150 psig, Satterfield and Cocchetto (1975) examined the composition of the pure-pyridine feed HDN reaction product mixture, and found it to approach its equilibrium composition as the temperature approached 400°C.

Goudriaan (1974), in studies using sulfided and un-

sulfided CoMo/Al₂O₃ catalysts, showed the hydrogenation of pyridine to be equilibrium limited at 400°C and 80 bars pressure.

II.B.3.c. Pyridine Hydrogenation: Equilibrium Constant Determination

An important part of this study is the examination of a possible thermodynamic limitation on the HDN of pyridine. This requires a reliable value of the equilibrium constant for pyridine saturation of piperidine. This equilibrium constant is available through two independent routes: directly from empirical equilibrium data, and by calculation from data for the free energies of formation of the reactants and products.

Free energies of formation are available for pyridine (McCullough et al., 1957) and piperidine (Scott, 1971), allowing calculation of the reaction equilibrium constant as a function of temperature (the free energy data used, principles of calculation, and sample calculations are included in the Appendix). The data use as a standard reference state the pure compound as an ideal gas, with the attendant one atmosphere standard pressure. On the basis of comparison with several published sets of empirical equilibrium data for this reaction, including his own,

Goudriaan (1974) determined that the data of McCullough was superior to earlier data by Kline and Turkevitch (1944). This type of revision of widely-used thermodynamic values is common, and illustrates the fact that such quantities as free energies of formation are themselves based on experimental data and are not absolute standards.

A detailed review of the techniques and results of investigators empirically determining the equilibrium constant is presented by Goudriaan (1974) in the introduction to his own experimental determination. Goudriaan's own careful study covered temperatures from 150°C to 350°C, and pressures from one to 80 bars. A continuous flow packed bed reactor utilized catalysts chosen for their activity and selectivity toward the pyridine-piperidine reaction. By passing a constant-composition mixture of pyridine and piperidine through the reactor with varying partial pressures of hydrogen at different temperatures, it was determined at which hydrogen partial pressures the hydrogenation of pyridine and dehydrogenation of piperidine took place. Interpolating to the point of no reaction gave a value for the equilibrium composition. Using the results of his kinetic analysis, this interpolated value was refined slightly to eliminate effects which side reactions might have on the equilibrium constant. The final result relating the equilibrium constant to temperature

is presented in the Appendix. This result agreed reasonably well with the equilibrium constant calculated from the thermodynamic data of McCullough, and Scott.

II.B.3.d. Pyridine HDN: Effects of Sulfur Compounds

In a study of the simultaneous hydrogenolysis of pyridine and thiophene at a total reaction pressure of 150 psig, thiophene was shown to inhibit pyridine conversion under certain reaction conditions, while enhancing it under others (Satterfield et al., 1975). The inhibitions of pyridine conversion were found at temperatures where the hydrogenation of pyridine was assumed to be rate limiting, due to competition for active catalytic sites between the thiophene and pyridine. At temperatures between 350° and 400°C, where the hydrogenolysis of piperidine was taken as the rate limiting step, thiophene enhanced the conversion of pyridine, probably due to the effects of the thiophene reaction product hydrogen sulfide on the catalyst. Hydrogen sulfide could both help keep the catalyst in a more fully-sulfided state, and increase the acidic character of the active sites.

Goudriaan (1974; Goudriaan et al., 1973) determined that the presence of hydrogen sulfide enhanced the hydrogenation of pyridine, which he attributed to the enhance-

ment of the acidic nature of the catalyst by proton donation by the hydrogen sulfide. In the earlier reference, Goudriaan was willing to attribute some enhancement to the maintainance of the sulfided state of the catalyst. The later reference assumed active sites to be void of sulfur (although adjacent to sulfur-containing sites), and assumed that presence of hydrogen sulfide would actually inhibit hydrogenation via competitive adsorption on these sites. In concidering such conclusions as this last one, it should be remembered that there are still many different proposals for the nature of the active sites, and that this conclusion was specific to the particular model assumed.

II.C. Thermodynamics of Thiophene HDS and Pyridine HDN

Figures 2-1 and 2-2 present the equilibrium constants for thiophene HDS and pyridine HDN reactions as a function of the inverse absolute reactor temperature. These were calculated from the free energy of formation data included in the Appendix.

The figures show that for both thiophene HDS and pyridine HDN, the overall hydrogenolysis reactions (labeled 1 on each figure) are thermodynamically favorable ($K_p > 1$ or $\log_{10}(K_p) > 0$) up to temperatures of nearly 600°C and 500°C, respectively. Examining the stepwise hydrogenolysis of each reaction according to the accepted mechanisms discussed in the literature review, however, shows that the first steps of the reactions, the hydrogenation of pyridine to piperidine, and the desulfurization of thiophene to butadiene and hydrogen sulfide, become thermodynamically unfavorable at approximately 250°C and 175°C, respectively. For thiophene desulfurization, in particular, this is a mild trend, and should not affect the overall rate of reaction unless some subsequent reaction step becomes rate limiting. For the pyridine hydrogenation to piperidine the effect is stronger. For this step, two lines are shown: No. 2, which was calculated from the free energy of formation data; and No. 2a, which was

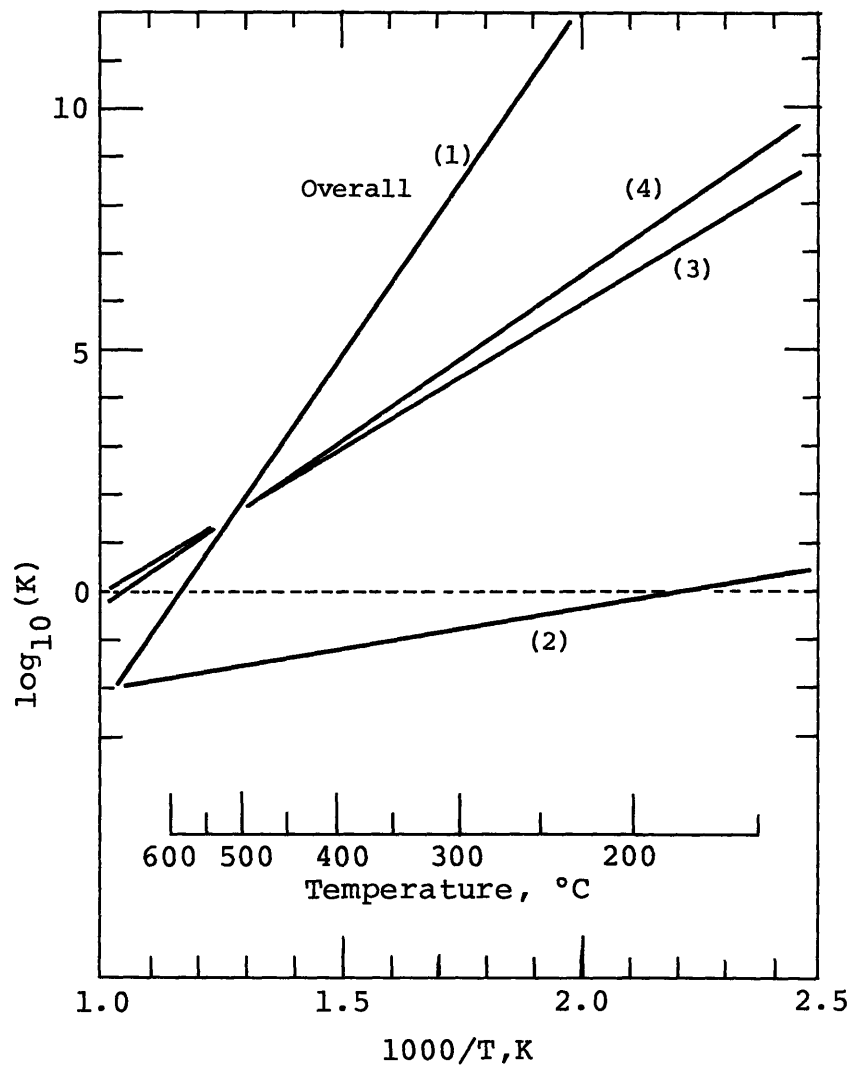
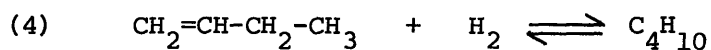
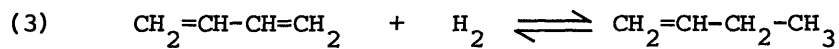
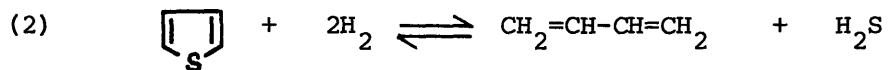
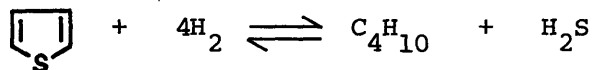


Figure 2-1: Thermodynamics of Thiophene HDS

(1) Overall reaction



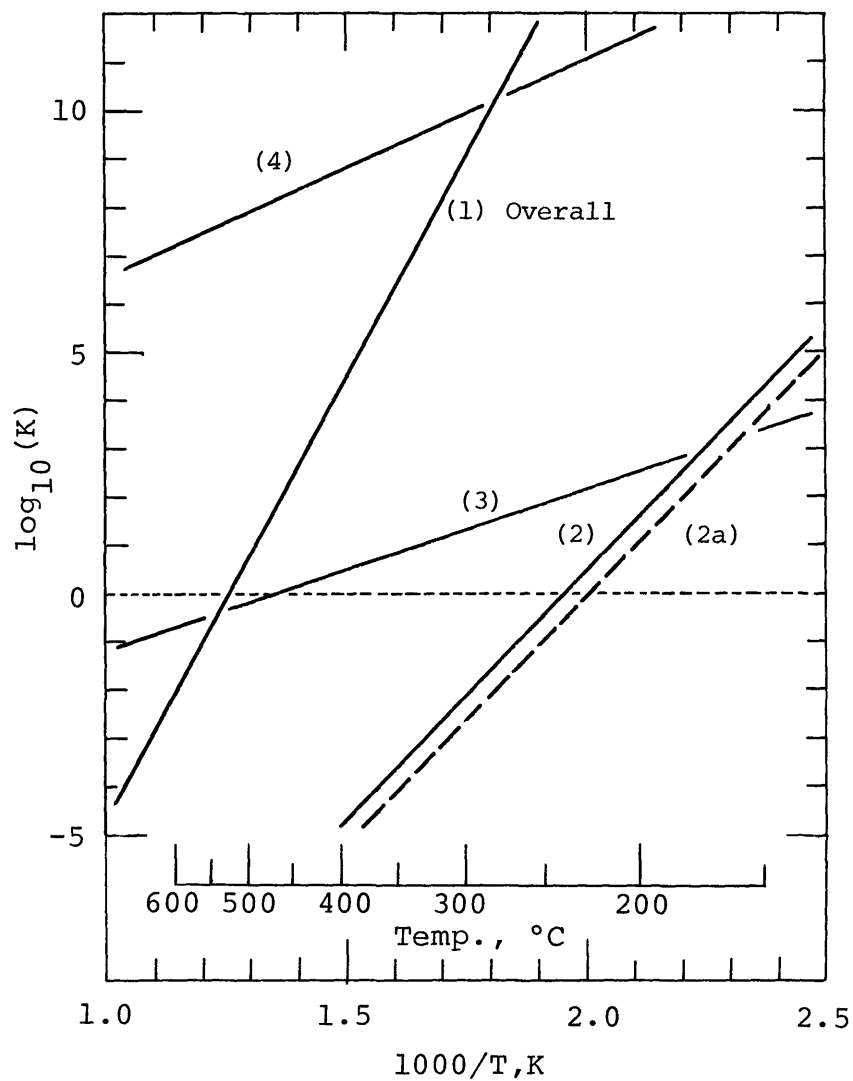
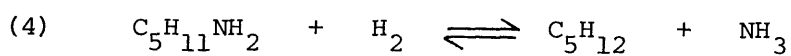
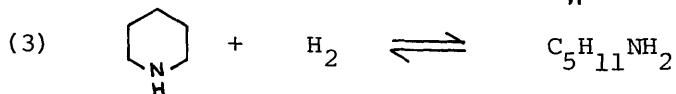
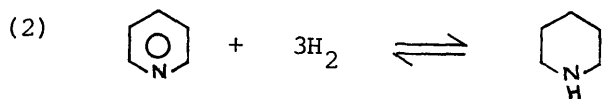
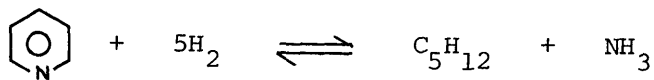


Figure 2-2: Thermodynamics of Pyridine HDN

(1) Overall reaction



calculated from the empirical equilibrium constant relationship determined for this reaction by Goudriaan (1974). These two lines are very close; both are presented because of their significance in the analyses of this thesis.

The second and ensuing steps of each reaction remain thermodynamically favorable to high temperatures, as did the overall reactions. Thus whether either of these reactions becomes thermodynamically limited will depend upon the nature of the rate limiting steps of the reaction mechanisms at temperatures where the equilibrium constants are less than one (logs less than zero).

II.D. Objectives

The overall objective of this long-term research program is to examine the interactions which result from the presence of both organic nitrogen and sulfur compounds in petroleum feedstocks derived from unconventional sources such as oil shale and coal. From a better understanding of these phenomena, suggestions should evolve for the improvement of industrial processing conditions.

This particular study focused on the interactions between the model compounds thiophene and pyridine in hydrogenolysis reactions at pressures up to 1000 psig (70

bars). It was desired to determine the inhibitions, enhancements, and changes in product distributions which might occur under temperature and pressure conditions similar to those of commercial processes. This would be accomplished by comparing the results of the hydrodenitrogenation (HDN) of pure pyridine and the hydrodesulfurization (HDS) of pure thiophene with the results of these reactions carried out using mixed pyridine-thiophene feeds.

Of particular importance was the examination of the potential equilibrium limitation on the reaction of pyridine. Specifically, if the reaction did reach equilibrium, then increasing the hydrogen partial pressure should help overcome the constraint by shifting the composition of the equilibrium mixture toward completion. The effect which the presence of thiophene would have on such a thermodynamic limitation was of great significance.

Chapter III - Apparatus and Procedure

The hydrodenitrogenation and hydrodesulfurization reactions of this study were carried out in the vapor phase in a packed-bed catalytic reactor using 1.5 grams of a sulfided NiMo/Al₂O₃ catalyst. Reaction pressures ranged from 150 to 1000 psig, and temperatures from 150° to 425°C. The continuous-flow system was run under steady-state, isothermal conditions. Liquid reactants were fed with a high-pressure metering pump, heated, and vaporized into a stream of heated hydrogen, and the resulting mixture fed to the reactor. The reactor effluent stream was sampled with an on-line heated gas sample valve which served as an interface between the reactor system and the gas chromatographic analysis system. Reactant conversions and product distributions were determined from the results of the chromatographic analysis.

Figure 3-1 with its key, Figure 3-3, together show the main components of the reactor facility. The heavy streamlines indicate primary flows through the system during steady-state reaction operation.

The different systems which make up the reactor facility are covered individually in the following sections, and further details are included in the Appendix.

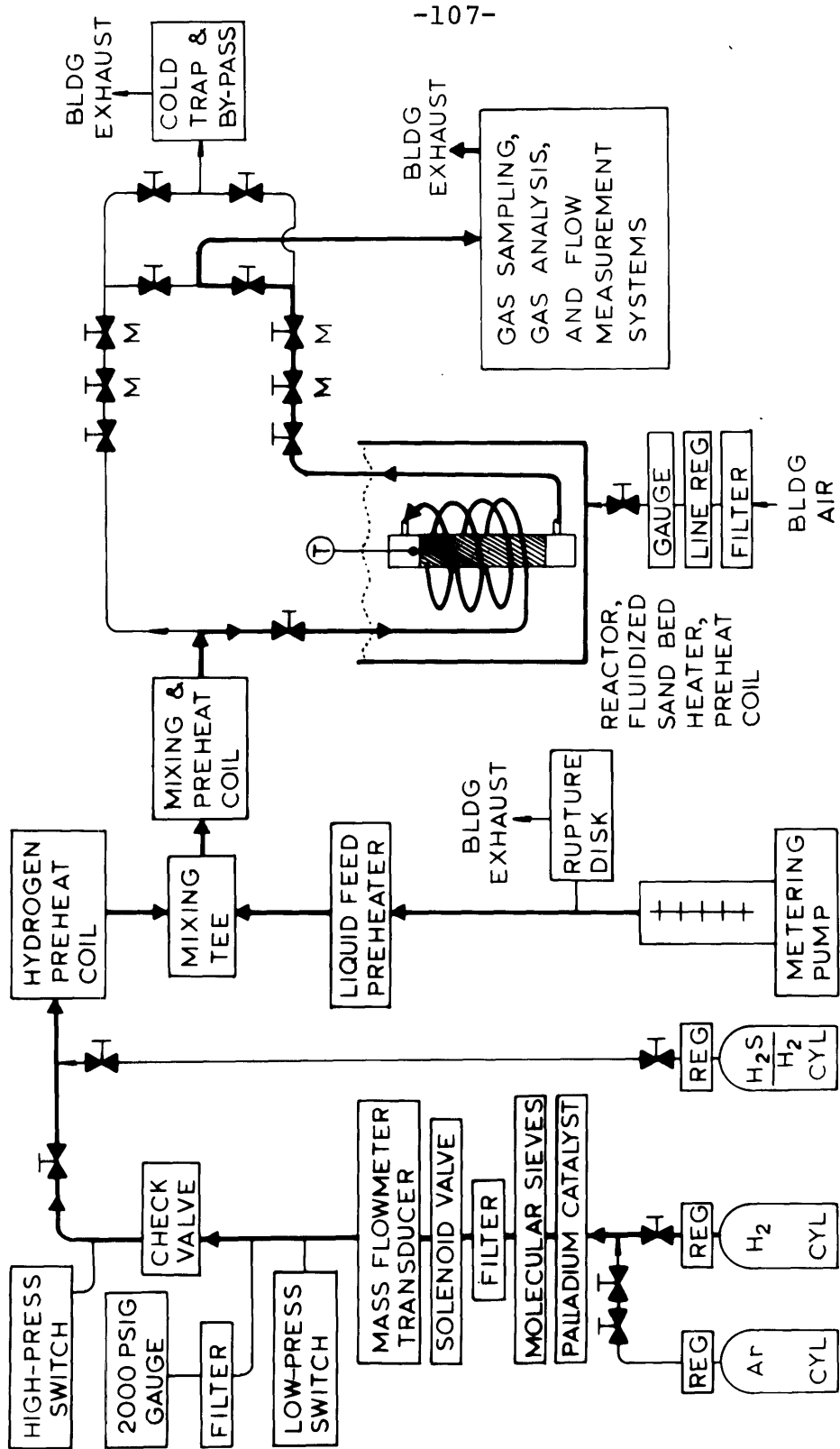


FIGURE 3-1: REACTOR SYSTEM: MAIN COMPONENTS AND PRIMARY FLOWS

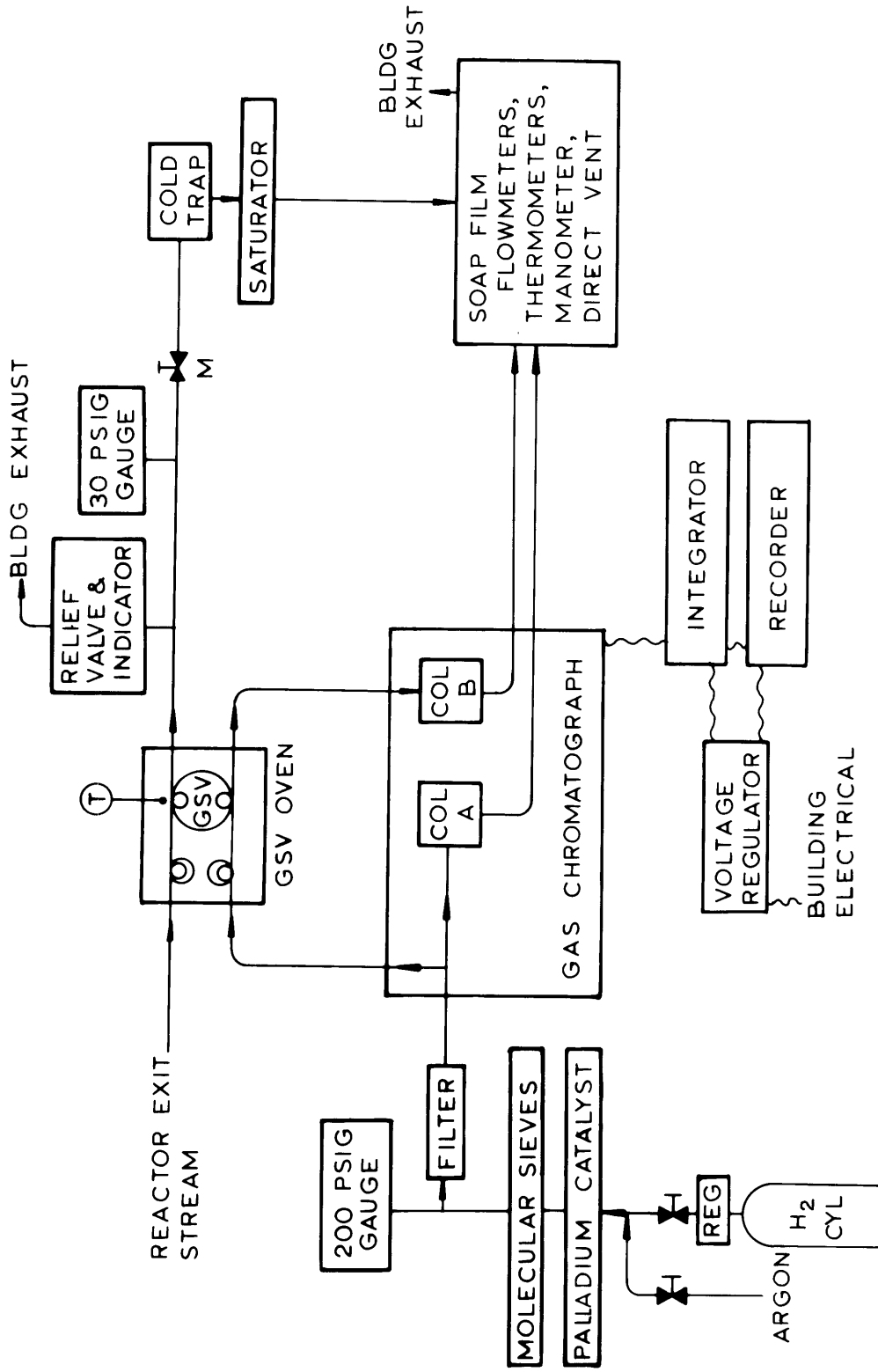
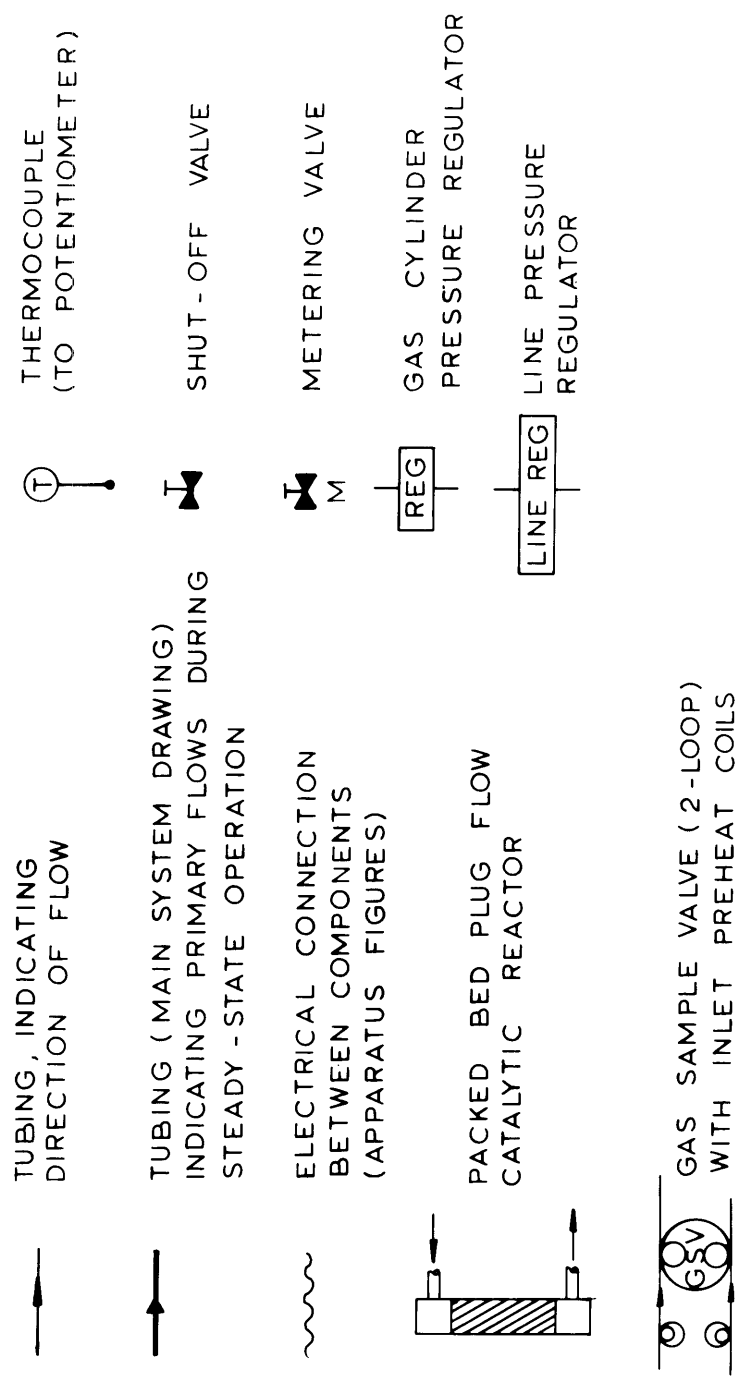


FIGURE 3-2 GAS SAMPLING, GAS CHROMATOGRAPH, AND FLOW MEASUREMENT SYSTEMS



NOTE: KEY APPLICABLE EXCEPT WHERE SUPERSEDED BY NOTES FOR INDIVIDUAL FIGURES.

FIGURE 3-3: KEY TO APPARATUS FIGURES

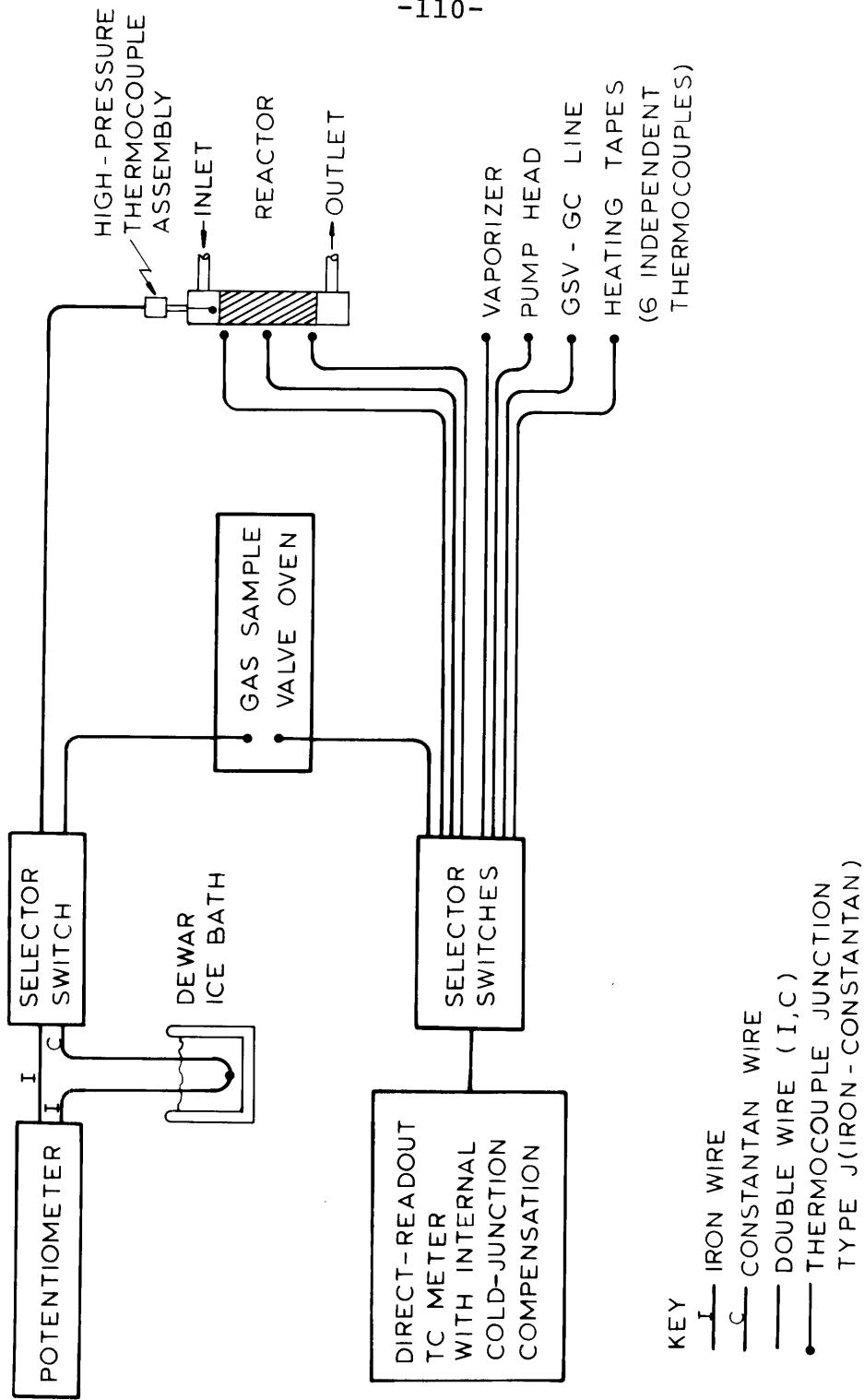


FIGURE 3-4: THERMOCOUPLE TEMPERATURE MEASUREMENT SYSTEMS

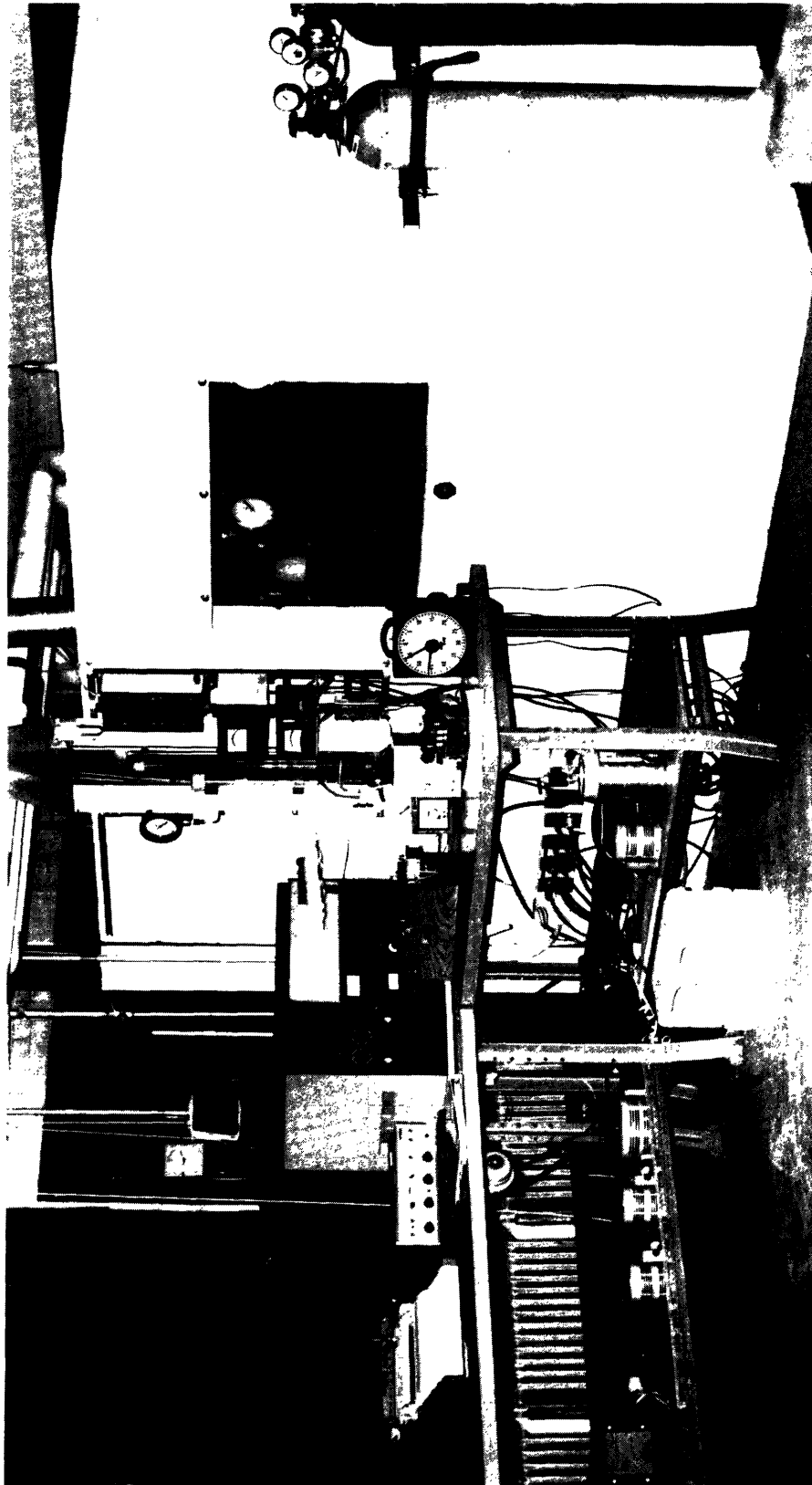


Figure 3-5:
Reactor Facility, Overall Exterior View;
Measurement, Control, and Analysis Systems; and Reactor Barricade

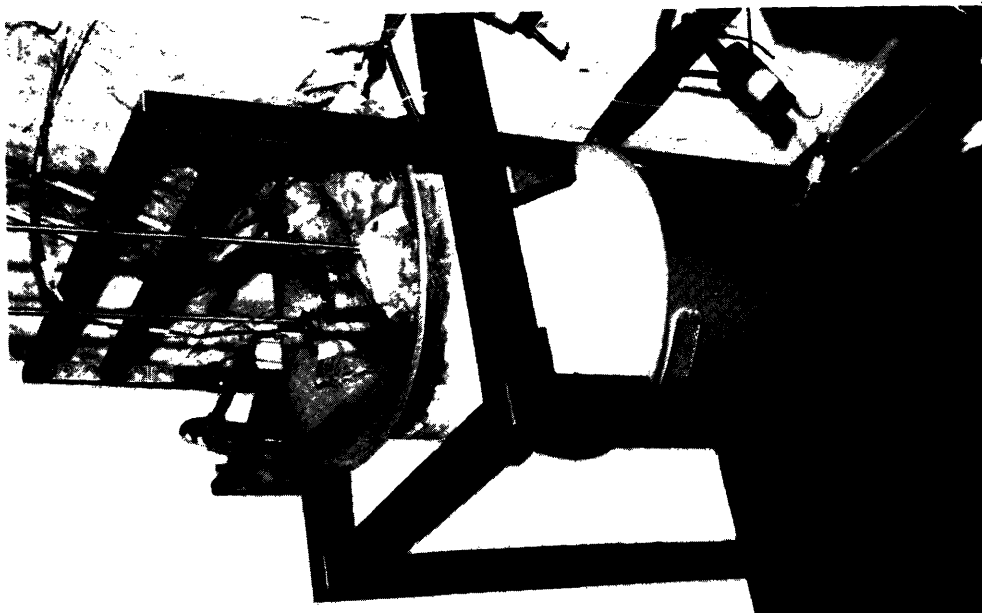


Figure 3-7:
Fluidized Sand Bed Heater and
Immersed Reactor Assembly

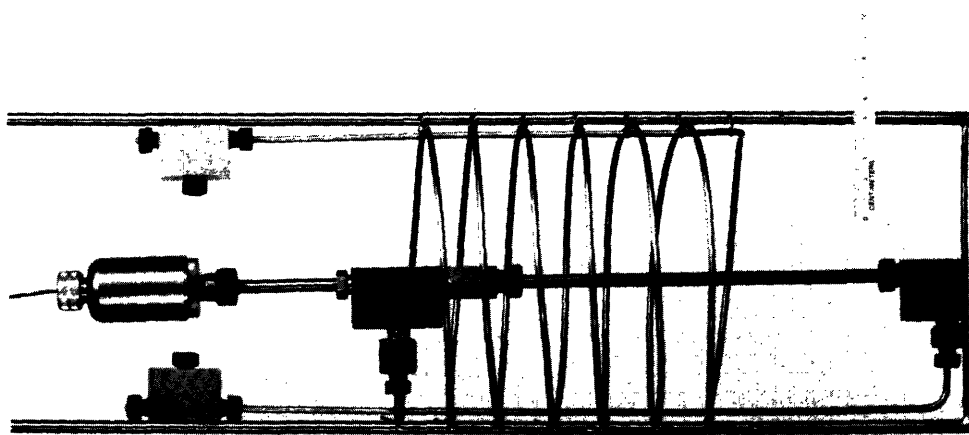


Figure 3-6:
Reactor Assembly; Reactor,
Preheat Coil, and Thermocouple;
On Support Frame

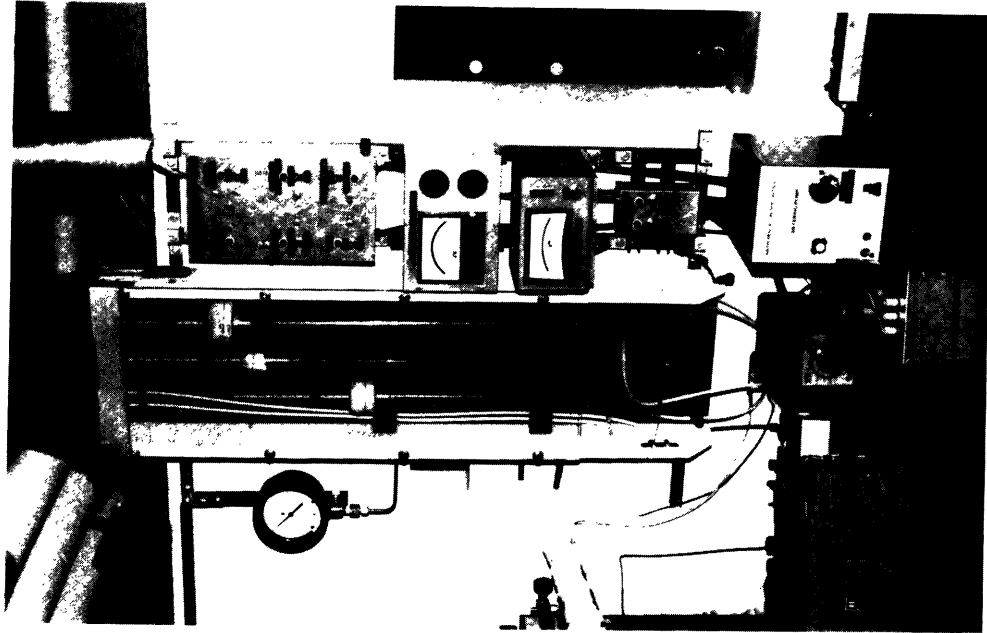


Figure 3-9:
Measurement and Control Systems
For Fluid Flow and Temperature

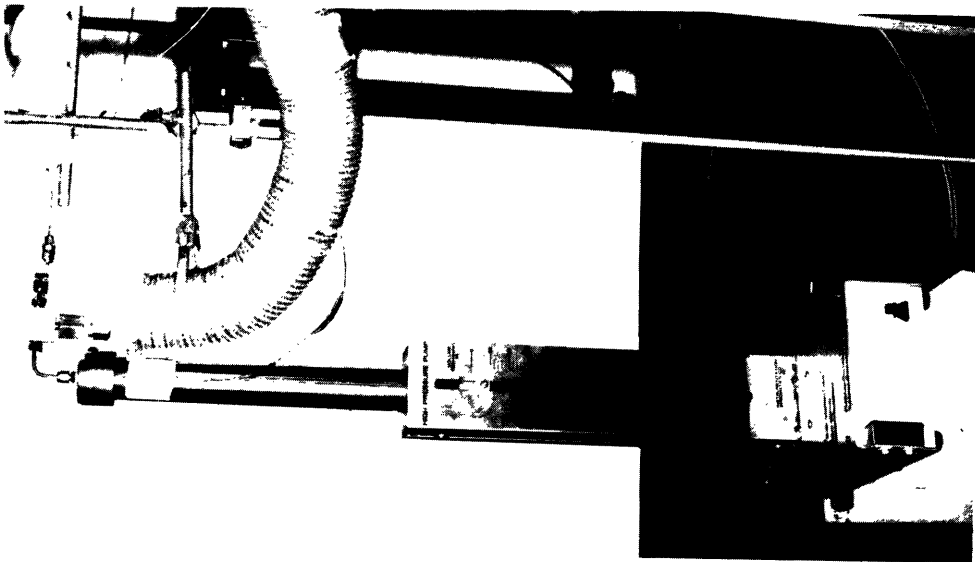


Figure 3-8:
Liquid Reactant Feed System:
Pump, Rupture Disk, and
Liquid Feed Preheater

III.A. Reactor Design Considerations

It was desired to operate the reactor in the absence of any heat or mass transfer limitations. The highly exothermic reactions ($\Delta H_{\text{rxn}} = -66$ kcal/gmole for thiophene HDS, and $\Delta H_{\text{rxn}} = -84$ kcal/gmole for pyridine HDN) necessitated rapid heat removal from the reactor. A fluidized sand bed heater was used for this purpose because of its good heat transfer qualities. To maximize the heat transfer from the packed bed, particularly the heat transfer in the radial direction across the catalyst bed (interparticle, or intrareactor heat transfer), it was desirable to reduce the reactor diameter to the smallest value which could not produce significant wall effects.

In previous work in this research group, catalysts ground and sieved to an average diameter of 0.77 mm had been used. Calculations showed this size to be small enough to avoid mass transfer limitations for the anticipated conversions of the higher-pressure reaction conditions of this study. For consistency with earlier work, then, this same particle size was used.

The lowest radial aspect ratio (ratio of the bed diameter to the catalyst particle diameter) for which channeling and wall heat transfer effects are not limiting,

is approximately four (Doraiswamy and Tajbl, 1974) to five. Given the constraints imposed by the fixed tubing sizes available, one-quarter inch OD tubing with an ID of 4.57 mm was chosen for the reactor, giving a radial aspect ratio of approximately six.

A minimum axial aspect ratio of 30 is needed to insure plug-flow operation of a reactor (Doraiswamy and Tajbl, 1974). For the 1.5 gram catalyst loading used in this study, this value was approximately 165. With plug-flow characteristics assured, axial dispersion and conduction effects could be neglected.

From the results of preliminary experiments, the maximum feed conversions possible without encountering heat transfer limitations were determined. This upper limit was used in the design of all final experiments. Details of the calculations of possible heat and mass transfer limitations for the run data presented in this work are given in the Appendix. They indicate that the system as run was free of heat and mass transfer limitations, but that the conversions (moles per hour) reached in this study were the greatest which could be tolerated in the present system without bringing on such limitations.

All tubing, components, and fittings subject to high pressures and heated reaction mixtures were constructed of

type 316 stainless steel. This austenitic stainless steel was determined to be adequate under the severe conditions of the study: high pressures and temperatures in the presence of both hydrogen and hydrogen sulfide (Fletcher and Elsea, 1964; Harper, 1968). The reactor tube (0.25 in.OD) and all connecting tubing (0.125 in.OD) were of 0.035 in.wall thickness, with basic working pressure ratings of approximately 6000 and 12,000 psi respectively. These were considered adequate safety factors for the conditions to be used, which would not exceed 1000 psig. Before use, all stainless steel tubing was cleaned with an H_2SO_4/HNO_3 mixture, trichloroethylene, acetone, and distilled water.

III.B. Reactor System

The reactor assembly is shown alone in Figure 3-6, and immersed in its fluidized sand bed heater in Figure 3-7. The reactor itself consisted of a straight, one-quarter inch OD stainless steel tube containing a packed catalyst bed of 4.57 mm diameter and 12.9 cm length. The catalyst particles were secured both above and below the bed by stainless steel screens and glass wool packing.

Reaction temperatures were measured with a thermocouple placed in the open reactor tube above the top

(entrance) of the catalyst bed. The high-pressure thermocouple assembly (Autoclave Engineers sheath-type) consisted of a one-sixteenth inch thermocouple probe welded into a one-quarter inch, coned-and-threaded tube. This thermocouple was read using a millivolt potentiometer (calibrated annually), in conjunction with a dewar ice bath cold junction. The temperature measurement systems are shown schematically in Figure 3-4.

Reaction temperatures were maintained by immersing the reactor in a fluidized sand bed heater, Tecam model SBS-4, with proportional temperature controller. This sand bed was modified to accommodate the reactor assembly by extending the original seven-inch-deep sand bed to give a depth of 13 to 14 inches when fluidized. An auxiliary heater was added to the extension to reduce the heatup times required by the large mass of sand. To determine that no temperature gradients were imposed on the reactor by the sand bed heater, three thermocouples were placed in the sand bed, 2 mm from the reactor tube, at the top, middle, and bottom of the catalyst bed. During steady-state operation, these three temperatures were always identical to within 1°C, the lowest detectable difference on the direct-readout thermocouple meter (Omega pyrometer, with internal cold junction compensation).

The reactor temperature, as measured by the internal thermocouple, was usually controlled to within $\pm 0.5^{\circ}\text{C}$ under steady-state conditions by the fluidized sand bed. This temperature reading refers to the bulk gas temperature at the catalyst bed inlet. That the internal bed temperature did not differ significantly from this temperature is shown in the discussion of possible heat transfer limitations in the reactor.

The heated, vapor-phase feed was passed through a final, 10 ft. preheating coil encircling the reactor in the sand bed, in order to bring the reaction mixture to the desired reactor temperature prior to entering the reactor.

The reactor pressure was controlled by a reactant hydrogen cylinder regulator allowing fine setting (to within 1 psi) of the pressure under the conditions studied (Precision Gas Products single-stage high-pressure regulator, 1200 series, mfg. by Tescom). The regulator maintained an even pressure in the system, but over the period required to obtain one set of isothermal samples, usually one to two hours, the pressure would gradually drop one to two psi. When greater pressure drops occurred under certain conditions, the pressure was adjusted during this time. The reactor pressure was measured with a 2000 psig Ametek Precision Test Gauge calibrated before installation

to its 0.25 percent factory specification. Reproducibility of pressure readings was to within ± 1 psi. The gauge was installed in the reactant hydrogen feed line and separated from the reactor by a check valve. The pressure drop between the gauge and the reactor inlet was calibrated as a function of the hydrogen flow rate, and was accounted for in all pressure readings. The gauge was partially protected from sudden pressure increases (as could occur as a result of the opening of a solenoid valve) by an in-line filter (Cajon "snubber").

The total flow rate through the system was controlled by valves downstream of the reactor, across which there was a pressure drop from the reaction pressure to approximately 15 psig. Initially, two metering valves (Autoclave Engineers micrometering valves) were used in series for this control. However, great difficulties with stem thread seizing led to the eventual use of just one valve, either metering or v-stem, with which very close control was still surprisingly possible.

The flow control valves, as well as tubing containing vaporized liquid reactants, were all wrapped with heating tapes individually controlled by variable transformers and monitored with thermocouples. Details of all heating circuits are given in the Appendix.

The total flow rate through the reactor was determined using three soap-film flowmeters (50, 250, and 1000 cc) to measure the volumetric flow rate of the reactor exit stream after it had been reduced to atmospheric pressure. The great excess of hydrogen in the reaction stream permitted accurate measurement of this flow rate after liquids in the stream had been condensed out in an ice-bath cold trap. The stream was passed through a two-stage saturator, bubblers packed with 0.5 mm glass beads, before entering the soap-film flowmeter to insure a defined (i.e. saturated) moisture content, and to aid in the successful operation of the flowmeters. The temperatures of the exit stream were measured with matched thermometers for correction to standard conditions and for determination of the proper vapor pressure of water. As the flowmeters were in a specially-constructed exhaust hood, the pressures of the columns were determined by subtracting the pressure drop from atmospheric to the column exit from the current barometric pressure. As this correction was always less than one mm of water, it was neglected. Barometric pressures were obtained from the continuous records of the Meteorology Department. The flowmeters, with other flow and temperature measurement components, are shown in Figure 3-9.

The cold trap preceding the saturator in the exit

stream was also used in some runs with dry ice to trap samples of the liquid reactants for further analysis.

III.C. The Catalyst Used, and Catalyst Sulfiding Procedures

The NiMo/Al₂O₃ catalyst used in this study was American Cyanamid AERO HDS-3A, containing 3.2 percent NiO and 15.1 percent MoO₃ by weight. In order that the results of the investigation be based on some recognizable standard for comparison, this well-known commercial catalyst was chosen. Nickel was chosen as the promoter for this study rather than the more-common cobalt (as in CoMo/Al₂O₃), as the former has been shown to have more activity toward denitrogenation, while keeping much the same desulfurization capability (Cir and Kubicka, 1972; Mayer, 1974). This particular catalyst has also been used as a standard for tests in the petroleum industry.

The initial catalyst pellet size is a 1/16-inch extrudate. For use in this microreactor study, it was ground, and sieved to a size fraction between 0.707 and 0.841 mm, for an average particle size of 0.774 mm.

The nickel and molybdenum are initially in their oxidic forms, but are activated by sulfiding before use. It is important that the catalysts not be contacted with pure hydrogen before sulfiding in order to avoid a permanent

loss of activity (American Cyanamid, 1969; Kolboe and Amberg, 1966). Three sulfiding procedures were used in this study to insure that long-term catalyst deactivation did not affect the results. The origins of these methods are covered in detail in the Results and Discussion of Results sections. The three processes are:

Type I, Formal Sulfiding

As specified by the manufacturer, and adapted for use on the microscale of this study, this multi-step procedure was used for each fresh catalyst loading, and as a technique to resulfide the catalyst after use with basic nitrogen compounds.

1. Heat reactor to 175°C under flow of argon.
2. Start 10% H₂S in H₂ mixture flowing over catalyst at a rate between 15 and 20 cc/hr at a total pressure of approximately 8 psig. Maintain flow and temperature for 12 hours.
3. Maintaining H₂S/H₂ flow rate, increase temperature to 315°C at a rate of 1°C per minute.
4. Maintain H₂S/H₂ flow and temperature of 315°C for one hour.
5. Cool reactor to 150°C under H₂S/H₂ flow
6. Cool reactor to room temperature under Argon.

Type II, Run Sulfiding

Sulfur compounds in the feed desulfurize, giving off

H₂S. This was shown in the catalyst activity section of this study to maintain the level of activity, by presumably maintaining the sulfided nature of the catalyst.

Type III, Shutdown Sulfiding

At the completion of a run using a pure-pyridine feed, the reactor was first cooled to 350°C under a hydrogen flow (the pyridine feed having been stopped). Flow of the H₂S/H₂ sulfiding mixture was then started, and the reactor cooled to 150°C. The reactor was then cooled to room temperature under argon.

The pore size distributions, surface areas, and other properties of both new, sulfided; and used, resulfided catalysts are given in Table 4-1, and covered in the Results and Discussion of Results Chapters.

III.D. Reactant Feed Systems

Liquid reactants, usually thiophene and/or pyridine, were injected into the system using a high-pressure metering pump, ISCO Model 314. This unit permitted continuous variation of flow rates over a wide range; the calibrations carried out for the low flow rates used in this study are presented in the Appendix. Individual calibration points represent weighed samples of distilled water metered by the pump in a measured amount of time.

As such, they represent integrated data points. Random fluctuations due to the pump operation over short time spans (seconds) could be imposed on such points in actual use. In order to improve the reproducibility of the pump results over those in its original condition, a rather crude factory control for the continuous variation capability was replaced with a ten-turn potentiometer. Improved performance was also achieved by supplying power to the pump control unit through a voltage regulator.

The liquid feed passed through a three-foot section of heated capillary (0.0625 in. OD, 0.0165 in. ID) tubing wrapped with heating tape. This temperature, also individually controlled and monitored, was usually maintained at approximately 275°C. This stream of heated liquid was then flashed into a stream of heated hydrogen, and this mixture passed through a 20 ft heated mixing and preheating coil, finally entering the final preheating coil in the fluidized sand bed. As the capillary preheater had a tendency to plug with continued use, a rupture disk was placed between the pump and the capillary entrance to protect the pump from overpressure.

Figure 3-8 shows the pump, rupture disk unit with exhaust line, and entrance to heated capillary (shown disconnected from pump).

Reactant hydrogen was passed over a palladium catalyst

(Engelhard Deoxo D-10-2500) to convert impurity oxygen to water and then over a bed of 4A molecular sieves, which were activated at elevated temperatures under a stream of Argon, to adsorb the water present. The hydrogen stream then passed through a 7 micron filter, to remove any catalyst or molecular sieve particulate traces, before entering an electronic mass flow meter transducer (Haystings-Raydist Model ALL-1K). The output from this transducer and its associated control unit were measured with a millivolt potentiometer after the output signal had been attenuated by an electronic buffer circuit (included in Appendix). After passing the reactor pressure gauge, the stream passed through a check valve installed to prevent back-up of the reaction mixture into the hydrogen feed system. The hydrogen was then preheated before entering the mixing tee, where it was contacted with the heated liquid reactant(s).

A mixture of 10% H₂S in H₂, used for sulfiding the catalyst, could be brought into the system in place of the purified hydrogen stream. An argon purge stream was also available at the entrance to the hydrogen purification section.

III.E. Reactant Stream Composition Analysis

The reaction stream was analyzed by gas chromatography, using a gas sample valve as an interface between the reactor and analysis systems.

The reactor exit stream was passed through an eight-port gas sample valve (Carle, model 2014) with two, 4 cc loops. These two loops were calibrated in situ, and the two percent volume difference accounted for in subsequent calculations. The gas sample valve was heated in a recirculating-air oven. The temperature was usually maintained to within $\pm 0.5^{\circ}\text{C}$ by use of a voltage regulator and variable transformer, as measured by a thermocouple in the oven, read on a millivolt potentiometer and using a Dewar ice bath cold junction.

The reactor stream pressure was dropped across the flow control valve, from that of the reaction (150, 500, or 1000 psig) to approximately atmospheric, the stream then passing through the gas sample valve. By installing a metering valve after the sampling unit, the pressure in the sampling valve was precisely maintained, between 14 and 18 psig, and measured with an Ametek Precision Test Gauge. Because the pressure drop from the reactor to the gas sample valve was much more than half the total pressure drop to atmospheric, the reactor pressure was independent

of this sampling pressure.

The gas sampling, gas chromatograph, and flow measurement systems are shown schematically in Figure 3-2. The chromatograph (Varian, model 2820-30) employed a thermal conductivity detector, and was used with a hydrogen carrier gas purified in the same manner as the reactant hydrogen.

The output of the chromatograph was recorded (Photovolt Microcord 44 recorder) and integrated using an electronic digital integrator (Autolab Vidar 6300). When the electronic integration results were inadequate due to peak characteristics beyond its capabilities (peaks of greatly different characteristics in the same chromatogram) or to false triggering of integrations by baseline noise, manual area determinations were used.

Erratic behavior of the integrator due to high building voltages was prevented by using a voltage regulator for the integrator power supply. The recorder and electronic mass flow meter, were also supplied with power from this unit.

The column packings used in the gas chromatograph for the separation of both the nitrogen-compound and sulfur-compound peaks were 10% SP-2310 supported on 100/120 mesh Supelcoport (Supelco, Inc.) The SP-2310 supported phase was 55% cyanopropylsilicone; and the Supelcoport, an acid-washed, silane-treated diatomite support. This packing

was used in glass columns, 1/4 inch OD, ten feet long. These columns were used because of their ability to separate both the nitrogen and sulfur reactants, and intermediate and side products, namely thiophene, tetrahydrothiophene, pyridine, piperidine, and n-pentylamine. The light reaction products, butane, pentane, hydrogen sulfide, and ammonia, could not be resolved, however, even with programming of the column temperature. The separations achieved did represent significant advances over those of other columns tried, particularly Carbowax 20M on 80/100 mesh Chromosorb W-HP. These latter columns were used for early runs (those of the catalyst activity study), but were inadequate because of the coincidence of the pyridine and piperidine peaks.

Peak identifications and separations were determined by syringe injection of the pure compounds and of mixtures of these compounds. The variables studied in the optimization of the component separations were the column carrier gas flow rates, and the column temperatures. The best column flow rates were determined to be 40 cc/min. Many isothermal temperatures and different temperature programs were studied to obtain the best separations in the least amount of analysis time. The optimization focused on the separation of the thiophene and piperidine peaks in the simultaneous HDS-HDN runs, as these were the only

peaks which were not easily resolved in relatively rapid analysis times.

The separations for pure thiophene HDS runs and for pure pyridine HDN runs were relatively simple, and isothermal column temperatures could be used which gave retention times of about seven minutes. The separation of piperidine and thiophene, however, was difficult, as under these column conditions they had the same retention times. Either temperature programming or a lower isothermal column temperature was used to separate these peaks during runs with simultaneous thiophene HDS and pyridine HDN. The different column conditions used did not affect the observed areas of any component except piperidine. For piperidine, due to a tailing tendency, the observed area was a function of column temperature for a given size sample. Thus, a calibration, developed by syringe injection of piperidine at different column temperatures, was used for normalizing the piperidine areas to those it would have had at the higher column temperatures. This removed the only difficulty of using different column temperatures.

Figures 3-10 through 3-12, together with a key in Table 3-1, show the separations achieved for the three types of runs. The figures show the actual chromatogram peaks under the reaction conditions specified in the table. The

Table 3-1

Key to Figures for the Chromatographic Product Separations
on 10% SP-2310 on 100/120 Mesh Supelcoport

<u>Parameter</u>	<u>Figure 3-10</u>	<u>Figure 3-11</u>	<u>Figure 3-12</u>
Reaction(s)	Thiophene HDS	Pyridine HDN	Pyridine HDN + Thiophene HDS
Column Temp.	100°C	110°C	80°C
Peak Attenuation	4	4	1
Run-Sample	46-18	41-25	53-23
Thiophene Feed	186 torr	---	93 torr
Pyridine Feed	---	186 torr	93 torr
Reaction Temp.	227°C	309°C	284°C
Thiophene Conv.	25%	---	44%
Pyridine Conv.	---	71%	56%

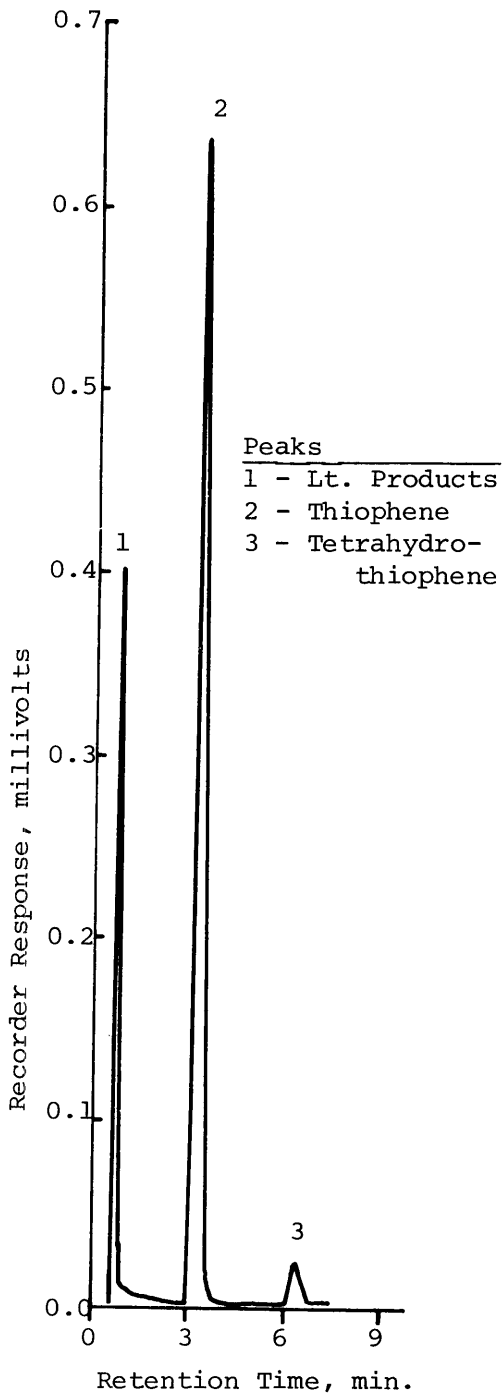


Figure 3-10: Separation of products of pure thiophene HDS (see Table 3-1)

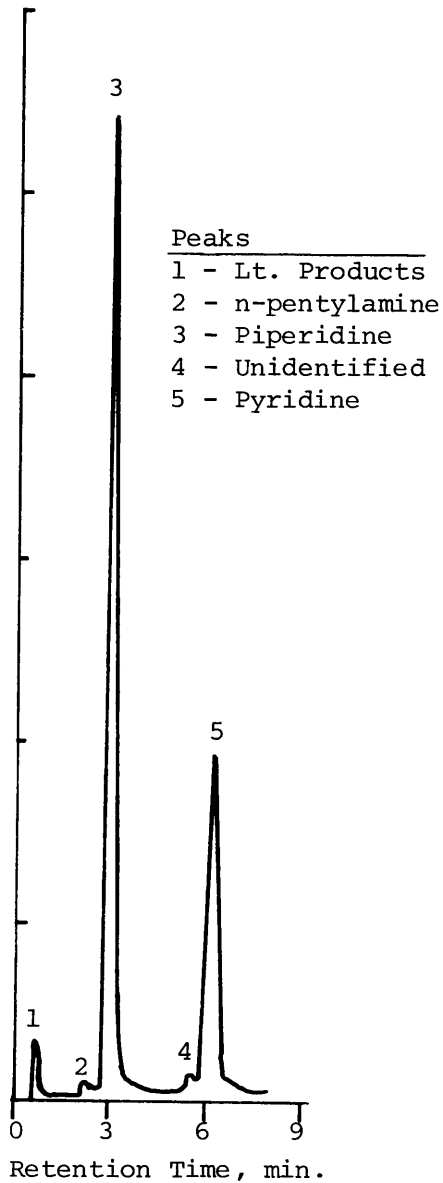


Figure 3-11: Separation of products of pure pyridine HDN (see Table 3-1)

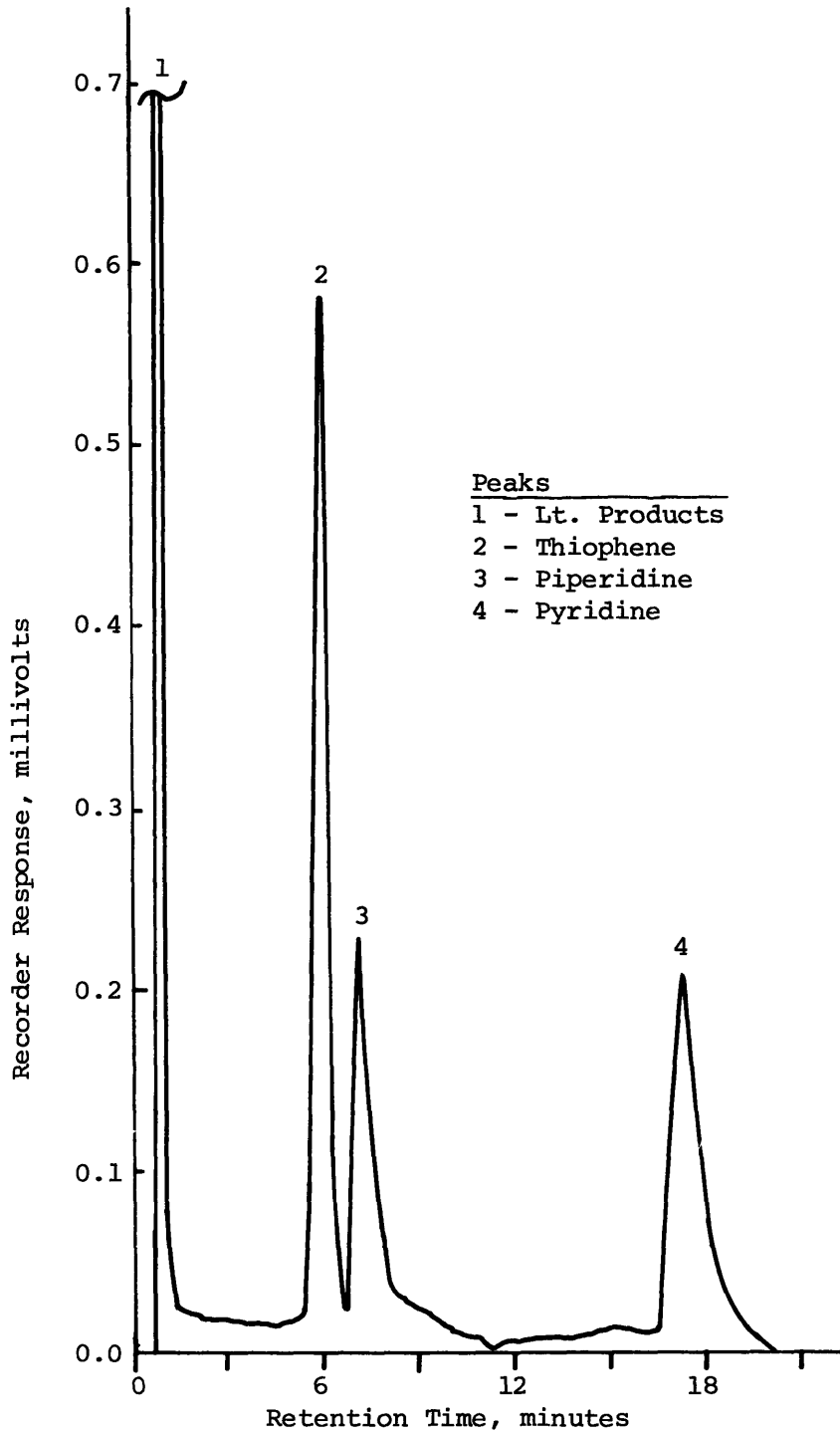


Figure 3-12: Separation of Products of Simultaneous Pyridine HDN and Thiophene HDS (see Table 3-1).

runs were chosen to illustrate the component separations, thus those with the largest tetrahydrothiophene and n-pentylamine concentrations are shown.

For pyridine runs, a quantitative analysis of the reaction products piperidine and n-pentylamine was made. To determine the mole fractions in the product stream from the chromatogram peak areas, the molar responses of the chromatograph to pyridine, piperidine, and n-pentylamine were determined. By injecting known quantities of each component into the chromatograph under the same detector conditions used for the run analyses, the peak area per mole of each component was determined.

For chromatogram areas in microvolt-seconds:

<u>Compound</u>	<u>Chromatograph response, microvolt-sec/gram mole</u>	<u>Relative Molar Response</u>
pyridine	7.077×10^{10}	1.00
piperidine	7.111×10^{10}	1.005
n-pentylamine	8.462×10^{10}	1.20

Here, the relative molar responses of piperidine and n-pentylamine are the ratio of the area per mole of the component to the area per mole of pyridine.

III.F. Safety Considerations

Several factors involved in this study combined to give

a high potential for serious safety problems. Accordingly, many precautions were taken in the design and operation of the experimental facility. First, the use of high-pressure, high-temperature hydrogen in the presence of hydrogen sulfide required type 316 stainless steel tubing and components (as previously discussed). The pressure rating of the tubing was a minimum of five times the maximum pressure to be used in the system. This was considered sufficient to prevent the so-called Hindenburg effect (Hottel, 1972). In addition, all high-pressure components and those which might be subject to a buildup of hydrogen-air mixtures were located behind a barricade, as can be seen in the overall exterior view of the facility in Figure 3-5.

Numerous other designs were oriented toward safety of operation. For example high-pressure valves were fitted with solid-center unions on handle extensions which would not permit the stems to pass through small openings in a 1/4-inch steel shield in the event that a stem should break off during operation.

An automatic shutdown system was activated by pressure switches set to a narrow range around the 1000 psig working pressure. In the event of an unintentional pressure increase, or a decrease due to rupture, the system automatically closed a solenoid valve in the hydrogen feed line,

turned off the metering pump, and sounded an alarm. Fortunately, this system was never needed. Diagrams giving details of this system are included in the Appendix.

As electrical heating tapes were in close contact with valves and tubing, all parts of the system were carefully grounded. Further, in the event of an emergency, all heating circuits could be shut down with one master switch.

Several of the chemicals used in this study were toxic, as detailed by Sax (1968), Steere (1971), Fairhall (1969), and Deichmann and Gerarde (1969). For thiophene, pyridine, and piperidine, some of the specifically-noted effects are: severe, irreparable eye damage; severe ataxia (loss of muscular coordination) through action on the central nervous system; respiratory disorders; kidney and liver damage; nausea and vomiting; nervousness; and external skin irritation. Further, chemical similarity to known carcinogens indicates another possible type of hazard. Hydrogen sulfide is also well-known for its severe toxicity. Of interest in the work of this research group was the fact that pyridine was noted to cause CNS depression (Sax, 1968).

Consideration of the above information, as well as the high flammability of some of the materials, led to

the extensive hooding of all chemical-handling operations. Also, potential sources of vapors, such as the rupture disk exit, were continuously connected into the exhaust system.

III.G. Experimental Procedure

An experimental run consisted of determining the conversion of the reactant(s) thiophene and/or pyridine at usually six reaction temperatures, for a constant feed composition and flow rate. The reactor system would first be brought to steady state with the reactor feed rates set to provide the desired component partial pressures, and the reactor at a temperature of 115°C. This temperature was sufficient to maintain the feed in a vapor state, but not high enough for reaction to occur. The chromatogram peak areas for the reactant under this condition were used as a base from which conversions would be calculated. The sand bed temperature was then raised to a level at which reaction would take place, and the system allowed to equilibrate. The chromatograms at this temperature would indicate the conversion of reactants by showing decreased reactant peak areas. Partial product distributions were also determined. The conversion of the reactants would then be calculated using the formulas described in detail and illustrated with sample calculations in the Appendix.

This procedure was repeated for each reaction temperature to be studied. The duration of a successful run varied from 10 to 20 hours, depending on the type of chromatographic analysis to be used and the number of samples taken at each reaction temperature (more samples were taken when there was a significant amount of scatter from among those of a set).

The reactor facility was always maintained in a standby state when not in use. The gas chromatograph, integrator, and recorder were run continuously; all heated lines, and the gas sample valve oven were kept at their steady-state temperatures.

A run began by bringing the temperature of the fluidized sand bed heater to 115°C, while maintaining the reactor under a flow of argon. With the pump loaded with the desired feed, the argon flow would be stopped and the pump connected to the liquid feed preheater. A flow of hydrogen would then be started, and the pressure of the system raised to the desired operating level. At this point, the pump would be temporarily run at a rate ten times its steady-state flow rate. Reducing the pump rate to the specified steady-state value quickly brought the partial pressure down to the desired level. For the base temperature conditions, an equilibration period of one hour was then permitted, while other pieces of equip-

ment were adjusted for the run conditions (for example, setting the gas chromatograph carrier gas flow rates). The pump rate, set initially, remained constant for the entire run. The total pressure required periodic readjustment to maintain the specified value. The flow rate through the system, measured with the soap-film flowmeters, was adjusted before the set of samples was taken.

For the determination of the base level of the reactant chromatograph peak area, six to eight samples were usually taken. At each sample, all relevant system conditions were recorded, as illustrated in the Appendix.

When the base peak areas had been taken, the fluidized sand bed temperature was raised to the first reaction temperature. Samples taken during the heatup from the base temperature indicated that a significant amount of desorption from the catalyst surface took place at this first step, but that the new steady-state level of conversion was quickly reached. An equilibration time of one-half to one hour was allowed before the sampling process was repeated. Four to six samples were usually taken at each reaction temperature. This process was repeated for each condition to be studied.

At the end of the final set of samples, the liquid feed was stopped, and the reactor depressurized. The pump

was then disconnected, and the reactor allowed to cool to room temperature under a stream of argon. Alternatively, the shutdown (Type III) sulfiding procedure could have been carried out, where the reactor was cooled from 350° to 150°C under a mixture of 10% H₂S in H₂, and then further cooled to room temperature under a flow of argon.

CHAPTER IV. RESULTS

The thiophene hydrodesulfurization (HDS) and pyridine hydrodenitrogenation (HDN) results presented in this thesis are all based on data from a continuous, plug-flow packed-bed catalytic reactor. One, 1.5 gram loading of a sulfided NiMo/Al₂O₄ catalyst was used for the catalyst activity study, and a second for the quantitative HDS and HDN runs. Methods devised in the activity study were used to prevent long-term catalyst deactivation in subsequent work.

The reaction data obtained from the plug-flow reactor were all of integral form, expressed as the conversion at the outlet of the catalyst bed as a function of the reaction temperature. The reactor was operated at constant space velocity, with the reactant stream residence time varying inversely with the absolute temperature. A detailed summary of the conditions and results for each run is given in the Appendix. Also given are the coordinates of the smooth curves through the data points for each reaction condition. This latter information was used in the quantitative analyses, and is useful for further computational purposes. Graphical data presentations all use the same temperature and conversion (or product composition) axes, so that direct comparisons can be easily made from one figure to another.

Total reactor pressures were set to nominal values of 150, 500, and 1000 psig, and the partial pressures of thiophene and pyridine to nominal values of either 93 or 186 torr. For clarity of presentation, these nominal pressures will be used in textual material and brief figure keys. Where relevant, each figure is also accompanied by a detailed key giving the actual values of all pressures for each separate run symbol used. Further details are included in the Appendix run summaries.

The units of measurement in this presentation are those used during the actual work, as they give the clearest picture of the different parameter variations. In the appropriate situations, the units used for pressure were: torr, psi, psig, psia, and bars. Temperatures were measured in degrees Celcius. For ease in adaptation of these results to the International System (SI) units, certain tables list temperatures in Kelvin as well as degrees Celcius, and pressures jointly in the appropriate working units and bars ($1 \text{ bar} = 10^5 \text{ pascal}$). To place the working pressures in their proper perspectives, the nominal values are converted below (using 1 atmosphere for the barometric pressure; the actual barometric pressure was used in run calculations):

<u>torr</u>	<u>psig</u>	<u>atm</u>	<u>bar (1 bar = 10⁵ pascal)</u>
93	----	0.1224	0.1240
186	----	0.2447	0.2480
---	150	11.21	11.36
---	500	35.02	35.49
---	1000	69.05	69.96

IV. A. Catalyst Activity

The methods used to maintain a constant level of activity for the sulfided NiMo/Al₂O₃ catalyst during this work were discussed in the section on catalyst sulfiding procedures. These methods were derived from the results presented in this section and the subsequent related discussion.

Early experimental runs using a pure-pyridine reactant feed showed a great loss of catalytic activity with continued use of a single loading of catalyst. A study was made to determine the reason for this behavior and techniques for achieving a consistent level of activity.

Figure 4-1 presents the activity with time on stream for a new catalyst loading. Activity is defined as the quasi-conversion of pyridine at 355°C for a pure-pyridine run at a total pressure of 150 psig and a pyridine feed

partial pressure of 93 torr. The "quasi" qualification is added because for the early runs, gas chromatograph columns were used which would not properly separate pyridine (reactant) and piperidine (reaction intermediate) peaks, giving erroneous, albeit reproducible, conversion values. The activity level was measured by repeating a standard run incorporating the conditions specified. Time on stream is defined as exposure of the catalyst to a heated stream of pyridine in hydrogen, with or without the additional presence of thiophene.

The three types of sulfiding procedures previously described: I. formal, II. run, and III. shutdown, were carried out as indicated in the figure. Except for the runs involved in the type II sulfiding procedure (those immediately preceding run 18), all used a pure pyridine feed, and there was no exposure of the catalyst to sulfur except during the type I and III procedures.

Activity decreased from an initial level of at least 34 percent (this being the quasi-conversion at 16 hours on stream) to a steady-state level of approximately 16 percent. The type I (formal) sulfiding at 50 hours did not restore the initial activity, but maintained it at approximately 24 percent.

The inclusion of thiophene in the reactor feed (type II sulfiding) before run 18 restored activity to 25 percent,

the same level as that for the previous formal procedure, to within the accuracy of the measurements. To determine whether the formal procedure would enhance the activity further, this was carried out before run 19, but the level remained unchanged. After two runs using pure pyridine, a type III (shutdown) sulfiding procedure was used, and the level of activity in run 21 was again the same as that after each of the sulfidings except the very first.

This catalyst loading was used for approximately 280 hours with pyridine and thiophene feeds, followed by approximately 240 hours with quinoline feeds. Then, after carrying out the formal sulfiding procedure, repetition of the standard reference run could produce only about one-half the activity found in the earlier study. The primary differences between the pyridine-thiophene and quinoline operations were that quinoline was likely to produce more heavy substances which could form carbon deposits, and the quinoline runs were made at slightly higher reaction temperatures (430°C) which stretched the acceptable limits of the temperature-sensitive catalyst.

After a total of 310 hours of pyridine contact and 240 hours of quinoline contact, the catalyst was formally sulfided, and removed and stored under nitrogen. A fresh catalyst was then formally sulfided, and also removed and stored under nitrogen. Both specimens were then examined

for their surface areas, pore volumes, pore size distributions, sulfur contents, and carbon contents. The results of these tests are given in Table 4-1 and Figure 4-2.

The surface area of the catalyst was unchanged by the prolonged use. There was approximately a ten percent reduction in specific pore volume; but the pore size distribution was remarkably similar for the two catalysts, with the used sample showing a slight shifting toward larger pores. While the analytical techniques used were carried out with great care, they were performed on one tenth of the total reactor loading (150 mg, or approximately 0.2 cc, was used for the tests), and could perhaps be subject to difficulties in obtaining a representative sample from the reactor loadings.

Although both catalysts were given the same formal sulfiding treatment before being tested, the used sample showed 12 percent less sulfur retention than did the new one. Another significant difference was the amount of carbon found on the two specimens. While for the new catalyst there was no detectable carbon (the catalyst was initially carbon-free, and was exposed only to hydrogen sulfide and hydrogen in the reactor), the used catalyst showed considerable carbon deposition.

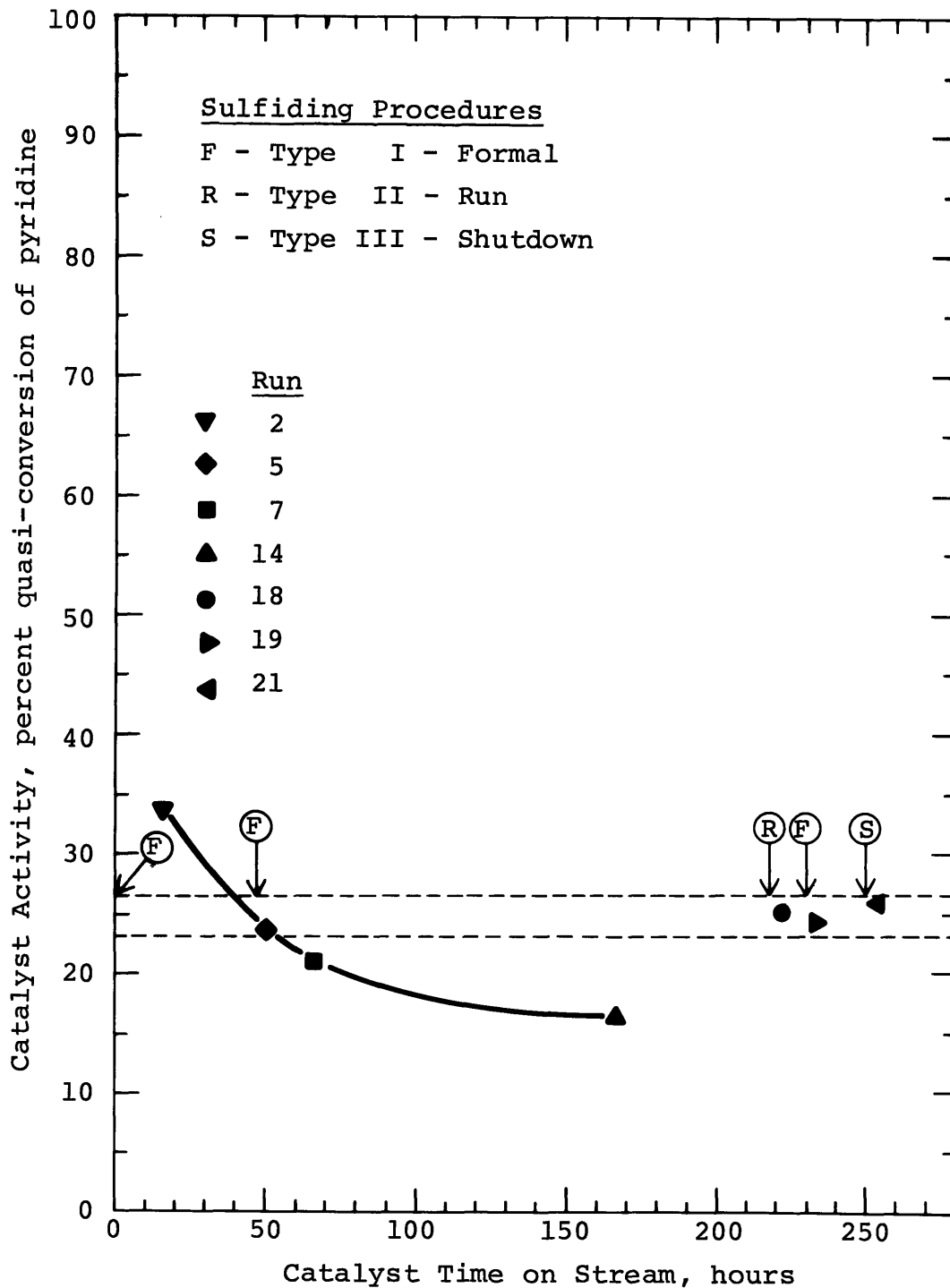


Figure 4-1: The Effects of Time on Stream and Sulfiding on the Activity of Sulfided NiMo/Al₂O₃ Catalyst.

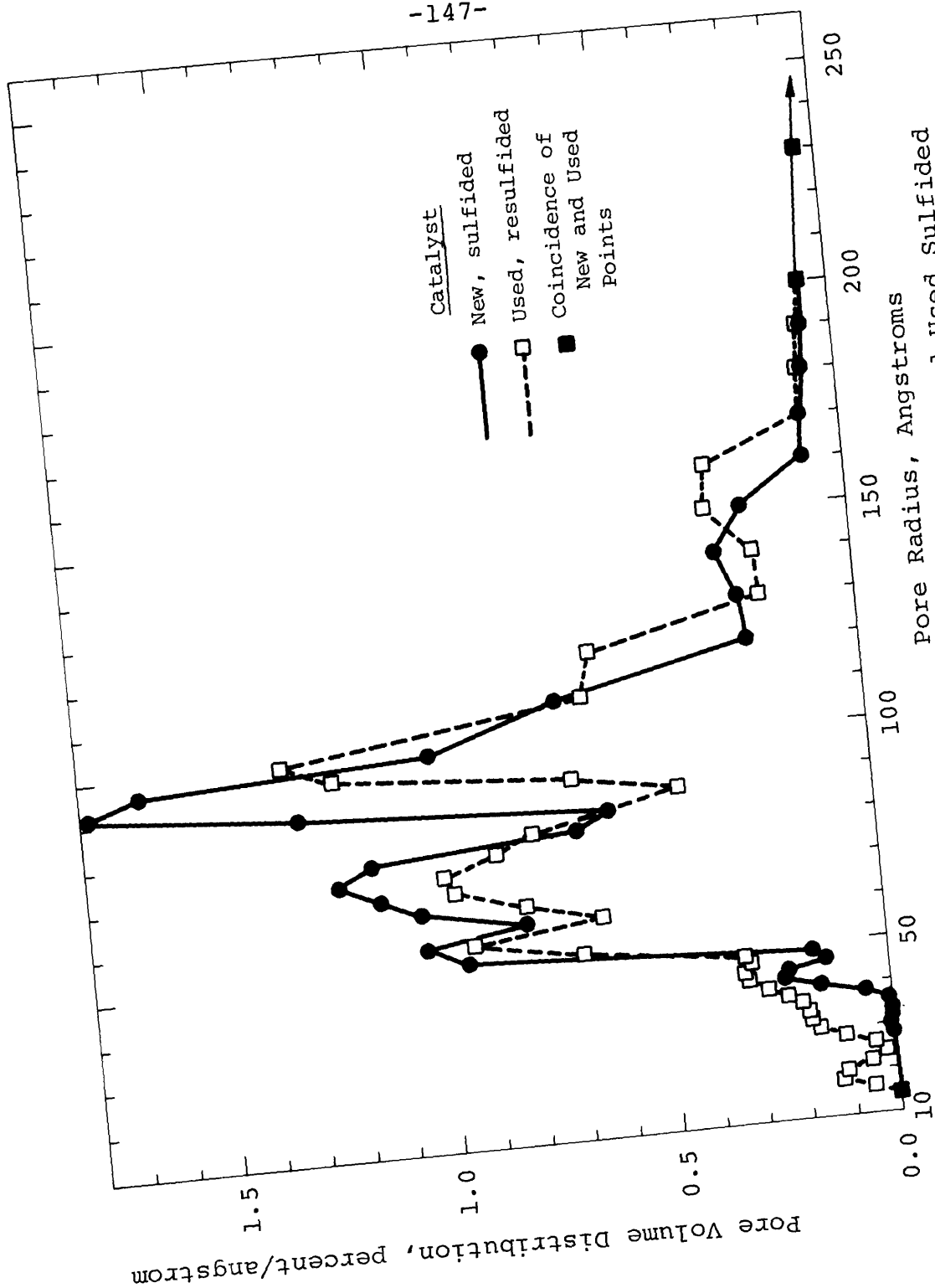


Figure 4-2: Pore Size Distributions for New and Used Sulfided NiMo/Al₂O₃ Catalysts

Table 4-1

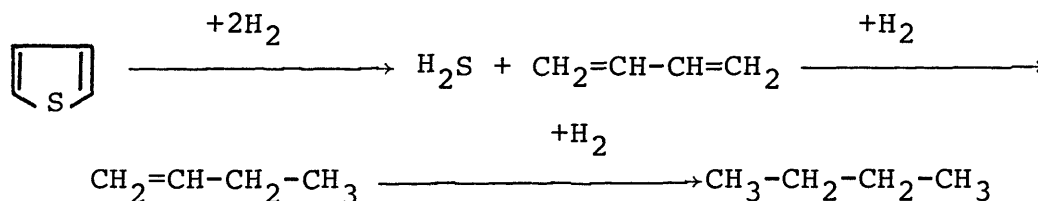
Analysis of New and Used Sulfided NiMo/Al₂O₃ Catalysts

<u>Property</u>	<u>Old Catalyst</u>	<u>New Catalyst</u>
Catalyst weight at loading, grams	1.48	1.48
Catalyst use history, hours on stream	550	0
Final sulfiding before tests, type (method)	I. (Formal)	I. (Formal)
.....		
Specific surface area (BET), m ² /gram catalyst	169	170
Specific pore volume, cm ³ /gram catalyst	0.46	0.51
Sulfur content, grams/kg catalyst	49	56
Carbon Content, grams/kg catalyst	37	<3*
.....		

*lower limit of analysis

IV. B. Thiophene Hydrodesulfurization

This hydrodesulfurization study was based on the use of thiophene as a model reactant representative of the family of organic sulfur compounds most difficult to remove from petroleum feedstocks. Experiments were designed to examine the desulfurization of thiophene both as a pure reactant and in the presence of basic nitrogen compounds. The specific reaction studied was, using the stepwise mechanism discussed earlier:



Reactor parameters applicable to this work are given in the introductory section. Quantitative HDS results are presented as the conversion (disappearance) of the reactant thiophene as a function of reactor temperature at constant space velocity.

Pure thiophene runs were carried out at total pressures of 150, 500, and 1000 psig, and thiophene partial pressures of 93 and 186 torr. Simultaneous HDS-HDN reactions were run at the same three total pressures, using equal partial pressures of thiophene and pyridine of 93 torr. Thiophene

and n-butylamine were also used at equal partial pressures of 93 torr in a study at 1000 psig.

A study was made to determine the effect of the methyl substitution of the thiophene molecule on its desulfurization. This was the Master's thesis of Selahattin Gultekin (1977), carried out with the facilities and direction of this author. Details of the methylthiophene work beyond those presented here can be found in the referenced thesis.

IV. B. 1. Pure Thiophene HDS

The influence of hydrogen partial pressure on the conversion of thiophene at total pressures of 150, 500, and 1000 psig for a thiophene feed partial pressure of 93 torr is shown in Figure 4-3, and a detailed figure key is given in Table 4-2. The curves present the conversion of thiophene at reaction temperatures from 150 to 310°C at the three reaction pressures.

The conversion of thiophene was rapidly effected over the catalyst used at pressures as low as 150 psig, where complete conversion was achieved by approximately 310°C. Increasing the total pressure by increasing the hydrogen partial pressure caused no significant changes in the observed conversion at temperatures below 190°C. At higher reaction temperatures, however, significant conversion

gains accompanied each pressure increase; complete conversion was achieved by 290° and 270° at 500 and 1000 psig, respectively. The behavior of the conversion curves was similar at all pressures, including the presence of decreases in the slope of the conversion vs. temperature curves as complete conversion was approached.

The effect on thiophene conversion of doubling the partial pressure of thiophene while keeping other parameters constant is shown in Figure 4-4 for total pressures of 150 and 1000 psig. The basic nature of the curves for the 186 torr thiophene feed partial pressure was the same as that of the 93 torr curves. Conversions were lower at any given reaction temperature, indicating a reaction order less than one in thiophene.

Tetrahydrothiophene was detected in the product streams at those temperatures which yielded thiophene conversions between five and 50 percent. At 150 psig, for a 186 torr thiophene feed, the maximum amount observed as approximately 0.3 mole percent of the amount of thiophene fed. At this condition, the conversion of thiophene was seven percent.

At 1000 psig, 186 torr thiophene feed, a maximum of five percent of the feed stream thiophene was saturated to tetrahydrothiophene at 230°C, at which temperature the conversion of thiophene was 25 percent. At a temperature

of 175°C, and a thiophene conversion of six percent, approximately one-third of this, or two percent of the thiophene fed, was reacted to tetrahydrothiophene. By 245°C, with about 50 percent thiophene conversion, there was very little tetrahydrothiophene in the product stream; none was present above this temperature.

IV. B. 2. Thiophene HDS in the Presence of Nitrogen Compounds

A study was made of the effect of the presence of pyridine on thiophene HDS by using a mixed thiophene-pyridine feed in a series of runs at 150, 500, and 1000 psig. For both pure-thiophene and thiophene-pyridine feed cases, the partial pressure of thiophene was maintained at 93 torr. For the mixed-feed cases pyridine was added to the reactant stream at the same partial pressure, 93 torr. Figure 4-5 shows the effect of the mixed feed on the conversion of thiophene by comparing the thiophene-pyridine data with the pure-thiophene data from Figure 4-3. For all pressures studied there was a strong inhibition, resulting in similar shifts of the three curves to higher temperature ranges. The qualitative behavior of the mixed-feed curves was again similar to that of the pure-thiophene feed curves.

To compare the effect of ammonia with that of pyridine on thiophene HDS, n-butylamine was added in equimolar

amounts with thiophene to a 93 torr thiophene feed at 1000 psig, intending that the decomposition of the amine would produce ammonia of the same partial pressure when decomposed. The butylamine, however, did not react as rapidly as had been expected, and, in fact, was converted at a rate closer to that of pyridine. Figure 4-6 shows the thiophene conversion for the thiophene-butylamine run, together with its conversions for the pure-feed and thiophene-pyridine feed cases. The inhibition by the resulting butylamine-ammonia mixture was nearly identical to that of pyridine, with the two mixed-feed curves showing a slight divergence at higher conversions.

Tetrahydrothiophene was not present in the product streams of the mixed thiophene-pyridine feed runs. Its qualitative presence could have been detected at levels as low as 0.1 percent of the amount of thiophene fed.

IV. B. 3. Effect of Methyl Substitution on Thiophene HDS

A study was carried out to determine the effect on thiophene HDS of the addition of methyl groups to the thiophene molecule. Thiophene, 2-methylthiophene, and 2,5-dimethylthiophene were fed separately to the reactor at partial pressures of 186 torr and a total pressure of 500 psig. The substituted compounds have the structures:

Table 4-2
Key for Thiophene HDS Figures:
4-3, 4-4, 4-5, 4-6, 4-7

<u>Symbol represents</u>	<u>Run Number</u>	<u>Total Pressure</u>	<u>Thiophene Feed</u>			<u>Pyridine Feed</u>		
			<u>psig</u>	<u>bars</u>	<u>Partial Pressure</u> <u>torr</u>	<u>Partial Pressure</u> <u>bars</u>	<u>Partial Pressure</u> <u>torr</u>	<u>Partial Pressure</u> <u>bars</u>
◇	THI	44	1000	69.95	93.6	0.1248	---	---
△	THI	43	499	35.43	93.6	0.1248	---	---
○	THI	42	150	11.34	92.2	0.1230	---	---
◊	THI	46	1000	69.96	192.1	0.2562	---	---
⊖	THI	45	150	11.34	184.7	0.2462	---	---
◆	THI	49	1000	69.96	94.5	0.1260	94.4	0.1259
◈	THI	53	999	69.90	95.0	0.1267	94.8	0.1264
▲	THI	50	500	35.44	95.5	0.1274	95.4	0.1271
●	THI	48	150	11.34	91.6	0.1221	91.5	0.1220
⊙	THI	51	149	11.30	92.5	0.1233	92.3	0.1230
⊚	THI	52	150	11.35	91.5	0.1219	91.3	0.1217
■	THI	55	1000	69.96	92.0	0.1227	92.0	0.1227

(n-butylamine)

Figure 4-7

□	THI	60	500	35.49	187.1	0.2495	---	---
△	DMT	61	500	35.47	189.4	0.2525 (DMT)	-	---
○	MT	62	498	35.36	188.0	0.2506 (MT)	--	---
⊖	MT	63	500	35.51	188.6	0.2514 (MT)	--	---

Notes:

THI = Thiophene

MT = 2-methylthiophene

DMT = 2,5-dimethylthiophene

Catalyst: sulfided NiMo/Al₂O₃

Details of each run are given in the Appendix

1 bar = 10⁵pascal = 10⁵N/m²

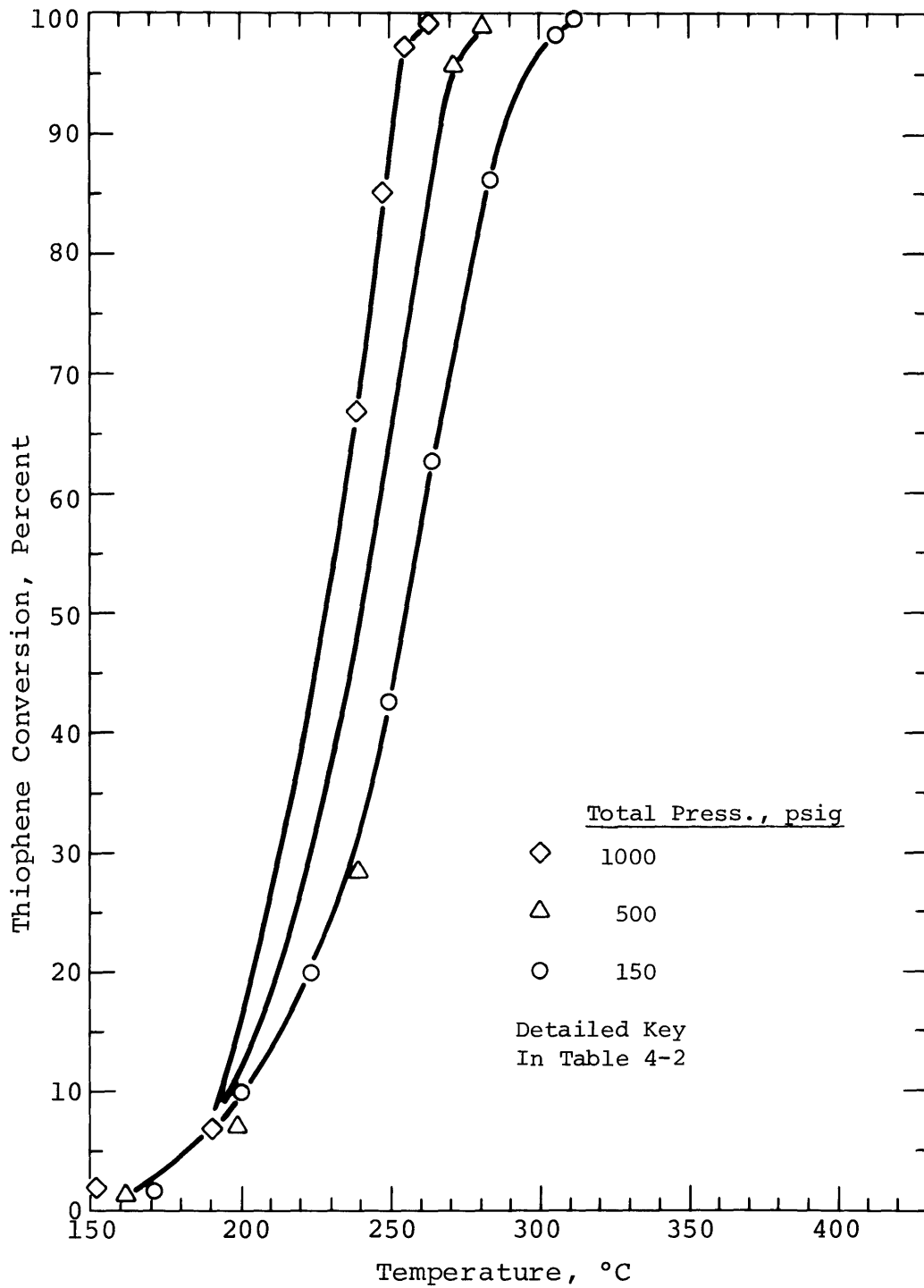


Figure 4-3: Thiophene HDS for Pure Thiophene (93 torr Partial Pressure) Feeds at Total Pressures of 150, 500, and 1000 psig.

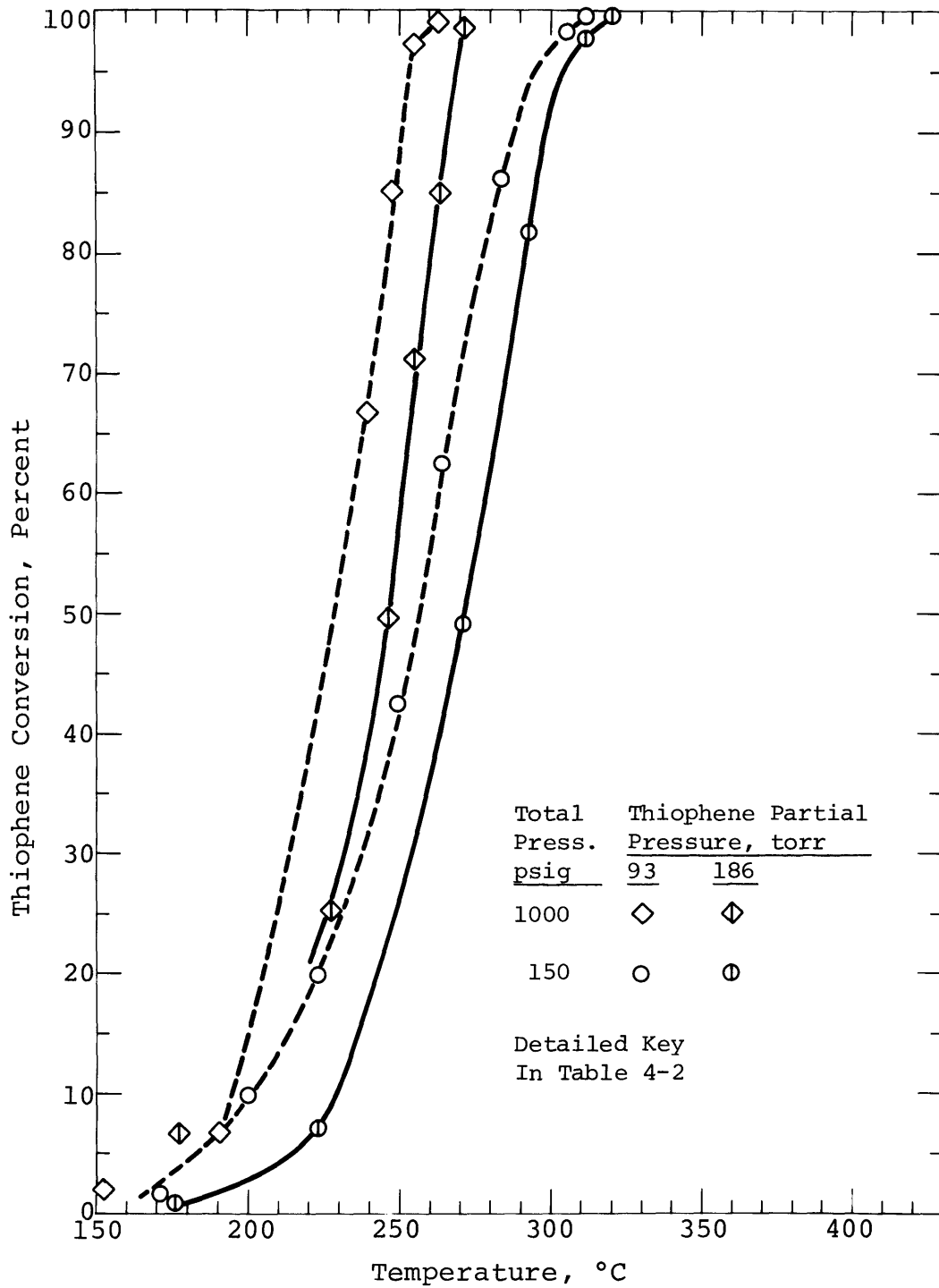


Figure 4-4: Thiophene HDS: Effect of the Partial Pressure of Thiophene on Thiophene Conversion at Total Pressures of 150 and 1000 psig.

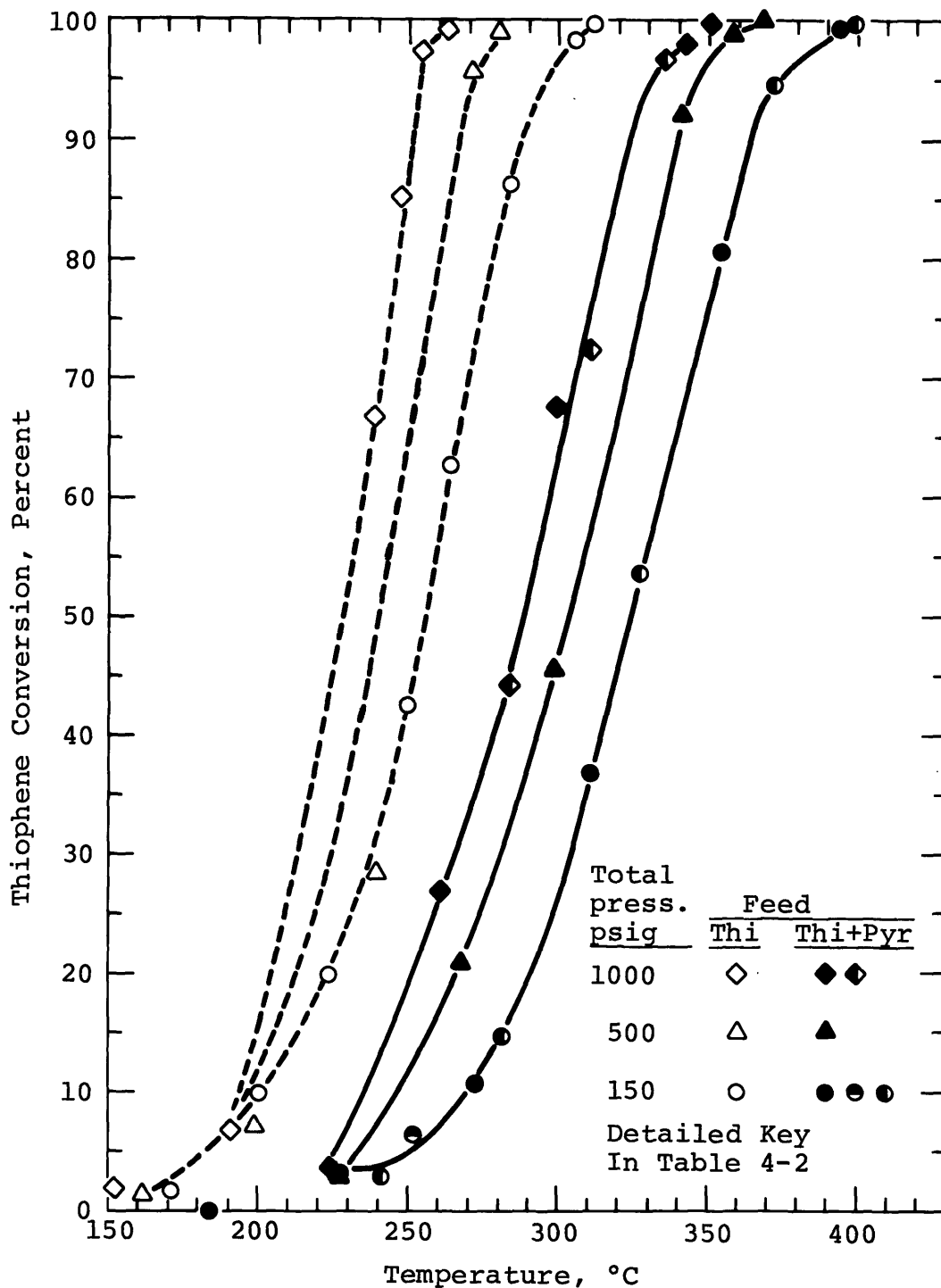


Figure 4-5: Thiophene HDS for Pure Thiophene (93 torr Partial Pressure) and Mixed Thiophene (93 torr)-Pyridine (93 torr) Feeds at Total Pressures of 150, 500, and 1000 psig.

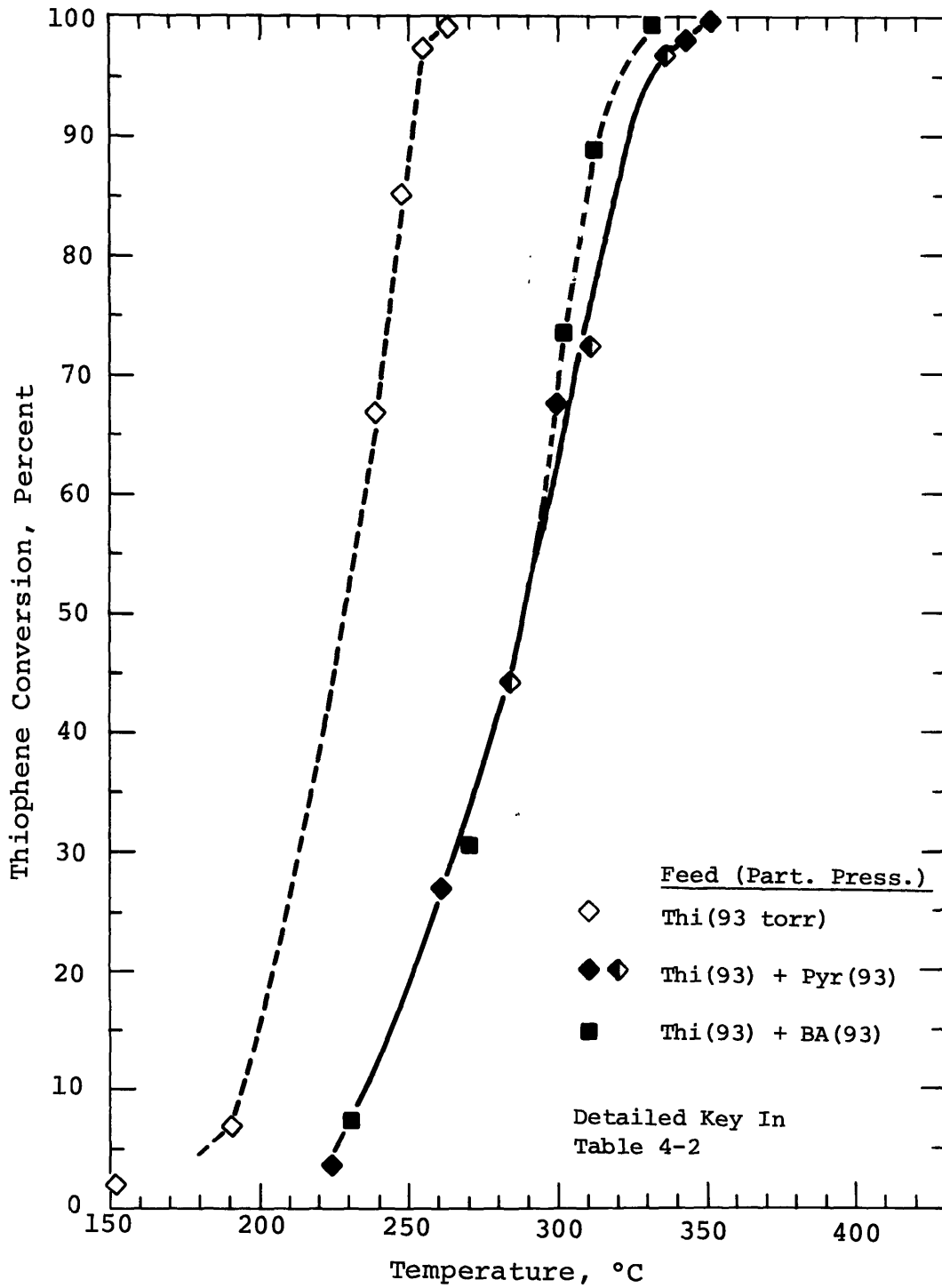


Figure 4-6: Comparison of the Effects of Pyridine and Combined Butylamine (BA) plus Ammonia on the Conversion of Thiophene at a Total Pressure of 1000 psig.

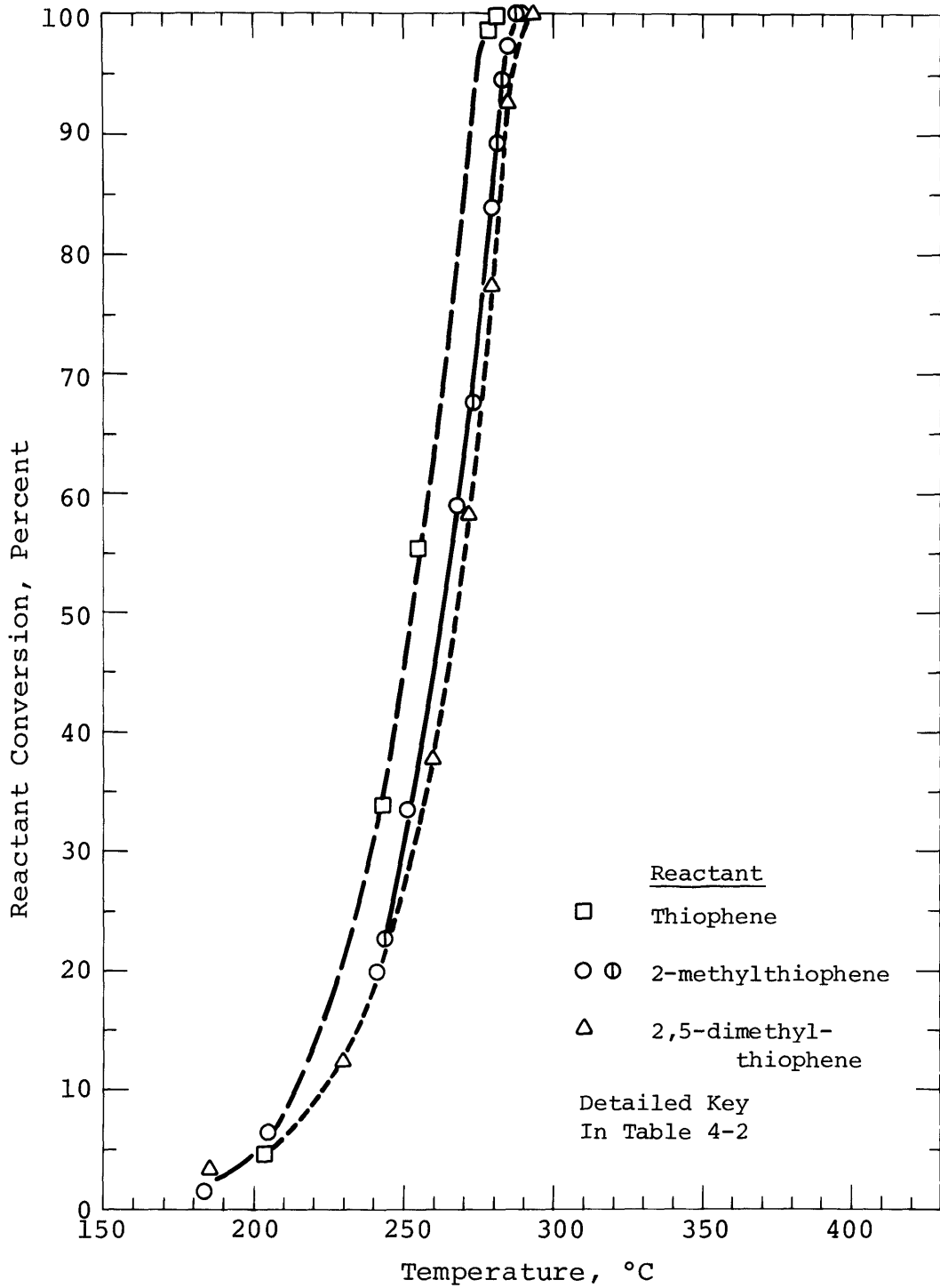


Figure 4-7: Thiophene HDS: Effect of Methyl Substitution of Thiophene on Reactant Conversion at a Total Pressure of 500 psig.

2-methylthiophene



2,5-dimethylthiophene

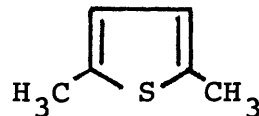
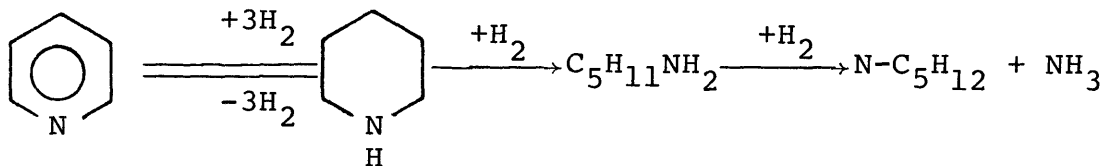


Figure 4-7 presents the conversion of the three compounds as a function of reaction temperature. The shifted conversion curves show that 2-methylthiophene exhibits an inhibition relative to thiophene, and that there is a small but distinct further inhibition for 2,5-dimethylthiophene.

IV. C. Pyridine Hydrodenitrogenation

This hydrodenitrogenation study is based on the use of pyridine as the model reactant representative of the family of organic nitrogen compounds most difficult to hydrogenate in petroleum feedstocks. Experiments were designed to examine the applicability of a stepwise reaction mechanism for pyridine HDN both as a pure reactant and in the presence of sulfur compounds; the results are all directed toward and should be examined in light of this purpose. The steps involved, as previously presented, are the reversible hydrogenation of pyridine to piperidine, followed by an irreversible hydrogenolysis of piperidine to n-pentylamine, with subsequent hydrogenolysis to n-pentane and ammonia:



Evidence of the extent of side reactions is discussed as well.

Reactor parameters applicable to this work were given in the overall Results introduction. Quantitative HDN results are presented in two forms: the conversion (disappearance) of reactant as a function of reactor temperature at constant space velocity; and the normalized concentration of components in the product stream, expressed as the moles of a component in the product stream per mole of pyridine in the feed stream of the reactor.

Pure pyridine reactions were carried out at total pressures of 150, 500, and 1000 psig, and pyridine partial pressures of 93 and 186 torr. Simultaneous HDN-HDS reactions were run at the same three total pressures, using equal pyridine and thiophene partial pressures of 93 torr. 1-propanethiol and pyridine were also used at equal partial pressures of 93 torr in a study at 1000 psig.

IV. C. 1. Pure Pyridine HDN

The influence of hydrogen partial pressure on the HDN of pyridine was studied at total reactor pressures of 150,

500, and 1000 psig. The effects on the conversion (hydrogenation) of pyridine for a pyridine feed partial pressure of 93 torr are shown in Figure 4-8, and a detailed figure key is given in Table 4-3. The curves present the conversion of pyridine at reaction temperatures from 190° to 410°C at the three reaction pressures.

Pyridine hydrogenation was independent of total pressure at temperatures less than 200°C, as the low conversions obtained in that range were indistinguishable, from 150 to 1000 psig. As the temperature increased, the effect of pressure was quite pronounced. Data at 150 psig showed increasing conversions until approximately 350°C, where the curve began to level off, exhibiting a maximum of 29 percent at 370°, and then decreasing to 20 percent at 410°. In contrast, at 1000 psig conversion increased rapidly with temperature until reaching levels greater than 90 percent. Complete conversion was achieved at 390°C. Results at 500 psig were expectedly intermediate between the other pressures, though more similar to the behavior at 1000 psig. Rapid increases in conversion tapered off until a maximum of 86 percent was achieved at 410°C. It is possible that denitrogenation at 500 psig would have reached a maximum similar to that at 150 psig, but the temperature limit of the catalyst precluded obtaining higher-temperature data.

The formation of the reaction intermediate piperidine in the HDN of pure pyridine is shown in Figure 4-9 as its normalized concentration as a function of reaction temperature. Expressed as the moles of piperidine in the product stream per mole of pyridine in the reactant stream, the concentration reached a maximum at approximately 315°C at each reaction pressure, the higher pressures greatly increasing the amounts present. By 400°, piperidine had essentially disappeared from the product stream.

For pure-pyridine runs, three components were identified in the product stream: pyridine, piperidine, and n-pentylamine. Figure 4-10 shows the relationship of these components as their normalized concentrations as a function of reaction temperature, for a total reactor pressure of 1000 psig. The pyridine curve is complementary to its conversion curve of Figure 4-8, and the piperidine curve is that of Figure 4-9. N-pentylamine in the product stream was never more than one mole percent of the amount of pyridine fed, and was only observed at this pressure at temperatures of 270° and 300°C. The relationship between the pyridine and piperidine curves should be noted. Whereas pyridine was rapidly converted, for instance, to four percent of its feed concentration at 330°C, the piperidine concentration increased as pyridine disappeared, and was still present in substantial quantities

(40 percent of the molar pyridine feed) at 350°C.

Similar results were obtained at 500 psig, although the lower pyridine conversions and piperidine presence did not lead to such extreme behavior. At 150 psig piperidine was always a small fraction of the amount of pyridine present, due to the very low pyridine conversions and piperidine concentrations. N-pentylamine was detected only in extremely small amounts at the two lower pressures, on the order of 0.001 mole per mole of pyridine fed. These 500 and 150 psig results are included in subsequent figures in comparisons with mixed pyridine-thiophene feed results.

The effect on pyridine conversion of doubling the partial pressure of pyridine, while keeping other parameters constant, was examined at total pressures of 150 and 1000 psig. As shown in Figure 4-11, the qualitative behaviors of the curves for 186 torr pyridine partial pressure were similar to those of 93 torr. Conversions for the higher partial pressures were less at any given temperature, indicating a reaction order less than one in pyridine.

Figure 4-12 shows the effect of doubling the pyridine partial pressure on the presence of piperidine in the product stream. At 150 psig there was no significant difference between the 93 and 186 torr results. At 1000 psig, the piperidine curves were shifted, for any given

concentration, to temperatures 15 to 20 degrees higher than those of the 93 torr curves. This shift was the same as that observed for the pyridine conversion data.

While the chromatographic identifications of pyridine, piperidine, and n-pentylamine were determined by direct injection of the pure compounds, there were three or four small peaks present in the product stream which were not the light reaction products ammonia and pentane. The total concentration of the small peak areas analyzed was approximately 0.5 mole percent of the pyridine fed to the reactor.

An attempt was made to identify these smaller product peaks using mass spectrometric (GC-MS) analysis. Reactor conditions for this analysis were chosen to be 150 psig total pressure, a pyridine partial pressure of 186 torr, and a temperature of 360°C, as these had produced the largest concentrations of the compounds in previous runs. The sensitivity of the flame ionization detector in the gas chromatograph (GC) with the mass spectrometer was greater than that of the thermal conductivity detector in the GC used for the on-line reactor stream analysis. Thus where the sample from the on-line GC indicated four peaks, with the smallest having an area of 0.1 percent of the amount of pyridine fed, the more sensitive unit detected a number of even smaller peaks in the condensed

effluent stream sample. Due to the extremely small, and not necessarily completely resolved peak areas, it was not possible to identify (with one exception), specific compounds in the GC-MS analysis. However, possible general classes of compounds were determined. Low-boiling compounds, those eluted before pyridine and piperidine, consisted mainly of unsaturated hydrocarbons. High boilers, those eluted after pyridine, consisted of substituted, unsaturated ring compounds, and possibly unsaturated rings linked by alkyl side chains. A specifically-identified example of the former was 4-n-pentylpyridine.

Table 4-3

Key for Pure-Pyridine Feed HDN Figures:

4-8, 4-9, 4-10, 4-11, 4-12

<u>Symbol</u>	<u>Symbol represents</u>	<u>Run number</u>	<u>Total pressure</u>		<u>Pyridine feed partial pressure</u>	
			<u>psig</u>	<u>bars</u>	<u>torr</u>	<u>bars</u>
<u>Figures 4-8, 4-9, 4-11, 4-12</u>						
◇	as per figure title	38	1000	69.95	95.1	0.1268
△	"	40	500	35.48	96.2	0.1283
○	"	39	151	11.40	89.6	0.1195
◈	"	41	1000	69.96	185.4	0.2472
⊙	"	47	150	11.36	181.0	0.2413

Figures 4-10

◇	PYR	}	38	1000	69.95	95.1	0.1268
○	PIP						
△	NPA						

Notes

PYR = Pyridine

PIP = Piperidine

NPA = N-pentyl amine

Catalyst: sulfided NiMo/Al₂O₃

1 bar = 10⁵ pascal = 10⁵N/m²

Details of each run are given in the Appendix

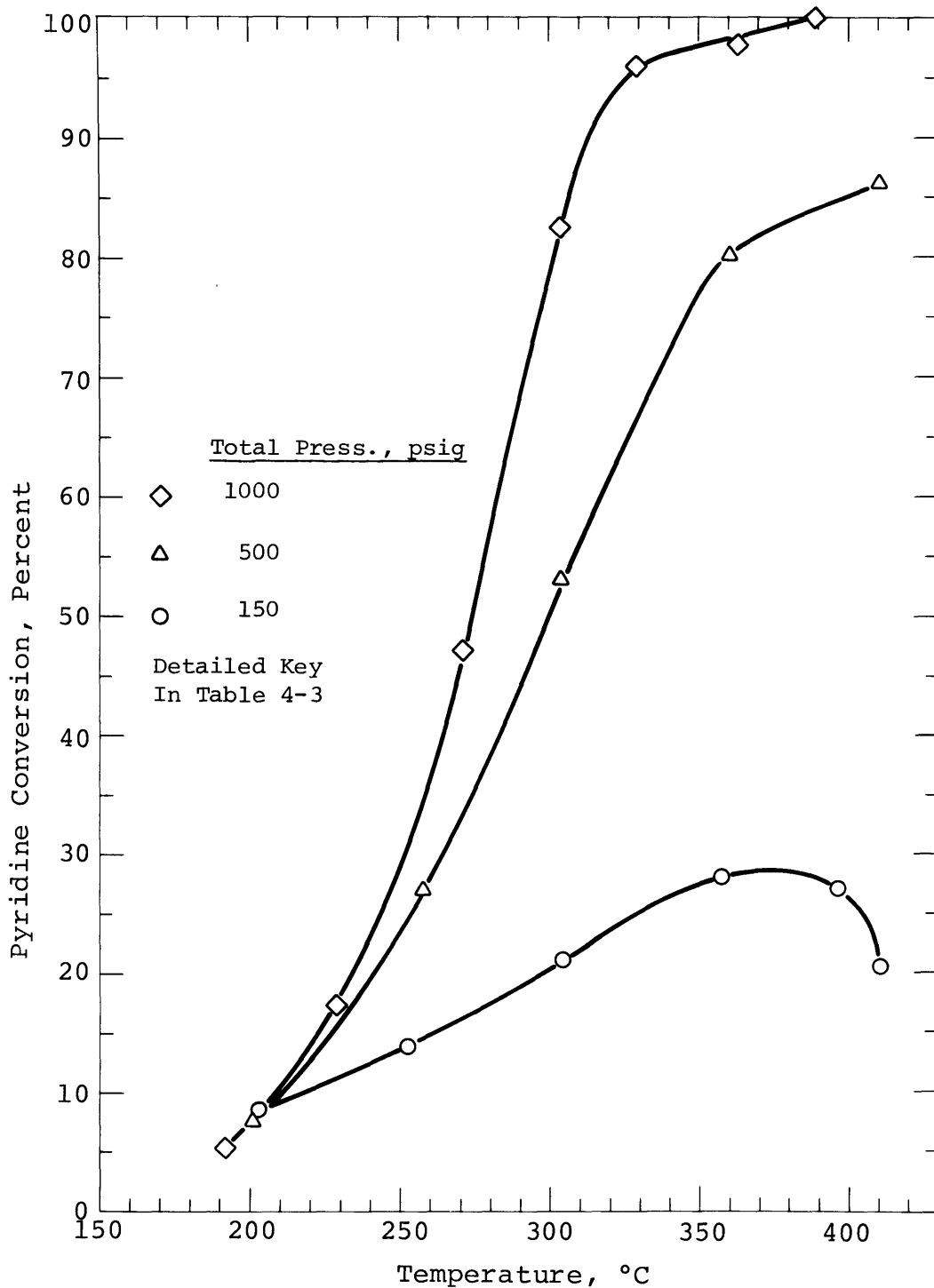


Figure 4-8: Pyridine HDN for Pure Pyridine (93 torr Partial Pressure) Feeds at Total Pressures of 150, 500, and 1000 psig.

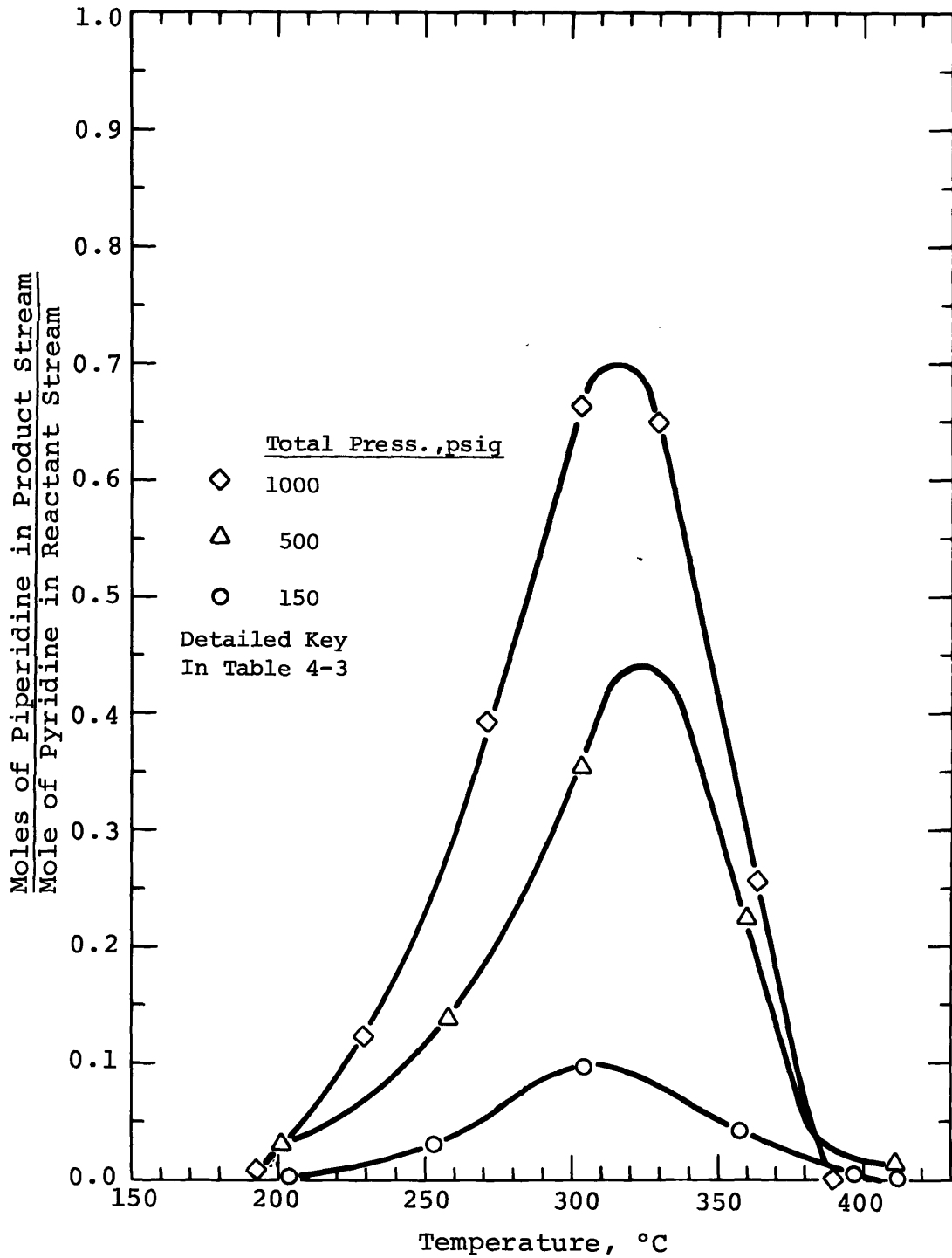


Figure 4-9: Piperidine Presence in the Product Stream for Pure-Pyridine (93 torr Partial Pressure) Feeds at Total Pressures of 150, 500, and 1000 psig.

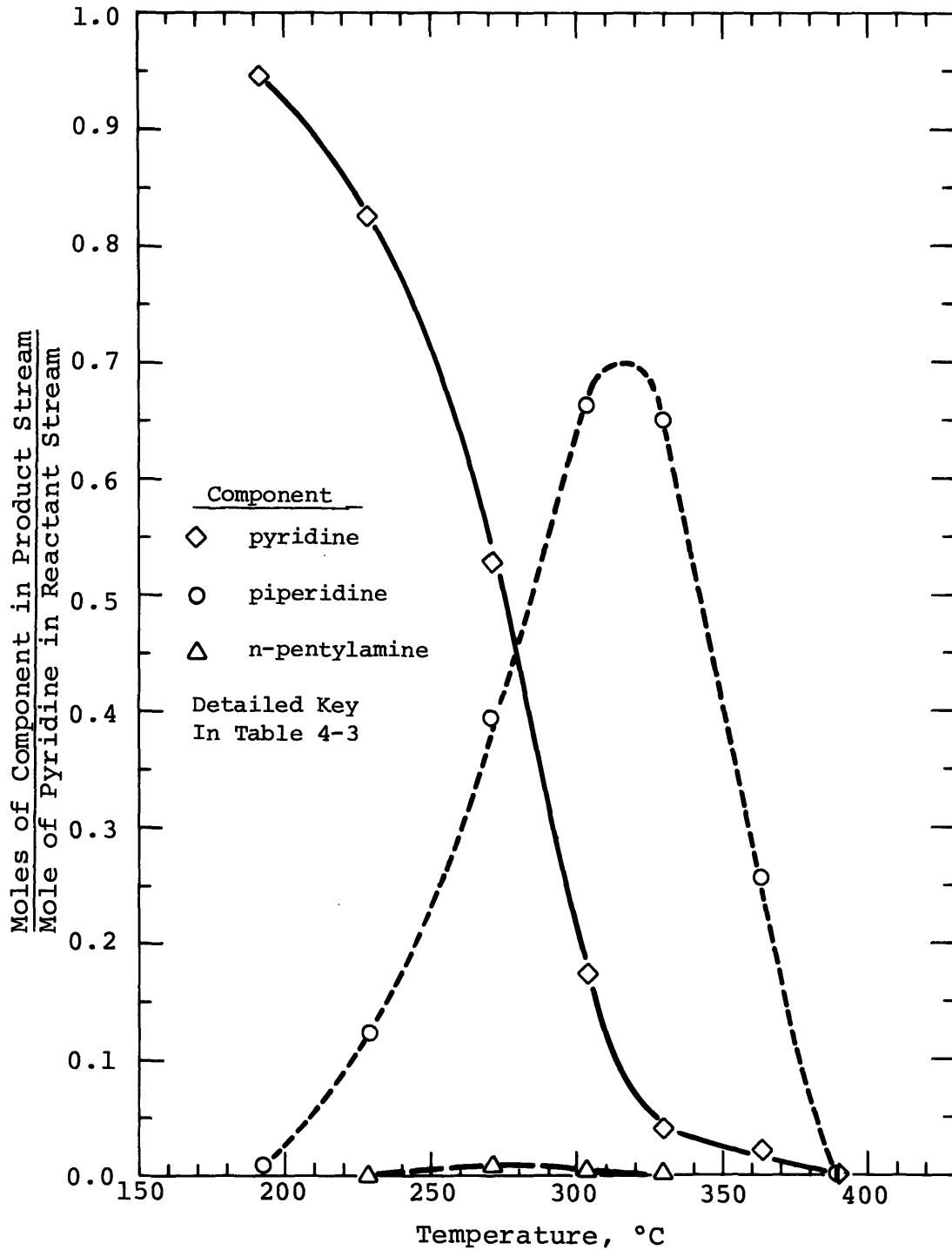


Figure 4-10: Product Distribution for Pyridine HDN
For a Pure Pyridine (93 torr Partial Pressure)
Feed at a Total Pressure of 1000 psig.

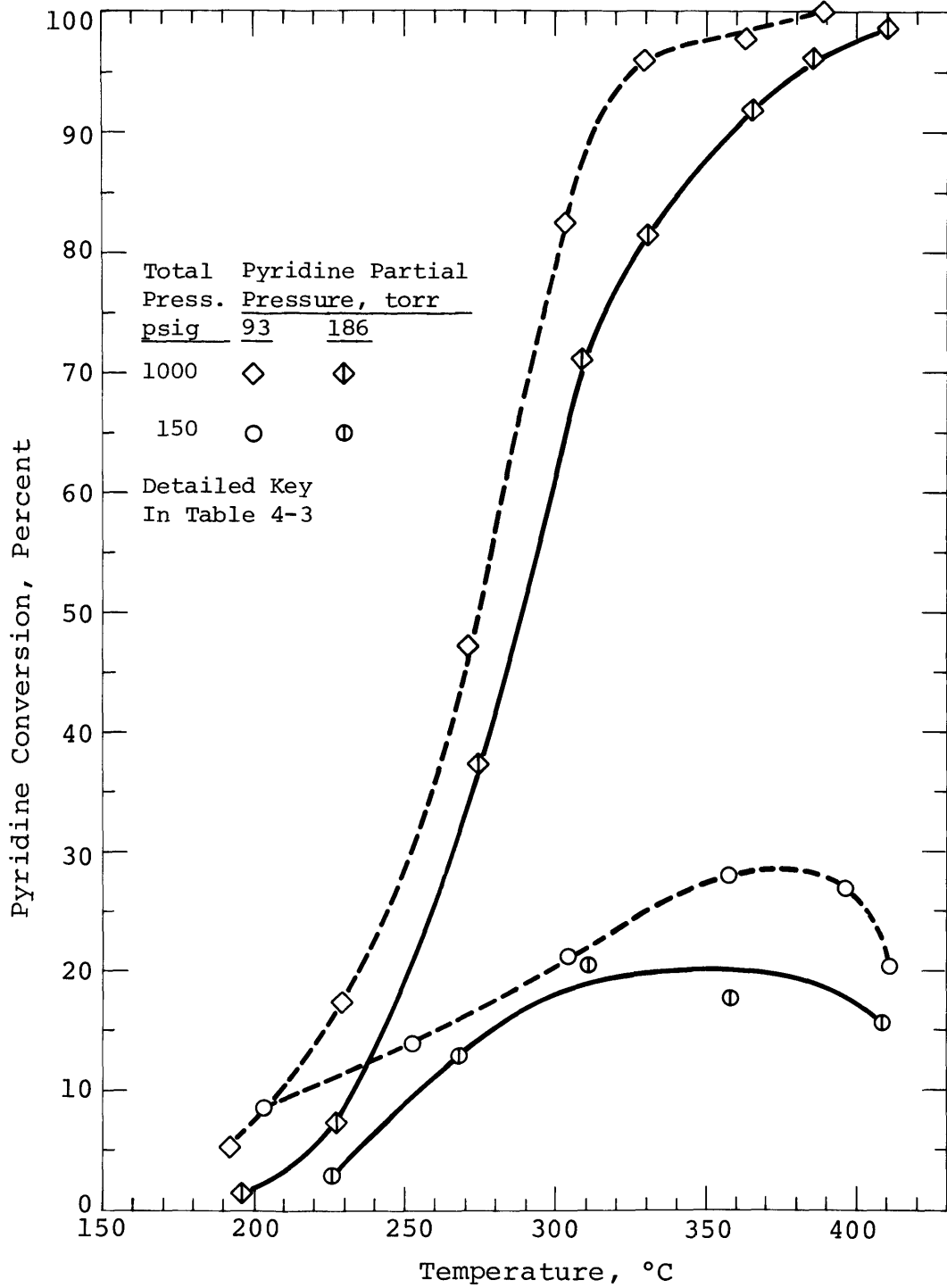


Figure 4-11: Pyridine HDN: Effect of the Partial Pressure of Pyridine on Pyridine Conversion at Total Pressures of 150 and 1000 psig.

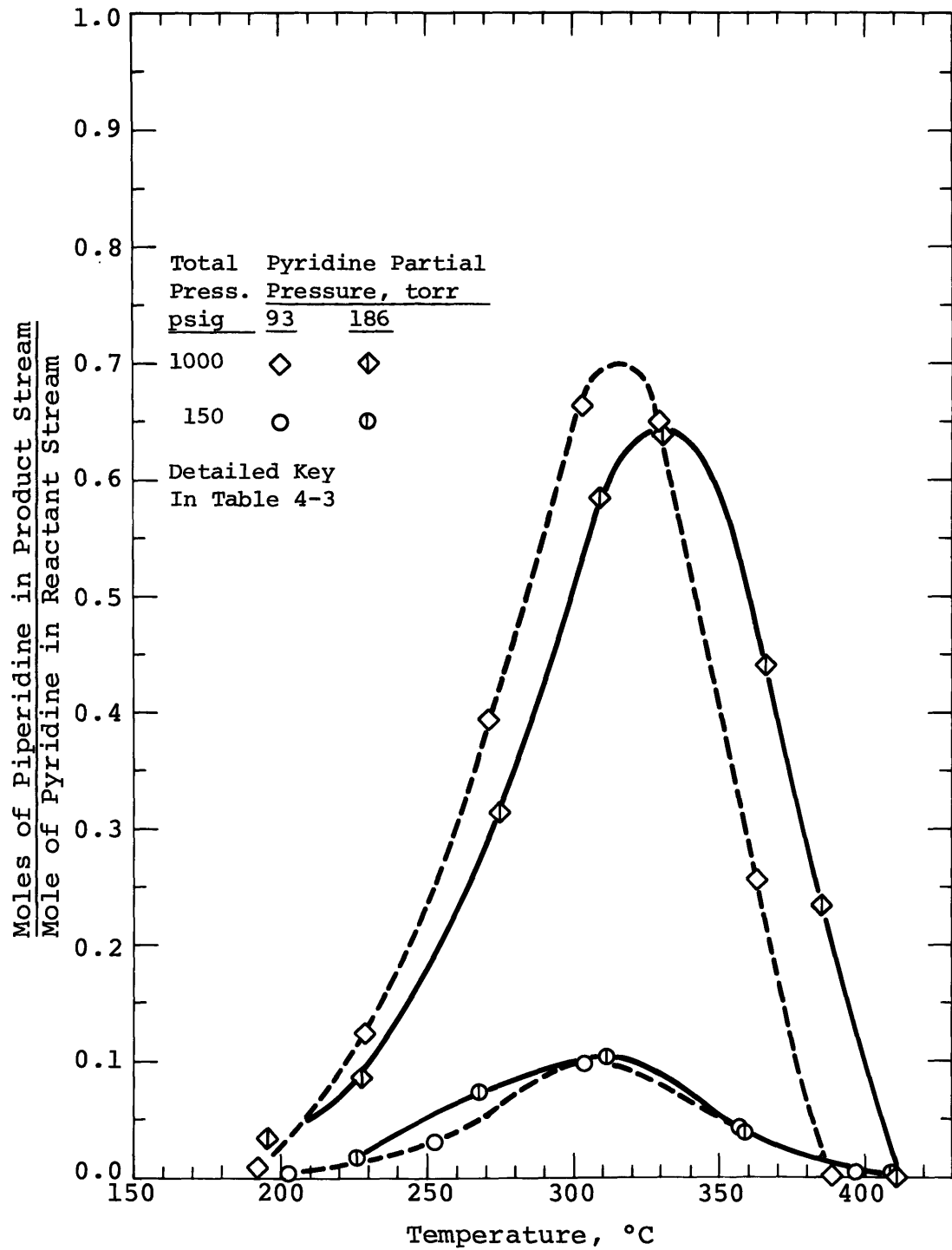


Figure 4-12: Pyridine HDN: Effect of the Partial Pressure of Pyridine on the Amount of Piperidine Present in the Product Stream at Total Pressures of 150 and 1000 psig.

IV. C. 2. Pyridine HDN in the Presence of Sulfur Compounds

The effect of the presence of thiophene on pyridine HDN was investigated by using the mixed pyridine-thiophene feed in a series of runs at 150, 500, and 1000 psig. For both pure-pyridine and pyridine-thiophene feeds, the partial pressure of pyridine was maintained at 93 torr. For the mixed-feed runs, thiophene was added to the reactant stream at the same partial pressure, 93 torr. Figure 4-13 shows the effect of the mixed feed on the conversion of pyridine by comparing the pyridine-thiophene data with the pure-pyridine data from Figure 4-8. At 150 and 500 psig a large inhibition at lower reaction temperatures was maintained until the pure-feed curves decreased their slopes, at which point an enhancement began. At 150 psig the previously observed downturn was eliminated, and at 500 psig complete conversion was achieved by 390°C. At 1000 psig a mild inhibition was observed above 280°C, until at 350° the same type of enhancement was seen as at the lower pressures, with the temperature required for complete conversion decreasing from 390° to 360°C.

The effect of hydrogen sulfide on pyridine HDN was studied for comparison with the effects of thiophene. With the pyridine partial pressure maintained at 93 torr, H₂S was added to the reactant mixture by feeding 1-propanethiol

in an equimolar amount with pyridine. The propanethiol was completely converted to H_2S at temperatures above $250^\circ C$, giving a reaction mixture with 93 torr of H_2S over most of the temperature range. Figure 4-14 shows the H_2S to have a stronger inhibiting effect than thiophene over the entire temperature range, except where enhancement at higher temperatures led to the same $360^\circ C$ point for complete conversion.

The addition of thiophene to the reactor feed in equal partial pressure with pyridine caused the amount of piperidine formed at all temperatures to decrease significantly. Figure 4-15 shows the normalized concentration of piperidine at 150 and 1000 psig total pressures for both pure-pyridine and pyridine-thiophene feeds. While the maxima maintained the same placement with temperature, the maximum amounts of piperidine formed were only from 20 to 60 percent of those for the pure-pyridine feeds. Also included in the 1000 psig results are data representing the run using 1-propanethiol to produce H_2S . These points are consistent with those of the pyridine-thiophene feed; if any real difference exists, it would be toward a slightly higher piperidine peak. Piperidine results at 500 psig are included as part of a further analysis in Figure 4-17.

The effects of the presence of thiophene on the product distribution for pyridine HDN are shown at 1000, 500, and

150 psig in Figures 4-16, 4-17, and 4-18, respectively. Figure 4-16 compares the 1000 psig product distribution for pyridine-thiophene runs with the distribution from Figure 4-10 for pure pyridine HDN. The relative effects of thiophene on pyridine and piperidine outputs are clearly shown. Whereas there was little change in the pyridine disappearance, there were, at the same temperatures, gross decreases in the amounts of piperidine present. For example at 330°C the ratio of piperidine to pyridine decreased from 16 to 4 with the addition of thiophene to the feed. The significance of the high-pressure reaction condition makes this result of particular importance in future discussion sections. Data for n-pentylamine are not available for pyridine-thiophene feed runs, as the amine peak in the chromatographic analysis was obscured by that of thiophene.

The 500 psig product distribution shown in Figure 4-17 displays the same decreasing piperidine characteristics as at 1000 psig, but the larger amounts of pyridine and lower amounts of piperidine remaining in the product stream result in piperidine-to-pyridine ratios on the order of one or less for the pure-pyridine-feed case, and far less than one for the mixed-feed case.

The 150 psig product distribution, shown in Figure 4-18, was different from the high-pressure results because its

much lower pyridine conversion characteristics both maintain a large amount of pyridine in the product stream, and produce much less piperidine intermediate. With the addition of thiophene producing the greatest decrease in the piperidine output of all three pressures, while simultaneously decreasing pyridine conversion, the piperidine-to-pyridine ratio for this case is the lowest of those studied.

The conversion beyond piperidine, i.e. the disappearance of both pyridine and piperidine, is shown in Figure 4-19. Below 300°C, the relative positions of the curves are a function of the formation and disappearance of piperidine at each reaction pressure. Above this temperature, definite trends are apparent. At 500 and 1000 psig, where significant conversions took place, there was much higher conversion at any given temperature for pyridine-thiophene feedstock than for the pure-pyridine feed case, particularly at the higher pressure. At 150 psig, there was much less difference between the two cases, and the mixed feed did not show higher conversions until a reaction temperature of nearly 400°C was reached.

Table 4-4
Key for Pyridine-Thiophene Feed HDN Figures:
4-13, 4-14, 4-15, 5-6, 5-7, 5-8

<u>Symbol</u>	<u>Symbol</u> <u>represents</u>	<u>Run</u> <u>Number</u>	<u>Total Pressure</u>		<u>Pyridine feed</u>		<u>Thiophene feed</u>	
			<u>psig</u>	<u>bars</u>	<u>torr</u>	<u>bars</u>	<u>torr</u>	<u>bars</u>
◇	as per figure title	38	1000	69.95	95.1	0.1268	---	---
△		40	500	35.48	96.1	0.1283	---	---
○	"	39	151	11.40	89.6	0.1195	---	---
◆	"	49	1000	69.96	94.4	0.1259	94.5	0.1260
◊	"	53	999	69.90	94.8	0.1264	95.0	0.1267
▲	"	50	500	35.44	95.4	0.1271	95.5	0.1274
●	"	48	150	11.34	91.5	0.1220	91.6	0.1221
◐	"	51	149	11.30	92.3	0.1230	92.5	0.1233
◑	"	52	150	11.35	91.3	0.1217	91.5	0.1219
■	"	54	1000	69.97	91.9	0.1226	91.8	0.1225 (propanethiol)

Notes

1 bar = 10^5 pascal = 10^5 N/m²
 Catalyst: sulfided NiMo/Al₂O₃
 Details of each run are given in the Appendix

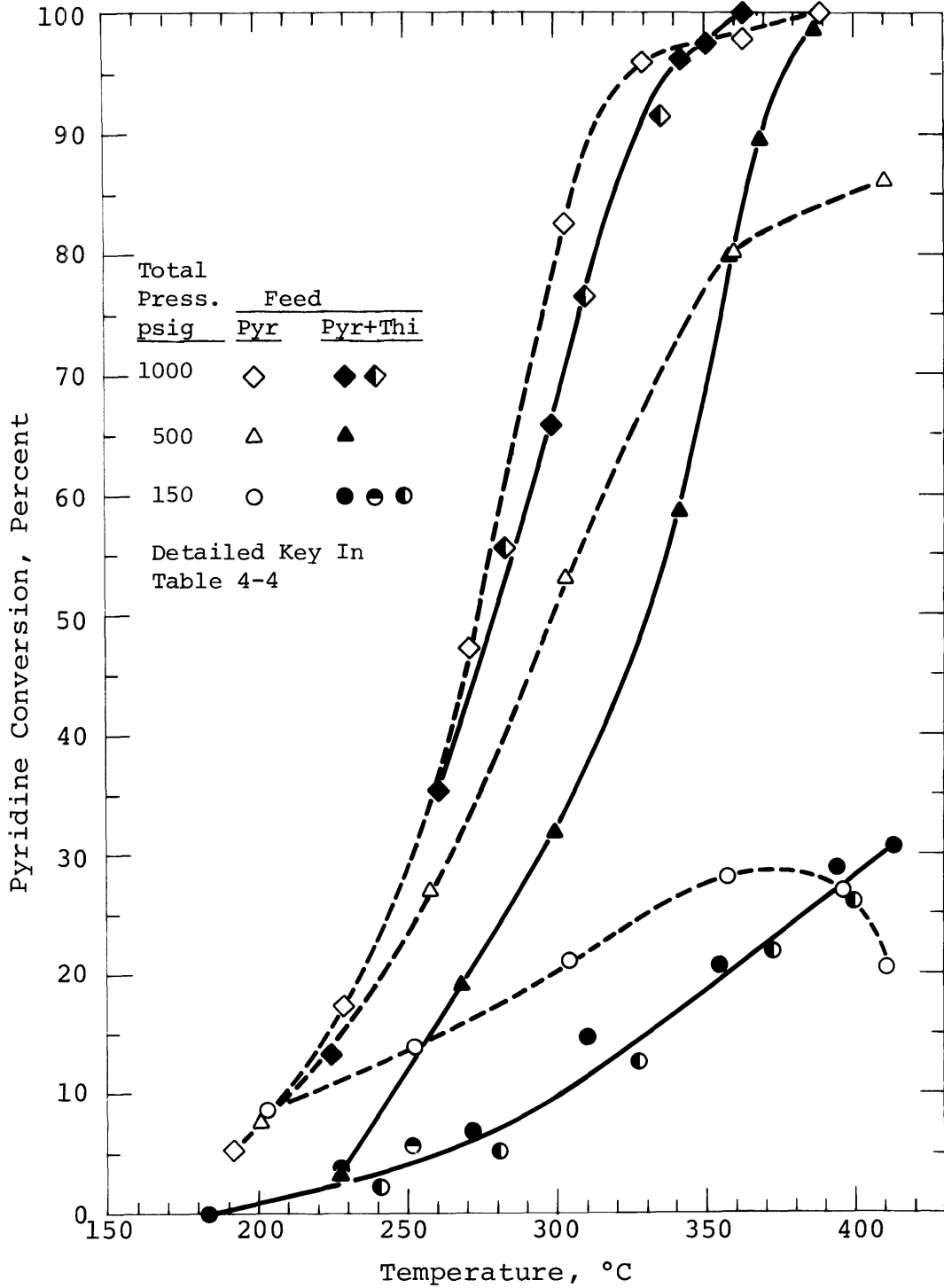


Figure 4-13: Pyridine HDN for Pure Pyridine (93 torr Partial Pressure) and Mixed Pyridine (93 torr)-Thiophene (93 torr) Feeds at Total Pressures of 150, 500, and 1000 psig.

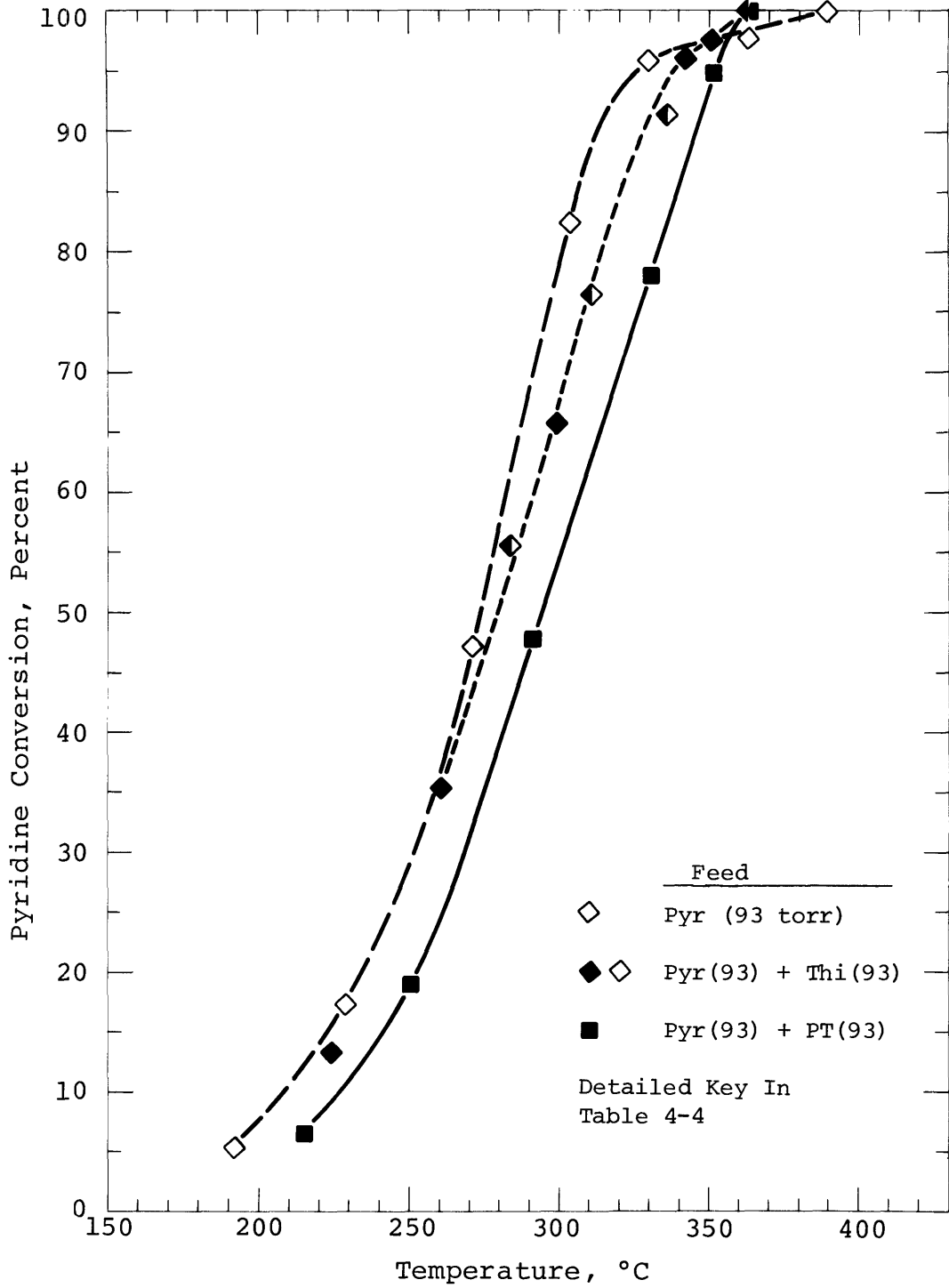


Figure 4-14: Comparison of the Effects of Hydrogen Sulfide and Thiophene on Pyridine Conversion at a Total Pressure of 1000 psig, using Propanethiol in Feed for Hydrogen Sulfide Generation.

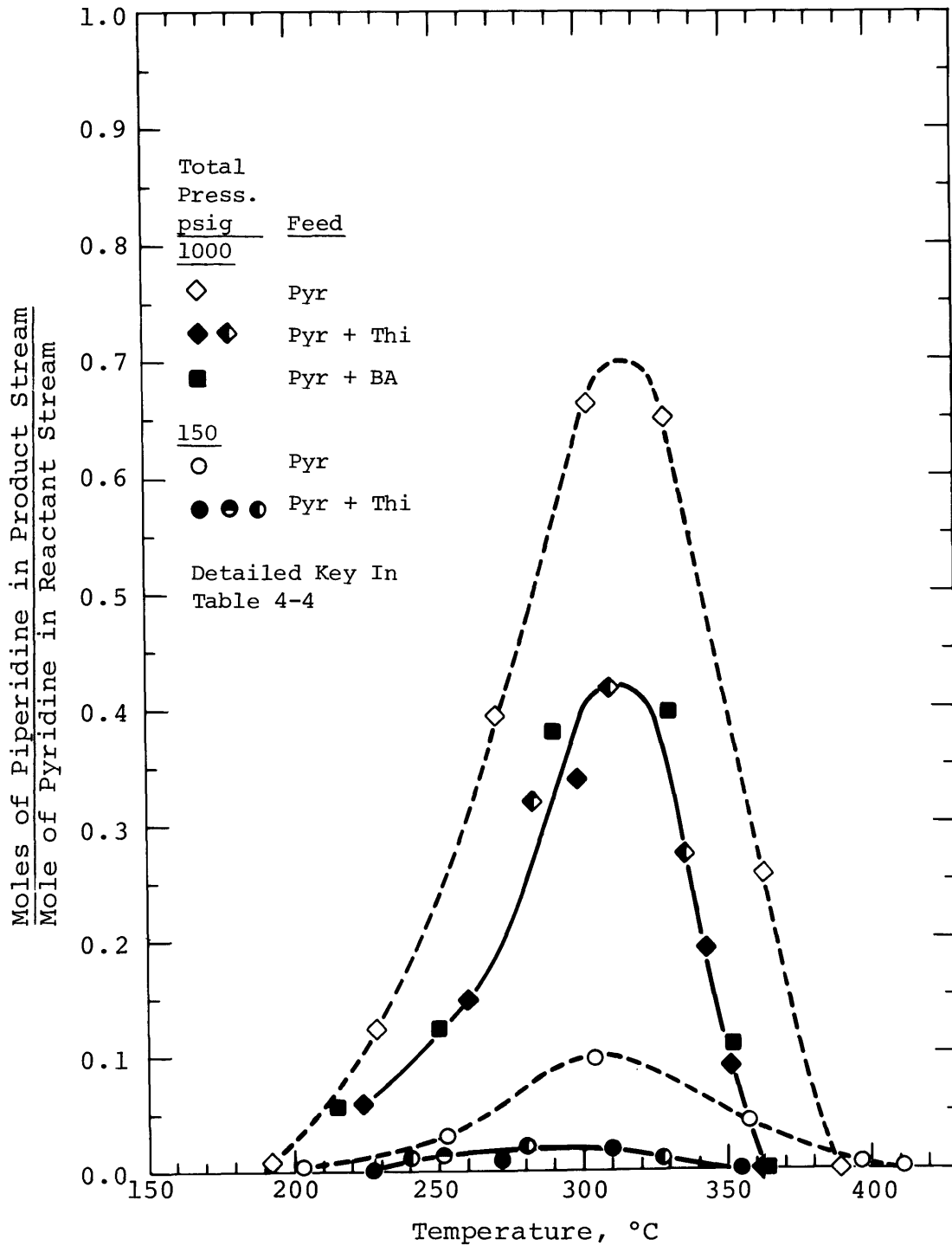


Figure 4-15: Piperidine Presence in the Product Stream For Pure Pyridine (93 torr partial press.) and Mixed Pyridine (93 torr)-Thiophene (93 torr) Feeds at Total Pressures of 150 and 1000 psig.

Table 4-5
Key for Pure-Pyridine and Pyridine-Thiophene Feed
HDN Product Distribution Figures:
4-16, 4-17- 4-18

<u>Symbol</u>	<u>Symbol represents</u>	<u>Run Number</u>	<u>Total Pressure</u>	<u>Pyridine feed</u>		<u>Thiophene feed</u>		
				<u>psig</u>	<u>bars</u>	<u>torr</u>	<u>bars</u>	<u>torr</u>
Figure 4-16								
◇	PYR	38	1000	69.95	95.1	0.1268	---	---
○	PIP							
△	NPA							
◆	PYR	49	1000	69.96	94.4	0.1259	94.5	0.1260
●	PIP							
◈	PYR	53	999	69.90	94.8	0.1264	95.0	0.1267
●	PIP							
Figure 4-17								
◇	PYR	40	500	35.48	96.2	0.1283	---	---
○	PIP							
△	NPA							
◆	PYR	50	500	35.44	95.4	0.1271	95.5	0.1274
●	PIP							
Figure 4-18								
◇	PYR	39	151	11.40	89.6	0.1195	---	---
○	PIP							
△	NPA							
◆	PYR	48	150	11.34	91.5	0.1220	91.6	0.1221
●	PIP							
◈	PYR	51	149	11.30	92.3	0.1230	92.5	0.1233
●	PIP							
◈	PYR	52	150	11.35	91.3	0.1217	91.5	0.1219
●	PIP							

Notes

PYR = Pyridine
 PIP = Piperidine
 NPA = n-Pentyl amine

1 bar = 10^5 pascal = 10^5 N/m²

Catalyst: sulfided NiMo/Al₂O₃

Details of each run are given in the Appendix

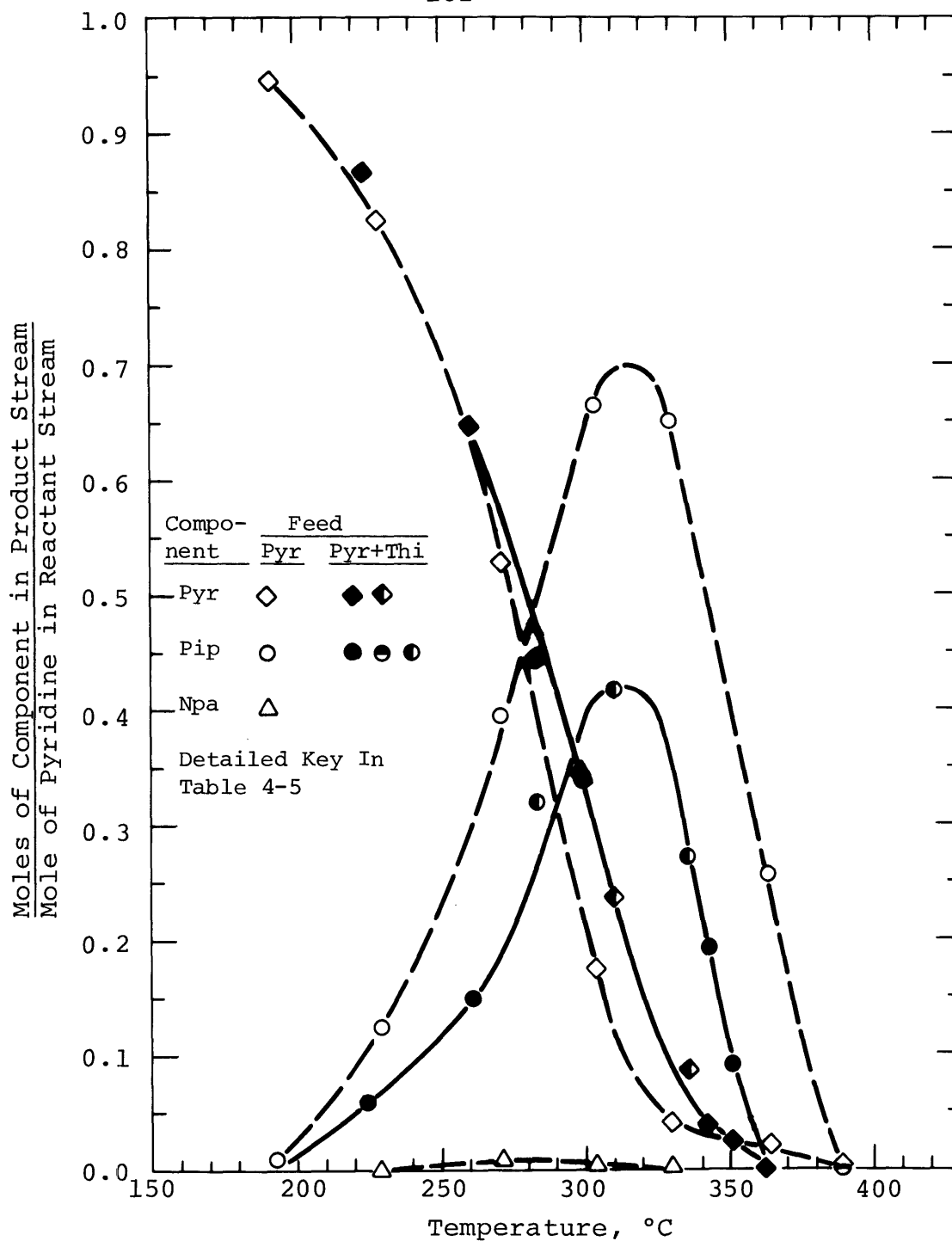


Figure 4-16: Product Distributions for Pyridine HDN For Pure Pyridine (93 torr partial press.) and Mixed Pyridine (93 torr)-Thiophene (93 torr) Feeds At a Total Pressure of 1000 psig. (Pip=piperidine, Npa=n-pentylamine)

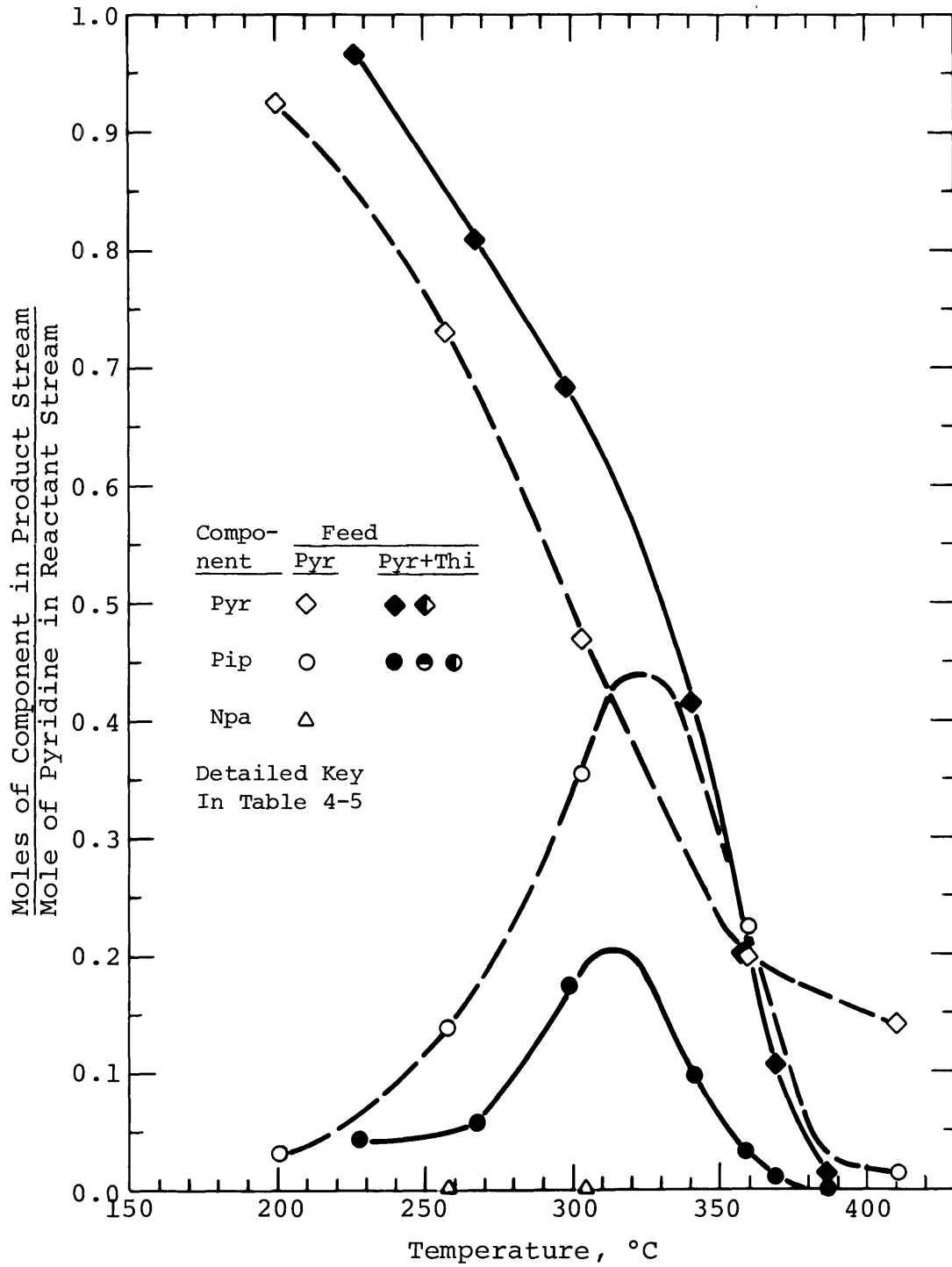


Figure 4-17: Product Distributions for Pyridine HDN For Pure Pyridine (93 torr partial press.) and Mixed Pyridine (93 torr)-Thiophene (93 torr) Feeds At a Total Pressure of 500 psig. (Pip=piperidine, Npa=n-pentylamine)

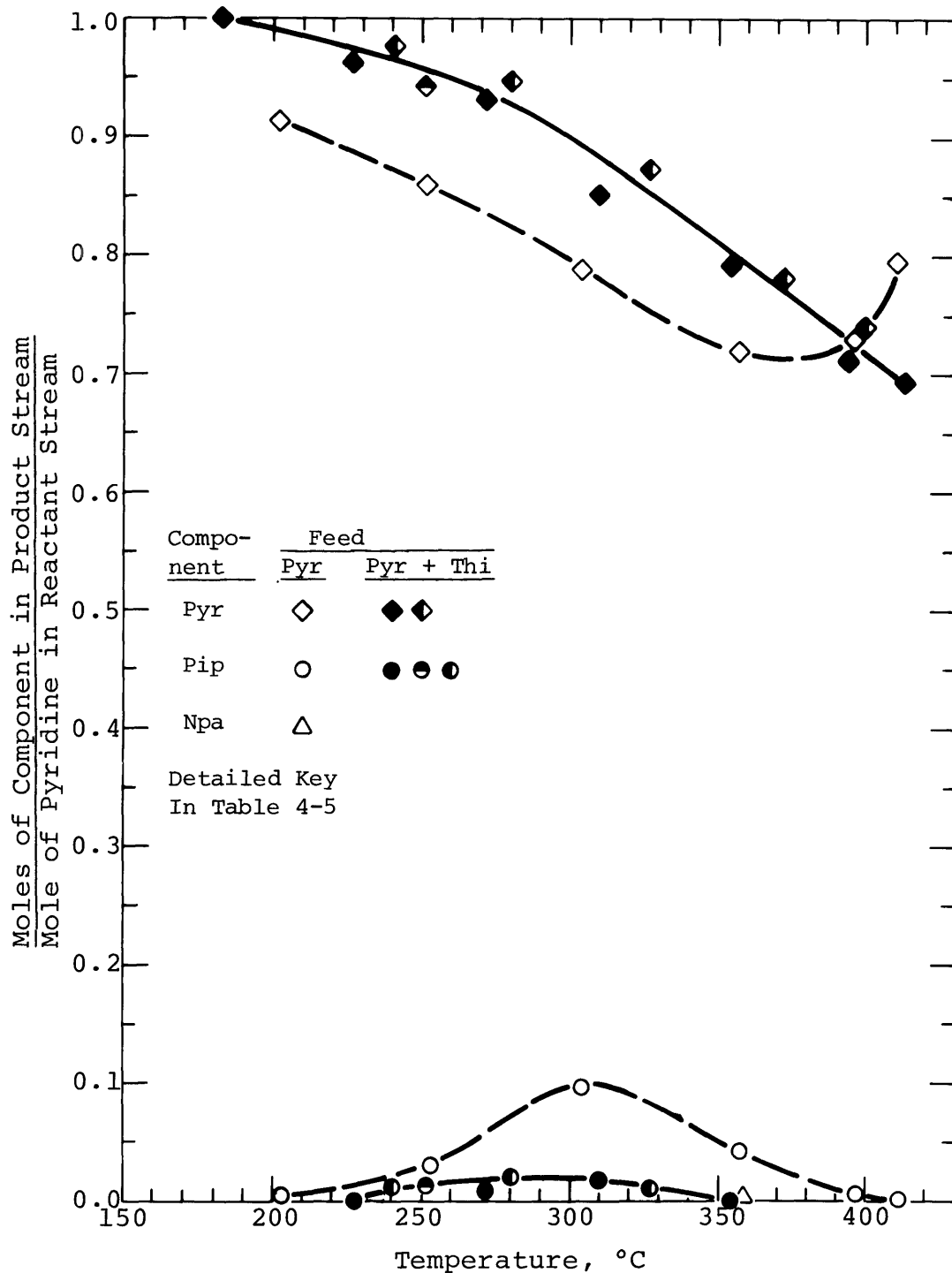


Figure 4-18: Product Distributions for Pyridine HDN For Pure Pyridine (93 torr partial press.) and Mixed Pyridine (93 torr)-Thiophene (93 torr) Feeds At a Total Pressure of 150 psig. (Pip=piperidine, Npa=n-pentylamine)

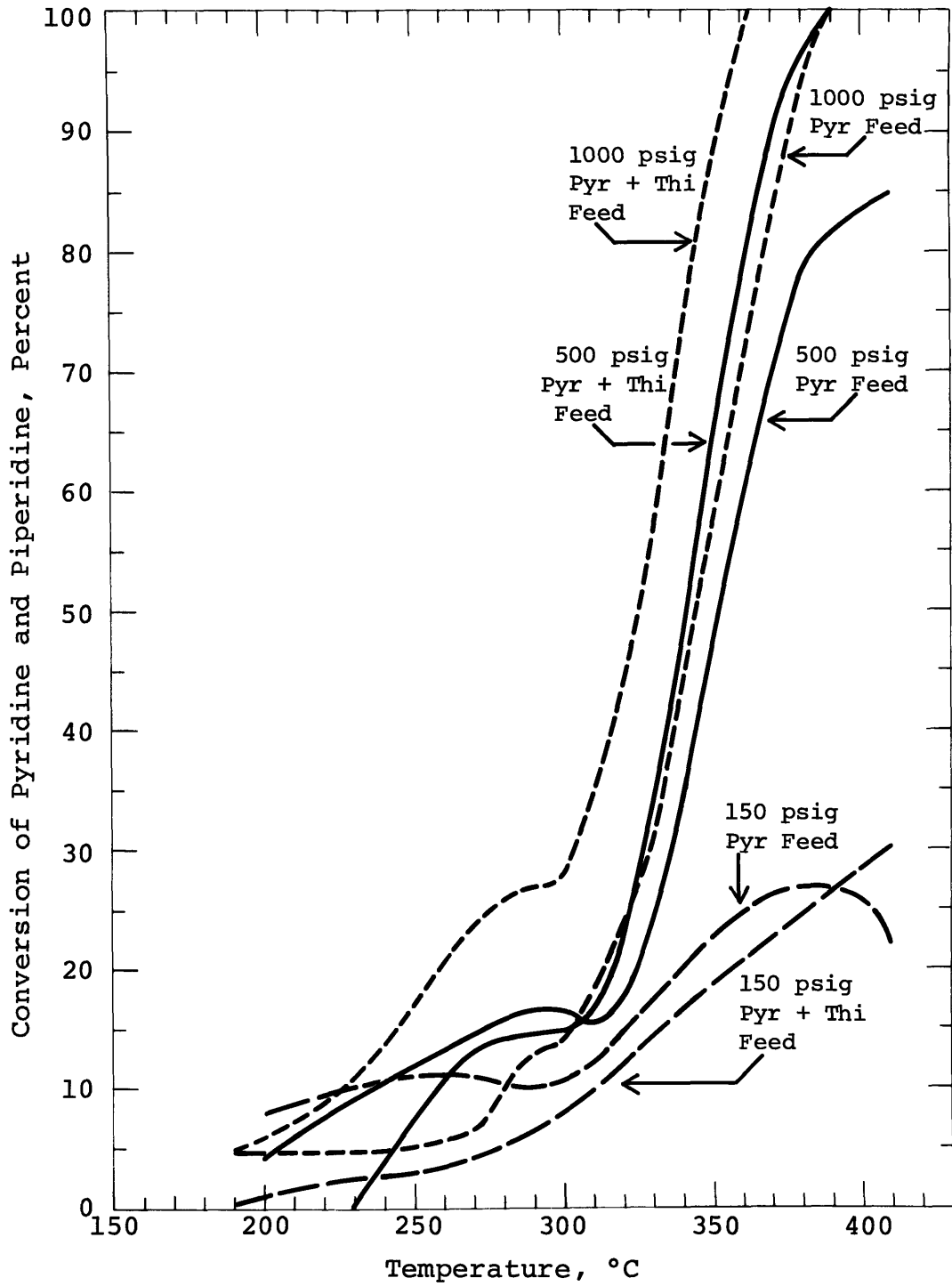


Figure 4-19: Conversion of Pyridine and Piperidine For Pure-Pyridine and Pyridine-Thiophene Feeds at Total Pressures of 150, 500, and 1000 psig.

CHAPTER V. DISCUSSION OF RESULTS

The sections of this discussion chapter are directly based on the analogous Results sections, beginning with the catalyst activity. For thiophene HDS and pyridine HDN, results related to the figures are covered first, followed by a kinetic analysis. For pyridine, a study of the equilibrium aspects of the reaction is also included. Following the individual examination of the HDS and HDN reactions and their interactions, the relative rates of thiophene HDS and pyridine HDN are discussed.

The quality of the experimental data is then examined. This includes a statistical analysis of individual data points and the use of statistical methods in the data analysis.

The results of the low-pressure runs of this study are not directly comparable to those of some earlier work in these laboratories (Mayer, 1974), for two reasons. First, the catalyst loading for quantitative analyses in this current work was used for approximately 200 hours before the runs presented here were made. This insured that the initial-activity effects were no longer present. Earlier work had used relatively fresh catalysts, which could have exhibited some of these effects. Second, the current gas chromatographic analyses separate pyridine

from its intermediate reaction product piperidine. The earlier work did not resolve these two components, and piperidine outputs were at least partially attributed to pyridine.

V.A. Catalyst Activity

The importance of maintaining a consistent state of catalyst activity required that both the type of deactivation observed in the early stages of catalyst use (as shown in Figure 4-1), and subsequent variations among runs, be eliminated. This was difficult because the catalyst was to be used under three greatly different types of feed conditions: pure pyridine, pure thiophene, and mixed pyridine-thiophene. The use of the three sulfiding procedures previously described overcame these difficulties. By carrying out one of the three sulfiding procedures, the catalyst could be returned to a standard state of activity for the start of the next run. That the procedures were effective was shown not only by the results of Figure 4-1, but also by the repetition of runs during the final data collection; the data generally showed very good reproducibility. Before carrying out runs 38 and following (those used quantitatively in this thesis), a new catalyst loading was used for approximately 200 hours,

overcoming the initial effects which were shown to result from using a fresh catalyst.

The deactivation of the catalyst after 550 hours on stream appeared to result primarily from the quinoline runs, as the catalyst had been used for the standard-state activity tests with pyridine until the time of the first quinoline work. Two factors could have significantly contributed to the decline in activity. First, the NiMo/Al₂O₃ catalyst was sensitive to overheating, and an upper temperature limit of approximately 425°C was recommended by the manufacturer (American Cyanamid, 1969). Both pyridine and quinoline runs were made near this limit, but the quinoline runs were consistently from five to ten degrees C higher than those of the pyridine work. Although this difference is small it may have been enough, after repeated application, to affect the catalyst, either by sintering, altering the pore structure, or enhancing the deposition of carbon.

Second, the presence of carbon deposits was a significant difference between the new and used catalyst samples. While no test was made after use with only pyridine, qualitative observations indicate that much of this deposit may have been due to the quinoline usage. The gas chromatographic analysis of the product stream for quinoline HDN showed a much larger amount of heavy material,

often aromatic rings linked by alkyl side chains. Further, while the chromatographic system remained clean after five years of pyridine and thiophene use, one month of quinoline work left heavy residues at points where temperature drops permitted condensation of heavier components. These depositions could indicate a significant tendency for quinoline to form carbon deposits on the catalyst surface.

The pore structure, as defined by the catalyst support, should not have been altered significantly by heat at the temperatures studied, as the alumina was stable to at least 550°C (American Cyanamid, 1969). Of the factors studied, however, small differences in pore structure would probably be due to the thermal treatment of and carbon deposition on the catalyst.

Perhaps the most significant difference between the catalysts was the amount of sulfur retained after the formal sulfiding procedures. The ten percent lower sulfur uptake of the used catalyst could represent a significant loss of active catalytic sites. This is the only test performed which had a degree of selectivity between the metallic sites and the alumina support, and thus represents an important factor where the sulfided metal catalyst provides the activity for the HDS and HDN reactions.

V.B. Thiophene Hydrodesulfurization

V.B. 1. Pure Thiophene HDS

The conversion of pure thiophene was shown in Figure 4-3 to be easily carried out at reaction pressures as low as 150 psig over the sulfided NiMo/Al₂O₃ catalyst. Increases in pressure up to 1000 psig produced even more-rapid desulfurization, while maintaining the same character of the conversion curve. This indicated that the same reaction mechanisms were probably in effect over the pressure range studied.

The S-shaped curves conform to expectations for a reaction order greater than zero in thiophene. For any positive order in the primary reactant, a point is reached at high temperatures (and thus high conversions) where the reactant falls to such low concentrations that decreases in the concentration driving force term in the rate expression are greater than the exponential increases in the reaction rate constant, and a decrease in the rate of reaction occurs. On a plot of the conversion as a function of the reaction temperature for plug flow reactor, this manifests itself as the S-shaped curves seen here.

The effect on the conversion of thiophene of doubling

its partial pressure, shown in Figure 4-4, was a decrease in the observed conversion at any given temperature. For the reactor type and plot used here, a first order reaction would show identical curves for the two partial pressures; the results here thus indicate a reaction order less than one. A quantitative discussion of the reaction order is deferred until the kinetic analysis section.

The presence of tetrahydrothiophene in the product stream indicated that at some operating conditions two parallel reaction mechanisms might be in effect: the main path for HDS being the route through the initial sulfur removal from thiophene and the subsequent saturation of butadiene; and a second, much-less-active path being the saturation of thiophene followed by the removal of the sulfur atom from the saturated species. An analysis of the light products to determine the amounts of butadiene, butenes, and butane present would be required to draw conclusions as to the extent of this second mechanism. Evidence from this type of analysis (Owens and Amberg, 1961) suggests that the former mechanism is by far the predominant form.

V.B. 2. Thiophene HDS in the Presence of Nitrogen Compounds

The inhibition of thiophene HDS by pyridine was shown

in Figure 4-5 to be a nearly-direct translation of the three pure-thiophene curves to higher temperatures. This implies that one basic type of HDS mechanism was active under both sets of conditions.

The run incorporating equal feed partial pressures of thiophene and n-butylamine produced useful results even though the conversion of the amine was much slower than expected. The basicity of the aliphatic amine is much closer to that of ammonia than to that of pyridine (Morrison and Boyd, 1966). It is thus possible to compare the effects of the combined butylamine and ammonia partial pressures, which should sum to 93 torr, with that of pyridine. There might have been a steric hindrance effect of the longer butylamine molecule relative to ammonia, but this would probably have been much less than the great difference in basicities between pyridine and the other two compounds.

As shown in Figure 4-6, the inhibitions caused by the butylamine-ammonia combination and by pyridine were nearly identical. From this, it appears that the action of either the aromatic pyridine or the aliphatic amine-ammonia combination affected the active sites in the same way, in spite of greatly different basicities. This could imply a type of threshold inhibiting quality, where once a certain strength of adsorption on active sites is reached,

their activity is decreased to a specific and constant level.

The complete disappearance of tetrahydrothiophene from the product stream in the presence of pyridine could indicate a blocking of the particular mechanism by which it was formed, with the continuing HDS occurring strictly by the sulfur-removal-then-saturation mechanism. This would be consistent with the assumptions made in the preceding section. Alternatively, pyridine could have enhanced the desulfurization of the saturated compound, reducing the concentration of the intermediate tetrahydrothiophene. This interpretation, however, is highly unlikely in light of the general inhibiting effect of pyridine.

The inhibiting effects of pyridine on thiophene conversion are summarized by Figure 5-1, which shows the ratio of the thiophene conversion in the presence of pyridine to that for the pure thiophene feed. The significant point here is that the proper combinations of high pressure and temperature will overcome the inhibition of pyridine and result in complete conversion of thiophene.

V.B.3. Effect of Methyl Substitution on Thiophene HDS

Two different methylthiophenes were examined to determine the degree to which methyl substitution would

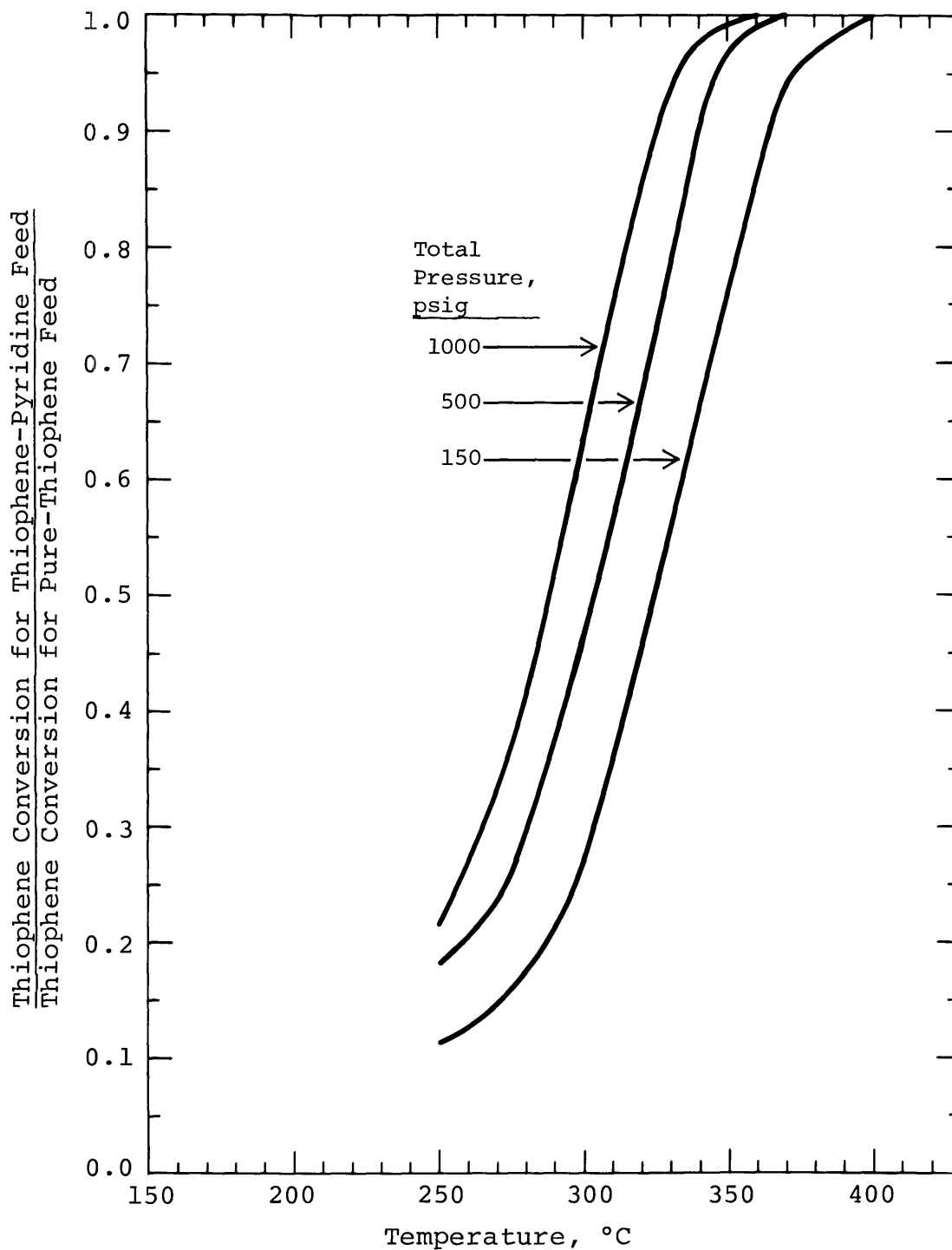


Figure 5-1: The Inhibition of Thiophene Conversion By Pyridine at Total Pressures of 150, 500, and 1000 psig.

decrease conversion relative to that of thiophene. Specifically of interest was the comparison between this effect and the inhibition of thiophene produced by the presence of pyridine.

A study by Desikan and Amberg (1963) showed 2-methylthiophene to be less reactive than 3-methylthiophene, in part due to chemical effects. Due to its proximity to the sulfur atom, 2-methylthiophene could also be expected to have a greater steric hindrance on the hydrogen attack of the sulfur. For these reasons, this compound was chosen for study. The addition of a second methyl group, to the other carbon adjacent to the sulfur atom, was expected to produce further steric hindrance; 2,5-dimethylthiophene was therefore also examined.

Three competing effects combine to produce a difference between the reaction of thiophene and its methyl-substituted analogs. First, steric hindrance could inhibit the attack of hydrogen on the sulfur atom, particularly if the thiophenic molecule were adsorbed onto the catalyst surface through the sulfur. Second, an inductive effect takes place, where the tendency of an alkyl group to release electrons increases the electron cloud density of the aromatic pi bond of the thiophene molecule, decreasing the molecule's stability and enhancing its reactivity. Third, a hyperconjugation effect of the methyl group in the

2-position enhances the stability, thereby decreasing the reactivity, of the thiophene molecule by increasing the delocalization of the pi electron cloud. Details of the action of these latter two effects may be found in Morrison and Boyd (1966).

The experimental results of Figure 4-7 show that the inhibiting effects overshadowed the enhancing effect; there was a decrease in the observed conversion of thiophene when the first methyl group was added, and a further small decrease with the addition of the second. It is considered that the steric hindrance was probably stronger than the hyperconjugation, and was thus primarily responsible for these effects. Even for the combined inhibition of the two methyl groups, however, the effect was significantly less than the inhibition produced by pyridine.

V.B.4. Thiophene HDS: Kinetic Analysis

To determine the best kinetic expression to describe the thiophene HDS results, it was necessary to compare proposed models with the integral reactor data obtained in this study. This required the assumption of specific models, integrating their associated rate expressions in

the plug-flow reactor performance equation, and comparing the predictions of these integrated forms with the actual experimental results. The data used for the pure-thiophene kinetic analysis were the 93 and 186 torr thiophene feed partial pressure runs at 150 and 1000 psig. For the addition of pyridine inhibition to the kinetic analysis, data were used from runs at 150 and 1000 psig with equal thiophene and pyridine partial pressures of 93 torr.

So as not to artificially complicate the situation, a first attempt was made to fit the pure-thiophene data to a power-law kinetic model. The thiophene conversion results had been shown to exhibit a reaction order between zero and one. The actual observed reaction order was calculated at each reaction temperature, but these values changed with temperature, and hence with extent of conversion. As was expected for a system with strong adsorption characteristics, power law kinetics was inadequate, and a model which accounted for these properties was then tried.

A series of Langmuir-Hinshelwood models was formulated to include various assumptions of the relative adsorption strengths of thiophene and hydrogen sulfide, and the nature of the chemisorptive bond between thiophene and the surface catalytic site. These assumptions, which were in addition to those inherent in the basic Langmuir-

Hinshelwood model, were designed to cover the most probable physical situations. So that the models could be explicitly written and integrated, each one was required to include specific assumptions before it was compared with experimental data. This method is distinctly different from techniques where either differential data or differentiated integral data can be compared with a potential expression, and the best values of a set of constants (corresponding to the assumptions here) determined. The form of the data of this study did not permit its differentiation, thus necessitating the more cumbersome techniques described above.

There is general agreement that thiophene and H_2S compete for the same active catalytic sites, thus requiring competitive adsorption terms in the Langmuir-Hinshelwood expression. There is less agreement, however, on the relative strengths of these adsorptions. Roberts (1965) found them to be of approximately the same magnitude in his study of thiophene HDS, while Desikan and Amberg (1964) found the relative adsorption of thiophene to be considerably stronger when the H_2S was formed from the HDS of thiophene rather than preadsorbed on the catalyst before introduction of thiophene. To examine these potential relationships, three cases were studied here, using ratios of adsorption constants (K_{H_2S}/K_{Thi}) of 0.0, 0.25, and 1.0.

Butane, butene, and butadiene were also present in the reaction stream as products and intermediates, and, therefore, need to be examined for competitive adsorption effects. The adsorption of the saturated hydrocarbon should be insignificant relative to that of thiophene when its presence in very low concentrations is due only to the decomposition of thiophene (Owens and Amberg, 1961, 1962a,b). A study (Owens and Amberg, 1961) has shown that butene adsorbs at least one order of magnitude less strongly than does thiophene. Thus, the presence of olefins, again when in the low concentrations resulting from the decomposition of thiophene, does not significantly affect the thiophene desulfurization reaction. The adsorption strengths of these three compounds were then considered to be much less than those of thiophene and H_2S , and competitive adsorption terms were not included for them.

The adsorption of hydrogen onto the catalyst surface to react with the adsorbed thiophene molecules has been discussed by Lipsch and Schuit (1969c). They propose an adsorption onto sites adjacent to but separate from those for thiophene adsorption. In the formulation of a Langmuir-Hinshelwood expression, this permits the use of an independent hydrogen functionality, a separate factor times the sulfur adsorption expression. Hydrogen is in

great excess in the reaction mixture, and its partial pressure thus remains fairly constant throughout a run. The hydrogen functionality then becomes a constant for each reaction pressure. Further, this expression will retain all of the above supporting assumptions for either molecular or atomic adsorption on the surface. The final evaluation of the change in the constant from one reaction pressure, and hence hydrogen partial pressure, to another will permit some statement concerning the type of adsorption taking place. A further relevant observation was made by Owens and Amberg (1961). As discussed in the literature section, they observed two types of hydrogen adsorption: strongly-held hydrogen, which competed with thiophene for active sites; and weakly-held hydrogen, which was assumed to be the source of hydrogen for the reactions of thiophene and unsaturated hydrocarbons. Thiophene was not able to compete with hydrogen for this second-site adsorption. The competition of hydrogen with thiophene could be significant, if the theory of Owens and Amberg (1961) is correct, rather than the total lack of competition noted by Lipsch and Schuit (1969c). If the latter case holds, then no competitive adsorption term for hydrogen is necessary. If there were competition, it would be necessary to account for it in a kinetic model. It is not possible to properly extrapolate from the near-

atmospheric-pressure pulse reactor results of Owens and Amberg to a continuous, high-pressure reactor with over 1000 psig of hydrogen. One method to account for such a competitive effect, which was a nearly-irreversible adsorption which rendered the hydrogen essentially unavailable for reaction, would be to assume that a certain percentage of the active sites were permanently unavailable for thiophene adsorption in the presence of a sufficiently-high partial pressure of hydrogen. In such a case, there would be no adsorption term in the Langmuir-Hinshelwood expression, as the assumption would represent a complete elimination of certain sites on which there would be no further competition. As there is in fact a great increase in thiophene reaction with increases in hydrogen pressure, it appears that some limit may be reached on the number of sites to be so deactivated. For purposes of this model, it is assumed that if the competition is significant, then, such a limit was reached by 150 psig.

Another undetermined factor is the nature of the adsorption of the thiophene molecule on the catalyst surface. Several groups, such as Roberts (1965), found the two-point adsorption of thiophene to give the best statistical fit for a Langmuir-Hinshelwood kinetic expression. Of these 2-point theory groups, some propose adsorption through two carbon atoms, and others through

one carbon and the sulfur atom. A one-point adsorption through the sulfur atom was also favored by some groups, such as Lipsch and Shuit (1969c). (These aspects are covered in detail in the literature review section.) The significance of this distinction is that the denominator of a Langmuir-Hinshelwood rate expression is taken to the power of the number of active sites involved in the controlling step of the reaction. For this study, both these cases were examined; the denominator was given powers of one and two in separate models.

The power of the thiophene partial pressure in the numerator driving force term is that of the number of molecules of thiophene taking part in the adsorption onto each catalytic site. Thiophene is taken to adsorb singly, thus its power is unity. This numerator power holds regardless of the number of sites required per molecule, as long as thiophene does not dissociate on adsorption.

The basic Langmuir-Hinshelwood expression resulting from these assumptions is:

$$-r_{\text{Thi}} = \frac{k_{\text{Thi}} K_{\text{Thi}} P_{\text{Thi}}}{(1 + K_{\text{Thi}} P_{\text{Thi}} + K_{\text{H}_2\text{S}} P_{\text{H}_2\text{S}})^m}$$

where: $-r_{\text{Thi}}$ = rate of disappearance of thiophene, gram moles of thiophene per hour per gram of catalyst

k_{Thi} = surface reaction rate constant for thiophene HDS, in appropriate units depending upon the functionality of the hydrogen term

α = hydrogen functionality, of form

$$K_{\text{H}_2}^n P_{\text{H}_2}^n / (1 + K_{\text{H}_2}^n P_{\text{H}_2}^n)$$

where $n=1$ for molecular adsorption of H_2 and $n=1/2$ for atomic adsorption of H_2

$K_{\text{Thi}}, K_{\text{H}_2\text{S}}$ = adsorption constants of thiophene and H_2S , respectively, torr^{-1}

$P_{\text{Thi}}, P_{\text{H}_2\text{S}}, P_{\text{H}_2}$ = partial pressures of thiophene, H_2S , and H_2 , torr (except H_2 , psi)

m = number of catalytic sites required for the adsorption of a thiophene molecule

From the stoichiometry of the desulfurization, one mole of thiophene yields one mole of H_2S . In the absence of significant side reactions producing other sulfur-containing species, the H_2S partial pressure is the difference between the thiophene feed partial pressure and the thiophene partial pressure at a particular reaction condition. This substitution was made before the integration of the reactor performance equation.

The performance equation for a plug flow catalytic reactor operating at conversions high enough to produce integral reactor data and derived on a mass-balance basis, is

$$\alpha = - \int_{P_{\text{Thi}}^0}^{P_{\text{Thi}}} \frac{dP_{\text{Thi}}}{-r_{\text{Thi}}}$$

The Langmuir-Hinshelwood expression for $-r_{\text{Thi}}$ was substituted into this equation, and the resulting total expression integrated for each set of assumptions. A total of six cases resulted from the variation of two parameters:

<u>Parameter</u>	<u>Cases Studied</u>
Ratio: $(K_{\text{H}_2\text{S}}/K_{\text{Thi}})$	$\begin{bmatrix} 0.0 \\ 0.25 \\ 1.00 \end{bmatrix}$
Number of catalytic sites used for adsorption of a pyridine molecule	$\begin{bmatrix} 1 \\ 2 \end{bmatrix}$

The integrated and adjusted expressions were then reduced to a form requiring the following experimental data for each total reaction pressure at ten degree C intervals: the actual feed partial pressures of thiophene for the nominal 93 and 186 torr feed conditions; and the partial pressure of thiophene under the particular reaction condition, derived from the smooth curves through the conversion data points of Figure 4-4. This amount of data was sufficient to solve these expressions, at each temperature, for values of two unknowns, K_{Thi} and $k_{\text{Thi}} \tau$; representing the adsorption constant for thiophene, and a reaction rate constant term including the hydrogen functionality and the reactor space time (a known quantity). Because a specific relationship between K_{Thi} and $K_{\text{H}_2\text{S}}$ is inherent in each model, this latter quantity is also uniquely determined. Because τ is a constant for each total pressure, and τ was a constant for all

experimental runs, the k^{app} product is a constant multiplier of k_{Th} at each reaction pressure. Since the logs of these numbers are used for further analysis, and the slopes rather than the actual values are of significance (as described next), then the quantity k^{app} can be used directly as the reaction rate constant for this purpose.

The quality of fit of the models was determined by the linearity of the natural logs of these K_{Th} and k^{app} values with the inverse absolute temperature. This linearity is expected for the two cases because of the functionality expressed by the integrated van't Hoff equation (Denbigh, 1966) and the Arrhenius temperature dependence (Levenspiel, 1972), respectively. There were great differences in the behavior of the K_{Th} and k^{app} values from model to model, ranging from excellent linearity to cases producing mathematically negative adsorption constants. These differences permitted discrimination among the models on the basis of the linearity of the two relationships.

It is important to emphasize that this kinetic analysis, and the subsequent one for pyridine hydrogenation, are not intended to provide unequivocal evidence that a particular fundamental kinetic model represents the precise mechanism by which the reaction is taking place. Rather, the conclusions reached here should be taken to indicate that certain assumptions are superior to others in the formulation of a simplified kinetic model representing this particular

set of experimental data. While the conclusions drawn from these analyses should indeed be useful, before extrapolating the results too far, one should keep in mind the warning of Satterfield (1977a) concerning such techniques, that "the utilization of this approach ... by chemical engineers has frequently led to an excess of enthusiasm over reality."

Two distinctions were sought from the kinetic analysis: between one- and two-point adsorption of thiophene; and among (K_{H_2S}/K_{Thi}) ratios of 0.0, 0.25, and 1.0. Examination of the linearity of the data included the quality of fit for all points; however, since the temperature ranges studied at each pressure were purposely extended to the extremes of high and low conversions, if only the two end points of a series showed deviation from linearity, this was not considered a serious deficiency. Plots of the results for the two best cases are shown in Figure 5-2; those of the other four are given in the Appendix.

First, examination of the K_{Thi} plots at both 150 and 1000 psig for the six models showed consistent differences between the one-point and two-point cases. The single-point models generally produced S-shaped curves, with the quality ranging from fairly good for the K-ratio of 0.0, to the extreme of negative calculated K_{Thi} values for the K-ratio of 1.0. The emergence of negative values for the adsorption constants was a result of the mathematical treatment; in a

physical sense, these are meaningless. The implication is that this particular model cannot account for the experimental results using magnitudes consistent with physical reality, and is, therefore, inadequate. For the single-point adsorption cases, if the extreme points are not included, a straight line through the remaining points would have a positive slope, implying an exothermic heat of adsorption. This is physically realistic. Of the single-point adsorption models, K-ratio = 0.0 gave the best results.

For the two-point adsorption models, the adsorption constants generally showed excellent linearity, especially when the extreme points were not considered. The order of quality was the same as for the single-point models, with the best at K-ratio = 0.0, followed by 0.25 and 1.0. The excellent linearity was accompanied by the curious fact that the lines were all nearly perfectly of zero slope, which would indicate an adsorption strength independent of temperature, and with no heat effects of adsorption. This is not as realistic physically as the exothermic adsorptions, which imply a decreasing adsorption with increasing temperature.

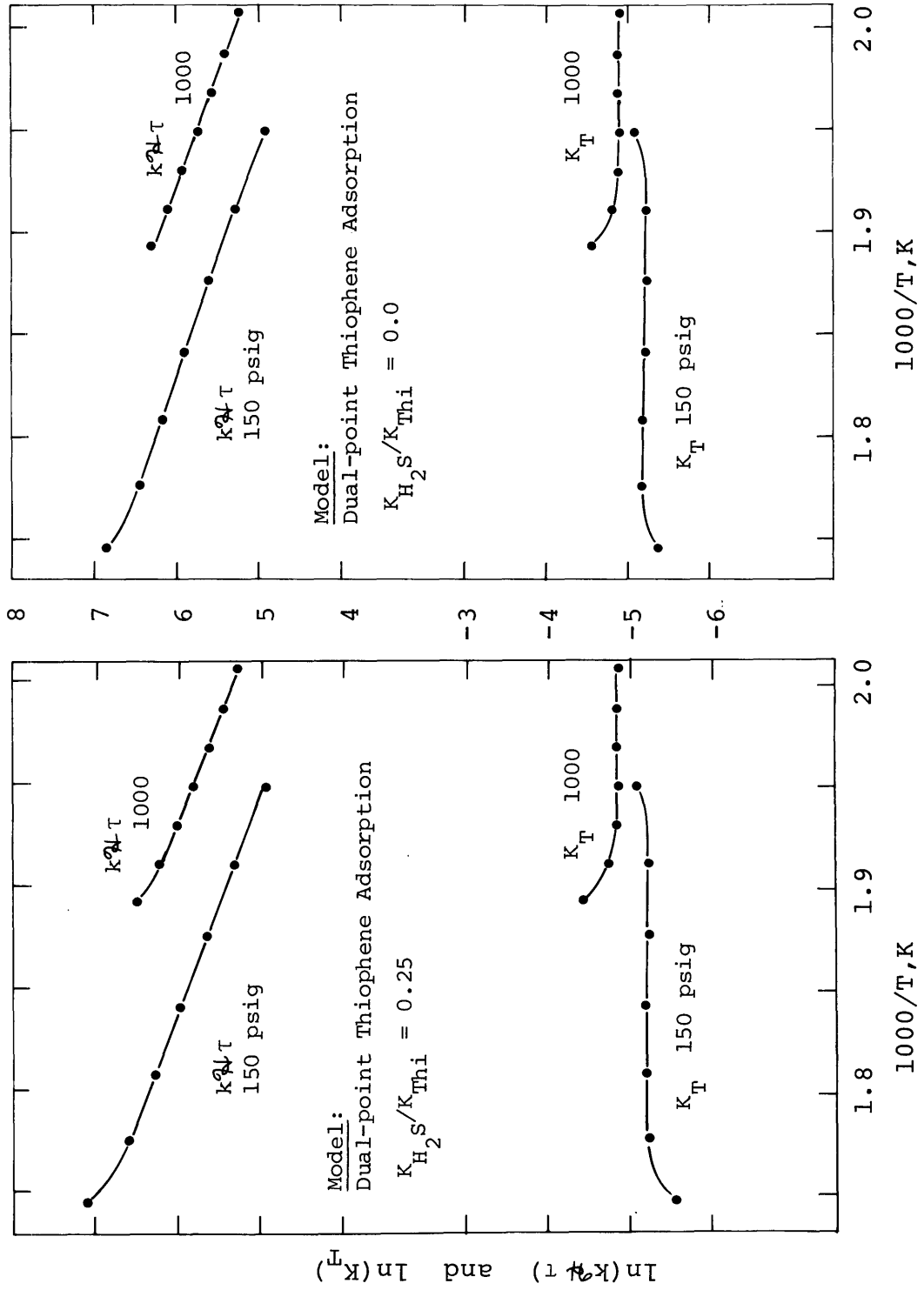
Examination of the k_{ad} plots showed all models to give good linearity, except that there was a distinct curve in both the one- and two-site cases with K-ratio = 1.0 which was not present in the other four models. For all models,

the two k^*_{τ} lines (or for the K-ratio = 1.0 cases, the linear portions) are nearly parallel, and give activation energies averaging 20 kcal/gram mole. This is a reasonable value for the thiophene HDS reaction. There was a slight but noticeable difference in the degree of parallelism of the k^*_{τ} lines between the single-point and dual-point models. For the dual-point cases, the activation energies for the two pressures differed by an average of approximately one kcal/gram mole, whereas the single-point differences averaged about two kcal/gmole. Although this distinction is small, its consistency among all of the models also favored the dual-site adsorption of thiophene.

From the above discussion, two trends were apparent for the application of models to this experimental data: first, the adsorption of hydrogen sulfide appeared to be weaker than that of thiophene; and second, two-point adsorption of thiophene showed a somewhat better correlation than did single-point adsorption.

Figure 5-2 presents the graphical results for the two best-fit models, $(K_{H_2S}/K_{Thi}) = 0.0$ and 0.25 , for dual-site adsorption of thiophene. The linearity of the results and the parallel nature of the lines for 150 and 1000 psig are clearly shown. For the best-fit cases, the activation energies derived from the slopes of the k^*_{τ} lines are:

Figure 5-2 : Performance of Langmuir-Hinshelwood Kinetic Models in Correlating Thiophene HDS Reaction Data



K_{H_2S}/K_{THI}	Thiophene adsorption, no. points	E_{act} kcal/gmole, 150 psig	E_{act} kcal/gmole, 1000 psig	E_{act} kcal/gmole, average
0.0	2	17.1	18.3	17.7
0.25	2	18.5	19.8	19.2

Insight into the adsorption of hydrogen can be gained from further examination of the $k_{\mathcal{A}}$ lines for these two models. The hydrogen functionality in the Langmuir-Hinshelwood expressions was based on hydrogen adsorption onto sites adjacent to, but distinctly different from those for thiophene. This led to an independent expression for hydrogen adsorption which was constant for each total reaction pressure, and hence hydrogen partial pressure. This expression, $\mathcal{A} = (K_{H_2}^n P_{H_2}^n / (1 + K_{H_2}^n P_{H_2}^n))$, was a constant multiplier of the reaction rate constant. Thus for any given reaction temperature, the ratio of \mathcal{A} at 1000 psig to that at 150 psig should be a direct measure of the nature of the hydrogen functionality. The previous discussion of the weakly-held hydrogen being responsible for reaction (Owens and Amberg, 1961, 1962b) agrees well with the separate type of site proposed for reactant hydrogen adsorption (Lipsch and Schuit, 1969c). The more-strongly-bonded hydrogen could be competing with the thiophene desulfurization sites, while the reactant hydrogen is being directed to the reaction by its own separate sites. With the possible-strongly-bonded hydrogen accounted for independently of the model

mathematics, and with relatively weak adsorption on the exclusively-hydrogen sites, the hydrogen functionality can be simplified. From $k_{Thi} = \text{constant}$ at any given reaction temperature, $\tau = \text{constant}$ for all runs; and for $K_{H_2} P_{H_2} \ll 1$, it follows that:

$$\frac{1000}{150} = \frac{(k_{Thi})1000}{(k_{Thi})150} = \frac{(P_{H_2}^n)1000}{(P_{H_2}^n)150}$$

All quantities here are known except n , the power of the hydrogen partial pressure in the numerator driving force. Using data from the midpoint of overlap between the low- and high-pressure lines, one gets, for a K-ratio of 0.0, $n = 0.45$; and for a K-ratio of 0.25, $n=0.50$. These values are extremely close to the theoretical value of 0.5 which, according to the Langmuir-Hinshelwood adsorption assumptions, implies dissociative adsorption of hydrogen onto active sites. If molecular, rather than atomic, adsorption were taking place, the power should be one. In practice, it has been observed that even on metallic catalysts, where atomic adsorption has been known to take place, the power of the hydrogen term has at times been near one (Satterfield, 1977). This indicates that one must regard these conclusions with caution.

The assumption of weak but unhindered hydrogen adsorption on its own separate sites made the denominator adsorption term for the hydrogen functionality approximately

unity. It is interesting to note that this is a reduction to a Rideal-Ely type of mechanism, where a strongly-adsorbed species reacts with either a gas-phase or a weakly-adsorbed species.

Using the best models from the pure-thiophene feed analysis, the addition of pyridine to the thiophene reaction was examined. The two-point thiophene adsorption models for $(K_{H_2S}/K_{Thi}) = 0.0$ and 0.25 were modified by adding a denominator adsorption term representing the presence of nitrogen compounds. For this analysis, pyridine, piperidine, and ammonia were combined into one term, which assumed the equal adsorption strength of all nitrogen compounds and a constant total partial pressure of these species. The resulting Langmuir-Hinshelwood expression was:

$$-r_{Thi} = \frac{k_{Thi} K_{Thi} P_{Thi}}{(1 + K_{Thi} P_{Thi} + K_{H_2S} P_{H_2S} + K_N P_N)^2}$$

where K_N = average adsorption constant for pyridine, piperidine, and ammonia; torr^{-1}

P_N = total feed partial pressure of pyridine, torr

This expression was integrated in the plug-flow reactor performance equation, and the resulting expression evaluated for those reaction temperatures which the pure- and mixed-feed data had in common. This was a severe restriction, as only high-conversion portions of the pure-feed curves overlapped the low-conversion portions of the mixed-feed curves.

While this precluded a detailed analysis, it was still possible to draw general conclusions about the interactions.

The analysis used the specific values for K_{Thi} and k_{tr} obtained for the two best models, and the data for thiophene-pyridine feed runs at 150 and 1000 psig derived from the smooth curves through the conversion points of Figure 4-5. With these data, all terms of the integrated expression were known at each temperature except $K_N P_N$, and this was then determined at each temperature.

The average value of $K_N P_N$ for both models and both pressures was 2.8, with a range from 2.4 to 3.3. This value can be compared with an average $K_{Thi} P_{Thi}$ value for the two models of 0.6. Thus, the trends of the data of Figure 4-5, which represent a strong inhibition of thiophene HDS by pyridine and pyridine reaction products, can be roughly accounted for by a model in which the nitrogen compounds competed for thiophene HDS sites with an adsorption strength approximately five times that of thiophene.

V.C. Pyridine Hydrodenitrogenation

V.C.1. Pure Pyridine HDN

Examination of the pure pyridine conversion curves of Figure 4-8 shows that at the three reaction pressures studied, there is a bend in the conversion curve beginning approxi-

mately at 340°C. Whereas at 500 and 1000 psig this is only a reduction in the slope of the curve, at 150 psig it becomes an actual decrease in the conversion as the temperature increases above 370°C. It is important to determine whether kinetics or thermodynamics is responsible for this behavior. Simple kinetics predicts a certain amount of such an effect at high conversion (sufficiently complex kinetics can predict almost anything), and the proposed equilibrium limitation might enhance it to varying degrees. For any reaction order greater than zero in pyridine, there should be a decrease in the rate of reaction at higher conversions due to the smaller amounts of pyridine remaining in the reaction stream. The decreases in the concentration driving force for the reaction are then great enough at high conversions to overcome the exponential increase in reaction rate constant with temperature, resulting in the observed S-shaped curves.

While simple kinetics may be responsible for much of this behavior at 1000 psig, there is no way for it to account for a downturn as seen at 150 psig. More advanced kinetic models, accounting for competitive adsorption of reactants and products on active catalytic sites, could predict such behavior if the products were much more strongly adsorbed than the reactants. To study

this, a Langmuir-Hinshelwood mechanism was examined, and is discussed later. If competitive adsorption of products were solely responsible for the downturn, then the most significant effects should be observed at 500 and 1000 psig, where there is a much higher concentration of products in the reaction stream. Instead, the downturn was present only at 150 psig, and it appears that another factor must also be at least partially responsible.

If a thermodynamic limitation were to cause the downturn, the piperidine hydrogenolysis step must first become rate limiting. If this step were rapid, then any piperidine formed would be quickly converted, primarily to n-pentane and ammonia, and with no appreciable concentration of piperidine in the reaction stream, equilibrium could not be reached. With a slow piperidine hydrogenolysis step, however, piperidine could accumulate in the reaction stream, and if the forward and reverse hydrogenation reactions were relatively rapid, then equilibrium could be attained.

If equilibrium between pyridine and piperidine were reached, then LeChatelier's principle would apply. The hydrogenation step involves the consumption of three moles of hydrogen to convert one mole of pyridine to piperidine. Thus, increasing the hydrogen partial pressure should force the equilibrium product composition to the right, in-

creasing the amount of pyridine converted to piperidine. Figure 4-9, which presents the amount of piperidine formed per mole of pyridine fed to the reactor, shows that when the pressure is increased from 150 to 1000 psig, the amount of piperidine present in the product stream increases sevenfold. Qualitatively, this is precisely the behavior expected for the equilibrium-limited case. A detailed examination of the approach of the reaction mixture to equilibrium is presented in a later section.

Product distributions for pyridine HDN at the three reaction pressures all focus on pyridine and piperidine. These were by far the largest components observed in the product distribution except for the unseparated light compounds, pentane and ammonia. N-pentylamine, always less than one mole percent of the amount of pyridine fed to the reactor, was apparently converted to pentane and ammonia at a rate much faster than it was formed. It is interesting to examine the behavior of butylamine hydrogenolysis in the 1000 psig run where it was added to the thiophene feed. It was expected that the butylamine would be converted readily at low reaction temperatures, producing ammonia to compete with thiophene for active catalytic sites. The butylamine, however, followed conversion behavior nearer to that of pyridine. This indicates that the rate of hydrogenolysis of pentylamine, while

significantly faster than the rate of piperidine hydrogenolysis, might not be rapid when itself present in large quantities as a feed.

There were very small quantities (less than one mole percent of the pyridine fed) of non-ammonia and non-pentane reaction products present in the reactor exit stream, which was analyzed by gas chromatography. The inability to separate ammonia in the chromatographic analysis prevented the calculation of a mass balance which could have indicated whether significant amounts of pyridine were forming heavy products which remained on the catalyst surface. The qualitative observations in the catalyst activity section indicated that this was not likely to be as significant for the pyridine runs as it would be for the higher molecular weight compounds such as quinoline. From the work of Beugeling (1971) one would have expected to find more products which would be in the proper boiling point range to be examined in the chromatograph. For the present work, however, few side reactions yielding products in this range appeared to be taking place. Those products which were examined by mass spectrometry indicated a wide variety of side reactions, although their total pyridine consumption was quite small. The most significant observation was that although, for the heavier compounds formed, there were alkyl substitutions

and perhaps chain linkages taking place, most of these compounds remained unsaturated. The lighter compounds formed were predominantly unsaturated. This indicated that there was a low hydrogenation capability of the catalyst toward many aromatics and olefins in spite of the ability to perform the hydrogenation of pyridine and the hydrogenolysis of piperidine and n-pentylamine. This is highly desirable, as in industrial operations it is important to maintain as high a proportion as possible of aromatics and unsaturated aliphatics.

The effect of doubling the partial pressure of pyridine on pyridine conversion was shown in Figure 4-11. The decreased conversion at the higher partial pressures indicated that the observed reaction order was less than one in pyridine; for the integral reactor used, a first-order reaction would have shown no change in the conversion-versus-temperature function with changes in partial pressure. As the conversion curve shift was not as much as would be expected for a zero order reaction, the observed order was between zero and one.

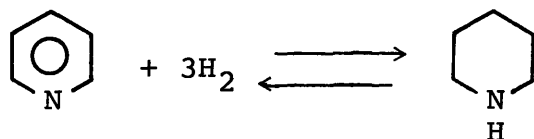
There was no significant effect of doubling the pyridine partial pressure on the percentage formation of piperidine at 150 psig, as shown in Figure 4-12. This implies that there may have been an inhibition of piperidine hydrogenolysis by the greater pyridine partial pressure. Since

there was a significant reduction in the amount of pyridine converted, there must have been a greater accumulation of piperidine in the higher partial pressure case. This could have occurred if there had been an inhibition of the hydrogenolysis reaction in the 186 torr case, as might have been caused by the increased amounts of pyridine present. At 1000 psig the curves for both pyridine conversion and piperidine presence were shifted equally to higher temperatures at the 186 torr feed conditions. This implies that the temperature-induced increases in the rate constants needed to compensate for the higher feed partial pressures produced similar effects on the two reactions, and the relative rates of the reactions remained unchanged.

V.C.2. Pyridine HDN: Equilibrium Analysis

One of the primary objectives of this thesis was to study the reversible hydrogenation of pyridine to piperidine, to determine whether this reaction step would reach and be limited to its equilibrium composition. This could occur if the hydrogenolysis and all other disappearance reactions of piperidine were slow enough so that a significant amount of piperidine could accumulate. If equilibrium were reached, then an important consideration would be the effect which the presence of thiophene would have on the attainment of equilibrium.

This section focuses on the first, reversible step of the series reaction mechanism for pyridine HDN, the hydrogenation of pyridine to piperidine:



The equilibrium constant as a function of temperature for pyridine hydrogenation was determined in two independent ways: by calculation from thermodynamic free energy of formation data; and by utilization of an empirical expression determined by Goudriaan (1974). Principles supporting and sample calculations illustrating the derivation from free energies and the calculation of various equilibrium quantities are given in the Appendix. Details of the experimental determination by Goudriaan and a discussion of the equilibrium constants for the different reaction steps are included in previous sections of this thesis. By estimating the activity coefficients of the components, Goudriaan determined that the non-idealities of pyridine and piperidine mutually compensated in the equilibrium constant expression. This permitted replacing the component activities by the partial pressures, giving:

$$K_p = \frac{P_{\text{Pip}}}{P_{\text{Pyr}} P_{\text{H}_2}^3}$$

where P_{Pip} , P_{Pyr} , and P_{H_2} are the partial pressures of pi-

peridine, pyridine, and hydrogen, respectively.

The first of two quantitative comparisons of thermodynamic equilibrium with the experimental results expresses the amount of piperidine at equilibrium as a fraction of the total pyridine and piperidine present:

$$\frac{\text{PIP}}{\text{PYR} + \text{PIP}}$$

where, through use of the ideal gas law, this expression represents either a mole or partial pressure fraction. For the theoretical case with only these two nitrogen components, this expresses the fraction of total nitrogen present as piperidine. For the experimental data, the fraction is based on only that nitrogen present as pyridine or piperidine (and hence affecting equilibrium), eliminating such other forms as ammonia and n-pentylamine. This representation is thus useful for comparing reaction data with the calculated equilibrium as it gives values on a relevant and well-defined basis, without interference by subsequent hydrogenation reactions or parallel side reactions.

Figure 5-3 shows the equilibrium values of this $\text{PIP}/(\text{PYR} + \text{PIP})$ ratio as a function of temperature. For each reaction pressure the solid line gives the ratios calculated from the empirical value of the equilibrium constant, and the dashed line, the values calculated from the K_p derived from thermodynamic data. For any given reactor pressure,

the difference in temperature required for the same PIP/(PYR + PIP) ratio is between 20°C and 30°C, with the empirical K_p results yielding the lower-temperature values. This difference is significant in subsequent comparison figures.

These calculated equilibrium curves can be compared with curves representing the experimental values of the PIP/(PYR + PIP) ratio for pyridine HDN data, for both pure-pyridine and pyridine-thiophene feeds. The experimental functions are derived from smooth curves through the pyridine and piperidine data of the product distribution figures. The calculated values from both the equilibrium situation and the experimental data are presented in tabular form in the Appendix.

Figure 5-4 shows the equilibrium curves derived from the empirical K_p superimposed on the experimental curves for the three reaction pressures. For the pure-pyridine feed cases at all three pressures, the experimental ratio rises with increasing temperature, peaks, and then falls nearly in concert with the equilibrium curve. (The apparent crossings of the equilibrium curves at 1000 and 150 psig pressures are not necessarily real effects. At these extremely low remaining fractions pyridine, e.g. 0.005 at 1000 psig and 380°C, the calculations are extremely sensitive to minute variations in the data.)

Similar behavior is observed for the three pyridine-thiophene feeds, except that the declining portions fall far short of the equilibrium curves. This difference reflects the decreased amount of piperidine present in the product stream for the mixed-feed runs.

Figure 5-5 superimposes over the same experimental curves the equilibrium values derived from the thermodynamically -calculated K_p values. This set of calculated curves was shown in Figure 5-3 to be translated 20°C to 30°C to the right of the empirically-based curves, and as expected holds a similar but shifted relationship to the experimental results.

From comparisons with the equilibrium curves, the product stream for pure pyridine appears to reach its equilibrium value at each of the three total pressures studied. At 1000 psig, the experimental ratio meets its equilibrium curve as complete conversion is achieved. At 500 and 150 psig, however, the exit composition of the reactor not only meets the equilibrium curve at some temperature less than that required for complete conversion, but as the temperature is raised further, the exit composition follows the equilibrium curve down to very low $PIP/(PYR + PIP)$ values. By contrast, the lower piperidine concentrations for the reaction in the presence of thiophene prevent the mixed-feed reaction from approaching

equilibrium.

A second method was used to assess the approach of the reactor product stream to its equilibrium concentration. This analysis entailed comparing experimental values of the equilibrium constant expression with those from the calculated K_p -temperature relationship on a plot of the integrated van't Hoff equation (Denbigh, 1966), $\log_{10}(K_p)$ as a function of the inverse absolute temperature. Figures 5-6, 5-7, and 5-8 show the plots of the $\log_{10}(K_p)$ for both the empirically-determined and thermodynamically-calculated K_p values. To compare experimental results with these K_p lines, the quantity:

$$\log_{10} \left(\frac{P_{\text{Pip}}}{P_{\text{Pyr}} P_{\text{H}_2}^3} \right)$$

was calculated from data at each experimental point. Figures 5-6, 5-7, and 5-8 present these experimental values for total pressures of 1000, 500, and 150 psig, respectively, each giving results for both pure-pyridine and pure-thiophene feed cases. Vertically-downward arrows indicate that, for mixed feed cases, the piperidine concentration was zero at those temperatures (with an ordinate value of negative infinity), and a curve thus drops off precipitously as it approaches such a temperature.

Once again, similar results were obtained at all three

reaction pressures. At each pressure the pure-pyridine-feed data starts out decades away from the equilibrium line at lower reaction temperatures, 200° to 250°C. As the temperature rises, the data approach the line, until at approximately 350°C the empirical equilibrium line is reached. Above this temperature the experimental curves follow the empirical equilibrium line down very closely, demonstrating the attainment of equilibrium in the reactor at all pressures studied, for pure-pyridine feeds.

For pyridine-thiophene feeds, the effects of the lower piperidine concentrations are clear: the mixed-feed data are always farther from the equilibrium lines than the pure-feed points, and drop off sharply well before reaching equilibrium.

Pure-pyridine hydrogenation appears to be equilibrium limited under all conditions studied. This is the result of a competition between the kinetic rate constant, which is increasing exponentially with temperature, and the equilibrium composition of the mixture, specifically determined at each temperature. At 1000 psig kinetics controls the reaction, and complete conversion is achieved. At 500 psig the approach to equilibrium reduces the concentration driving force and retards the reaction so that when the temperature limit of the catalyst is reached, conversion is still incomplete. From examination of the 500 psig curve

of Figure 4-8 in light of the equilibrium behavior, one might conclude that if higher reaction temperatures were to be possible (i.e. no limit on the catalyst temperature), there would be a downturn similar to that at 150 psig. The calculated equilibrium curve at 150 psig is at far lower temperatures than the others, setting a firm ceiling on the extent of reaction, as seen in the downturn in the pyridine conversion curve of Figure 4-8.

The addition of thiophene to the pyridine feed has been shown to have a much greater effect on the amount of piperidine present in the product stream than on the conversion of pyridine. In reducing the amount of piperidine present, the addition of thiophene removes a necessary criterion for the attainment of pyridine-piperidine equilibrium, specifically the relatively slow hydrogenolysis step which permits the piperidine concentration to build up, starting the entire sequence of events. Thus, through enhancement and inhibitions (discussed in the following section), thiophene has effectively prevented the attainment of equilibrium which was reached in its absence.

The data of this study have been shown to reach equilibrium quite precisely, when the equilibrium constant was defined by the empirical correlation of Goudriaan. The equilibrium constant derived from thermodynamic data differed slightly from the empirical value, showing the approach to,

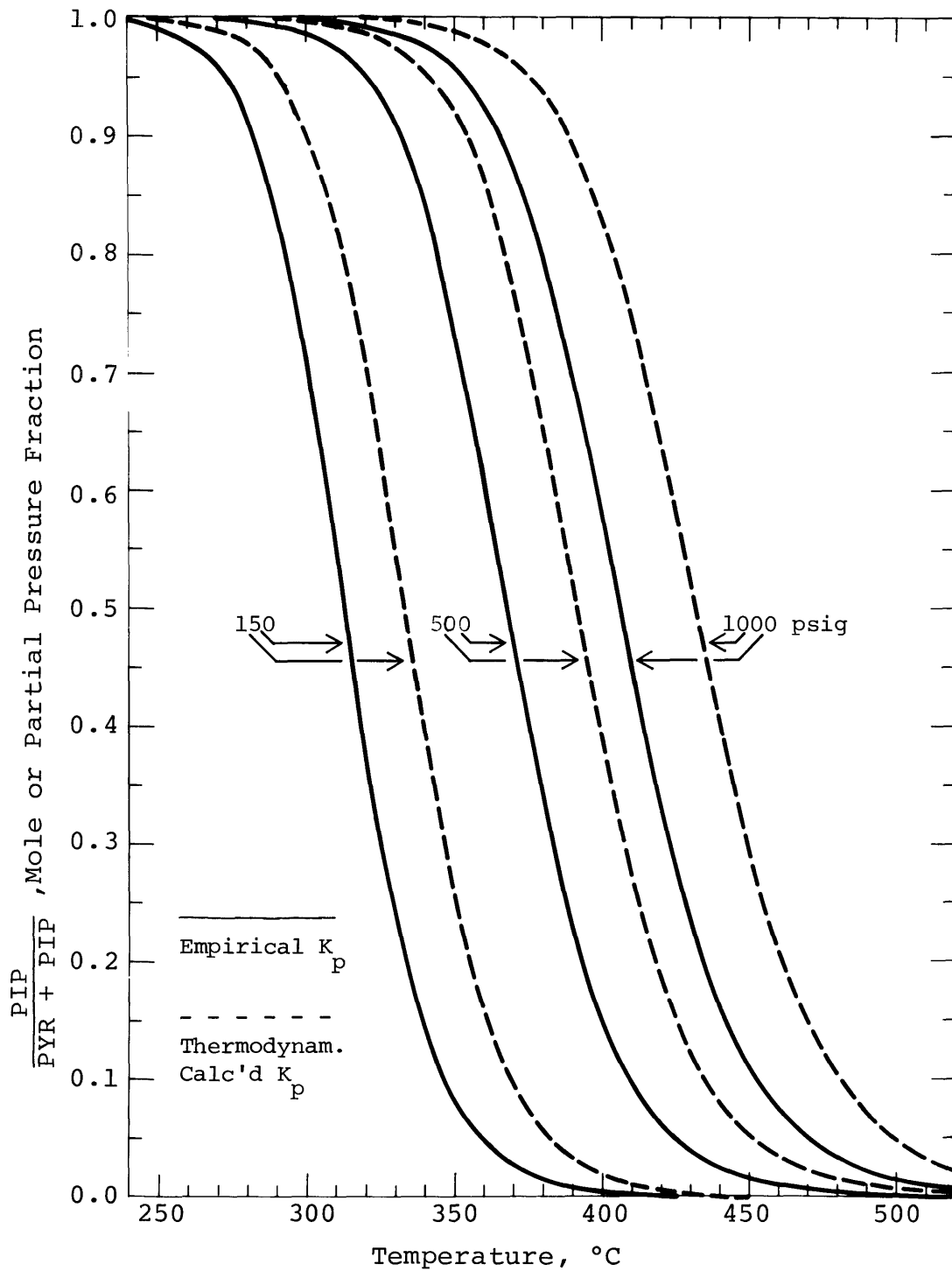


Figure 5-3: Equilibrium Compositions for Pyridine Saturation to Piperidine at Total Pressures of 150, 500, and 1000 psig.

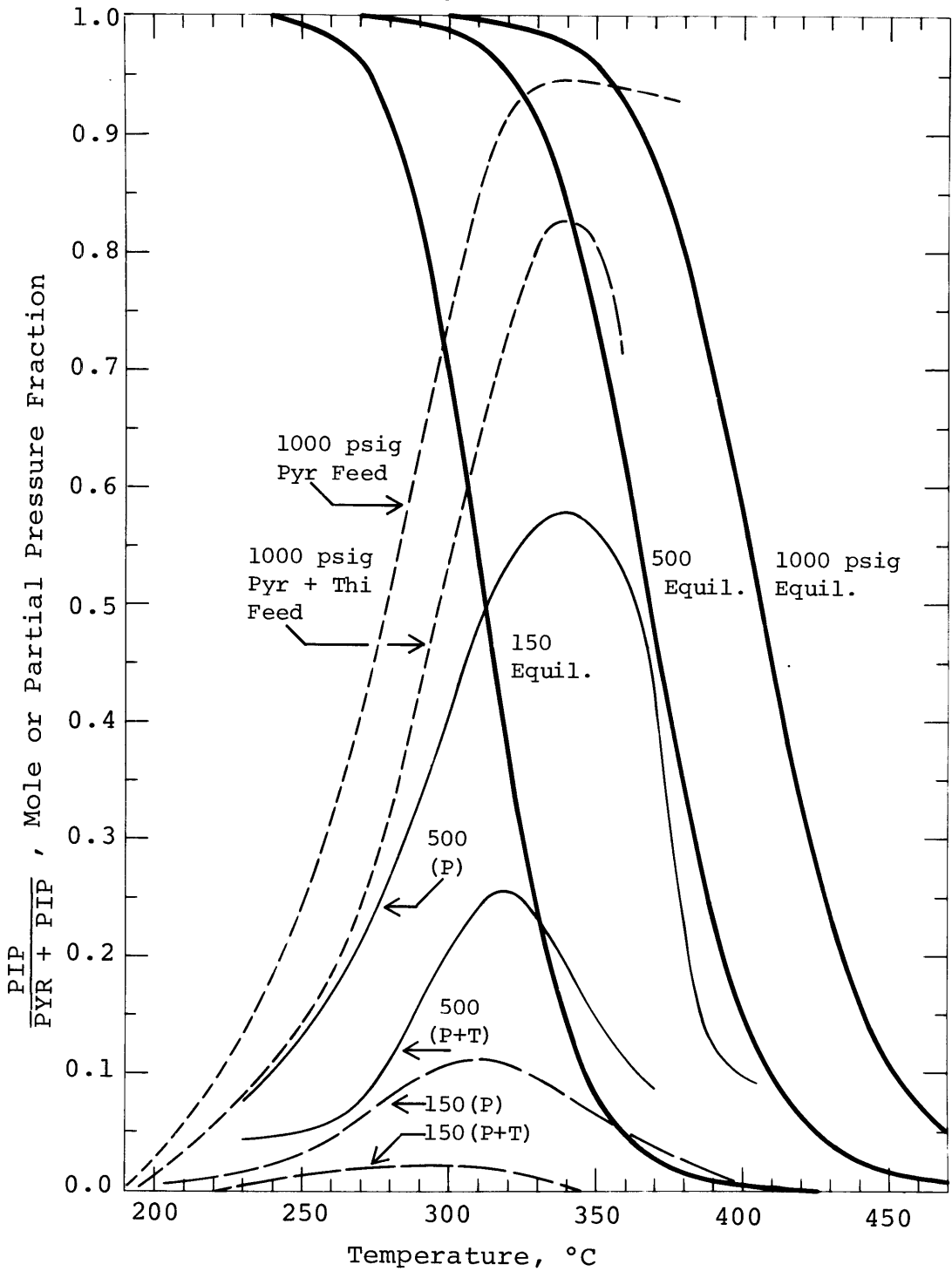


Figure 5-4: Comparison of Pyridine HDN Product Composition With Calculated Equilibrium Values (Empirical K_p) for Pure-Pyridine and Pyridine-Thiophene Feeds at Total Pressures of 150, 500, and 1000 psig.

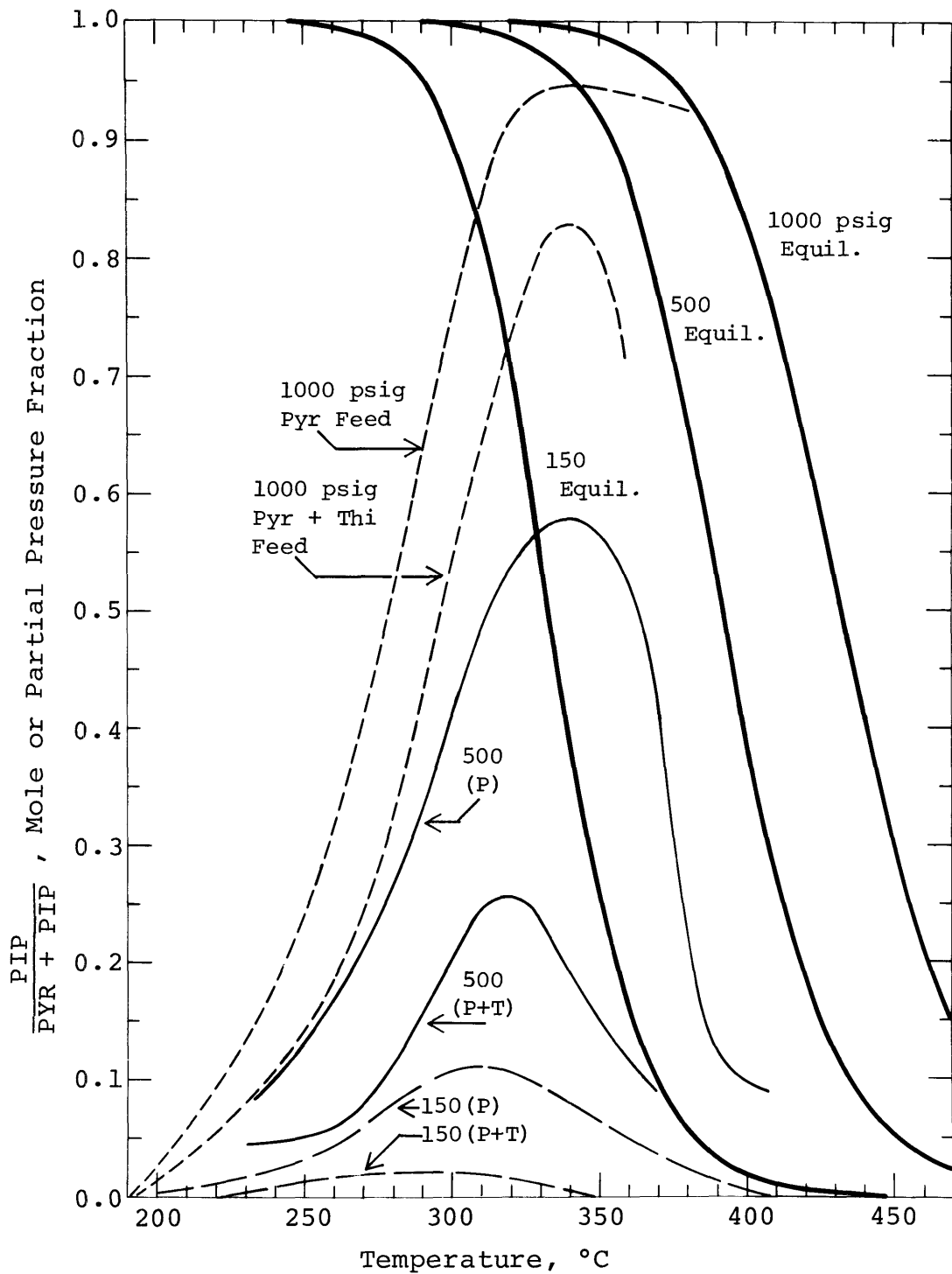


Figure 5-5: Comparison of Pyridine HDN Product Composition with Calculated Equilibrium Values (Thermodynamically-calculated K_p) for Pure-Pyridine and Pyridine-Thiophene Feeds^p at Total Pressures of 150, 500, and 1000 psig.

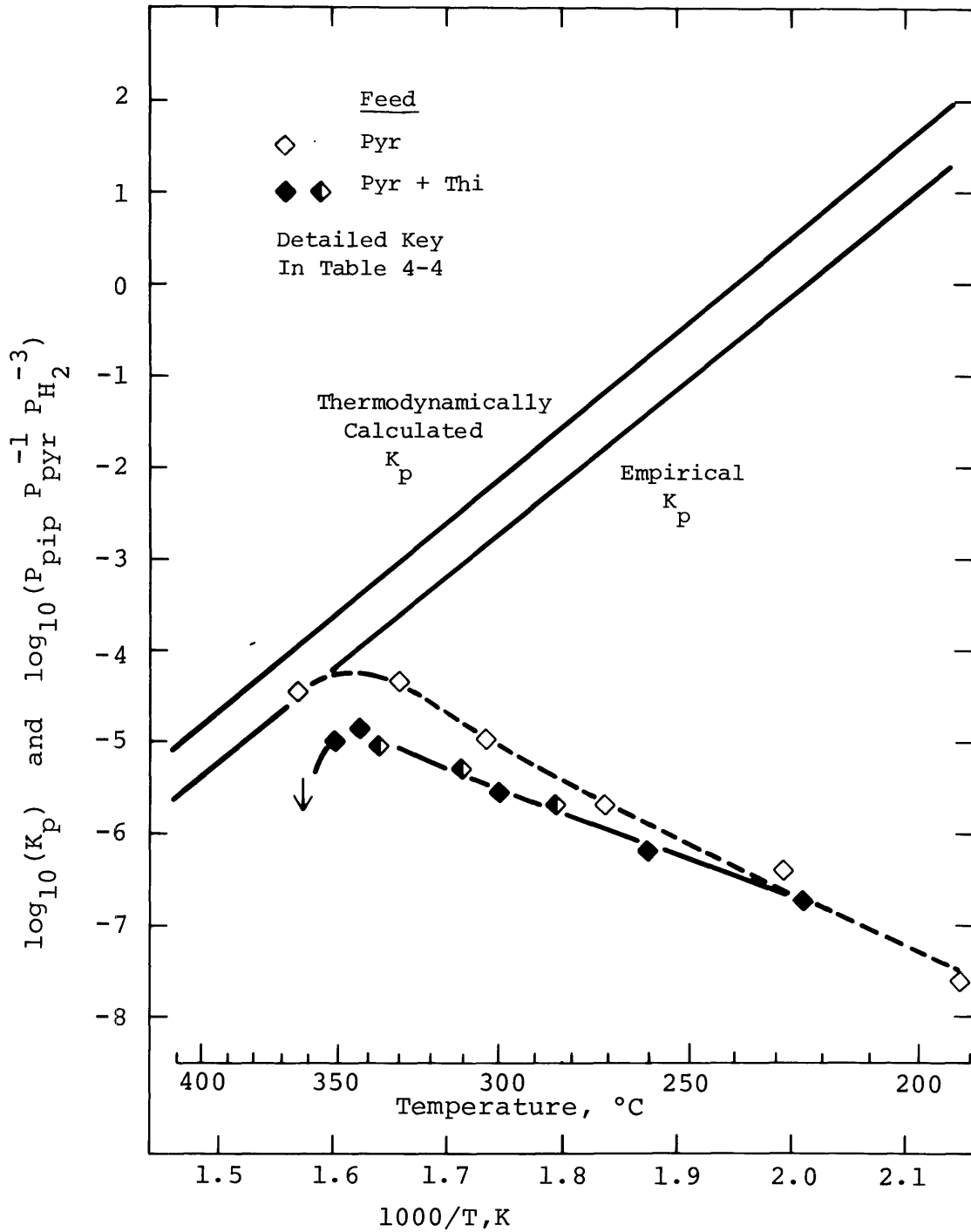


Figure 5-6: Comparison of the Experimental Values of The Equilibrium Constant Expression for Pyridine Hydrogenation with the Equilibrium Constant, for Pure-Pyridine and Pyridine-Thiophene Feeds at a Total Pressure of 1000 psig.

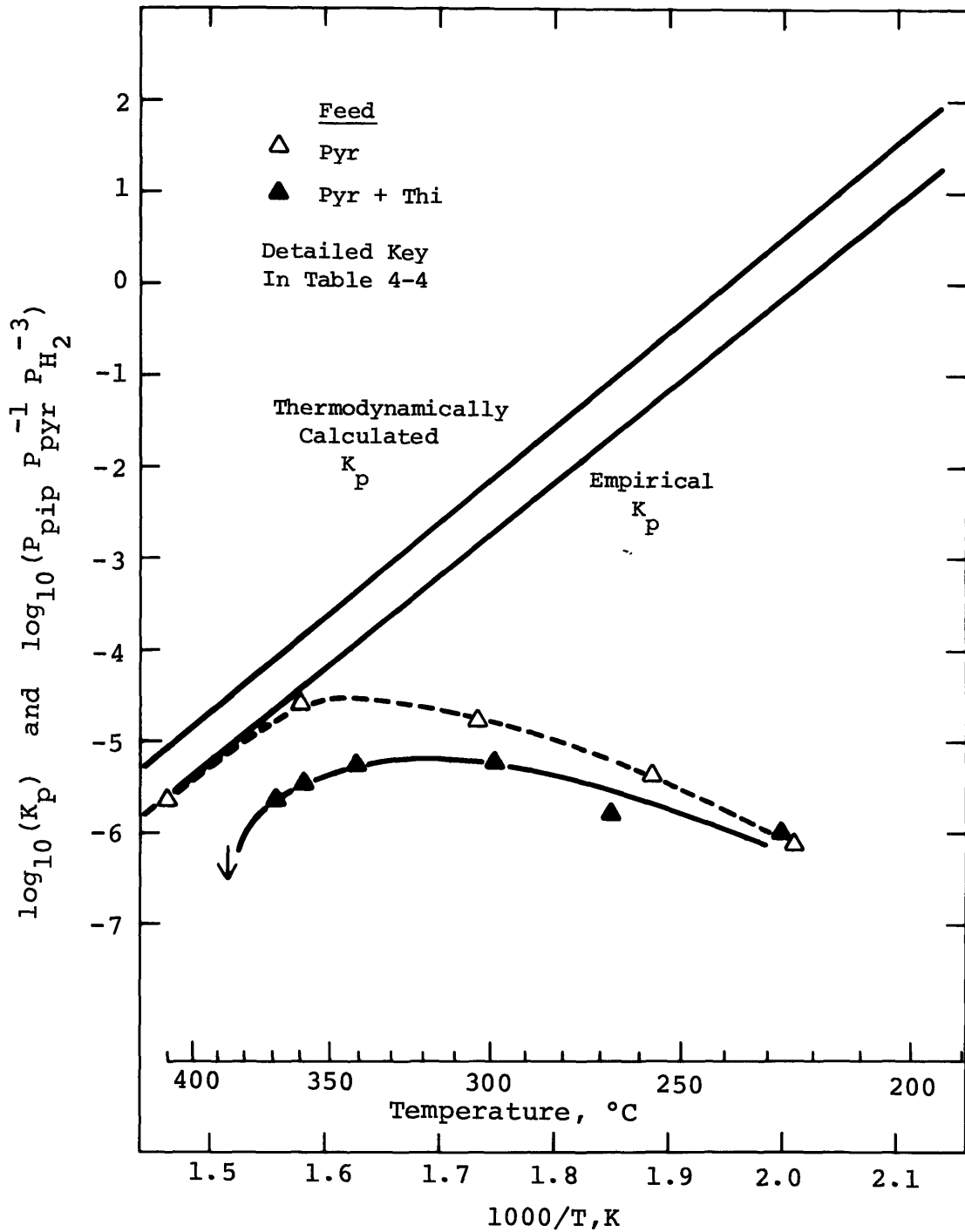


Figure 5-7: Comparison of the Experimental Values of The Equilibrium Constant Expression for Pyridine Hydrogenation with the Equilibrium Constant, for Pure-Pyridine and Pyridine-Thiophene Feeds at a Total Pressure of 500 psig.

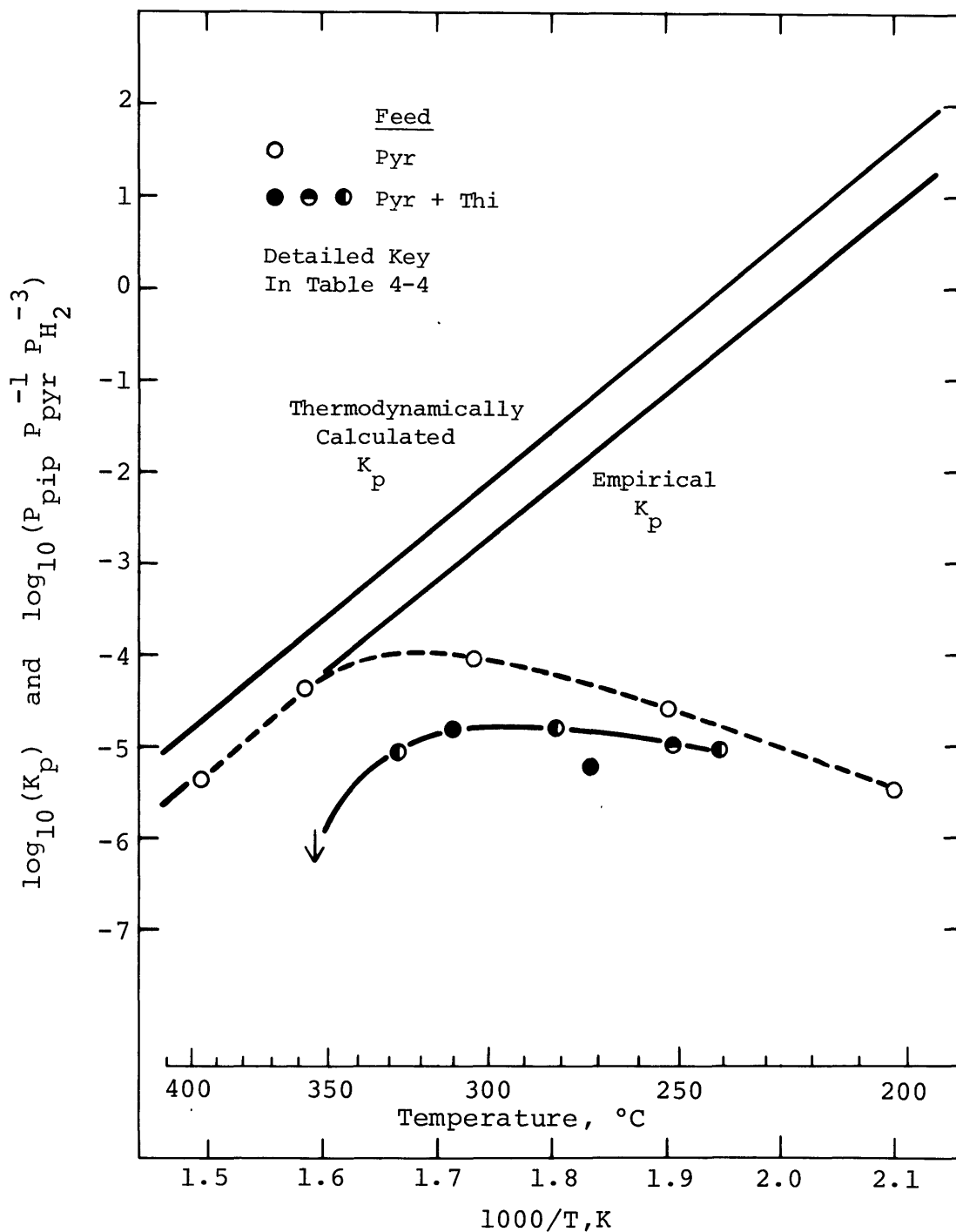


Figure 5-8: Comparison of the Experimental Values of The Equilibrium Constant Expression for Pyridine Hydrogenation with the Equilibrium Constant, for Pure-Pyridine and Pyridine-Thiophene Feeds at a Total Pressure of 150 psig.

but not the same precise attainment of, equilibrium. It should be remembered that the free energy of formation values upon which the thermodynamically-calculated equilibrium constant was based, were themselves based upon experimental data. These data have been significantly revised through the years, and also represent empirical, rather than absolute, thermodynamic values. The present results indicate that the data of Goudriaan may be more accurate than the data upon which the free energies were based.

In summary, these data indicate that pure-pyridine hydrogenation appears to reach equilibrium at reaction pressures from 150 to 1000 psig, particularly when viewed in light of results predicted by the empirical equilibrium constant. The addition of thiophene to the pyridine feed reduces the amount of piperidine present, preventing the attainment of equilibrium, and no thermodynamic limitation is encountered.

V.C.3. Pyridine HDN in the Presence of Sulfur Compounds

The addition of thiophene to the pyridine feed has been shown to have significant effects on pyridine HDN. The results section described the observed effects on pyridine hydrogenation and piperidine hydrogenolysis,

and the equilibrium discussion covered the way in which the lower concentrations of piperidine in the presence of thiophene affected the attainment of equilibrium between pyridine and piperidine. This discussion will apply the above results and analyses to other aspects of pyridine HDN.

The effect of the presence of thiophene on the hydrogenation of pyridine was shown in Figure 4-13. The rate-limiting reaction step before the onset of the equilibrium limitation was expected to be the hydrogenation of pyridine. The behavior of the 500 and 1000 psig data show the inhibiting effect of thiophene under these conditions. This was most likely due to competition between pyridine and thiophene for active catalytic sites.

The enhancement breakthroughs in the 500 and 1000 psig curves occurred at 360° and 350°C, respectively. From Figures 5-7 and 5-6, it is seen that equilibrium was reached at these same temperatures. It is thus likely that the 500 and 1000 psig pure-pyridine curves displayed a decreasing slope above these temperatures due not only to kinetic effects, but also very strongly due to an equilibrium limitation. The reaction rates represented by the pyridine-thiophene feed curves at temperatures greater than breakthrough were thus those of pyridine hydrogenation in the absence of a blocking piperidine concentration. Because

this hydrogenation was once again rate limiting, the competition for active sites remained a significant rate-determining factor. The results at 150 psig show similar behavior, with slight low-pressure conversion characteristics.

An understanding of the behavior of the disappearance of piperidine is important, as it is this component which is responsible for the equilibrium limitation, and enhancement of its removal is a primary objective. Figure 5-9 shows the percentage of the pyridine converted (hydrogenated to piperidine) which remains as piperidine in the product stream, for both pure-pyridine and pyridine-thiophene feeds, and total pressure of 500 and 1000 psig. For each pressure, there was a large decrease in this percentage when thiophene was added to the feed. There was a remarkable similarity of behavior between the two pure-feed cases and between the two mixed-feed cases. Since the percentages of removal were the same at the two pressures for temperatures greater than approximately 315°C, and since the amount of pyridine converted to piperidine was greater at 1000 psig than at 500 psig, then based strictly upon the amount of piperidine present, the piperidine hydrogenolysis appears to be precisely first order in piperidine under these conditions. This effect could also have been achieved with a reaction order less than one in piperidine if the

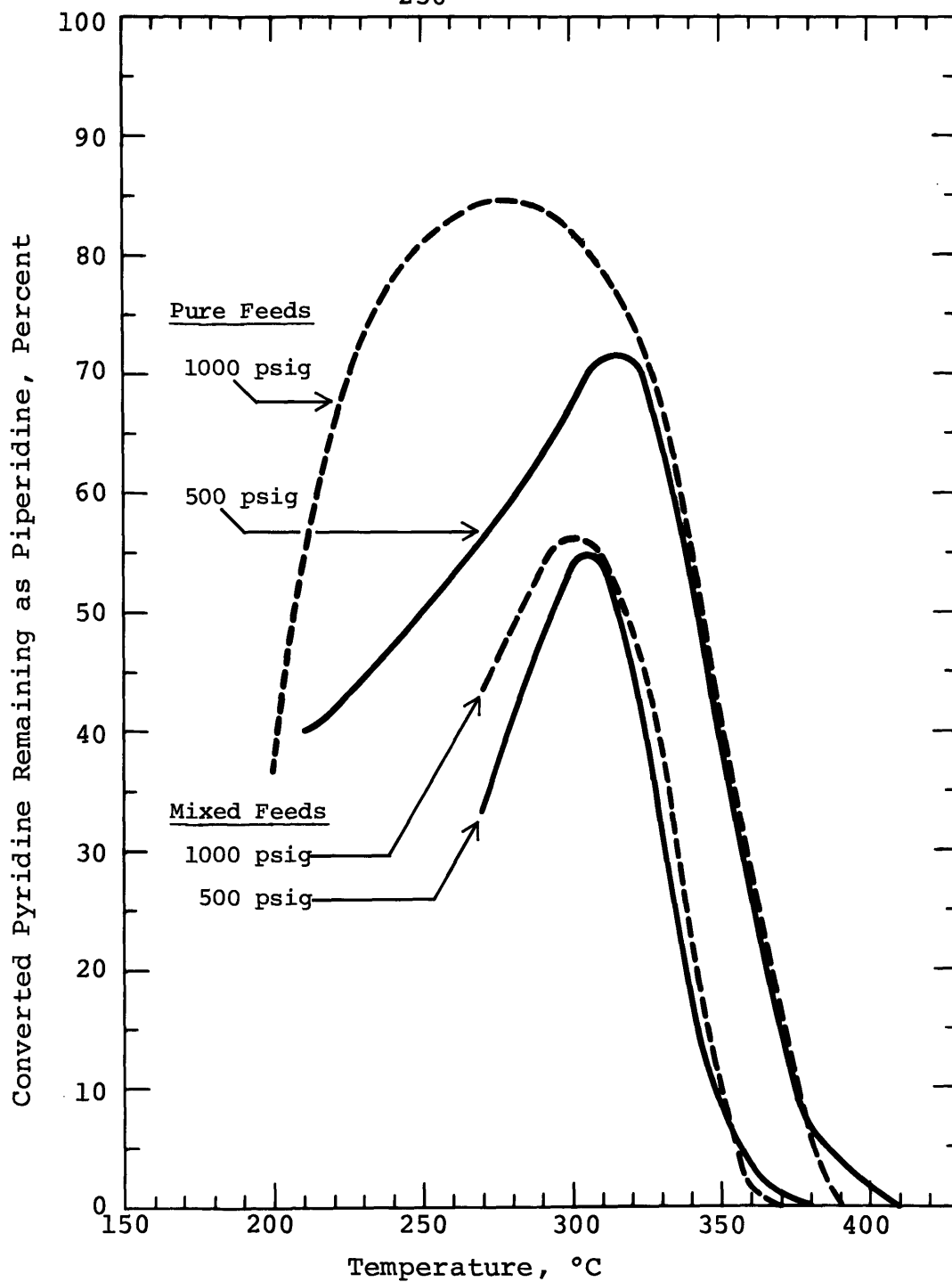


Figure 5-9: Percentage of Converted Pyridine Remaining As Piperidine in the Product Stream for Pure-Pyridine and Pyridine-Thiophene Feeds at 500 and 1000 psig.

increase in hydrogen partial pressure were also to increase the rate. The actual case is probably a combination of the piperidine order, the hydrogen effect, and the amounts of pyridine present.

Thiophene affects the amount of piperidine present in the product stream in at least two ways: by inhibition of pyridine hydrogenation; and by the enhancement of piperidine hydrogenolysis. The extent to which each of these mechanisms is significant appears to be a function of the total pressure.

At 1000 psig, the decreases in the piperidine concentration due to the addition of thiophene were always greater than could be accounted for by decreases in the amount of pyridine being hydrogenated. At low temperatures there was a significantly lower amount of piperidine present, while at the same time there was no inhibition of the pyridine conversion. For the entire temperature range, the decrease in piperidine was two to three times the amount which could be accounted for by lower pyridine conversions. At this pressure, then, the increase in piperidine hydrogenolysis must be the primary mechanism for the decrease in the piperidine concentration in the product stream.

The other extreme was represented by the performance at 150 psig. At this pressure, the inhibition of pyridine hydrogenation was always enough by a factor of two, to ac-

count for the lower piperidine concentrations. That this might imply a decreased rate of piperidine reaction in the presence of thiophene is not altogether satisfying, and this result should be used with caution.

The results at 500 psig, while once again between those at the pressure extremes, showed more of the 1000-psig character. At this intermediate pressure, the decreases in piperidine concentration and pyridine conversion were of the same general magnitude below 330°C. Above this temperature, there were much greater decreases in the piperidine concentration than in the pyridine hydrogenation inhibition. In fact, as at 1000 psig, there was a significantly lower amount of piperidine present in the product stream even with a hydrogenation enhancement.

Thiophene could enhance the hydrogenolysis of piperidine in several ways. First, H_2S , a product of thiophene HDS, could help maintain the catalyst in a more fully sulfided state; the sulfided condition of the catalyst has been shown to be important in the maintenance of catalytic activity. The acidity of H_2S could also enhance the hydrogenolysis activity through its ability to improve the acidity of the catalyst. Third, the acidic compound could help to remove basic nitrogen compounds from the catalyst surface.

Examination of the effect of hydrogen sulfide on pyridine HDN indicated that H₂S had a stronger inhibiting effect on pyridine conversion than did thiophene. The effects of the two compounds on the presence of piperidine in the product stream were quite similar. The effect on pyridine conversion would imply a stronger adsorption of H₂S than thiophene on the catalytic sites. This order is the reverse of that found for the adsorption of the two compounds on thiophene HDS sites. While the effects of H₂S on the presence of piperidine were similar to those of thiophene, if one were to infer from the data that the H₂S-related piperidine peak were higher than that from the thiophene-related runs, then the H₂S results would be intermediate between those of pyridine-thiophene and pure-pyridine feeds. This in turn, would imply a weaker adsorption of H₂S than thiophene. Thus, while it is possible to say that H₂S has effects similar to those of thiophene, more data would be needed to draw detailed conclusions.

To summarize the effects of thiophene on the removals of pyridine and piperidine, Figure 5-10 shows the ratios:

$$\begin{aligned} \text{RX(P)} &= \left[\frac{\text{conversion of pyridine} \\ \text{in a pyridine-thiophene feed}}{\text{conversion of pyridine} \\ \text{in a pure-pyridine feed}} \right] \\ \text{RX(P+P)} &= \left[\frac{\text{conversion beyond piperidine} \\ \text{in a pyridine-thiophene feed}}{\text{conversion beyond piperidine} \\ \text{in a pure-pyridine feed}} \right] \end{aligned}$$

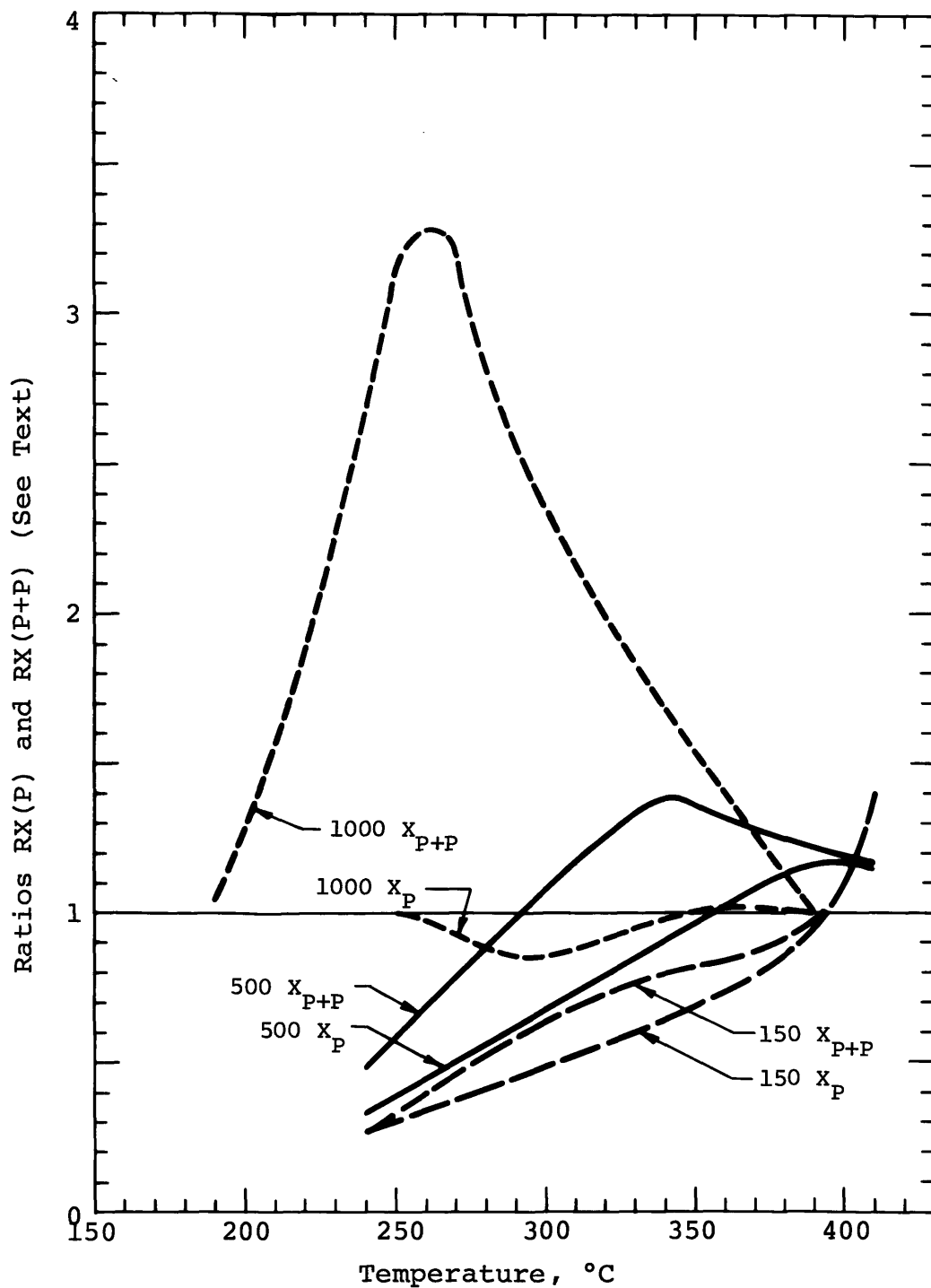


Figure 5-10: Comparison of the Effects of Thiophene on the Conversion of Pyridine with the Effects of Thiophene on Conversion of Pyridine and Piperidine at Total Pressures of 150, 500, and 1000 psig.

For the conversion of pyridine, there was an inhibition relative to the pure case under most conditions, with enhancements present only at the highest reaction temperatures. For the conversion beyond piperidine (disappearance of both pyridine and piperidine), however, there was a significant further enhancement for the two higher pressures, at intermediate temperatures, caused by the decrease in the piperidine concentration. This is an important effect, as any nitrogen remaining as piperidine in a petroleum stream would be as undesirable as pyridine, and the reduction of the levels of both should be examined. The most important point here is that at the higher reaction pressures of significance to industrial operation, whereas thiophene primarily causes an inhibition in pyridine hydrogenation, it enhances the conversion beyond piperidine.

V.C.4. Pyridine HDN: Kinetic Analysis

It was desired to see if the pyridine HDN data could be fitted to a kinetic model. Because the results obtained in this study were all integral data of a form not amenable to differentiations it was necessary to assume a particular kinetic model and integrate it for the case of a plug flow reactor. The experimental data could then be compared with the results predicted by the integrated model. The data

to be used for the pure-pyridine kinetic analysis were the 93 and 186 torr pyridine partial pressure runs at 150 and 1000 psig.

In order to properly examine models in the order of their complexity, it was first attempted to fit the pyridine data to power-law kinetic models. A first-order reaction in pyridine would have shown identical conversion curves for the two feed partial pressures, and a zero-order reaction would have produced an inhibition at the higher partial pressure greater than was observed. Thus the observed order was between zero and one. By calculating the actual observed order at ten-degree intervals, it was seen that this order changed with temperature, and hence with the extent of conversion. These results indicated that power-law kinetics was inadequate to describe the data. This was expected; the strong adsorption of both reactants and products indicated that an adsorption-oriented model would be required.

A Langmuir-Hinshelwood expression was then written to account for the competitive adsorption of all nitrogen species and the approach to equilibrium. Several assumptions for the specific model were required, in addition to those inherent in all Langmuir-Hinshelwood expressions. The basic set of parameters was varied from one model to another.

First, the inclusion of a term for the reversibility of the pyridine hydrogenation was added to the concentration driving force term. Cases were run both with and without the equilibrium term present.

The second type of assumption covered the choice of relative adsorption constants for pyridine, piperidine, and ammonia. Because the experimental data had to be compared with the integrated results, a specific relationship among the three adsorption constants had to be chosen for each model. There is great disagreement in the literature on the relevant relative strengths of adsorption. From adsorption studies using both metallic catalysts supported on alumina, and on an alumina support alone (Sonnemans, 1973), it is evident that any adsorption study utilizing the total available catalyst surface will indiscriminately adsorb compounds on active sites and non-active support areas. This decreases the usefulness of the derived results, as there are indications that in addition to the support material, there are perhaps two different types of catalyst sites on which one should carry out independent adsorption studies. Such a direct adsorption study under relevant reaction conditions would be extremely difficult at best.

A second way to arrive at the relative adsorptions is to attempt to draw conclusions on the effect of a particular component's concentration on the observed reaction rate.

This approach was used for example by Goudriaan(1974).

Adsorption of the product pentane on the acidic catalyst surface was taken to be much less than that of the basic nitrogen compounds present, following reasoning similar to that for the thiophene model, and the adsorption term for pentane was taken to be negligible. Although aliphatic amines are quite basic, the extremely low concentrations of n-pentylamine relative to pyridine and piperidine warranted elimination of this term from the denominator. Similarly, the low concentrations of the products of side reactions led to their exclusion. Thus, for the pure-pyridine feed cases, adsorption terms were included for pyridine, piperidine, and ammonia. A frequent assumption in the literature is that the adsorption constants for these three compounds are equal (Sonnemans, 1973; McIlvried, 1971). As there are a number of conflicting references relating to the relative adsorptivities of these compounds (see Literature review), this provided a neutral starting point, and was thus one of the adsorption cases studied. Goudriaan (1974) found different relative adsorptivities on pyridine hydrogenation and piperidine hydrogenolysis sites. The former type of site, which is applicable here, showed an ammonia adsorption five times stronger than that of pyridine. Other works did not necessarily discriminate among different types of sites,

but are at least considered here. Sonnemans (1973), for example, found ammonia to be adsorbed less strongly than pyridine by a factor of four, and piperidine to be adsorbed six times more strongly than pyridine. This, however, is due to a large extent to adsorption on the catalyst support, and is not necessarily applicable to the metallic sites. The stronger adsorption of piperidine is reasonable, however, if one considers piperidine to have much of the character of an aliphatic alkyl amine, as aliphatic amines are known to have stronger basicity than pyridine (Morrison and Boyd, 1966).

To cover the most likely adsorption relationships in the modeling process, piperidine was given three relative adsorption levels: equal to; twice; and four times that of pyridine. Ammonia was similarly given three relative levels of adsorption: equal to; one-fourth of; and four times that of pyridine.

An additional parameter accounted for the reaction of some nitrogen to heavy compounds which might form a tar on the catalyst surface, or in some other way not be involved in the actual adsorption process. For this, each other case was examined for two values of the amount of nitrogen compounds converted beyond piperidine (later termed "converted nitrogen") not present as ammonia. The values chosen were zero and 15 percent.

The number of catalytic sites required for the adsorption of the pyridine molecule on the surface is significant, as this number becomes the power to which the denominator of a Langmuir-Hinshelwood expression is raised. Two modes of adsorption have been proposed for pyridine: one-point adsorption onto a single catalytic site through the nitrogen atom (Goudriaan, 1974); and flat adsorption of the molecule onto several catalytic sites (Aboul-Gheit and Abdou, 1973; Balandin, 1964). The single-point adsorption seems more reasonable when one considers that it is the character of the nitrogen atom which gives pyridine its strong adhesion; flat adsorption would subordinate the nitrogen character of pyridine to its aromatic character, which would not account for the stronger adsorption than benzene. Further, single-point adsorption results in a denominator power of one, whereas the multiple sites of the second case result in an undefined and quantitatively rather intractable situation. For purposes of this model, then, single-point adsorption will be assumed, with its attendant denominator power of one.

The power of the pyridine partial pressure in the driving force term of the Langmuir-Hinshelwood expression represents the number of molecules of pyridine involved in the adsorption onto each catalytic site, this being inde-

pendent of the number of sites required per molecule as long as it does not adsorb dissociatively. As pyridine molecules adsorb individually, this power is one.

The adsorption of reactant hydrogen is taken to be on sites adjacent to but distinct from the sites for pyridine adsorption. This is analogous to the situation discussed previously for thiophene. The resulting hydrogen functionality in a Langmuir-Hinshelwood expression is then an independent factor times the nitrogen expression. As the great excess of hydrogen in the reaction mixture keeps its partial pressure essentially constant through a run, this hydrogen functionality will become a constant at each reaction pressure. This relationship holds for either the atomic or molecular adsorption of hydrogen on the catalytic sites, and all aspects of the model examination except the hydrogen functionality are independent of the type of hydrogen adsorption. In addition to the weak adsorption of reactant hydrogen, there may be a strong adsorption of hydrogen on pyridine-adsorption sites similar to that discussed for thiophene. Although this competition has not been considered a significant factor in the literature (Sonnemans, 1973; Goudriaan, 1974; McIlvried, 1971), the possibility should be kept in mind.

The Langmuir-Hinshelwood expression for the hydrogenation of pyridine which results from these assumptions, and was

used as the model for further analysis, is:

$$-r_{\text{Pyr}} = \frac{k_{\text{Pyr}} \alpha K_{\text{Pyr}} \left(P_{\text{Pyr}} - \frac{P_{\text{Pip}}}{K_{\text{eq}} P_{\text{H}_2}^3} \right)}{1 + K_{\text{Pyr}} P_{\text{Pyr}} + K_{\text{Pip}} P_{\text{Pip}} + K_{\text{NH}_3} P_{\text{NH}_3}}$$

where: $-r_{\text{Pyr}}$ = rate of disappearance of pyridine, gmoles pyridine/hr-gr catalyst

K_{Pip} = surface reaction rate constant for pyridine hydrogenation; appropriate units depending upon the functionality of the hydrogen term

α = hydrogen functionality, of form:

$$\frac{K_{\text{H}_2}^n P_{\text{H}_2}^n}{1 + K_{\text{H}_2}^n P_{\text{H}_2}^n}$$

where: $n = 1$ for molecular adsorption of H_2

$n = 1/2$ for atomic adsorption of H_2

$K_{\text{Pyr}}, K_{\text{Pip}}, K_{\text{NH}_3}, K_{\text{H}_2}$ = adsorption constants for pyridine, piperidine, ammonia, and hydrogen, respectively, torr^{-1} (except H_2 , psi^{-1})

$P_{\text{Pyr}}, P_{\text{Pip}}, P_{\text{NH}_3}, P_{\text{H}_2}$ = partial pressures of pyridine, piperidine, ammonia, and hydrogen, respectively, torr (except H_2 , psi)

E_{eq} = equilibrium constant for pyridine hydrogenation to piperidine, psi^{-3}

$$\left(\frac{P_{\text{Pip}}}{K_{\text{eq}} P_{\text{H}_2}^3} \right) = \text{equilibrium-approach term, torr}$$

This expression for $-r_{\text{Pyr}}$ was then used in the mass-bal-

ance-derived expression for reactor performance for an integral plug flow reactor:

$$\tau = \int_{P_{\text{Pyr}}^{\circ}}^{P_{\text{Pyr}}} \frac{dP_{\text{Pyr}}}{-r_{\text{Pyr}}}$$

The resulting expression was integrated, and then adjusted for 36 cases, representing all combinations of the following:

<u>Parameter</u>	<u>Cases Studied</u>
Pyridine-piperidine equilibrium accounted for (approach term included in concentration driving force) ?	[yes no]
Ratio: $\frac{K_{\text{NH}_3}}{K_{\text{Pyr}}}$	[0.25 1.00 4.00]
Ratio: $\frac{K_{\text{Pip}}}{K_{\text{Pyr}}}$	[1.0 2.0 4.0]
Percentage of converted nitrogen lost as heavy products	[0.0 15.0]

The method of analysis of the various HDN models was the same as that described for the thiophene expressions. Here, the experimental data used was: the actual pyridine feed partial pressure for the nominal 93 and 186 torr runs at 150 and 1000 psig; the partial pressures of pyridine and piperidine under the above reaction conditions.

For the pyridine evaluation, discrimination among models was accomplished by studying the linearity of the k_{tr} relationships. The results for the K_{PYR} values were quite erratic; a determination of the response of the K_{PYR} behavior to small shifts in the drawn conversion curves indicated that the data would not support the use of the K_{PYR} analysis. Thus, the following discussion focuses on the k_{tr} results. Also, the results for the 186 torr feed at 150 psig left much uncertainty as to the precise behavior of this pyridine conversion curve. Thus, the following discussion will use the results at a total pressure of 1000 psig.

Several strong trends permitted a number of models to be classified as definitely inferior in the modeling of these data, and yield general conclusions about the best results. First, in every case where $(K_{\text{NH}_3}/K_{\text{PYR}}) = 4.0$, for all values of the other parameters studied, the model showed extreme deviations from linearity at higher reaction temperatures. At lower temperatures, where conversions were low and the concentration of ammonia in the product stream was therefore also low, there was little difference from the models where this ratio equaled 0.25 or 1.00. The relatively poor performance of this model suggests the adsorption of ammonia to be equal to or less strong than that of pyridine on the hydrogenation sites. The per-

formance of the 0.25 ratio curve may be considered slightly better than that of the 1.0 curve, but the difference is far less than that between these two ratios and the higher one.

Second, the assumption of a 15 percent loss of converted (beyond piperidine) nitrogen caused no significant differences in the results for cases where $(K_{\text{NH}_3}/K_{\text{Pyr}})$ was not equal to four. Only in those cases of very strong ammonia adsorption did this make a real difference, and then it did not improve the model. As the strong ammonia adsorption case has already been shown to be inferior, and there was virtually no effect of the 15 percent loss criterion on the other cases, the criterion can also be disregarded.

The very strong adsorption of piperidine, $(K_{\text{Pip}}/K_{\text{Pyr}}) = 4.0$, also reduced the quality of each case over similar cases with this ratio equal to one or two. Thus from these data, the adsorption of piperidine on the hydrogenation sites could be said to be less than four times as strong as that of pyridine.

The addition of the driving force term to account for the reversible nature of the hydrogenation should have improved the results at temperatures where equilibrium was reached. At high temperatures there was always a slight difference between the equilibrium and non-equilibrium cases, other factors held constant, but it did not affect

differentiation among the other model parameters.

This leaves two criteria, giving four cases, which appear to indicate the best level of performance and thus of the underlying assumptions. The best, and approximately equal, results are obtained for:

$$\frac{K_{\text{NH}_3}}{K_{\text{Pyr}}} = \begin{array}{c} \boxed{0.25} \\ \text{or} \\ \boxed{1.00} \end{array} \quad \frac{K_{\text{Pip}}}{K_{\text{Pyr}}} = \begin{array}{c} \boxed{1.0} \\ \text{or} \\ \boxed{2.0} \end{array}$$

From the fitting of these models to the data, it can be concluded that on the catalytic sites active for hydrogenation of pyridine to piperidine: 1) the adsorption of ammonia is on the order of or less than that of pyridine, and 2) the adsorption of piperidine is on the order of that of pyridine, or slightly greater.

Six cases are shown in Figure 5-11. For a total pressure of 1000 psig and $(K_{\text{Pip}}/K_{\text{Pyr}}) = 1.0$, both equilibrium-corrected and non-equilibrium-corrected models are presented for $(K_{\text{NH}_3}/K_{\text{Pyr}}) = 0.25, 1.0$ and 4.0 . The natural log of the k_{tr} term is given as a function of inverse absolute temperature. Three distinct sections of the curves can be discerned. These correspond to the three types of behavior present in the pyridine conversion curves of Figure 4-11: below 250°C, where the 93 and 186 torr curves separated and then closed slightly as temperature rose; between 250° and 300°, where the curves remained fairly

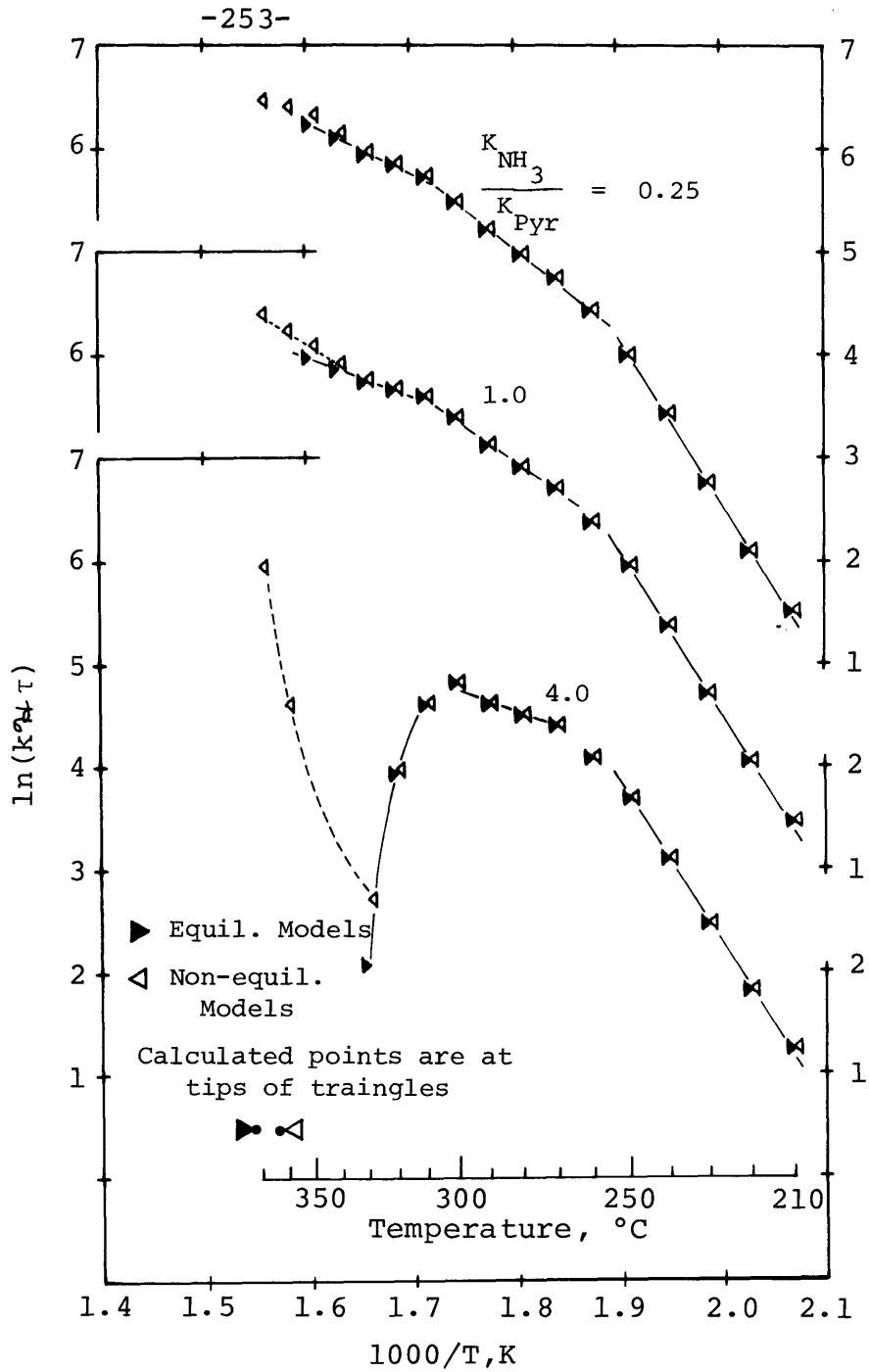


Figure 5-11: The Relative Performance of Six Langmuir-Hinshelwood Models for Correlating Pyridine Hydrogenation Data at a Total Pressure of 1000 psig for $K_{Pip}/K_{Pyr} = 1.0$

parallel; and above 300°C, where equilibrium and kinetic effects began to show. These results are qualitatively similar to those of other workers, who found shifts in reaction mechanisms among different temperature regions (Sonnemans, 1973; Goudriaan, 1974). The effect of the equilibrium correction can be seen as a divergence of the solid and open symbols at temperatures above 300°C. Finally, whereas there was but a small difference between the 0.25 and 1.0 ratio curves, the 4.0 ratio curve illustrates the poor behavior described earlier which was used as the basis for rejection of the strong adsorption of ammonia.

The initial, low-temperature sections of the curves, before product adsorption interactions took effect, had the same straight section with the same slope for all four of the best models. This slope gave an activation energy of 32.1 kcal/gmole. The observed activation energy decreases for the middle-temperature portion of the 0.25 and 1.0 curves, to approximately 15 kcal/gmole. A line drawn to take all the points into consideration yields an activation energy of approximately 20 kcal/gmole.

Of the four best cases, two ($K_{\text{NH}_3}/K_{\text{Pyr}} = 0.25$ and 1.0, for $K_{\text{Pip}}/K_{\text{Pyr}} = 1.0$) were shown in Figure 5-11. The other two, for the same relative ammonia strengths but for $K_{\text{Pip}}/K_{\text{Pyr}} = 2.0$, are included in the Appendix.

One comment can be made concerning the general magnitude of the observed adsorption coefficients for all the cases described above as giving the more-reasonable fits. The magnitude of the sum of the products $\sum K_{ads_i} P_i$ is of the order 1, implying that all terms of the denominator of the model are significant. Specifically, the 1.0 term is not negligible, thus removing the possibility of reducing the best fit for this data to a power-law model with a reaction rate constant which is a function of the initial partial pressure of pyridine, the so-called "poisoned first order" reaction mechanism of Sonnemans (1973).

Because of the general nature of the conclusions from this analysis, it was not possible to extend it further to incorporate the interactions with thiophene.

V.D. Relative Rates of Thiophene HDS and Pyridine HDN

In pure-reactant form the reactions of thiophene were relatively rapid compared with those of pyridine. However, the mutual interactions have been shown to produce several different effects on the various reactions and reaction steps. First, the conversions (disappearances) of thiophene and pyridine were each inhibited in the presence of the other under most reaction conditions. The inhibition of the thiophene conversion, however, was much

greater than that of pyridine. As a result, the ratio of thiophene conversion to pyridine conversion decreased significantly for the mixed-feed cases. Figure 5-12 presents these interactions as the ratio of conversions of thiophene and pyridine as a function of the reaction temperature. The curves for 500 and 1000 psig show this decrease in the ratio of conversions for the mixed-feed cases relative to the pure-feed cases. Where thiophene had been as much as three times more active toward reaction than pyridine when pure, the maxima decreased to 1.0 to 1.5 for the mixed feed data. The ratios at these pressures approach unity at higher temperatures as the conversions of both thiophene and pyridine approach 100 percent. A significant factor here is that this reduction was achieved through inhibitions of both reactions, rather than enhancements. The results at 150 psig appear quite different, as the pyridine conversions remain low at all temperatures. As this pressure is significantly below those of commercial petroleum processing conditions, attention should be focused on the higher-pressure results.

The actual parameter of interest in the treatment of a petroleum feedstock is the complete removal of an offensive atom from the liquid fuel. In the case of thiophene, this is accomplished in the first step of the thiophene

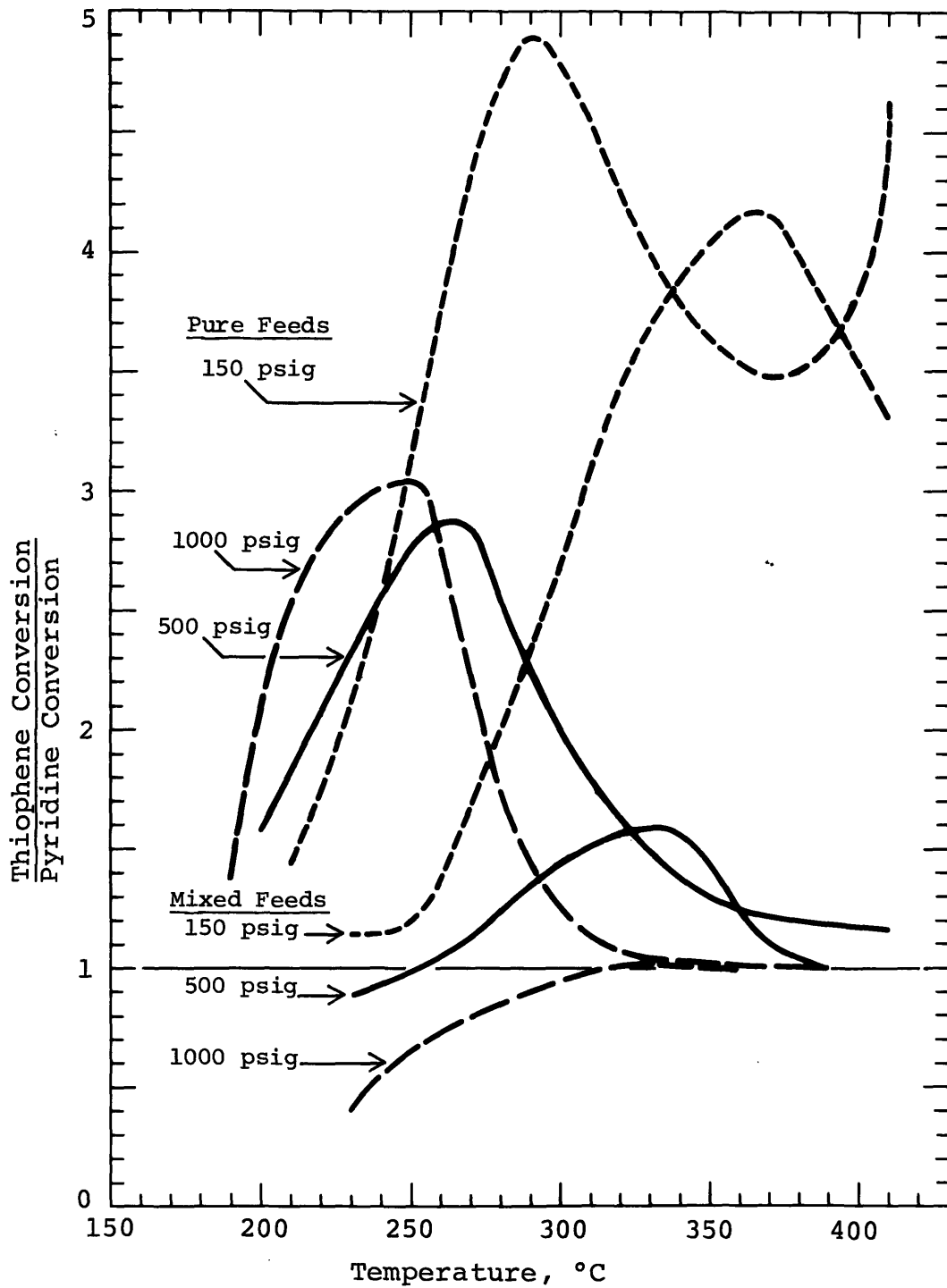


Figure 5-12: The Ratio of Thiophene Conversion to Pyridine Conversion for Pure and Mixed Feeds At Total Pressures of 150, 500, and 1000 psig.

conversion, where hydrogen sulfide is formed and can be separated from the liquid phase. For pyridine, however, its conversion results in the immediate formation of piperidine, itself undesirable in the product liquid. Although some heavy side products will form, the disappearance of both pyridine and piperidine can be examined as an approximation of the conversion pyridine to ammonia.

Figure 5-13 presents the ratio of thiophene conversion to the conversion of both pyridine and piperidine as a function of reaction temperature. Accounting for piperidine changes the sulfur-nitrogen relationship considerably. At 1000 psig, for example, with the great amount of piperidine formed, the ratio in the pure-feed case rises to sixteen instead of the previous three, at intermediate reaction temperatures. The mixed-feed case shows a much smaller peak due to the reduction of piperidine levels. At temperatures approaching 400°C, all of the high-pressure curves approach one, as complete conversion is approached for all components. This observation is important, as it demonstrates that a combination of sufficiently high temperatures and pressures can overcome some of the adverse effects of mixed-feed reactions.

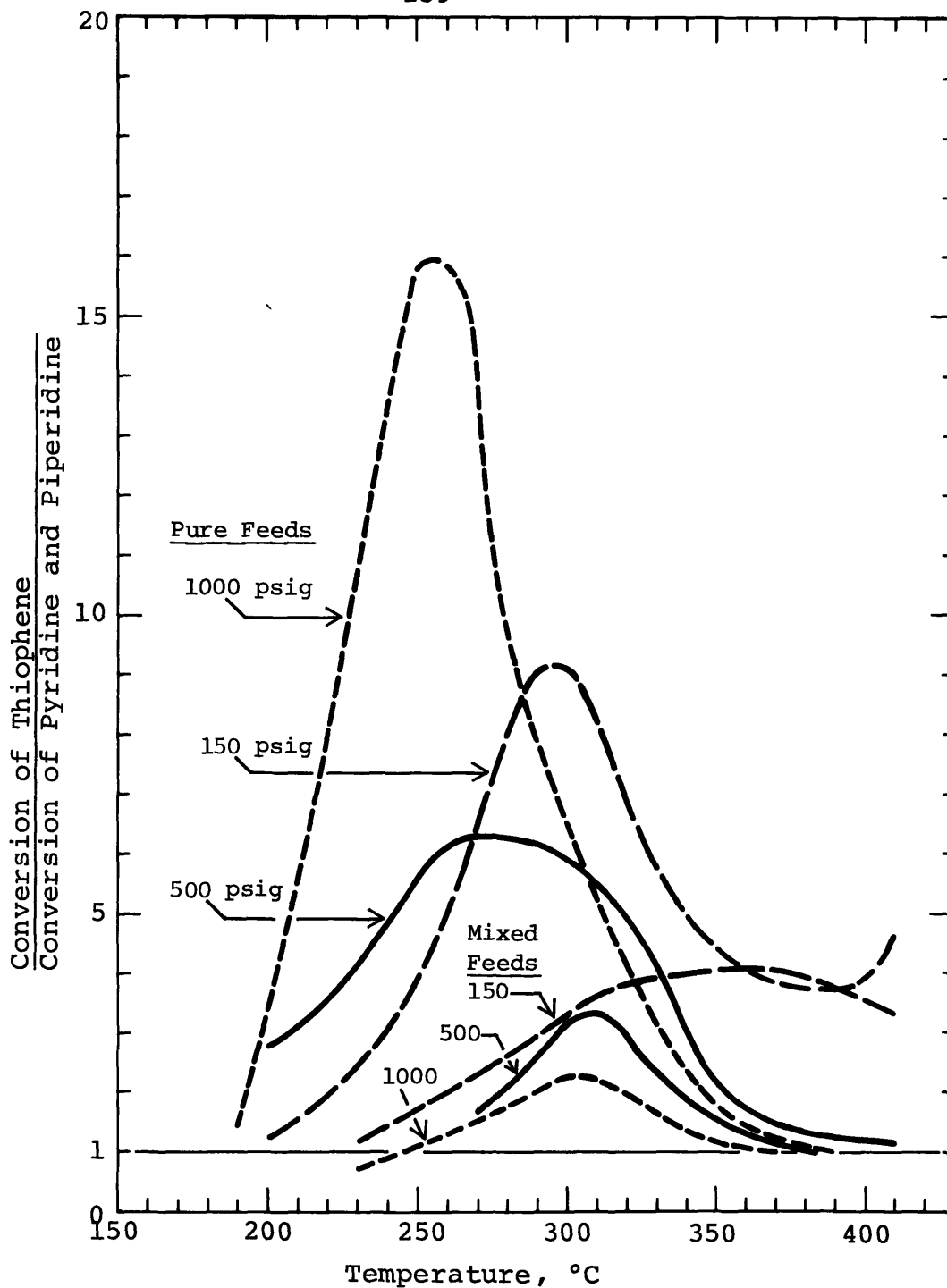


Figure 5-13: The Ratio of the Conversion of Thiophene to the Conversion of Pyridine and Piperidine For Pure and Mixed Feeds at Total Pressures of 150, 500, 1000 psig.

V.E. Quality of the Experimental Data

Two types of errors are present in experimental data: determinate, or systematic error; and indeterminate, or random error (Shoemaker and Garland, 1974; Skoog and West, 1969). Both types of error and their significance and treatment in this study are discussed below. Additionally, the determinate error associated with each piece of equipment is covered in the separate apparatus discussion. The specific mathematical treatment of indeterminate error is detailed in the Appendix section covering the derivation and principles of equations.

Determinate errors are subdivided by Skoog into those of the instruments, the methods, and the personnel. The first, difficulties with the experimental apparatus, was the most significant in this study. Great care was taken to identify and eliminate many systematic errors associated with the equipment and its use. Where appropriate, all pieces of equipment were calibrated; for example, pressure gauges by local manufacturer's representatives or Institute services, the gas chromatograph by direct injection of reactants and products, and the reactant metering pump by weighing metered samples.

Experimental methods were worked out and performed with great care. Further, much experience was gained before obtaining the final set of data appearing in this thesis. Regarding personnel error, the author attempted to be as

careful in the acquisition of data and as objective in its treatment as possible.

Shoemaker states that "sad experience hath shown... that more often than not systematic errors are undetected and uncorrected." In this study, all systematic errors which were recognized were either corrected or accounted for by equipment calibration. Any such error remaining was indeed not detected.

Indeterminate errors, such as random variations in equipment performance, instrument indications, and personal reading of instruments or operation of the apparatus, are relatively easy to express quantitatively. Whereas systematic error will bias results in a specific direction, random error is assumed to produce a scatter approximating a Gaussian, or normal, distribution of values about a mean, thus allowing statistical treatment.

For the data of this study, every conversion point presented was calculated from two sets of several gas chromatograms each, taken at two different steady-state conditions of the reactor system. Four to six samples were usually taken for each set; more were made if necessary due to large fluctuations in the first areas obtained. Each gas chromatograph sample exhibits the net effect of all control and measurement errors present in the system at that particular moment. The spread of each

set of such samples has been statistically analyzed and presented as the relative standard deviation.

By propogating the errors through the mathematical analysis as shown in the Appendix, confidence intervals were calculated. As at least thirty samples would be needed to approximate the behavior of a Gaussian distribution, t-values were used to properly size the intervals according to the number of samples used (Anderson, 1963; Crow et al., 1960). For each conversion point, both 68 percent and 95 percent confidence intervals were calculated, corresponding to intervals of plus or minus one and two standard deviations from the mean, respectively, for a normal distribution.

Figure 5-14 presents the pyridine hydrogenation results of Figure 4-13 with the addition of bars on each data point representing the 95 percent confidence intervals. Where the bars were smaller than the sizes of the drawn data point, they were not shown. The analogous bars for the 68 percent confidence intervals were of course smaller.

In addition to providing quantitative and visual estimates of the quality of the data, these bars were useful indetermining whether curves drawn precisely through sets of data points were reflecting a true difference between sets of conditions, or whether one curve should represent

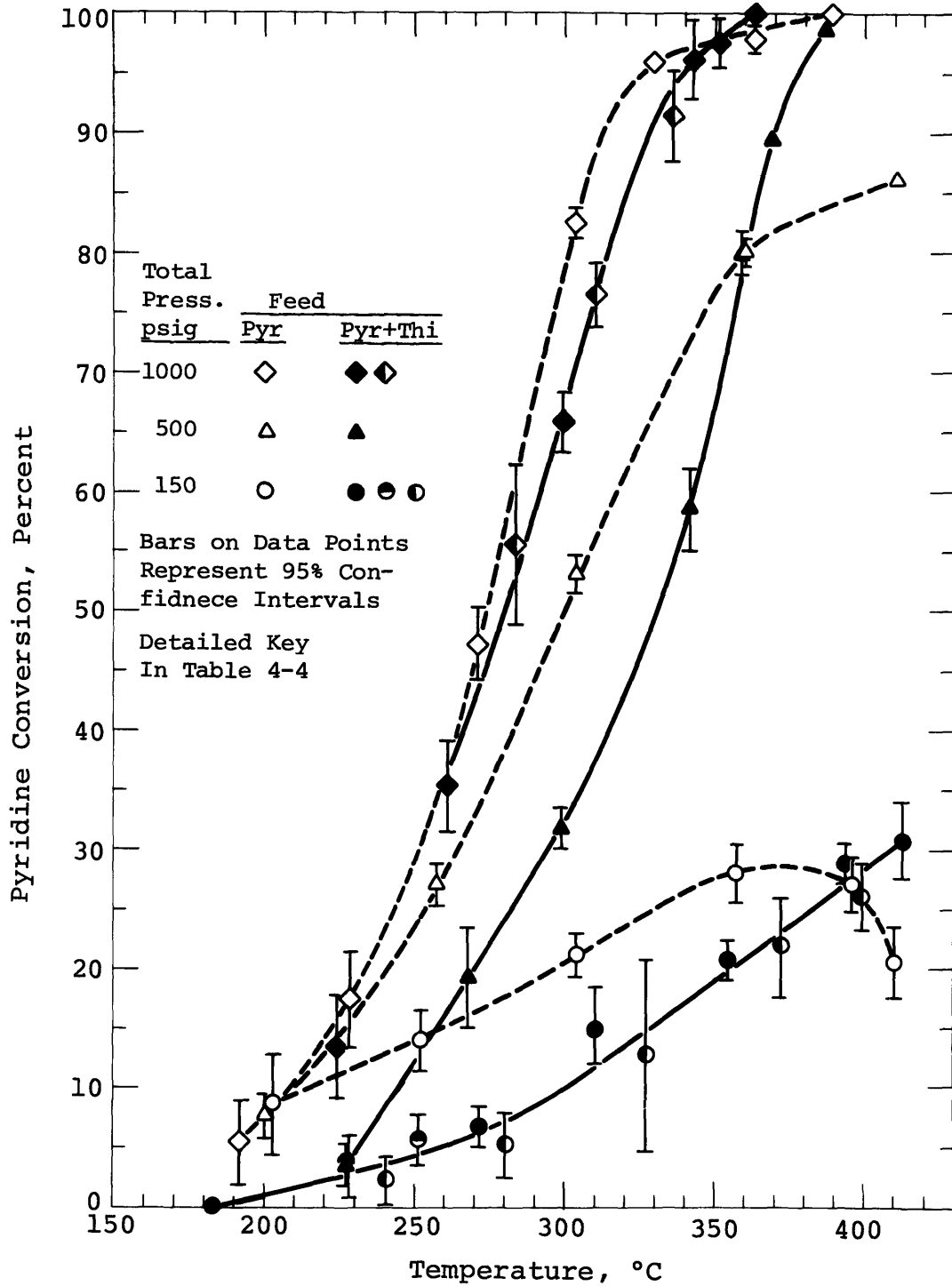


Figure 5-14: 95 Percent Confidence Limits for Pyridine Conversion Data

both sets of data. This criterion was applied in the drawing and analysis of the graphical results. An example of this technique in Figure 5-14 is the drawing of the curves for the pure-pyridine and pyridine-thiophene feeds at 1000 psig total pressure. From examination of the confidence intervals it was clear that at temperatures above 270°C the curves were indeed different, with 95 percent confidence. The single mixed-feed data point at 224°C was shown by its error bars to be not significantly different from the pure-pyridine data, and both sets of data were represented by the single curve drawn at lower temperatures.

Another important use for the confidence levels was in the methylthiophene analysis. The conclusion that there was a difference between the 2-methylthiophene and 2,5-dimethylthiophene curves was made on the basis of this type of statistical evidence.

The reproducibility of the data was demonstrated by the repetition of runs. Mixed thiophene-pyridine runs were chosen for the reproducibility runs because each contained two complete sets of reaction data (one for each reactant) which would have to fit the reproducibility criteria simultaneously, a severe test. There were thus several mixed-feed runs made at 150 and 1000 psig, and the consistency of their results can be seen for both conversions and inter-

mediate reaction products in Figures 4-5, -13, -16, -17, and -18.

Without the chromatographic separation of the light reaction products it was not possible to calculate a mass balance for the reactions. However, for the pyridine runs, where absolute calibrations for the molar responses had been made for the product distribution calculations, it was possible to make a mass balance on the feed stream for the no-reaction conditions. This was a check on the independent calibrations of the reactor metering and flow measurement systems and the gas chromatographic analysis system. First, from metered and measured reactor flow rates the number of moles of pyridine which should have been in the gas sample valve could be calculated. Second, from the chromatograph peak areas and the absolute calibrations of the GC response for pyridine, the number of moles of pyridine detected could be obtained. These totally-independently-determined quantities were calculated for two pure-pyridine runs, and showed mass balances for pyridine to within 0.4 and 0.9 percent. This demonstrates, at least for those runs checked, that the pyridine fed to the reactor was well accounted for in the analysis stream.

Chapter VI - Conclusions

VI.A. Catalyst Activity

The activity of sulfided NiMo/Al₂O₃ catalysts is strongly dependent upon the state of sulfiding of the catalyst. The addition of easily-decomposed sulfur compounds to a reactor feed will maintain activity in the presence of basic nitrogen compounds such as pyridine.

VI.B. Thiophene Hydrodesulfurization

Thiophene HDS is inhibited by the presence of the basic aromatic nitrogen compound pyridine at all temperatures, and pressures from 150 to 1000 psig (11 to 70 bars). Aliphatic amines appear to cause the same degree of inhibition as does pyridine. Complete conversion is still possible under inhibited conditions, but at higher reaction temperatures than for the pure-thiophene reaction.

Pyridine competes strongly with thiophene for active catalytic sites, showing an adsorption strength greater than that of thiophene. Hydrogen sulfide is also competitive, but appears to have weaker adsorption than thiophene when present as a product of thiophene hydrogenolysis. Two-point adsorption of thiophene gives better kinetic

correlations for these data than does single-point adsorption.

VI.C. Pyridine Hydrodenitrogenation

The HDN of pure pyridine is subject to a thermodynamic limitation above 350°C at pressures from 150 to 1000 psig, where pyridine reaches equilibrium with its saturated reaction intermediate piperidine. The higher hydrogen partial pressures, however, shift the equilibrium composition toward piperidine, and complete conversion of pyridine is then possible.

The presence of thiophene inhibits the hydrogenation of pyridine at temperatures below which the equilibrium limitation would be in effect for the pure feed reaction. At temperatures above which pure pyridine hydrogenation would be equilibrium-limited, thiophene enhances pyridine reaction, giving conversions greater than those observed for the pure-feed case.

The concentration of piperidine greatly decreases with the addition of thiophene, caused by both the inhibition of pyridine hydrogenation and the enhancement of piperidine hydrogenolysis. This reduction in the piperidine concentration removes a necessary criterion for equilibrium; there is no thermodynamic limitation on

pyridine HDN in the presence of thiophene.

The conversion of pyridine beyond piperidine is enhanced by thiophene for temperatures greater than 300°C at pressures of 500 and 1000 psig. This is a better measure of the removal of the nitrogen atom from the liquid reactant stream than is the conversion of pyridine.

Piperidine competes with pyridine for active catalytic sites with an adsorption strength equal to or slightly greater than that of pyridine. Ammonia adsorption is equal to or weaker than pyridine on the active catalytic sites.

Chapter VII - Recommendations

1. Determine adsorption constants and reaction rate constants for both the pure-feed and mixed-feed cases with thiophene and pyridine. Make this a primary objective of a run program. This would entail taking data as conversion as a function of inverse feed rate at constant temperature, rather than conversion as a function of temperature at a constant feed rate. With the data of this present study already providing the overall picture, the narrower temperature limits of such a study should not be bothersome if the reaction conditions were carefully chosen. This alternate data form would permit differentiation of the data and direct application to Langmuir-Hinshelwood modeling procedures. This should than improve the distinctions among the relative adsorptions of the various compounds on the active catalytic sites.

2. Study the effect of the addition of thiophene on the product distribution of pyridine HDN. (It would seem that some of the many reaction products observed by Sonnemans, for example, would not be found under the mixed-feed conditions.) This would require improved chromatographic separations, possibly utilizing two different column packings, with column switching, for

separating both the low and medium boilers. It might also require the use of a flame ionization detector on the gas chromatograph.

3. Compare the effects of thiophene and of hydrogen sulfide on pyridine HDN in more detail. This study raised questions as to the relative effects of the two compounds. An improved understanding of this should give a better picture of the role of H_2S as both necessary for catalyst activity and as an inhibitor of reactions.

4. Extension of the study to other nitrogen and sulfur compounds, still emphasizing the interactions between sulfur and nitrogen. These studies could also involve the use of simulated feed stocks for naphtha reactions. Trickle-bed operations would also be interesting, as these add another dimension to the problem. Comparisons of the same heterocompounds in the gas-phase and trickle-bed operation could be an interesting bridge from our present work.

5. A detailed catalyst study is not the purpose of the current line of research in this group, but it would be interesting to carefully consider what commercial catalysts should be used in future work, as new developments have improved the activity for hydrodenitrogenation.

Chapter VIII - Appendix

VIII.A. Apparatus - Further Details

Apparatus figures referred to in the text and indicated as being in the Appendix are included in Appendix A.

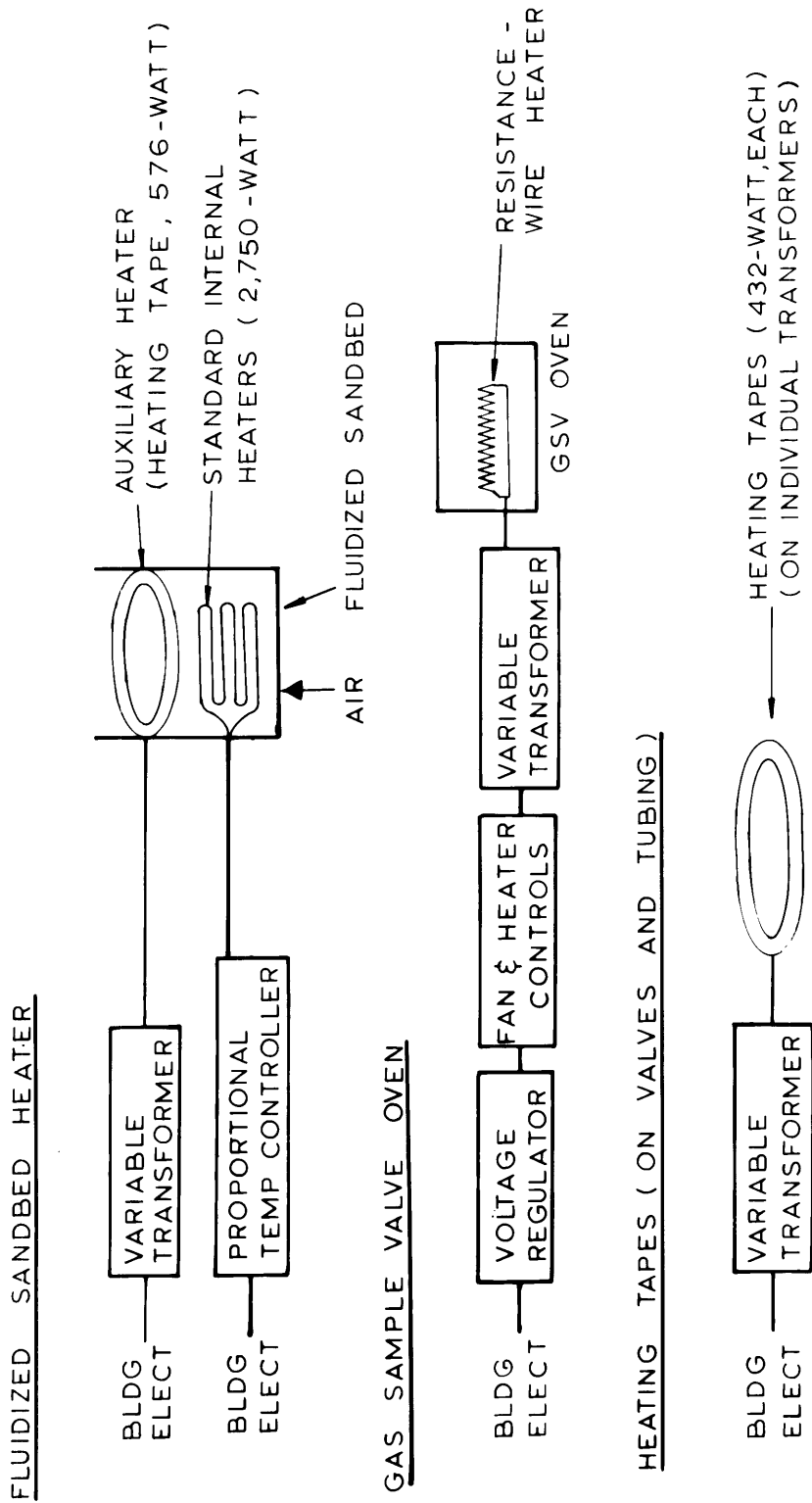


FIGURE 8-1: HEATING CIRCUITS

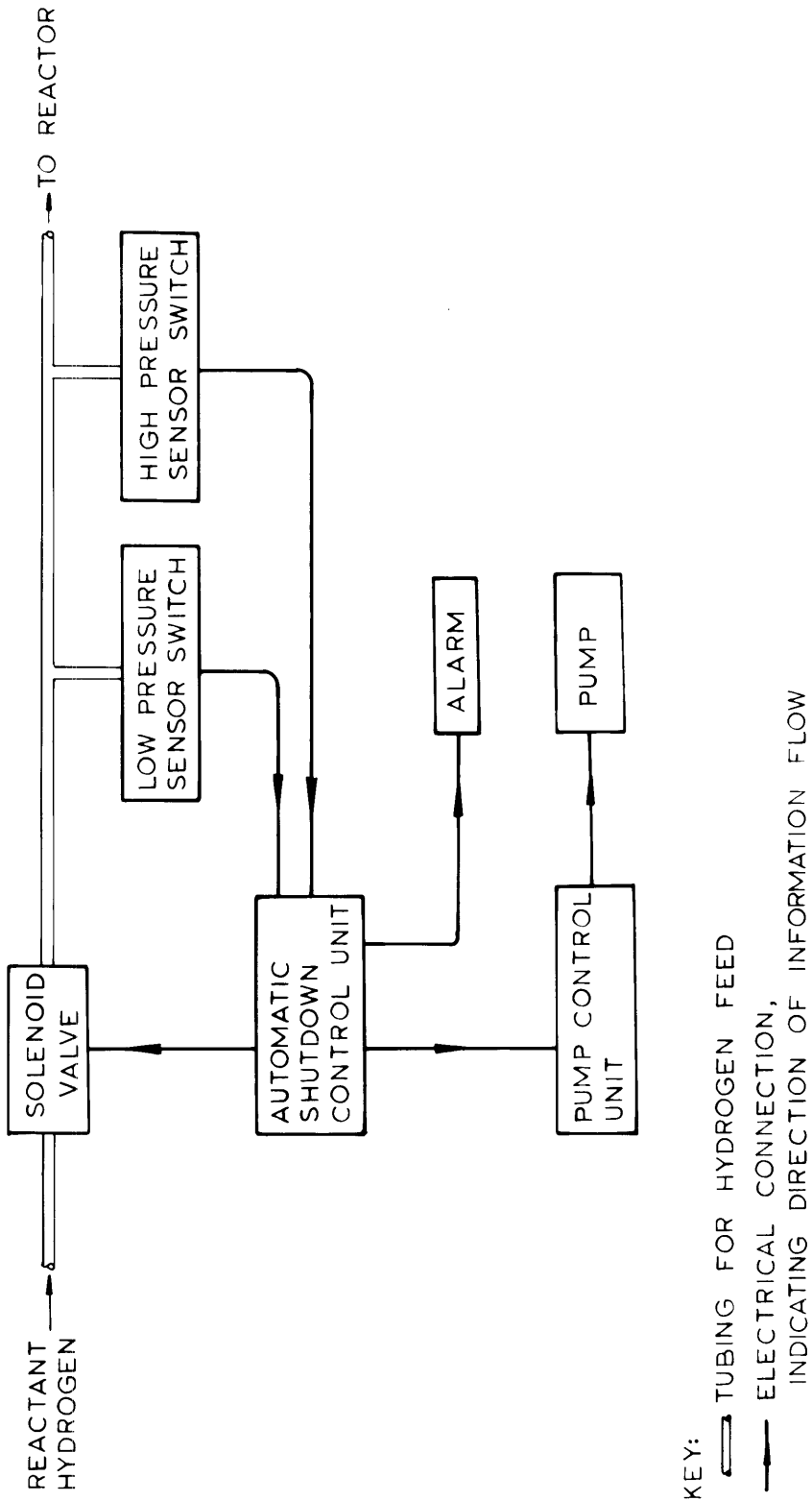


FIGURE 8-2: AUTOMATIC SAFETY SYSTEM - BASIC COMPONENT INTERACTIONS

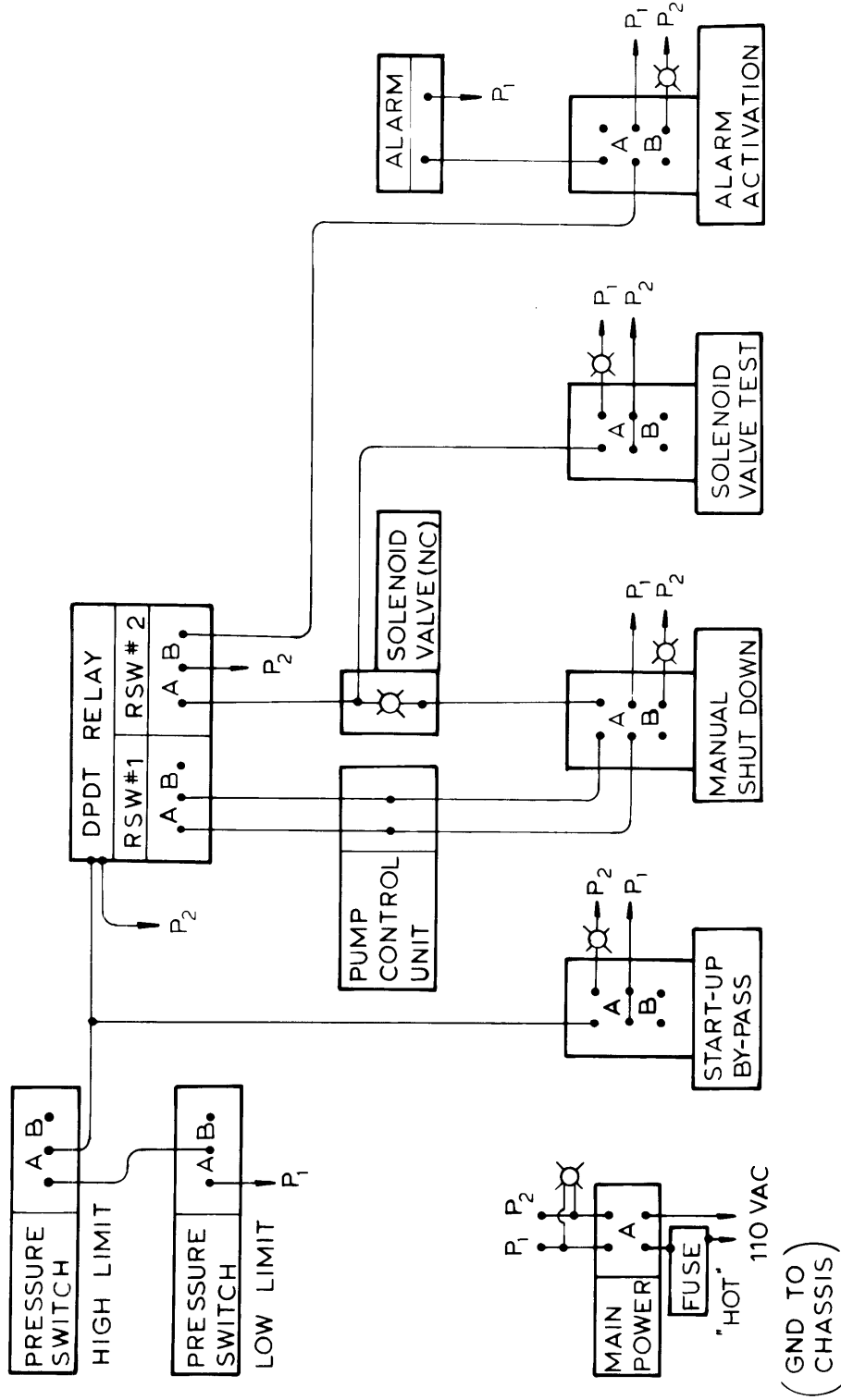


FIGURE 8-3 AUTOMATIC SHUTDOWN SYSTEM - CONTROL CIRCUIT

SWITCH POSITIONS FOR ALL MODES OF OPERATION

SWITCH TYPE	SWITCH NAME	SWITCH MODE	CONTACTS A	CONTACTS B	PILOT LIGHT
PANEL ELECTRIC	MAIN POWER	ON	CLOSED	—	ON
		OFF	OPEN	—	OFF
	STARTUP BY-PASS	RUN	OPEN	CLOSED	OFF
		START-UP	CLOSED	OPEN	ON
PANEL ELECTRIC	MANUAL SHUTDOWN	RUN	CLOSED	OPEN	OFF
		SHUTDOWN	OPEN	CLOSED	ON
	ALARM MODE	ACT.	CLOSED	OPEN	OFF
		DEACT.	OPEN	CLOSED	ON
PRESSURE-ACTIVATED	SOLENOID VALVE TEST	OFF	OPEN	CLOSED	OFF
		ON	CLOSED	OPEN	ON
	HIGH LIMIT PRESSURE	PRESS.OK	CLOSED	OPEN	—
		PRESS.HIGH	OPEN	CLOSED	—
RELAY-ACTIVATED	LOW LIMIT PRESSURE	PRESS OK	CLOSED	OPEN	—
		PRESS LOW	OPEN	CLOSED	—
	RELAY SWITCH 1	RUN	OPEN	CLOSED	—
		SHUTDOWN	CLOSED	OPEN	—
RELAY SWITCH 2	RUN	CLOSED	OPEN	—	
	SHUTDOWN	OPEN	CLOSED	—	

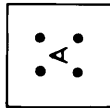
PILOT LIGHT



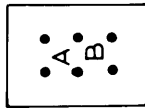
ELECTRICAL WIRES, INDICATING JUNCTION



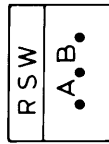
DPST SWITCH



DPDT SWITCH



SPDT SWITCH, RELAY-OPERATED (HALF OF DPDT RELAY)



SPDT SWITCH, PRESSURE-ACTIVATED

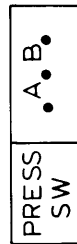


FIGURE 8-4: KEY FOR AUTOMATIC SHUTDOWN CONTROL CIRCUIT DIAGRAM

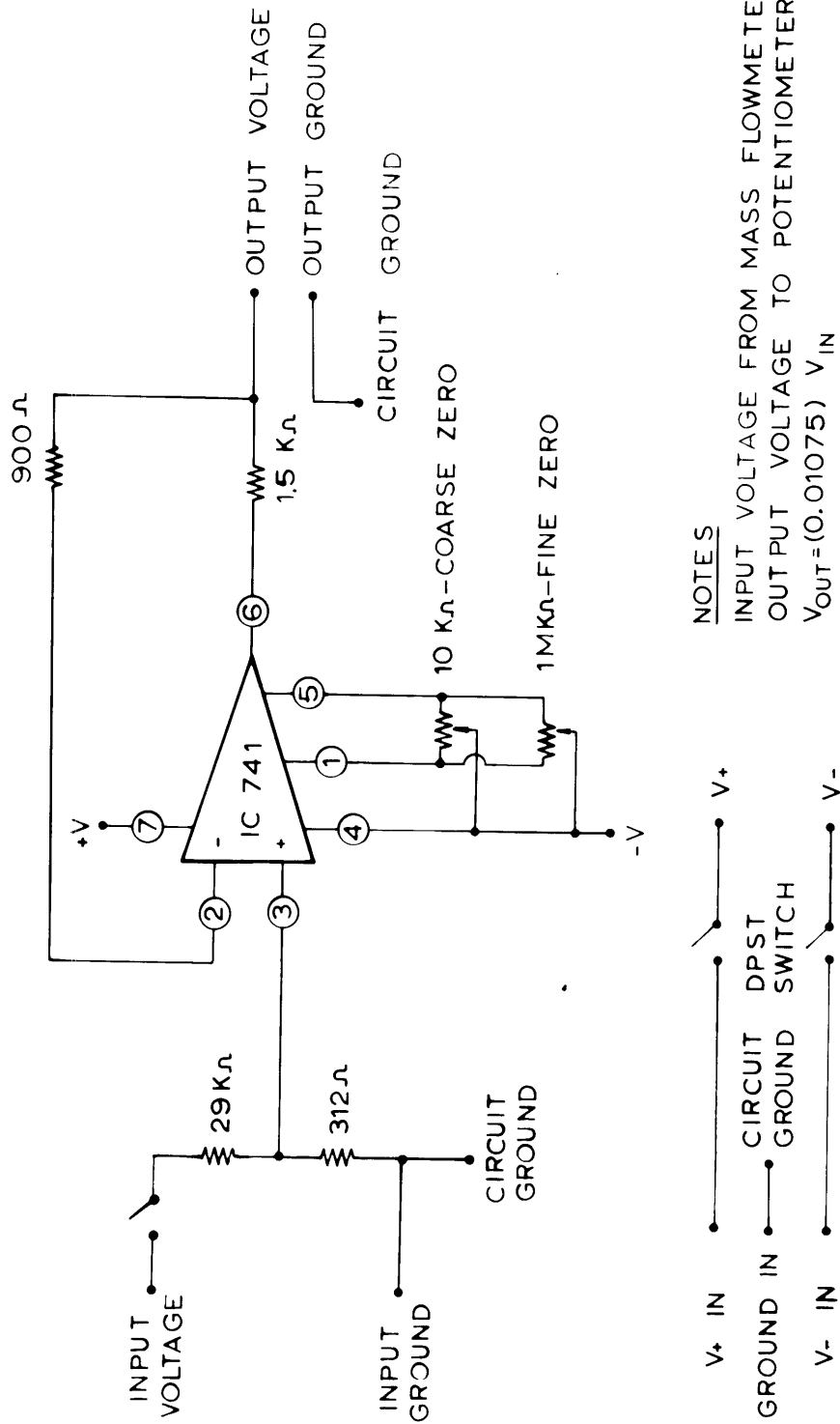


FIGURE 8-5: MASS FLOW METER OUTPUT SIGNAL BUFFER CIRCUIT

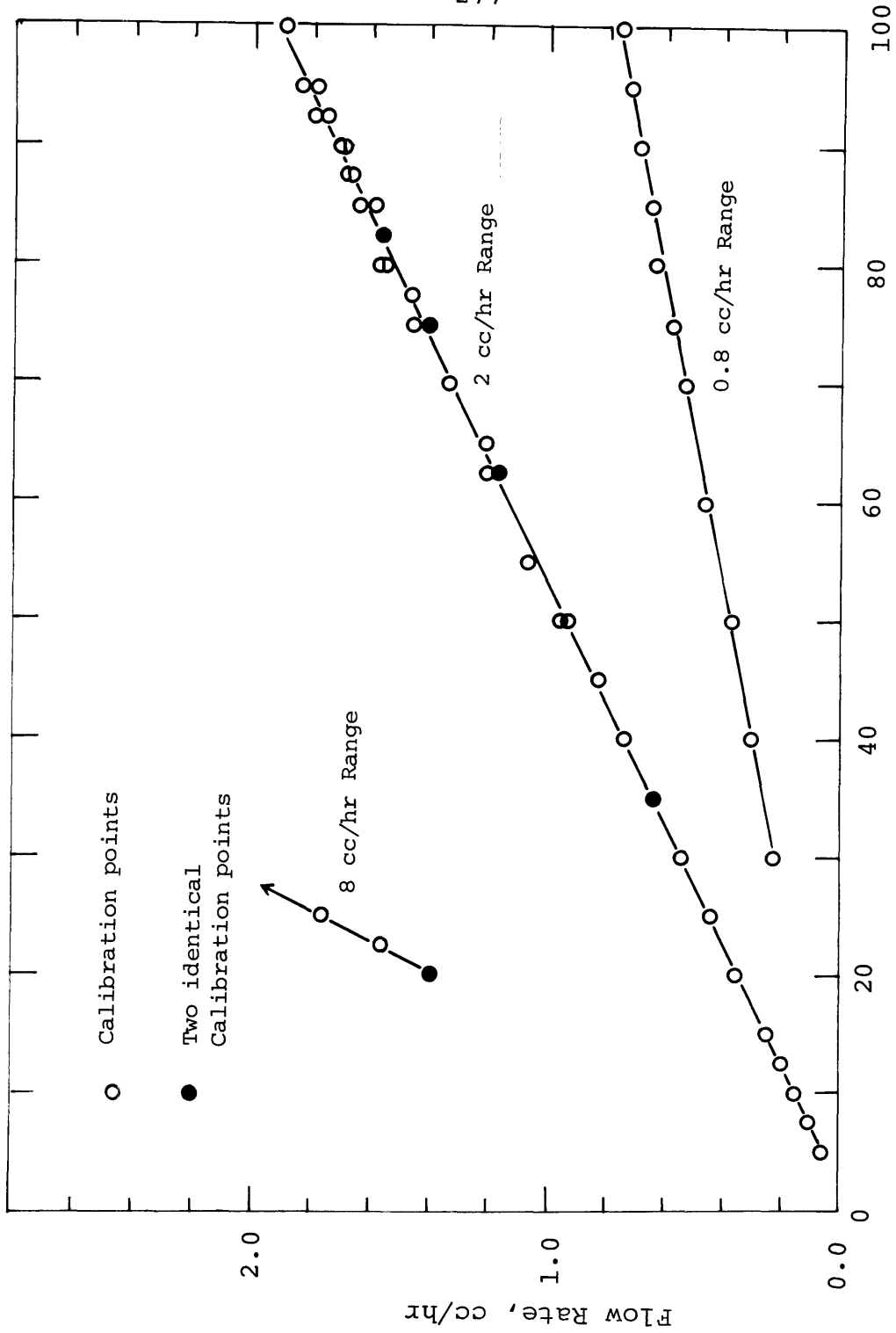


Figure 8-6 : High-Pressure Metering Pump Calibrations

VIII.B. Physical Property Data

Appendix B contains tables of physical and thermodynamic properties of compounds relevant to this study.

Table 8-1
Properties of Chemicals Used

<u>Property</u>	<u>Thiophene</u>	<u>Pyridine</u>
Formula	C ₄ H ₄ S	C ₅ H ₅ N
Molecular Weight	84.14	79.10
Melting Point, °C	-38.2	-42
Boiling Point, °C	84.2	115.5
Density, g/cc	1.051	0.978
Critical Temperature, °C	307	347
Critical Pressure, atm.	56.2	55.6
.....		
Brand, purity used	Aldrich, Gold Label	Aldrich, Gold Label
Purity	99+ %	99+ %
.....		

Hydrogen Used:

Airco, pre-purified

purity: 99.95%

dew point: -75°F

oxygen: 1 ppm

(table continued)

Table 8-1 (continued)

Structure and Synonyms

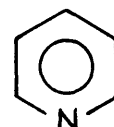
Thiophene (C_4H_4S)
divinylene sulfide
thiofuran
thiofurfuran
thiole
thiotetrole



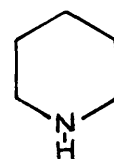
Tetrahydrothiophene (C_4H_8S)
tetramethylene sulfide
thiacyclopentane
thiolane
thiophane



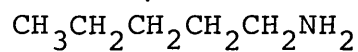
Pyridine (C_5H_5N)
azine



Piperidine ($C_5H_{11}N$)
hexahydropyridine
pentamethyleneimine



n-Pentylamine ($C_5H_{11}NH_2$)
1-aminopentane
n-amylamine



1-Propanethiol (C_3H_7SH)
n-propyl mercaptan

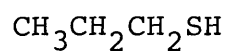


Table 8-2
 Free Energies and Heats of Formation for Compounds Relevant to this Study
 Temperature, °K

Component	300	400	500	600	700	800	900	1000
(Reference)	ΔG_f° , kcal/gmole	ΔG_f° , kcal/gmole						
pyridine (1)	45.54	49.74	54.18	58.77	63.47	68.21	72.99	77.79
piperidine (2)	26.53	39.52	53.03	66.85	80.84	94.89	109.0	123.0
n-pentylamine (3)	17.58	32.53	48.09	63.99	80.11	96.35	112.71	128.90
n-pentane (4)	-1.80	+9.60	21.51	33.76	46.20	58.77	71.46	84.18
ammonia (5)	-3.82	-1.33	+1.27	3.95	6.69	9.47	12.28	15.11
thiophene (6)	20.60	23.58	26.72	29.95	33.25	36.58	39.93	43.29
hydrogen sulfide (7)	-17.45	-16.48	-15.44	-14.36	-13.25	-12.11	-10.97	-9.80
1,3-butadiene (4)	36.07	39.46	43.05	46.78	50.60	54.48	58.40	62.36
1-butene (4)	17.19	23.23	29.55	36.07	42.73	49.45	56.25	63.07
n-butane (4)	-3.94	+5.09	14.54	24.28	34.19	44.21	54.34	64.50
n-butylamine (3)	14.85	27.22	40.12	53.30	66.67	80.15	93.73	107.15
1-propanethiol (6)	-8.75	-0.95	+7.17	15.49	23.95	32.49	41.08	49.69
	ΔH_f° , kcal/gmole							
pyridine (1)	33.48	32.38	31.52	30.88	30.41	30.07	29.86	29.76
piperidine (2)	-11.30	-13.67	-15.46	-16.68	-17.42	-17.68	-17.61	-17.23
n-pentylamine (3)	26.45	28.77	30.67	32.18	33.33	34.12	34.63	34.89
n-pentane (4)	-35.04	-37.18	-38.94	-40.37	-41.48	-42.29	-42.87	-43.21
ammonia (5)	-11.05	-11.54	-11.97	-12.33	-12.64	-12.89	-13.08	-13.23
thiophene (6)	12.03	11.30	10.74	10.33	10.02	9.82	9.68	9.62
hydrogen sulfide (7)	-20.24	-20.50	-20.74	-20.95	-21.13	-21.27	-21.38	-21.45
1,3-butadiene (4)	25.41	25.38	24.70	24.11	23.63	23.25	22.95	22.75
1-butene (4)	-0.06	-1.49	-2.70	-3.70	-4.51	-5.15	-5.62	-5.95
n-butane (4)	-30.18	-32.00	-33.51	-34.73	-35.70	-36.42	-36.94	-37.26
n-butylamine (3)	21.52	23.52	25.16	26.47	27.47	28.17	28.63	28.87
1-propanethiol (6)	-13.51	-32.89	-34.03	-34.93	-35.60	-36.07	-36.36	-36.49

Note: Properties are for the ideal gas state

References: (1) McCullough, et al., 1957; (2) Scott, 1971; (3) Rihani, 1968; (4) Rossini et al., 1953; (5) Kobe and Crawford, 1958; (6) El-Sabban and Scott, 1970; (7) Evans and Wagman, 1952.

VIII.C. Run Data Summaries

Table 8-3

Catalyst History - Final Catalyst Loading

<u>Run Number</u>	<u>Run Feed</u>	<u>Run Pressure (psig)</u>	<u>Sulfiding Type Used</u>	<u>Total Hours of Catalyst Use Before Start of Run</u>
38	Pyr	1000	1	215
39	Pyr	150	3	228
40	Pyr	500	3	246
41	Pyr	1000	3	259
42	Thi	150	3	272
43	Thi	500	2	286
44	Thi	1000	2	300
45	Thi	150	2	313
46	Thi	1000	2	324
47	Pyr	150	2	335
48	Pyr-Thi	150	3	350
49	Pyr-Thi	1000	3	366
50	Pyr-Thi	500	2	384
51	Pyr-Thi	150	2	400
52	Pyr-Thi	150	2	411
53	Pyr-Thi	1000	2	430
54	Pyr-PT	1000	3	449
55	Thi-BA	1000	3	468
56	Pyr	150	2	489
60	Thi	500	2	495
61	DMT	500	2	-
62	MT	500	2	-
63	MT	500	2	-

Notes: Feeds - Pyr = Pyridine; Thi = Thiophene; PT = Propane-thiol; BA = Butylamine, DMT = 2,5-Dimethylthiophene; MT = 2-Methylthiophene

Total use before Run 38 all with pure Pyr feed, with periodic sulfiding

Hours of use includes runs with all feeds, including aborted run times, but does not include type I or III sulfiding times

Run 60 directly followed Run 56; Runs 60 through 63 were made by Gultekin

Sulfiding Type: 1. Formal, 2. Run, 3. Shutdown

Data Summaries for Individual Runs

DATA SUMMARY - RUN 38

PURPOSE - To study pure pyridine HDN at a total pressure of 1000 psig and a pyridine partial pressure of 93 torr.

OVERALL RUN PARAMETERS

TOTAL PRESSURE = 999.8 PSIG = 69.04 ATM = 69.95 BARS
 LHSV = 0.305 INVERSE HOURS (1)
 SPACE VELOCITY, AVG = 0.429 INVERSE SECONDS (2)
 MOLES HYDROGEN PER MOLE LIQUID REACTANT (1) = 550.8

REACTOR FEED

	GRAMS/HR	G MOL/HR	MOLE FRACTION	PARTIAL PRESSURES		
				BARS	TORR	PSI
THIOPHENE	0.0000	0.00000	0.000000	0.0000	0.0	0.00
PYRIDINE	0.6340	0.00802	0.001812	0.1268	95.1	1.84
HYDROGEN (3)	8.8995	4.4144	0.99819	69.82	-NA-	1012.7
TOTAL	9.5335	4.4224	1.00000	69.95	-NA-	1014.6

CATALYST - NIMO/AL2O3, HDS-3A

TOTAL BED VOLUME = 2.123 CC
 CATALYST WEIGHT = 1.4829 GRAMS
 SULFIDING TYPE = 1

SULFIDING TYPE

0 - NONE
 1 - FORMAL
 2 - RUN
 3 - SHUTDOWN

EXPERIMENTAL RESULTS FOR INDIVIDUAL DATA POINTS

REACTOR TEMPERATURE, DEG C	THIOPHNE CONVRSN, PERCENT	PYRIDINE CONVRSN, PERCENT	PIP OUT/ PYR IN, MOL/MOL	NPA OUT/ PYR IN, MOL/MOL	SPACE TIME, SEC (2)	RESDNC TIME, SEC (4)
192.0	0.0	5.4	0.0079	0.0000	2.33	3.12
228.5	0.0	17.4	0.1241	0.0000	2.33	2.90
271.0	0.0	47.2	0.3928	0.0082	2.34	2.68
303.5	0.0	82.5	0.6643	0.0039	2.35	2.54
329.8	0.0	96.0	0.6503	0.0000	2.36	2.44
363.3	0.0	97.9	0.2567	0.0000	2.30	2.25
389.0	0.0	100.0	0.0000	0.0000	2.34	2.20

NOTES

- (1) BASED ON THIOPHENE PLUS PYRIDINE LIQUID FEED
- (2) BASED ON TOTAL BED VOLUME AT 350. DEG C AND 1000. PSIG
- (3) BY DIFFERENCE
- (4) BASED ON TOTAL BED VOLUME AT REACTOR CONDITIONS
- (-) PYR = PYRIDINE, PIP = PIPERIDINE, NPA = NPENTYLAMINE
- (-) DATA FORM -- CONST SPACE VELOCITY, INDEP VARIABLE = TEMP
- (-) 1 BAR = 10**5 PASCAL = 10**5 N/M**2

-284-
DATA SUMMARY - RUN 39

PURPOSE - To study pure pyridine HDN at a total pressure of 150 psig and a pyridine partial pressure of 93 torr.

OVERALL RUN PARAMETERS

TOTAL PRESSURE = 150.6 PSIG = 11.25 ATM = 11.40 BARS
 LHSV = 0.305 INVERSE HOURS (1)
 SPACE VELOCITY, AVG = 0.456 INVERSE SECONDS (2)
 MOLES HYDROGEN PER MOLE LIQUID REACTANT (1) = 94.4

REACTOR FEED

	GRAMS/HR	G. MOL/HR	MOLE FRACTION	PARTIAL PRESSURES		
				BARS	TORR	PSI
THIOPHENE	0.0000	0.00000	0.000000	0.0000	0.0	0.00
PYRIDINE	0.6340	0.00802	0.010485	0.1195	89.6	1.73
HYDROGEN (3)	1.5249	0.7564	0.98951	11.28	-NA-	163.6
TOTAL	2.1589	0.7644	1.00000	11.40	-NA-	165.3

CATALYST - NIMO/AL2O3, HDS-3A

TOTAL BED VOLUME = 2.123 CC
 CATALYST WEIGHT = 1.4829 GRAMS
 SULFIDING TYPE = 3

SULFIDING TYPE

0 - NONE
 1 - FORMAL
 2 - RUN
 3 - SHUTDOWN

EXPERIMENTAL RESULTS FOR INDIVIDUAL DATA POINTS

REACTOR TEMPERATURE, DEG C	THIOPHNE CONVRSN, DFG K	PYRIDINE CONVRSN, PERCENT	PIP OUT/ PYR IN, MOL/MOL	NPA OUT/ PYR IN, MOL/MOL	SPACE TIME, SEC (2)	RESDNC TIME, SEC (4)	
203.0	476.2	0.0	8.6	0.0040	0.0000	2.17	2.86
252.6	525.7	0.0	13.9	0.0306	0.0000	2.20	2.63
304.0	577.2	0.0	21.1	0.0969	0.0000	2.20	2.39
357.6	630.8	0.0	28.0	0.0417	0.0020	2.20	2.18
396.3	669.5	0.0	27.1	0.0043	0.0012	2.18	2.03
410.6	683.7	0.0	20.5	0.0000	0.0000	2.18	1.99

NOTES

- (1) BASED ON THIOPHENE PLUS PYRIDINE LIQUID FEED
- (2) BASED ON TOTAL BED VOLUME AT 350. DEG C AND 150. PSIG
- (3) BY DIFFERENCE
- (4) BASED ON TOTAL BED VOLUME AT REACTOR CONDITIONS
- (-) PYR = PYRIDINE, PIP = PIPERIDINE, NPA = NPENTYLAMINE
- (-) DATA FORM -- CONST SPACE VELOCITY, INDEP VARIABLE = TEMP
- (-) 1 BAR = 10**5 PASCAL = 10**5 N/M**2

DATA SUMMARY - RUN 40

PURPOSE - To study pure pyridine HDN at a total pressure of 500 psig and a pyridine partial pressure of 93 torr.

OVERALL RUN PARAMETERS

TOTAL PRESSURE = 500.3 PSIG = 35.01 ATM = 35.48 BARS
 LHSV = 0.305 INVERSE HOURS (1)
 SPACE VELOCITY, AVG = 0.423 INVERSE SECONDS (2)
 MOLES HYDROGEN PER MOLE LIQUID REACTANT (1) = 275.5

REACTOR FEED

	GRAMS/HR	G MOL/HR	MOLE FRACTION	PARTIAL PRESSURES		
				BARS	TORR	PSI
THIOPHENE	0.0000	0.00000	0.000000	0.0000	0.0	0.00
PYRIDINE	0.6340	0.00802	0.003616	0.1283	96.2	1.86
HYDROGEN (3)	4.4520	2.2083	0.99638	35.35	-NA-	512.7
TOTAL	5.0860	2.2163	1.00000	35.48	-NA-	514.6

CATALYST - NIMO/AL2O3, HDS-3A

TOTAL BED VOLUME = 2.123 CC
 CATALYST WEIGHT = 1.4829 GRAMS
 SULFIDING TYPE = 3

SULFIDING TYPE

0 - NONE
 1 - FORMAL
 2 - RUN
 3 - SHUTDOWN

EXPERIMENTAL RESULTS FOR INDIVIDUAL DATA POINTS

REACTOR TEMPERATURE, DEG C	THIOPHENE CONVRSN, PERCENT	PYRIDINE CONVRSN, PERCENT	PIP OUT/ PYR IN, MOL/MOL	NPA OUT/ PYR IN, MOL/MOL	SPACE TIME, SEC (2)	RESDNC TIME, SEC (4)
200.6	0.0	7.6	0.0303	0.0000	2.37	3.11
257.4	0.0	27.0	0.1383	0.0008	2.36	2.78
303.8	0.0	53.1	0.3545	0.0004	2.37	2.56
360.0	0.0	80.2	0.2244	0.0000	2.37	2.33
410.5	0.0	86.2	0.0135	0.0000	2.34	2.14

NOTES

- (1) BASED ON THIOPHENE PLUS PYRIDINE LIQUID FEED
- (2) BASED ON TOTAL BED VOLUME AT 350. DEG C AND 500. PSIG
- (3) BY DIFFERENCE
- (4) BASED ON TOTAL BED VOLUME AT REACTOR CONDITIONS
- (-) PYR = PYRIDINE, PIP = PIPERIDINE, NPA = NPENTYLAMINE
- (-) DATA FORM -- CONST SPACE VELOCITY, INDEP VARIABLE = TEMP
- (-) 1 BAR = 10**5 PASCAL = 10**5 N/M**2

-286-
DATA SUMMARY - RUN 41

PURPOSE - To study pure pyridine HDN at a total pressure of 1000 psig and a pyridine partial pressure of 186 torr.

OVERALL RUN PARAMETERS

TOTAL PRESSURE = 1000.0 PSIG = 69.05 ATM = 69.96 BARS
 LHSV = 0.612 INVERSE HOURS (1)
 SPACE VELOCITY, AVG = 0.441 INVERSE SECONDS (2)
 MOLES HYDROGEN PER MOLE LIQUID REACTANT (1) = 282.0

REACTOR FEED

	GRAMS/HR	G MOL/HR	MOLE FRACTION	PARTIAL PRESSURES		
				BARS	TORR	PSI
THIOPHENE	0.0000	0.00000	0.000000	0.0000	0.0	0.00
PYRIDINE	1.2714	0.01607	0.003533	0.2472	185.4	3.59
HYDROGEN (3)	9.1391	4.5333	0.99647	69.71	-NA-	1011.1
TOTAL	10.4105	4.5494	1.00000	69.96	-NA-	1014.7

CATALYSE - NiO/AL₂O₃, HDS-3A

TOTAL BED VOLUME = 2.123 CC
 CATALYST WEIGHT = 1.4829 GRAMS
 SULFIDING TYPE = 3

SULFIDING TYPE

0 - NONE
 1 - FORMAL
 2 - RUN
 3 - SHUTDOWN

EXPERIMENTAL RESULTS FOR INDIVIDUAL DATA POINTS

REACTOR TEMPERATURE, DEG C	THIOPHENE CONVRSN, PERCENT	PYRIDINE CONVRSN, PERCENT	PIP OUT/ PYR IN, MOL/MOL	NPA OUT/ PYR IN, MOL/MOL	SPACE TIME, SEC (2)	RESDNC TIME, SEC (4)
195.5	0.0	1.4	0.0333	0.0000	2.27	3.01
227.0	0.0	7.4	0.0865	0.0000	2.26	2.81
274.4	0.0	37.3	0.3150	0.0047	2.25	2.56
308.9	0.0	71.1	0.5851	0.0029	2.25	2.41
330.5	0.0	81.5	0.6413	0.0014	2.29	2.37
365.5	0.0	91.9	0.4419	0.0000	2.26	2.20
385.8	0.0	96.2	0.2331	0.0000	2.25	2.13
410.5	0.0	98.7	0.0015	0.0000	2.28	2.08

NOTES

- (1) BASED ON THIOPHENE PLUS PYRIDINE LIQUID FEED
- (2) BASED ON TOTAL BED VOLUME AT 350. DEG C AND 1000. PSIG
- (3) BY DIFFERENCE
- (4) BASED ON TOTAL BED VOLUME AT REACTOR CONDITIONS
- (-) PYR = PYRIDINE, PIP = PIPERIDINE, NPA = NPENTYLAMINE
- (-) DATA FORM -- CONST SPACE VELOCITY, INDEP VARIABLE = TEMP
- (-) 1 BAR = 10**5 PASCAL = 10**5 N/M**2

-287-
DATA SUMMARY - RUN 42

PURPOSE - To study pure thiophene HDS at a total pressure of 150 psig and a thiophene partial pressure of 93 torr.

OVERALL RUN PARAMETERS

TOTAL PRESSURE = 150.0 PSIG = 11.19 ATM = 11.34 BARS
 LHSV = 0.301 INVERSE HOURS (1)
 SPACE VELOCITY, AVG = 0.440 INVERSE SECONDS (2)
 MOLES HYDROGEN PER MOLE LIQUID REACTANT (1) = 91.2

REACTOR FEED

	GRAMS/HR	G MOL/HR	MOLE FRACTION	PARTIAL PRESSURES		
				BARS	TORR	PSI
THIOPHENE	0.6720	0.00799	0.010845	0.1230	92.2	1.78
PYRIDINE	0.0000	0.00000	0.000000	0.0000	0.0	0.00
HYDROGEN (3)	1.4685	0.7284	0.98915	11.22	-NA-	162.7
TOTAL	2.1405	0.7364	1.00000	11.34	-NA-	164.5

CATALYST - NIMO/AL2O3, HDS-3A

TOTAL BED VOLUME = 2.123 CC
 CATALYST WEIGHT = 1.4829 GRAMS
 SULFIDING TYPE = 3

SULFIDING TYPE

0 - NONE
 1 - FORMAL
 2 - RUN
 3 - SHUTDOWN

EXPERIMENTAL RESULTS FOR INDIVIDUAL DATA POINTS

REACTOR TEMPERATURE, DEG C	THIOPHNE CONVRSN, PERCENT	PYRIDINE CONVRSN, PERCENT	PIP OUT/ PYR IN, MOL/MOL	NPA OUT/ PYR IN, MOL/MOL	SPACE TIME, SEC (2)	RESDNC TIME, SEC (4)
171.0	1.6	0.0	0.0000	0.0000	2.28	3.19
200.0	9.9	0.0	0.0000	0.0000	2.28	3.00
223.3	19.9	0.0	0.0000	0.0000	2.26	2.84
249.5	42.5	0.0	0.0000	0.0000	2.29	2.73
264.0	62.6	0.0	0.0000	0.0000	2.25	2.61
284.0	86.2	0.0	0.0000	0.0000	2.31	2.58
305.3	98.4	0.0	0.0000	0.0000	2.26	2.43
312.0	99.7	0.0	0.0000	0.0000	2.26	2.40

NOTES

- (1) BASED ON THIOPHENE PLUS PYRIDINE LIQUID FEED
- (2) BASED ON TOTAL BED VOLUME AT 35C. DEG C AND 150. PSIG
- (3) BY DIFFERENCE
- (4) BASED ON TOTAL BED VOLUME AT REACTOR CONDITIONS
- (-) PYR = PYRIDINE, PIP = PIPERIDINE, NPA = NPENTYLAMINE
- (-) DATA FORM -- CONST SPACE VELOCITY, INDEP VARIABLE = TEMP
- (-) 1 BAR = 10**5 PASCAL = 10**5 N/M**2

-288-
DATA SUMMARY - RUN 43

PURPOSE - To study pure thiophene HDS at a total pressure of 500 psig and a thiophene partial pressure of 93 torr.

OVERALL RUN PARAMETERS

TOTAL PRESSURE = 499.3 PSIG = 34.97 ATM = 35.43 BARS
 LHSV = 0.301 INVERSE HOURS (1)
 SPACE VELOCITY, AVG = 0.433 INVERSE SECONDS (2)
 MOLES HYDROGEN PER MOLE LIQUID REACTANT (1) = 282.9

REACTOR FEED

	GRAMS/HR	G MOL/HR	MOLE FRACTION	PARTIAL PRESSURES		
				BARS	TORR	PSI
THIOPHENE	0.6720	0.00799	0.003522	0.1248	93.6	1.81
PYRIDINE	0.0000	0.00000	0.000000	0.0000	0.0	0.00
HYDROGEN (3)	4.5550	2.2594	0.99648	35.31	-NA-	512.1
TOTAL	5.2270	2.2674	1.00000	35.43	-NA-	513.9

CATALYST - NIMO/AL2O3, HDS-3A

TOTAL BED VOLUME = 2.123 CC
 CATALYST WEIGHT = 1.4829 GRAMS
 SULFIDING TYPE = 2

SULFIDING TYPE

0 - NONE
 1 - FORMAL
 2 - RUN
 3 - SHUTDOWN

EXPERIMENTAL RESULTS FOR INDIVIDUAL DATA POINTS

REACTOR TEMPERATURE, DEG C	THIOPHNE CONVRSN, PERCENT	PYRIDINE CONVRSN, PERCENT	PIP OUT/ PYR IN, MOL/MOL	NPA OUT/ PYR IN, MOL/MOL	SPACE TIME, SEC (2)	RESDNC TIME, SEC (4)
161.7	1.2	0.0	0.0000	0.0000	2.32	3.32
198.4	7.0	0.0	0.0000	0.0000	2.29	3.03
239.6	28.4	0.0	0.0000	0.0000	2.33	2.82
271.8	95.6	0.0	0.0000	0.0000	2.30	2.62
280.5	99.0	0.0	0.0000	0.0000	2.29	2.57

NOTES

- (1) BASED ON THIOPHENE PLUS PYRIDINE LIQUID FEED
- (2) BASED ON TOTAL BED VOLUME AT 350. DEG C AND 500. PSIG
- (3) BY DIFFERENCE
- (4) BASED ON TOTAL BED VOLUME AT REACTOR CONDITIONS
- (-) PYR = PYRIDINE, PIP = PIPERIDINE, NPA = NPENTYLAMINE
- (-) DATA FORM -- CONST SPACE VELOCITY, INDEP VARIABLE = TEMP
- (-) 1 BAR = 10**5 PASCAL = 10**5 N/M**2

DATA SUMMARY - RUN 44

PURPOSE - To study pure thiophene HDS at a total pressure of 1000 psig and a thiophene partial pressure of 93 torr.

OVERALL RUN PARAMETERS

TOTAL PRESSURE = 1000.0 PSIG = 69.04 ATM = 69.95 BARS
 LHSV = 0.301 INVERSE HOURS (1)
 SPACE VELOCITY, AVG = 0.434 INVERSE SECONDS (2)
 MOLES HYDROGEN PER MOLE LIQUID REACTANT (1) = 559.4

REACTOR FEED

	GRAMS/HR	G MOL/HR	MOLE FRACTION	PARTIAL PRESSURES		
				BARS	TORR	PSI
THIOPHENE	0.6720	0.00799	0.001784	0.1248	93.6	1.81
PYRIDINE	0.0000	0.00000	0.000000	0.0000	0.0	0.00
HYDROGEN (3)	9.0073	4.4679	0.99822	69.83	-NA-	1012.8
TOTAL	9.6793	4.4759	1.00000	69.95	-NA-	1014.6

CATALYSE - NIMO/AL2O3, HDS-3A

TOTAL BED VOLUME = 2.123 CC
 CATALYST WEIGHT = 1.4829 GRAMS
 SULFIDING TYPE = 2

SULFIDING TYPE

0 - NONE
 1 - FORMAL
 2 - RUN
 3 - SHUTDOWN

EXPERIMENTAL RESULTS FOR INDIVIDUAL DATA POINTS

REACTOR TEMPERATURE, DEG C	THIOPHENE CONVRSN, PERCENT	PYRIDINE CONVRSN, PERCENT	PIP OUT/ PYR IN, MOL/MOL	NPA OUT/ PYR IN, MOL/MOL	SPACE TIME, SEC (2)	RESDNC TIME, SEC (4)
152.0	1.9	0.0	0.0000	0.0000	2.29	3.36
190.6	6.8	0.0	0.0000	0.0000	2.31	3.10
239.0	66.8	0.0	0.0000	0.0000	2.30	2.80
247.3	85.1	0.0	0.0000	0.0000	2.30	2.75
255.0	97.4	0.0	0.0000	0.0000	2.32	2.74
263.0	99.2	0.0	0.0000	0.0000	2.31	2.69

NOTES

- (1) BASED ON THIOPHENE PLUS PYRIDINE LIQUID FEED
- (2) BASED ON TOTAL BED VOLUME AT 350. DEG C AND 1000. PSIG
- (3) BY DIFFERENCE
- (4) BASED ON TOTAL BED VOLUME AT REACTOR CONDITIONS
- (-) PYR = PYRIDINE, PIP = PIPERIDINE, NPA = NPENTYLAMINE
- (-) DATA FORM -- CONST SPACE VELOCITY, INDEP VARIABLE = TEMP
- (-) 1 BAR = 10**5 PASCAL = 10**5 N/M**2

-290-
DATA SUMMARY - RUN 45

PURPOSE - To study pure thiophene HDS at a total pressure of 150 psig and a thiophene partial pressure of 186 torr.

OVERALL RUN PARAMETERS

TOTAL PRESSURE = 150.0 PSIG = 11.19 ATM = 11.34 BARS
 LHSV = 0.602 INVERSE HOURS (1)
 SPACE VELOCITY, AVG = 0.439 INVERSE SECONDS (2)
 MOLES HYDROGEN PER MOLE LIQUID REACTANT (1) = 45.0

REACTOR FEED

	GRAMS/HR	G MOL/HR	MOLE FRACTION	PARTIAL PRESSURES		
				BARS	TORR	PSI
THIOPHENE	1.3440	0.01597	0.021721	0.2462	184.7	3.57
PYRIDINE	0.0000	0.00000	0.000000	0.0000	0.0	0.00
HYDROGEN (3)	1.4504	0.7194	0.97828	11.09	-NA-	160.9
TOTAL	2.7944	0.7354	1.00000	11.34	-NA-	164.4

CATALYST - NIMO/AL2O3, HDS-3A

TOTAL BED VOLUME = 2.123 CC
 CATALYST WEIGHT = 1.4829 GRAMS
 SULFIDING TYPE = 2

SULFIDING TYPE

0 - NONE
 1 - FORMAL
 2 - RUN
 3 - SHUTDOWN

EXPERIMENTAL RESULTS FOR INDIVIDUAL DATA POINTS

REACTOR TEMPERATURE, DEG C	THIOPHNE CONVRSN, PERCENT	PYRIDINE CONVRSN, PERCENT	PIP OUT/ PYR IN, MOL/MOL	NPA OUT/ PYR IN, MOL/MOL	SPACE TIME, SEC (2)	RESDNC TIME, SEC (4)
176.0	0.9	0.0	0.0000	0.0000	2.21	3.07
223.0	7.1	0.0	0.0000	0.0000	2.26	2.83
271.0	49.2	0.0	0.0000	0.0000	2.35	2.68
292.3	81.8	0.0	0.0000	0.0000	2.30	2.53
312.0	97.8	0.0	0.0000	0.0000	2.32	2.47
320.3	99.6	0.0	0.0000	0.0000	2.28	2.40

NOTES

- (1) BASED ON THIOPHENE PLUS PYRIDINE LIQUID FEED
- (2) BASED ON TOTAL BED VOLUME AT 350. DEG C AND 150. PSIG
- (3) BY DIFFERENCE
- (4) BASED ON TOTAL BED VOLUME AT REACTOR CONDITIONS
- (-) PYR = PYRIDINE, PIP = PIPERIDINE, NPA = NPENTYLAMINE
- (-) DATA FORM -- CONST SPACE VELOCITY, INDEF VARIABLE = TEMP
- (-) 1 BAR = 10**5 PASCAL = 10**5 N/M**2

-291-
DATA SUMMARY - RUN 46

PURPOSE - To study pure thiophene HDS at a total pressure of 1000 psig and a thiophene partial pressure of 186 torr.

OVERALL RUN PARAMETERS

TOTAL PRESSURE = 1000.1 PSIG = 69.04 ATM = 69.96 BARS
 LHSV = 0.602 INVERSE HOURS (1)
 SPACE VELOCITY, AVG = 0.423 INVERSE SECONDS (2)
 MOLES HYDROGEN PER MOLE LIQUID REACTANT (1) = 272.1

REACTOR FEED

	GRAMS/HR	G. MOL/HR	MOLE FRACTION	PARTIAL PRESSURES		
				BARS	TORR	PSI
THIOPHENE	1.3440	0.01597	0.003662	0.2562	192.1	3.72
PYRIDINE	0.0000	0.00000	0.000000	0.0000	0.0	0.00
HYDROGEN (3)	8.7615	4.3460	0.99634	69.70	-NA-	1010.9
TOTAL	10.1055	4.3619	1.00000	69.96	-NA-	1014.6

CATALYST - NIMO/AL2O3, HDS-3A

TOTAL BED VOLUME = 2.123 CC
 CATALYST WEIGHT = 1.4829 GRAMS
 SULFIDING TYPE = 2

SULFIDING TYPE

0 - NONE
 1 - FORMAL
 2 - RUN
 3 - SHUTDOWN

EXPERIMENTAL RESULTS FOR INDIVIDUAL DATA POINTS

REACTOR TEMPERATURE, DEG C	THIOPHNE CONVRSN, PERCENT	PYRIDINE CONVRSN, PERCENT	PIP OUT/ PYR IN, MOL/MOL	NPA OUT/ PYR IN, MOL/MOL	SPACE TIME, SEC (2)	RESDNC TIME, SEC (4)
177.0	6.6	0.0	0.0000	0.0000	2.38	3.29
227.0	25.3	0.0	0.0000	0.0000	2.35	2.93
246.0	49.7	0.0	0.0000	0.0000	2.36	2.84
255.1	71.2	0.0	0.0000	0.0000	2.39	2.82
263.5	85.1	0.0	0.0000	0.0000	2.35	2.73
271.8	98.7	0.0	0.0000	0.0000	2.33	2.66

NOTES

- (1) BASED ON THIOPHENE PLUS PYRIDINE LIQUID FEED
- (2) BASED ON TOTAL BED VOLUME AT 350. DEG C AND 1000. PSIG
- (3) BY DIFFERENCE
- (4) BASED ON TOTAL BED VOLUME AT REACTOR CONDITIONS
- (-) PYR = PYRIDINE, PIP = PIPERIDINE, NPA = NPENTYLAMINE
- (-) DATA FORM -- CONST SPACE VELOCITY, INDEP VARIABLE = TEMP
- (-) 1 BAR = 10**5 PASCAL = 10**5 N/M**2

-292-
DATA SUMMARY - RUN 47

PURPOSE - To study pure pyridine HDN at a total pressure of 150 psig and a pyridine partial pressure of 186 torr.

OVERALL RUN PARAMETERS

TOTAL PRESSURE = 150.2 PSIG = 11.21 ATM = 11.36 BARS
 LHSV = 0.612 INVERSE HOURS (1)
 SPACE VELOCITY, AVG = 0.452 INVERSE SECONDS (2)
 MOLES HYDROGEN PER MOLE LIQUID REACTANT (1) = 46.1

REACTOR FEED

	GRAMS/HR	G. MOL/HR	MOLE FRACTION	PARTIAL PRESSURES		
				BARS	TORR	PSI
THIOPHENE	0.0000	0.00000	0.000000	0.0000	0.0	0.00
PYRIDINE	1.2714	0.01607	0.021247	0.2413	181.0	3.50
HYDROGEN (3)	1.4927	0.7404	0.97875	11.12	-NA-	161.2
TOTAL	2.7641	0.7565	1.00000	11.36	-NA-	164.7

CATALYST - NIMO/AL2O3, HDS-3A

TOTAL BED VOLUME = 2.123 CC
 CATALYST WEIGHT = 1.4829 GRAMS
 SULFIDING TYPE = 2

SULFIDING TYPE

0 - NONE
 1 - FORMAL
 2 - RUN
 3 - SHUTDOWN

EXPERIMENTAL RESULTS FOR INDIVIDUAL DATA POINTS

REACTOR TEMPERATURE, DEG C	THIOPHENE CONVRSN, PERCENT	PYRIDINE CONVRSN, PERCENT	PIP OUT/ PYR IN, MOL/MOL	NPA OUT/ PYR IN, MOL/MOL	SPACE TIME, SEC (2)	RFS DNC TIME, SEC (4)
226.0	0.0	2.9	0.0170	0.0000	2.23	2.77
268.0	0.0	12.9	0.0732	0.0000	2.21	2.54
310.4	0.0	20.5	0.1040	0.0000	2.20	2.35
358.3	0.0	17.7	0.0393	0.0035	2.20	2.17
409.0	0.0	15.6	0.0046	0.0000	2.22	2.05

NOTES

- (1) BASED ON THIOPHENE PLUS PYRIDINE LIQUID FEED
- (2) BASED ON TOTAL BED VOLUME AT 350. DEG C AND 150. PSIG
- (3) BY DIFFERENCE
- (4) BASED ON TOTAL BED VOLUME AT REACTOR CONDITIONS
- (-) PYR = PYRIDINE, PIP = PIPERIDINE, NPA = NPENTYLAMINE
- (-) DATA FORM -- CONST SPACE VELOCITY, INDEP VARIABLE = TEMP
- (-) 1 BAR = 10**5 PASCAL = 10**5 N/M**2

-293-
DATA SUMMARY - RUN 48

PURPOSE - To study simultaneous pyridine HDN and thiophene HDS at a total pressure of 150 psig and equal pyridine and thiophene partial pressures of 93 torr.

OVERALL RUN PARAMETERS

TOTAL PRESSURE = 149.8 PSIG = 11.19 ATM = 11.34 BARS
 LHSV = 0.606 INVERSE HOURS(1)
 SPACE VELOCITY, AVG = 0.446 INVERSE SECONDS(2)
 MOLES HYDROGEN PER MOLE LIQUID REACTANT(1) = 45.4

REACTOR FEED

	GRAMS/HR	G. MOL/HR	MOLE FRACTION	PARTIAL PRESSURES		
				BARS	TORR	PSI
THIOPHENE	0.6768	0.00804	0.010768	0.1221	91.6	1.77
PYRIDINE	0.6358	0.00804	0.010761	0.1220	91.5	1.77
HYDROGEN (3)	1.4735	0.7309	0.97847	11.09	-NA-	160.9
TOTAL	2.7861	0.7470	1.00000	11.34	-NA-	164.4

CATALYST - NiMo/Al₂O₃, HDS-3A

TOTAL BED VOLUME = 2.123 CC
 CATALYST WEIGHT = 1.4829 GRAMS
 SULFIDING TYPE = 3

SULFIDING TYPE

0 - NONE
 1 - FORMAL
 2 - RUN
 3 - SHUTDOWN

EXPERIMENTAL RESULTS FOR INDIVIDUAL DATA POINTS

REACTOR TEMPERATURE, DEG C	THIOPHENE CONVRSN, PERCENT	PYRIDINE CONVRSN, PERCENT	PIP OUT/ PYR IN, MOL/MOL	NPA OUT/ PYR IN, MOL/MOL	SPACE TIME, SEC (2)	RESDNC TIME, SEC (4)
227.8	3.1	3.6	0.0000	0.0000	2.27	2.83
272.0	10.7	6.8	0.0078	0.0000	2.19	2.50
310.1	36.9	14.9	0.0182	0.0000	2.22	2.37
354.8	80.6	20.7	0.0000	0.0000	2.27	2.26
394.3	99.3	28.9	0.0000	0.0000	2.26	2.11
413.8	100.0	30.7	0.0000	0.0000	2.25	2.03

NOTES

- (1) BASED ON THIOPHENE PLUS PYRIDINE LIQUID FEED
- (2) BASED ON TOTAL BED VOLUME AT 350. DEG C AND 150. PSIG
- (3) BY DIFFERENCE
- (4) BASED ON TOTAL BED VOLUME AT REACTOR CONDITIONS
- (-) PYR = PYRIDINE, PIP = PIPERIDINE, NPA = NPENTYLAMINE
- (-) DATA FORM -- CONST SPACE VELOCITY, INDEP VARIABLE = TEMP
- (-) 1 BAR = 10**5 PASCAL = 10**5 N/M**2
- (-) BY INSPECTION: PYR CONV = THI CONV = 0.0 AT 183.5°C

DATA SUMMARY - RUN 49

PURPOSE - To study simultaneous pyridine HDN and thiophene HDS at a total pressure of 1000 psig and equal pyridine and thiophene partial pressures of 93 torr.

OVERALL RUN PARAMETERS

TOTAL PRESSURE = 999.8 PSIG = 69.04 ATM = 69.96 BARS
 LHSV = 0.606 INVERSE HOURS (1)
 SPACE VELOCITY, AVG = 0.433 INVERSE SECONDS (2)
 MOLES HYDROGEN PER MOLE LIQUID REACTANT (1) = 276.8

REACTOR FEED

	GRAMS/HR	G MOL/HR	MOLE FRACTION	PARTIAL PRESSURES		
				BARS	TORR	PSI
THIOPHENE	0.6768	0.00804	0.001801	0.1260	94.5	1.83
PYRIDINE	0.6358	0.00804	0.001800	0.1259	94.4	1.83
HYDROGEN (3)	8.9725	4.4506	0.99640	69.71	-NA-	1011.0
TOTAL	10.2851	4.4667	1.00000	69.96	-NA-	1014.7

CATALYST - NIMO/AL2O3, HDS-3A

TOTAL BED VOLUME = 2.123 CC
 CATALYST WEIGHT = 1.4829 GRAMS
 SULFIDING TYPE = 3

SULFIDING TYPE

0 - NONE
 1 - FORMAL
 2 - RUN
 3 - SHUTDOWN

EXPERIMENTAL RESULTS FOR INDIVIDUAL DATA POINTS

REACTOR TEMPERATURE, DEG C	THIOPHENE CONVRSN, PERCENT	PYRIDINE CONVRSN, PERCENT	PIP OUT/ PYR IN, MGL/MOL	NPA OUT/ PYR IN, MOL/MOL	SPACE TIME, SEC (2)	RESDNC TIME, SEC (4)
224.1	3.5	13.4	0.0593	0.0000	2.29	2.86
260.5	26.9	35.4	0.1479	0.0000	2.32	2.71
299.5	67.6	65.8	0.3396	0.0000	2.35	2.56
342.6	98.1	96.2	0.1914	0.0000	2.29	2.32
351.0	99.8	97.6	0.0900	0.0000	2.31	2.31
362.3	100.0	100.0	0.0000	0.0000	2.31	2.27

NOTES

- (1) BASED ON THIOPHENE PLUS PYRIDINE LIQUID FEED
- (2) BASED ON TOTAL BED VOLUME AT 350. DEG C AND 1000. PSIG
- (3) BY DIFFERENCE
- (4) BASED ON TOTAL BED VOLUME AT REACTOR CONDITIONS
- (-) PYR = PYRIDINE, PIP = PIPRIDINE, NPA = NPENTYLAMINE
- (-) DATA FORM -- CONST SPACE VELOCITY, INDEP VARIABLE = TEMP
- (-) 1 BAR = 10**5 PASCAL = 10**5 N/M**2

DATA SUMMARY - RUN 50

PURPOSE - To study simultaneous pyridine HDN and thiophene HDS at a total pressure of 500 psig and equal pyridine and thiophene partial pressures of 93 torr.

OVERALL RUN PARAMETERS

TOTAL PRESSURE = 499.6 PSIG = 34.98 ATM = 35.44 BARS
 LHSV = 0.606 INVERSE HOURS (1)
 SPACE VELOCITY, AVG = 0.428 INVERSE SECONDS (2)
 MOLES HYDROGEN PER MOLE LIQUID REACTANT (1) = 138.3

REACTOR FEED

	GRAMS/HR	G MOL/HR	MOLE FRACTION	PARTIAL PRESSURES		
				BARS	TORR	PSI
THIOPHENE	0.6771	0.00805	0.003594	0.1274	95.5	1.85
PYRIDINE	0.6354	0.00803	0.003587	0.1271	95.4	1.84
HYDROGEN (3)	4.4821	2.2233	0.99282	35.19	-NA-	510.4
TOTAL	5.7946	2.2394	1.00000	35.44	-NA-	514.1

CATALYST - NIMO/AL2O3, HDS-3A

TOTAL BED VOLUME = 2.123 CC
 CATALYST WEIGHT = 1.4829 GRAMS
 SULFIDING TYPE = 2

SULFIDING TYPE

0 - NONE
 1 - FORMAL
 2 - RUN
 3 - SHUTDOWN

EXPERIMENTAL RESULTS FOR INDIVIDUAL DATA POINTS

REACTOR TEMPERATURE, DEG C	REACTOR TEMPERATURE, DEG K	THIOPHENE CONVRSN, PERCENT	PYRIDINE CONVRSN, PERCENT	PIP OUT/ PYR IN, MOL/MOL	NPA OUT/ PYR IN, MOL/MOL	SPACE TIME, SEC (2)	RESDNC TIME, SEC (4)
227.3	500.4	2.6	3.4	0.0433	0.0000	2.31	2.88
267.7	540.8	20.8	19.2	0.0571	0.0000	2.33	2.68
298.8	571.9	45.4	31.8	0.1743	0.0000	2.31	2.51
341.3	614.4	92.0	58.6	0.0983	0.0000	2.36	2.39
358.9	632.0	98.9	80.0	0.0302	0.0000	2.35	2.31
368.6	641.8	100.0	89.6	0.0103	0.0000	2.38	2.30
386.5	659.7	100.0	98.8	0.0000	0.0000	2.33	2.20

NOTES

- (1) BASED ON THIOPHENE PLUS PYRIDINE LIQUID FEED
- (2) BASED ON TOTAL BED VOLUME AT 350. DEG C AND 500. PSIG
- (3) BY DIFFERENCE
- (4) BASED ON TOTAL BED VOLUME AT REACTOR CONDITIONS
- (-) PYR = PYRIDINE, PIP = PIPERIDINE, NPA = NPENTYLAMINE
- (-) DATA FORM -- CONST SPACE VELOCITY, INDEP VARIABLE = TEMP
- (-) 1 BAR = 10**5 PASCAL = 10**5 N/M**2

-296-
DATA SUMMARY - RUN 51

PURPOSE - To study simultaneous pyridine HDN and thiophene HDS at a total pressure of 150 psig and equal pyridine and thiophene partial pressures of 93 torr.

OVERALL RUN PARAMETERS

TOTAL PRESSURE = 149.3 PSIG = 11.16 ATM = 11.30 BARS
 LHSV = 0.606 INVERSE HOURS (1)
 SPACE VELOCITY, AVG = 0.441 INVERSE SECONDS (2)
 MOLES HYDROGEN PER MOLE LIQUID REACTANT (1) = 44.9

REACTOR FEED

	GRAMS/HR	G MOL/HR	MOLE FRACTION	PARTIAL PRESSURES		
				BARS	TORR	PSI
THIOPHENE	0.6771	0.00805	0.010903	0.1233	92.5	1.79
PYRIDINE	0.6354	0.00803	0.010884	0.1230	92.3	1.78
HYDROGEN (3)	1.4555	0.7220	0.97821	11.06	-NA-	160.4
TOTAL	2.7680	0.7380	1.00000	11.30	-NA-	164.0

CATALYST - NIMO/AL2O3, HDS-3A

TOTAL BED VOLUME = 2.123 CC
 CATALYST WEIGHT = 1.4829 GRAMS
 SULFIDING TYPE = 2

SULFIDING TYPE

0 - NONE
 1 - FORMAL
 2 - RUN
 3 - SHUTDOWN

EXPERIMENTAL RESULTS FOR INDIVIDUAL DATA POINTS

REACTOR TEMPERATURE, DEG C	THIOPHNE CONVRSN, PERCENT	PYRIDINE CONVRSN, PERCENT	PIP OUT/ PYR IN, MOL/MOL	NPA OUT/ PYR IN, MOL/MOL	SPACE TIME, SEC (2)	RESDNC TIME, SEC (4)
251.5	6.4	5.6	0.0132	0.0000	2.25	2.66

NOTES

- (1) BASED ON THIOPHENE PLUS PYRIDINE LIQUID FEED
- (2) BASED ON TOTAL BED VOLUME AT 350. DEG C AND 150. PSIG
- (3) BY DIFFERENCE
- (4) BASED ON TOTAL BED VOLUME AT REACTOR CONDITIONS
- (-) PYR = PYRIDINE, PIP = PIPERIDINE, NPA = NPENTYLAMINE
- (-) DATA FORM -- CONST SPACE VELOCITY, INDEP VARIABLE = TEMP
- (-) 1 BAR = 10**5 PASCAL = 10**5 N/M**2

-297-
DATA SUMMARY - RUN 52

PURPOSE - To study simultaneous pyridine HDN and thiophene HDS
 at a total pressure of 150 psig and equal pyridine and
 thiophene partial pressures of 93 torr.

OVERALL RUN PARAMETERS

TOTAL PRESSURE = 149.9 PSIG = 11.21 ATM = 11.35 BARS
 LHSV = 0.606 INVERSE HOURS (1)
 SPACE VELOCITY, AVG = 0.447 INVERSE SECONDS (2)
 MOLES HYDROGEN PER MOLE LIQUID REACTANT (1) = 45.6

REACTOR FEED

	GRAMS/HR	G MOL/HR	MOLE FRACTION	PARTIAL PRESSURES		
				BARS	TORR	PSI
THIOPHENE	0.6771	0.00805	0.010739	0.1219	91.5	1.77
PYRIDINE	0.6354	0.00803	0.010720	0.1217	91.3	1.77
HYDROGEN (3)	1.4783	0.7333	0.97854	11.11	-NA-	161.2
TOTAL	2.7908	0.7494	1.00000	11.35	-NA-	164.7

CATALYST - NiMo/Al₂O₃, HDS-3A

TOTAL BED VOLUME = 2.123 CC
 CATALYST WEIGHT = 1.4829 GRAMS
 SULFIDING TYPE = 2

SULFIDING TYPE

0 - NONE
 1 - FORMAL
 2 - RUN
 3 - SHUTDOWN

EXPERIMENTAL RESULTS FOR INDIVIDUAL DATA POINTS

REACTOR	THIOPHENE	PYRIDINE	PIP OUT/	NPA OUT/	SPACE	RESDNC	
TEMPERATURE,	CONVRSN,	CONVRSN,	PYR IN,	PYR IN,	TIME,	TIME,	
DEG C	DEG K	PERCENT	PERCENT	MOL/MOL	MOL/MOL	SEC (2)	SEC (4)
240.5	513.7	2.8	2.2	0.0120	0.0000	2.21	2.68
280.8	553.9	14.6	5.2	0.0204	0.0000	2.22	2.49
327.2	600.3	53.6	12.7	0.0105	0.0000	2.26	2.35
372.5	645.7	94.6	21.8	0.0000	0.0000	2.26	2.18
400.0	673.2	99.7	26.0	0.0000	0.0000	2.25	2.07

NOTES

- (1) BASED ON THIOPHENE PLUS PYRIDINE LIQUID FEED
- (2) BASED ON TOTAL BED VOLUME AT 350. DEG C AND 150. PSIG
- (3) BY DIFFERENCE
- (4) BASED ON TOTAL BED VOLUME AT REACTOR CONDITIONS
- (-) PYR = PYRIDINE, PIP = PIPERIDINE, NPA = NPENTYLAMINE
- (-) DATA FORM -- CONST SPACE VELOCITY, INDEP VARIABLE = TEMP
- (-) 1 BAR = 10**5 PASCAL = 10**5 N/M**2

-298-
DATA SUMMARY - RUN 53

PURPOSE - To study simultaneous pyridine HDN and thiophene HDS
 at a total pressure of 1000 psig and equal pyridine and
 thiophene partial pressures of 93 torr.

OVERALL RUN PARAMETERS

TOTAL PRESSURE = 999.3 PSIG = 68.99 ATM = 69.90 BARS
 LHSV = 0.606 INVERSE HOURS (1)
 SPACE VELOCITY, AVG = 0.430 INVERSE SECONDS (2)
 MOLES HYDROGEN PER MOLE LIQUID REACTANT (1) = 275.2

REACTOR FEED

	GRAMS/HR	G MOL/HR	MOLE FRACTION	PARTIAL PRESSURES		
				BARS	TORR	PSI
THIOPHENE	0.6771	0.00805	0.001812	0.1267	95.0	1.84
PYRIDINE	0.6354	0.00803	0.001809	0.1264	94.8	1.83
HYDROGEN (3)	3.9217	4.4255	0.99633	69.65	-NA-	1010.2
TOTAL	10.2342	4.4415	1.00000	69.90	-NA-	1013.9

CATALYST - NIMO/AL2O3, HDS-3A

TOTAL BED VOLUME = 2.123 CC
 CATALYST WEIGHT = 1.4829 GRAMS
 SULFIDING TYPE = 2

SULFIDING TYPE

0 - NONE
 1 - FORMAL
 2 - RUN
 3 - SHUTDOWN

EXPERIMENTAL RESULTS FOR INDIVIDUAL DATA POINTS

REACTOR TEMPERATURE, DEG C	THIOPHENE CONVRSN, DEG K	PYRIDINE CONVRSN, PERCENT	PIP OUT/ PYR IN, PERCENT	NPA OUT/ PYR IN, MOL/MOL	SPACE TIME, SEC (2)	RESDNC TIME, SEC (4)	
283.9	557.0	44.2	55.6	0.3193	0.0000	2.32	2.59
310.5	583.7	72.3	76.5	0.4152	0.0000	2.33	2.49
336.0	609.2	96.9	91.5	0.2724	0.0000	2.31	2.36

NOTES

- (1) BASED ON THIOPHENE PLUS PYRIDINE LIQUID FEED
- (2) BASED ON TOTAL BED VOLUME AT 350. DEG C AND 1000. PSIG
- (3) BY DIFFERENCE
- (4) BASED ON TOTAL BED VOLUME AT REACTOR CONDITIONS
- (-) PYR = PYRIDINE, PIP = PIPERIDINE, NPA = NPENTYLAMINE
- (-) DATA FORM -- CONST SPACE VELOCITY, INDEP VARIABLE = TEMP
- (-) 1 BAR = 10**5 PASCAL = 10**5 N/M**2

DATA SUMMARY - RUN 54

PURPOSE - To study pyridine HDN at a total pressure of 1000 psig and a pyridine partial pressure of 93 torr, in the presence of a 93 torr partial pressure of propanethiol.

OVERALL RUN PARAMETERS

TOTAL PRESSURE = 1000.1 PSIG = 69.06 ATM = 69.97 BARS
 LHSV = 0.331 INVERSE HOURS (1)
 SPACE VELOCITY, AVG = 0.445 INVERSE SECONDS (2)
 MOLES HYDROGEN PER MOLE LIQUID REACTANT (1) = 569.9

REACTOR FEED

	GRAMS/HR	G MOL/HR	MOLE FRACTION	PARTIAL PRESSURES		
				BARS	TORR	PSI
THIOPHENE	0.0000	0.00000	0.000000	0.0000	0.0	0.00
PYRIDINE	0.6359	0.00804	0.001752	0.1226	91.9	1.78
PROPANETHIOL				0.1225	91.8	1.78

CATALYST - NIMO/AL2O3, HDS-3A

TOTAL BED VOLUME = 2.123 CC
 CATALYST WEIGHT = 1.4829 GRAMS
 SULFIDING TYPE = 3

SULFIDING TYPE

0 - NONE
 1 - FORMAL
 2 - RUN
 3 - SHUTDOWN

EXPERIMENTAL RESULTS FOR INDIVIDUAL DATA POINTS

REACTOR TEMPERATURE, DEG C	THIOPHNE CONVRSN, PERCENT	PYRIDINE CONVRSN, PERCENT	PIP OUT/ PYR IN, MOL/MOL	NPA OUT/ PYR IN, MOL/MOL	SPACE TIME, SEC (2)	RESDNC TIME, SEC (4)
215.0	0.0	6.5	0.0560	0.0000	2.26	2.88
250.1	0.0	19.0	0.1233	0.0000	2.26	2.69
291.0	0.0	47.7	0.3802	0.0000	2.23	2.47
330.8	0.0	78.1	0.3957	0.0000	2.23	2.30
352.0	0.0	94.9	0.1090	0.0000	2.24	2.24
363.5	0.0	100.0	0.0000	0.0000	2.26	2.21

NOTES

- (1) BASED ON THIOPHENE PLUS PYRIDINE LIQUID FEED
- (2) BASED ON TOTAL BED VOLUME AT 350. DEG C AND 1000. PSIG
- (3) BY DIFFERENCE
- (4) BASED ON TOTAL BED VOLUME AT REACTOR CONDITIONS
- (-) PYR = PYRIDINE, PIP = PIPERIDINE, NPA = NPENTYLAMINE
- (-) DATA FORM -- CONST SPACE VELOCITY, INDEP VARIABLE = TEMP
- (-) 1 BAR = 10**5 PASCAL = 10**5 N/M**2

-300-
DATA SUMMARY - RUN 55

PURPOSE - To study thiophene HDS at a total pressure of 1000 psig and a thiophene partial pressure of 93 torr, in the presence of a 93 torr partial pressure of butylamine.

OVERALL RUN PARAMETERS

TOTAL PRESSURE = 999.8 PSIG = 69.04 ATM = 69.96 BARS
 LHSV = 0.361 INVERSE HOURS (1)
 SPACE VELOCITY, AVG = 0.443 INVERSE SECONDS (2)
 MOLES HYDROGEN PER MOLE LIQUID REACTANT (1) = 569.1

REACTOR FEED

	GRAMS/HR	G MOL/HR	MOLE FRACTION	PARTIAL PRESSURES		
				BARS	TORR	PSI
THIOPHENE	0.6752	0.00802	0.001754	0.1227	92.0	1.78
PYRIDINE	0.0000	0.00000	0.000000	0.0000	0.0	0.00
BUTYLAMINE				0.1227	92.0	1.78

CATALYST - NIMO/AL2O3, HDS-3A

TOTAL BED VOLUME = 2.123 CC
 CATALYST WEIGHT = 1.4829 GRAMS
 SULFIDING TYPE = 3

SULFIDING TYPE

0 - NONE
 1 - FORMAL
 2 - RUN
 3 - SHUTDOWN

EXPERIMENTAL RESULTS FOR INDIVIDUAL DATA POINTS

REACTOR TEMPERATURE, DEG C	REACTOR TEMPERATURE, DEG K	THIOPHENE CONVRSN, PERCENT	PYRIDINE CONVRSN, PERCENT	PIP OUT/ PYR IN, MOL/MOL	NPA OUT/ PYR IN, MOL/MOL	SPACE TIME, SEC (2)	RESDNC TIME, SEC (4)
230.3	503.4	7.3	0.0	0.0000	0.0000	2.26	2.79
270.0	543.2	30.6	0.0	0.0000	0.0000	2.24	2.58
302.0	575.2	73.5	0.0	0.0000	0.0000	2.27	2.46
312.0	585.2	88.8	0.0	0.0000	0.0000	2.26	2.41
332.0	605.2	99.3	0.0	0.0000	0.0000	2.25	2.32

NOTES

- (1) BASED ON THIOPHENE PLUS PYRIDINE LIQUID FEED
- (2) BASED ON TOTAL BED VOLUME AT 350. DEG C AND 1000. PSIG
- (3) BY DIFFERENCE
- (4) BASED ON TOTAL BED VOLUME AT REACTOR CONDITIONS
- (-) PYR = PYRIDINE, PIP = PIPERIDINE, NPA = NPENTYLAMINE
- (-) DATA FORM -- CONST SPACE VELOCITY, INDEP VARIABLE = TEMP
- (-) 1 BAR = 10**5 PASCAL = 10**5 N/M**2

-301-
DATA SUMMARY - RUN 60

PURPOSE - To study the HDS of thiophene at a total pressure of 500 psig and a thiophene partial pressure of 186 torr.

OVERALL RUN PARAMETERS

TOTAL PRESSURE = 500.0 PSIG = 35.03 ATM = 35.49 BARS
 LHSV = 0.605 INVERSE HOURS (1)
 SPACE VELOCITY, AVG = 0.436 INVERSE SECONDS (2)
 MOLES HYDROGEN PER MOLE LIQUID REACTANT (1) = 141.2

REACTOR FEED

	GRAMS/HR	G. MOL/HR	MOLE FRACTION	PARTIAL PRESSURES		
				BARS	TORR	PSI
THIOPHENE	1.3507	0.01605	0.007030	0.2495	187.1	3.62
PYRIDINE	0.0000	0.00000	0.000000	0.0000	0.0	0.00
HYDROGEN (3)	4.5712	2.2675	0.99297	35.24	-NA-	511.1
TOTAL	5.9219	2.2835	1.00000	35.49	-NA-	514.7

CATALYST - NIMO/AL2O3, HDS-3A

TOTAL BED VOLUME = 2.123 CC
 CATALYST WEIGHT = 1.4829 GRAMS
 SULFIDING TYPE = 2

SULFIDING TYPE

0 - NONE
 1 - FORMAL
 2 - RUN
 3 - SHUTDOWN

EXPERIMENTAL RESULTS FOR INDIVIDUAL DATA POINTS

REACTOR TEMPERATURE, DEG C	THIOPHENE CONVRSN, PERCENT	PYRIDINE CONVRSN, PERCENT	PIP OUT/ PYR IN, MOL/MOL	NPA OUT/ PYR IN, MOL/MOL	SPACE TIME, SEC (2)	RESDNC TIME, SEC (4)
203.8	4.7	0.0	0.0000	0.0000	2.29	2.99
243.0	33.9	0.0	0.0000	0.0000	2.29	2.76
278.4	98.8	0.0	0.0000	0.0000	2.31	2.62
255.0	55.4	0.0	0.0000	0.0000	2.30	2.72
281.5	99.8	0.0	0.0000	0.0000	2.30	2.59

NOTES

- (1) BASED ON THIOPHENE PLUS PYRIDINE LIQUID FEED
- (2) BASED ON TOTAL BED VOLUME AT 350. DEG C AND 500. PSIG
- (3) BY DIFFERENCE
- (4) BASED ON TOTAL BED VOLUME AT REACTOR CONDITIONS
- (-) PYR = PYRIDINE, PIP = PIPERIDINE, NPA = NPENTYLAMINE
- (-) DATA FORM -- CONST SPACE VELOCITY, INDEP VARIABLE = TEMP
- (-) 1 BAR = 10**5 PASCAL = 10**5 N/M**2
- (-) Run by Gultekin

-302-
DATA SUMMARY - RUN 61

PURPOSE - To study the HDS of 2,5-dimethylthiophene at a total pressure of 500 psig and a 2,5-dimethylthiophene partial pressure of 186 torr.

OVERALL RUN PARAMETERS

TOTAL PRESSURE = 499.7 PSIG = 35.00 ATM = 35.47 BARS
 LHSV = 0.838 INVERSE HOURS(1)
 SPACE VELOCITY, AVG = 0.432 INVERSE SECONDS(2)
 MOLES HYDROGEN PER MOLE LIQUID REACTANT(1) = 139.5

REACTOR FEED

	GRAMS/HR	G MOL/HR	MOLE FRACTION	PARTIAL PRESSURES		
				BARS	TORR	PSI
THIOPHENE	1.8040	0.01608	0.007118	0.2525	189.4	3.66
PYRIDINE	0.0000	0.00000	0.000000	0.0000	0.0	0.00
HYDROGEN (3)	4.5217	2.2429	0.99288	35.22	-NA-	510.8
TOTAL	6.3257	2.2590	1.00000	35.47	-NA-	514.4

CATALYST - NIMO/AL2O3, HDS-3A

TOTAL BED VOLUME = 2.123 CC
 CATALYST WEIGHT = 1.4829 GRAMS
 SULFIDING TYPE = 2

SULFIDING TYPE

0 - NONE
 1 - FORMAL
 2 - RUN
 3 - SHUTDOWN

EXPERIMENTAL RESULTS FOR INDIVIDUAL DATA POINTS

REACTOR TEMPERATURE, DEG C	THIOPHNE CONVRSN, PERCENT	PYRIDINE CONVRSN, PERCENT	PIP OUT/ PYR IN, MOL/MOL	NPA OUT/ PYR IN, MOL/MOL	SPACE TIME, SEC (2)	RESDNC TIME, SEC (4)
185.5	3.3	0.0	0.0000	0.0000	2.30	3.12
229.8	12.4	0.0	0.0000	0.0000	2.31	2.86
259.7	37.8	0.0	0.0000	0.0000	2.33	2.72
271.3	58.2	0.0	0.0000	0.0000	2.35	2.69
279.6	77.4	0.0	0.0000	0.0000	2.32	2.61
293.0	100.0	0.0	0.0000	0.0000	2.33	2.56
284.8	92.7	0.0	0.0000	0.0000	2.32	2.59

NOTES

- (1) BASED ON THIOPHENE PLUS PYRIDINE LIQUID FEED
- (2) BASED ON TOTAL BED VOLUME AT 350. DEG C AND 500. PSIG
- (3) BY DIFFERENCE
- (4) BASED ON TOTAL BED VOLUME AT REACTOR CONDITIONS
- (-) PYR = PYRIDINE, PIP = PIPERIDINE, NPA = NPENTYLAMINE
- (-) DATA FORM -- CONST SPACE VELOCITY, INDEP VARIABLE = TEMP
- (-) 1 BAR = 10**5 PASCAL = 10**5 N/M**2
- (-) Run by Gultekin

-303-
DATA SUMMARY - RUN 62

PURPOSE - To study the HDS of 2-methylthiophene at a total pressure of 500 psig and a 2-methylthiophene partial pressure of 186 torr.

OVERALL RUN PARAMETERS

TOTAL PRESSURE = 498.0 PSIG = 34.89 ATM = 35.36 BARS
 LHSV = 0.755 INVERSE HOURS (1)
 SPACE VELOCITY, AVG = 0.433 INVERSE SECONDS (2)
 MOLES HYDROGEN PER MOLE LIQUID REACTANT (1) = 140.1

REACTOR FEED

	GRAMS/HR	G MOL/HR	MOLE FRACTION	PARTIAL PRESSURES		
				BARS	TORR	PSI
THIOPHENE	1.5785	0.01608	0.007089	0.2506	188.0	3.64
PYRIDINE	0.0000	0.00000	0.000000	0.0000	0.0	0.00
HYDROGEN (3)	4.5404	2.2522	0.99291	35.11	-NA-	509.2
TOTAL	6.1189	2.2683	1.00000	35.36	-NA-	512.8

CATALYST - NIMO/AL2O3, HDS-3A

TOTAL BED VOLUME = 2.123 CC
 CATALYST WEIGHT = 1.4829 GRAMS
 SULFIDING TYPE = 2

SULFIDING TYPE

0 - NONE
 1 - FORMAL
 2 - RUN
 3 - SHUTDOWN

EXPERIMENTAL RESULTS FOR INDIVIDUAL DATA POINTS

REACTOR TEMPERATURE, DEG C	THIOPHNE CONVRSN, PERCENT	PYRIDINE CONVRSN, PERCENT	PIP OUT/ PYR IN, MOL/MOL	NPA OUT/ PYR IN, MOL/MOL	SPACE TIME, SEC (2)	RESDNC TIME, SEC (4)
183.6	1.5	0.0	0.0000	0.0000	2.28	3.11
204.3	6.4	0.0	0.0000	0.0000	2.30	3.00
241.0	19.9	0.0	0.0000	0.0000	2.32	2.81
268.0	59.0	0.0	0.0000	0.0000	2.32	2.66
279.8	84.0	0.0	0.0000	0.0000	2.32	2.59
289.3	100.0	0.0	0.0000	0.0000	2.33	2.56
285.0	97.4	0.0	0.0000	0.0000	2.33	2.58
251.6	33.5	0.0	0.0000	0.0000	2.32	2.73

NOTES

- (1) BASED ON THIOPHENE PLUS PYRIDINE LIQUID FEED
- (2) BASED ON TOTAL BED VOLUME AT 350. DEG C AND 500. PSIG
- (3) BY DIFFERENCE
- (4) BASED ON TOTAL BED VOLUME AT REACTOR CONDITIONS
- (-) PYR = PYRIDINE, PIP = PIPERIDINE, NPA = NPENTYLAMINE
- (-) DATA FORM -- CONST SPACE VELOCITY, INDEP VARIABLE = TEMP
- (-) 1 BAR = 10**5 PASCAL = 10**5 N/M**2
- (-) Run by Gultekin

DATA SUMMARY - RUN 63

PURPOSE - To study the HDS of 2-methylthiophene at a total pressure of 500 psig and a 2-methylthiophene partial pressure of 186 torr.

OVERALL RUN PARAMETERS

TOTAL PRESSURE = 500.2 PSIG = 35.04 ATM = 35.51 BARS
 LHSV = 0.755 INVERSE HOURS (1)
 SPACE VELOCITY, AVG = 0.434 INVERSE SECONDS (2)
 MOLES HYDROGEN PER MOLE LIQUID REACTANT (1) = 140.2

REACTOR FEED

	GRAMS/HR	G MOL/HR	MOLE FRACTION	PARTIAL PRESSURES		
				BARS	TORR	PSI
THIOPHENE	1.5785	0.01608	0.007080	0.2514	188.6	3.65
PYRIDINE	0.0000	0.00000	0.000000	0.0000	0.0	0.00
HYDROGEN (3)	4.5459	2.2549	0.99292	35.26	-NA-	511.3
TOTAL	6.1244	2.2710	1.00000	35.51	-NA-	515.0

CATALYST - NIMO/AL2O3, HDS-3A

TOTAL BED VOLUME = 2.123 CC
 CATALYST WEIGHT = 1.4329 GRAMS
 SULFIDING TYPE = 2

SULFIDING TYPE

0 - NONE
 1 - FORMAL
 2 - RUN
 3 - SHUTDOWN

EXPERIMENTAL RESULTS FOR INDIVIDUAL DATA POINTS

REACTOR TEMPERATURE, DEG C	THIOPHNE CONVRSN, PERCENT	PYRIDINE CONVRSN, PERCENT	PIP OUT/ PYR IN, MOL/MOL	NPA OUT/ PYR IN, MOL/MOL	SPACE TIME, SEC (2)	RESDNC TIME, SEC (4)
243.4	22.6	0.0	0.0000	0.0000	2.28	2.75
273.1	67.7	0.0	0.0000	0.0000	2.29	2.61
281.5	89.4	0.0	0.0000	0.0000	2.33	2.61
288.0	100.0	0.0	0.0000	0.0000	2.33	2.59
283.0	94.5	0.0	0.0000	0.0000	2.34	2.63

NOTES

- (1) BASED ON THIOPHENE PLUS PYRIDINE LIQUID FEED
- (2) BASED ON TOTAL BED VOLUME AT 350. DEG C AND 500. PSIG
- (3) BY DIFFERENCE
- (4) BASED ON TOTAL BED VOLUME AT REACTOR CONDITIONS
- (-) PYR = PYRIDINE, PIP = PIPERIDINE, NPA = NPENTYLAMINE
- (-) DATA FORM -- CONST SPACE VELOCITY, INDEP VARIABLE = TEMP
- (-) 1 BAR = 10**5 PASCAL = 10**5 N/M**2
- (-) Run by Gultekin

Table 8-5

Catalyst Activity Run Data

<u>Run</u>	<u>Time on Stream at Maximum Pyridine Conversion, hours</u>	<u>Maximum Pyridine Conversion, percent</u>	<u>Reactor Temp., °C</u>
2	16	33.8	350
5	50	23.6	352
7	66	21.0	352
14	166	16.4	357
18	222	25.1	360
19	234	24.2	362
21	254	~25.9	361

Table 8-6
Pyridine HDN Conversion Curve Values

Reactor Temp, °C	Total pressure = 1000 psig				500 psig		150 psig			
	PYR(93)	PYR(186)	THI(93)	PYR(93)	PYR(93)	THI(93)	PYR(93)	PYR(186)	PYR(93)	THI(93)
190	5.0	---	5.0	---	---	---	---	---	---	0.4
200	7.4	1.9	7.4	---	7.5	---	8.4	---	---	1.0
210	10.4	3.3	10.4	---	10.0	---	9.4	---	---	1.5
220	13.8	5.3	13.8	8.0	12.8	---	10.4	---	---	2.1
230	17.8	8.6	17.8	10.9	15.9	4.3	11.6	3.9	---	2.7
240	22.8	13.4	22.8	14.5	19.5	8.2	12.7	6.4	---	3.4
250	28.7	19.2	28.7	18.8	23.4	12.0	13.8	8.8	---	4.2
260	36.0	25.6	35.0	24.0	27.8	15.9	15.0	11.2	---	5.1
270	45.0	33.0	42.2	31.2	32.9	19.8	16.3	13.3	---	6.0
280	56.8	41.6	50.0	39.0	38.4	23.9	17.5	15.2	---	7.2
290	68.6	51.0	58.3	46.7	44.5	28.0	18.8	16.8	---	8.4
300	78.9	61.2	67.2	54.6	50.8	32.2	20.3	18.1	---	9.9
310	88.2	71.2	76.5	62.3	56.2	37.0	21.9	18.9	---	11.6
320	93.3	76.9	84.9	70.1	61.5	42.7	23.7	19.4	---	13.4
330	96.0	81.3	91.3	77.9	66.9	49.4	25.2	19.8	---	15.2
340	97.0	84.7	95.5	85.6	72.0	57.7	26.5	20.0	---	17.0
350	97.5	87.7	97.5	93.3	77.0	67.8	27.6	20.2	---	18.8
360	98.2	90.4	99.3	99.1	80.2	79.9	28.3	20.1	---	20.7
370	98.8	93.0	100.0	100.0	81.8	90.1	28.7	19.8	---	22.6
380	99.5	94.9			83.0	96.4	28.5	19.4	---	24.4
390	100.0	96.5			84.0	100.0	27.8	18.6	---	26.3
400		97.7			85.1		26.2	17.3	---	28.3
410		98.5			86.1		21.7	15.3	---	30.2

Notes: All table values (except temperatures) are percent conversion (disappearance) of reactant pyridine, representing values of curves through experimental data points on conversion vs. temperature figures.

Feed Code: PYR =Pyridine; THI = Thiophene; PT = Propanethiol

Feed Partial pressures (nominal) are shown in parenthesis

Table 8-7
Thiophene HDS Conversion Curve Values

Reactor Temp, °C	Total Pressure = 1000 psig				500 psig		150 psig		THI (93) PYR (93)	
	THI (93)	THI (186)	THI (93) PYR (93)	THI (93) BA (93)	THI (93)	THI (93) PYR (93)	THI (93)	THI (93) PYR (93)	THI (93)	THI (93) PYR (93)
190	6.8	---	---	---	6.8	---	6.8	---	1.8	---
200	15.7	---	---	---	11.7	---	9.7	---	2.8	---
210	26.2	---	---	---	18.2	---	13.4	---	4.2	---
220	38.4	20.7	---	---	26.3	---	18.2	---	6.4	---
230	52.5	28.5	7.2	7.2	36.5	3.7	24.3	3.1	10.6	3.1
240	68.2	40.3	12.7	12.7	49.7	7.4	32.1	3.8	18.4	3.8
250	87.5	58.2	18.9	18.9	64.6	11.7	42.8	4.9	26.7	4.9
260	98.4	79.2	26.0	26.0	80.2	16.5	55.9	6.9	36.7	6.9
270	100.0	97.1	33.5	33.5	93.8	22.2	69.8	10.1	48.5	10.1
280		100.0	41.3	41.3	98.5	29.2	82.2	14.2	62.0	14.2
290			52.0	52.0	100.0	37.3	92.0	19.4	77.2	19.4
300			63.3	69.0		46.3	97.1	26.2	91.8	26.2
310			75.2	85.4		56.1	99.2	35.5	97.5	35.5
320			85.7	94.7		66.8	100.0	45.8	99.5	45.8
330			94.1	98.5		78.4		55.7	100.0	55.7
340			97.6	100.0		90.4		65.7		65.7
350			99.5			96.8		75.8		75.8
360			100.0			99.1		85.8		85.8
370						100.0		93.9		93.9
380								96.6		96.6
390								98.4		98.4
400								100.0		100.0

Notes: All table values (except temperatures) are percent conversion (disappearance) of reactant thiophene, representing values of curves through experimental data points on conversion vs. temperature figures.

Feed Code: THI = Thiophene; PYR = Pyridine; BA = Butylamine
Feed partial pressures (nominal) are shown in parenthesis

PYRIDINE HDN PRODUCT DISTRIBUTION

PYRIDINE AND PIPERIDINE RELATIVE MOLAR OUTPUTS

PURE PYRIDINE FEED DATA

REACTOR TEMP, DEG C	<u>1000 PSIG</u>		<u>500 PSIG</u>		<u>150 PSIG</u>	
	<u>PYR OUT/ PYR IN, MOL/MOL</u>	<u>PIP OUT/ PYR IN, MOL/MOL</u>	<u>PYR OUT/ PYR IN, MOL/MOL</u>	<u>PIP OUT/ PYR IN, MOL/MOL</u>	<u>PYR OUT/ PYR IN, MOL/MOL</u>	<u>PIP OUT/ PYR IN, MOL/MOL</u>
190.	0.950	0.002	9.000	9.000	9.000	9.000
200.	0.926	0.027	0.925	0.033	0.916	0.005
210.	0.896	0.056	0.900	0.040	0.906	0.007
220.	0.862	0.090	0.872	0.053	0.896	0.010
230.	0.822	0.130	0.841	0.071	0.884	0.015
240.	0.772	0.177	0.805	0.092	0.873	0.021
250.	0.713	0.232	0.766	0.117	0.862	0.028
260.	0.640	0.298	0.722	0.147	0.850	0.039
270.	0.550	0.380	0.671	0.183	0.837	0.055
280.	0.432	0.462	0.616	0.227	0.825	0.072
290.	0.314	0.550	0.555	0.281	0.812	0.087
300.	0.211	0.647	0.492	0.341	0.797	0.097
310.	0.118	0.694	0.438	0.408	0.781	0.098
320.	0.067	0.697	0.385	0.439	0.763	0.091
330.	0.040	0.648	0.331	0.433	0.748	0.078
340.	0.030	0.524	0.280	0.385	0.735	0.065
350.	0.025	0.402	0.230	0.300	0.724	0.050
360.	0.018	0.285	0.198	0.216	0.717	0.037
370.	0.012	0.166	0.182	0.132	0.713	0.027
380.	0.005	0.063	0.170	0.050	0.715	0.018
390.	0.000	0.000	0.160	0.023	0.722	0.010
400.	0.000	0.000	0.149	0.016	0.738	0.004
410.	0.000	0.000	0.139	0.013	0.783	0.000

NOTES

FRACTIONS REPRESENT VALUES OF CURVES THROUGH EXPERIMENTAL
DATA POINTS ON PRODUCT DISTRIBUTION FIGURES

9.000 = NO EXPERIMENTAL DATA AT THIS REACTION CONDITION

PYRIDINE HDN PRODUCT DISTRIBUTION

PYRIDINE AND PIPERIDINE RELATIVE MOLAR OUTPUTS

SIMULTANEOUS PYRIDINE-THIOPHENE FEED DATA

REACTOR TEMP, DEG C	<u>1000 PSIG</u>		<u>500 PSIG</u>		<u>150 PSIG</u>	
	<u>PYR OUT/ PYR IN, MOL/MOL</u>	<u>PIP OUT/ PYR IN, MOL/MOL</u>	<u>PYR OUT/ PYR IN, MOL/MOL</u>	<u>PIP OUT/ PYR IN, MOL/MOL</u>	<u>PYR OUT/ PYR IN, MOL/MOL</u>	<u>PIP OUT/ PYR IN, MOL/MOL</u>
190.	0.950	0.000	9.000	9.000	0.996	0.000
200.	0.926	0.013	9.000	9.000	0.990	0.000
210.	0.896	0.030	9.000	9.000	0.985	0.000
220.	0.862	0.048	9.000	9.000	0.979	0.000
230.	0.822	0.069	0.957	0.042	0.973	0.003
240.	0.772	0.093	0.918	0.044	0.966	0.009
250.	0.713	0.117	0.880	0.047	0.958	0.013
260.	0.650	0.146	0.841	0.052	0.949	0.016
270.	0.578	0.183	0.802	0.066	0.940	0.017
280.	0.500	0.241	0.761	0.099	0.928	0.018
290.	0.417	0.313	0.720	0.134	0.916	0.019
300.	0.328	0.394	0.678	0.174	0.901	0.019
310.	0.235	0.419	0.630	0.203	0.884	0.019
320.	0.151	0.413	0.573	0.198	0.866	0.014
330.	0.087	0.350	0.506	0.153	0.848	0.009
340.	0.045	0.220	0.423	0.100	0.830	0.004
350.	0.025	0.102	0.322	0.058	0.812	0.000
360.	0.007	0.017	0.201	0.026	0.793	0.000
370.	0.000	0.000	0.099	0.009	0.774	0.000
380.	0.000	0.000	0.036	0.000	0.756	0.000
390.	0.000	0.000	0.000	0.000	0.737	0.000
400.	0.000	0.000	0.000	0.000	0.717	0.000
410.	0.000	0.000	0.000	0.000	0.698	0.000

NOTES

FRACTIONS REPRESENT VALUES OF CURVES THROUGH EXPERIMENTAL
DATA POINTS ON PRODUCT DISTRIBUTION FIGURES

9.000 = NO EXPERIMENTAL DATA AT THIS REACTION CONDITION

VIII.D. Derivation of Equations and Supporting Principles

VIII.D.1 Plug Flow Reactor Parameters

For plug-flow reactors, the basic performance equation is:

$$\frac{V}{F} = \int \frac{dx}{-r}$$

where: V = volume of catalyst bed

F = volumetric feed rate

dx = differential conversion taking place
in a differential section of the catalyst
bed

-r = rate of disappearance of reactant

This is derived from a mass balance on the reactor, and hence relates the conversion to mass flow parameters (Satterfield, 1970; Levenspiel, 1972; Smith, 1970). The flow component of the equation is its left-hand side, where V/F , a natural product of the mathematical derivation, is the space time (space time = space velocity⁻¹ = time required to process one reactor volume of feed measured at specified conditions; Levenspiel, 1972). In terms of the physical flows of material through the reactor, only the space time is represented in the equation as a direct mathematical result of the mass balance derivation. The actual residence time (contact time, holding time) of the reactant mixture does not appear. Given a constant space

time, the residence time can vary, as with the reactor temperature or pressure, without affecting the mathematical performance of the reactor.

For this study, the space time and space velocity conditions were defined as 350°C and the nominal pressure of the reaction, either 150, 500, or 1000 psig. Since the total volumetric flow rate of the reactor stream was held constant during a run, and this flow rate was varied in direct proportion to the total absolute reactor pressure from one nominal pressure to another, the space velocity (and hence space time) was a constant for all runs.

VIII.D.2 Conversion of Reactants

Conversion is defined for this study as the disappearance of reactant, thiophene or pyridine. As the total reaction gas mixture is of approximately constant molar density at all extents of reaction, changes in the absolute amounts of the reactants present can be determined by following variations in the individual component concentrations, measured as partial pressures. The use of partial pressures also permits the comparison of values at different total pressures (i.e. different hydrogen partial pressures). Thus:

$$X = 1 - \frac{P}{P_0}$$

where X = fractional conversion of reactant

P = partial pressure of reactant under specific reaction conditions

P₀ = initial feed partial pressure of reactant

In this study, changes in the concentrations (partial pressures) were determined by the gas chromatographic analysis of the reactor exit stream, utilizing the linear response of the integrated chromatograph signal to the amount of each component present. This permits substitution of the ratio of chromatograph peak areas in the above equation.

Experimentally, the reactor system is first brought to a steady state condition where all feeds to the reactor have been set to values which will remain constant for the entire run, but the reactor itself is at a temperature, approximately 115°C, at which no reaction occurs. A series of gas chromatograms under this condition will give an average reactant peak area, A_B , for the no-reaction condition which will be used as a base, indicating the amount of reactant present in the feed to the reactor under any other set of reactor conditions. When the reactor temperature is subsequently increased to give finite conversion, the observed reactant peak area in the product stream chromatogram is decreased. Comparison of this peak area at reaction temperature, A_T , with the base area gives the expression for reactant conversion:

$$x = 1 - \frac{A_T}{A_B}$$

Several factors in addition to chemical reaction may influence the observed reactant peak areas. To avoid distorting the calculated conversions, the observed chromatogram areas of a run are all normalized to a standard set of conditions. The temperature and pressure of the gas sample valve, and thus the contained gas volume, may change. Each area is corrected to a standard sample valve temperature and pressure, for example 200°C and 14 psig,

using the ideal gas law. The volumes of the two loops of the gas sample valve differed by nearly two percent, so a correction factor was added to normalize the resulting sample sizes. These three correction factors combine to give the partially-standardized peak area (for pressures in psi and temperatures in degrees C):

$$\left(\begin{array}{c} \text{standardized} \\ \text{area} \end{array} \right) = \left(\begin{array}{c} \text{measured} \\ \text{area} \end{array} \right) \left(\frac{\text{stnd.press.}+14.7}{\text{actual GSV press.}+ \text{barometric press.}} \right) \times \left(\frac{\text{actual GSV temp.}+273}{\text{stnd.temp.} + 273} \right) \left(\begin{array}{c} \text{loop size} \\ \text{factor} \end{array} \right)$$

The most important correction needed is that for variations in the total flow rate through the reactor. For any given conversion and reactant feed rate, an increase in total flow rate (due to an increase in hydrogen flow) would dilute the reactant in the product stream, giving smaller observed peaks. By normalizing all sample sizes according to the associated reactor flow rates, this dilution effect is eliminated. For computational purposes, this was accomplished by replacing the standardized chromatographic areas with the products of these standardized areas and the standardized reactor flow rate associated with each sample.

For this calculation, reactor flow rates were corrected to standard conditions of 1 atmosphere pressure and 0°C

(the actual physical state of the reactants at this temperature has no bearing on the use of these conditions). Flow rates were measured with a soap-film flowmeter preceded by a saturator. The temperature of the gas stream inside the flowmeter was measured. The pressure of the stream equaled the barometric pressure. As the flowmeter was preceded by a saturator, the vapor pressure of water at the temperature of the gas flow was subtracted from the barometric pressure to give the true partial pressure of the dry exhaust gas. These correction factors combine to give, for pressures in torr and temperature in degrees C:

$$\left(\begin{array}{c} \text{standardized} \\ \text{reactor flow} \end{array} \right) = \left(\begin{array}{c} \text{measured} \\ \text{reactor flow} \end{array} \right) \left(\frac{\text{barometric press.} - \text{vapor press. water}}{760} \right) \times \left(\frac{273}{\text{gas temp.} + 273} \right)$$

The vapor pressure of water, VP_{H_2O} , in torr, was determined for each temperature, $T^\circ C$, by the equation:

$$VP_{H_2O} = 3.717 + (0.4958)T + (0.000210)T^2 + (0.000497)T^3$$

This correlation was determined by fitting, using graphical techniques (Lipka, 1918), vapor pressure-temperature data for water over the temperature range of interest (Weast, 1966).

Replacing the areas in the previous conversion

equation by the products (SAFR) of the standardized areas (SA_B and SA_T) and standardized flow rates (SF_B and SF_T) one gets:

$$X = 1 - \frac{(SA_T)(SF_T)}{(SA_B)(SF_B)} = 1 - \frac{SAFR_T}{SAFR_B}$$

It is this equation which is used in the actual computations, and illustrated in the sample calculation section.

VIII.D.3 Data Quality - Statistical Determination

The statistical quality of the data is expressed in two ways. First, the relative standard deviation of the normalized gas chromatograph peak areas is given for each isothermal set of samples. Second, each reactant conversion value is accompanied by two sets of confidence intervals, for 68 and 95 percent confidence limits.

As a measure of the statistical quality of a set of samples, the normalized peak areas (or, for calculation purposes the standardized area-flow rate products, SAFR), the variance is the most rigorous, as it is independent of the number of samples taken; it can be combined through successive calculations; it can be used for quantitative comparisons of different data groups, and gives good indications of the determinate or indeterminate nature of the data scatter (Department of Chemistry, M.I.T., 1964;

Skoog and West, 1969). For dimensional consistency and better order-of-magnitude comparisons of the scatter with the mean, the square root of the variance, the standard deviation, is usually preferred. In this study the relative standard deviation, the standard deviation of a set of samples expressed as a percentage of the mean value, is given for each isothermal set of gas chromatograph samples.

The variance is calculated using a form of the defining equation particularly suited to computational methods. For n values of any variable x :

$$\text{variance} = s^2 = \frac{1}{n(n-1)} \left(n \sum_{i=1}^n x_i^2 - \left(\sum_{i=1}^n x_i \right)^2 \right) \quad (3-1)$$

The standard deviation and relative standard deviation, for a mean value \bar{x} are:

$$\text{standard deviation} = s = (\text{variance})^{1/2} \quad (3-2)$$

$$\text{relative standard deviation} = \text{RSD} = \frac{100s}{\bar{x}} \quad (3-3)$$

To specify confidence limits for a conversion value calculated from equations of the previous section, variances must be propagated through the calculations (Skoog and West, 1969). Naming the SAFR quotient Z , the final conversion equation becomes:

$$X = 1 - \frac{\text{SAFR}_T}{\text{SAFR}_B} = 1 - Z \quad (3-4)$$

The relative standard deviation of Z, RSD_Z , is determined by summing the relative deviations of $SAFR_T$ and $SAFR_B$, RSD_T and RSD_B respectively:

$$RSD_Z = RSD_B + RSD_T \quad (3-5)$$

The variance of Z then becomes, using equation (3-3):

$$s_Z^2 = \left(\frac{RSD_Z \times Z}{100} \right)^2 \quad (3-6)$$

For subtraction, variances are additive. In equation (3-4), then for zero variance in the number one:

$$s_X^2 = 0 + s_Z^2 \quad (3-7)$$

Confidence intervals of 68 and 95 percent follow from the standard deviation of the conversion. At least 30 samples would be required to use statistical values based on a normal distribution in the confidence limit calculation. Instead, t-values, which account for the deviations from the normal distribution found in smaller sample numbers are used. Confidence limits are then (Crow et al., 1960):

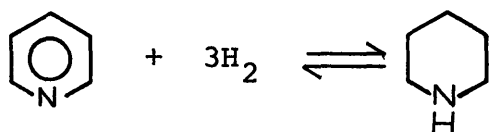
$$\bar{x} \pm \frac{(t_{\alpha/2, n-1})(s_X)}{n^{1/2}} \quad (3-8)$$

where $t_{\alpha/2, n-1}$ is the appropriate t-value for the desired confidence level and number of degrees of freedom. The number of samples, n, and hence the number of degrees of

freedom, $n-1$, for this calculation are conservatively based on the smaller of the number of samples in the base and at the reaction temperature.

VIII.D.4 Pyridine-Piperidine Equilibrium - Principles of Calculation

For the hydrogenation of pyridine to piperidine:



the relative quantities of pyridine (Pyr) and piperidine (Pip) present at equilibrium over the range of reaction temperatures are calculated using the equilibrium constant determined as a function of temperature. This equilibrium constant is obtained in two ways for use in this study: by calculation from thermodynamic free energy of formation data, and by utilization of an empirically-determined temperature functionality. The principles supporting the determinations are discussed here, and sample calculations are presented in a subsequent Appendix section.

Thermodynamic data for the free energy of formation as a function of temperature is available for both pyridine (McCullough et al., 1957) and piperidine (Scott, 1971), and are tabulated elsewhere in the Appendix. This permits calculation of the change in free energy for the reaction,

$\Delta G_{\text{rxn}}^{\circ}$, at any given temperature, from the free energy of formation for each reactant and product in its standard state at the specified temperature according to the summation (Modell and Reid, 1970):

$$\Delta G_{\text{rxn}}^{\circ} = \sum_1^n v_i \Delta G_{f_i}^{\circ} \quad (4-1)$$

where $\Delta G_{f_i}^{\circ}$ is the free energy of formation for each species i (for all reactants and products) in their standard states (with $\Delta G_{f_i}^{\circ} = 0$ for elements), and v_i is the stoichiometric coefficient of species i (positive for products, negative for reactants). All data used here are based upon an ideal gas reference state, with its inherent one atmosphere standard pressure. The justification for utilizing the ideal gas assumption for all calculations for the reaction conditions used has been previously presented. For the pyridine saturation reaction, with $\Delta G_{f_{\text{H}_2}}^{\circ} = 0$:

$$\Delta G_{\text{rxn}}^{\circ} = \Delta G_{f_{\text{Pip}}}^{\circ} - \Delta G_{f_{\text{Pyr}}}^{\circ} \quad (4-2)$$

The equilibrium constant follows directly from $\Delta G_{\text{rxn}}^{\circ}$. For the ideal gas case the activity-based constant K_a reduces to the partial pressure-based equilibrium constant, K_p . Thus, for any absolute temperature, T , with universal gas constant R :

$$\Delta G_{\text{rxn}}^{\circ} = -RT \ln(K_p) \quad (4-3)$$

$$\text{and } K_p = \exp\left(\frac{-\Delta G_{\text{rxn}}^{\circ}}{RT}\right) \quad (4-4)$$

To remove the free energy term from the equation and obtain a simple relationship for K_p as a function of temperature, °K, one takes advantage of the linearity of $\Delta G_{\text{rxn}}^{\circ}$ as a function of absolute temperature. $\Delta G_{\text{rxn}}^{\circ}$ values calculated at several temperatures give a series of K_p and T pairs, which produce a straight line when plotting the alternate form of equation (4-3):

$$\log_{10}(K_p) = \frac{-\Delta G_{\text{rxn}}^{\circ}}{2.303 R} \left(\frac{1}{T}\right) \quad (4-5)$$

Eliminating the $\Delta G_{\text{rxn}}^{\circ}$ dependence by this plot, the final equilibrium constant-temperature relationship is of the form, for constants a and b:

$$\log_{10}(K_p) = a \left(\frac{1}{T}\right) + b \quad (4-6)$$

An experimental determination of the equilibrium constant by Goudriaan (1974) discussed in the literature review also gave a temperature dependence of the form of equation (4-6). While giving constants a and b quite close to those derived from thermodynamic data, the empirical values give equilibrium concentrations different enough to warrant separate presentation.

Equilibrium for the pyridine hydrogenation reaction is expressed, where the ideal gas assumption permits replacing component activities by partial pressures, as:

$$K_p = \frac{p_{\text{Pip}}}{p_{\text{Pyr}} p_{\text{H}_2}^3} \quad (4-7)$$

For quantitative comparison of thermodynamic equilibrium with experimental results, the amount of piperidine at equilibrium is given as a fraction of the total pyridine and piperidine present:

$$\frac{p_{\text{Pip}}}{p_{\text{Pyr}} + p_{\text{Pip}}} = \frac{\text{moles Pip}}{\text{moles Pyr} + \text{moles Pip}} \quad (4-8)$$

where p_{Pip} and p_{Pyr} are the partial pressures of piperidine and pyridine, respectively. For the case with only these components present reaching equilibrium, this expresses the fraction of total nitrogen present as piperidine. For experimental data presentation, the fraction is based on only that nitrogen present as pyridine or piperidine (and hence affecting equilibrium), eliminating such other forms as ammonia and n-pentylamine. This representation is then useful as a form for comparison with reaction data, as it gives values comparable on a constant basis, without interference by subsequent hydrogenation reactions or side

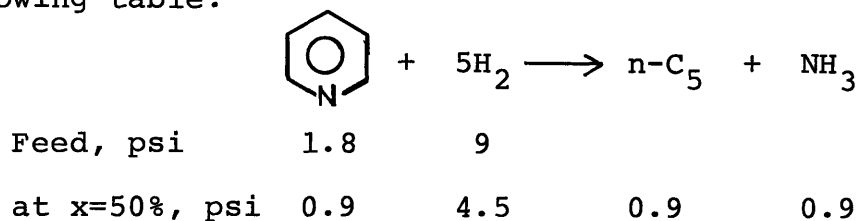
reactions. The fractions of equation (4-8) as a function of temperature thus become an equilibrium functionality presented in this thesis. From equation (4-8), let:

$$x = \left(\frac{p_{\text{Pip}}}{p_{\text{Pyr}}} \right) = (K_p) (p_{\text{H}_2})^3 \quad (4-9)$$

then

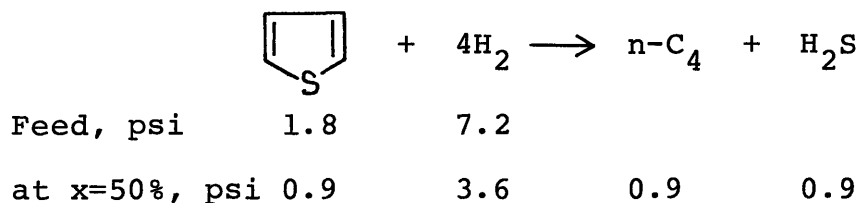
$$\frac{p_{\text{Pip}}}{p_{\text{Pyr}} + p_{\text{Pip}}} = \frac{x}{1+x} \quad (4-10)$$

The hydrogen partial pressure for use in equation (4-9) is taken as the average of that at the several different reaction conditions, and is calculated by subtracting all non-hydrogen partial pressures from the total pressure. All runs for this equilibrium analysis used a pyridine feed of approximately 1.8 psig partial pressure. The hydrogen partial pressure at 50 percent pyridine conversion was used, assuming complete conversion of reactant pyridine to pentane and ammonia, as calculated in the following table:



Total non-hydrogen partial pressure = 0.9 + 0.9 + 0.9 = 2.7 psi.

Half of the runs for the equilibrium comparison contained equimolar feeds of pyridine and thiophene. Thus, one-half of the non-hydrogen partial pressure is taken into account:



One-half of the non-hydrogen partial pressure = $0.5(0.9 + 0.9 + 0.9) = 1.35$ psi. The average hydrogen partial pressure used for the equilibrium calculations is then:

$$p_{\text{H}_2}, \text{ psi} = \text{total pressure, psig} + 14.7 - 2.7 \text{ psi} - 1.35 \text{ psi}$$

With K_p and p_{H_2} both known, the equilibrium fraction follows directly from equations (4-9) and (4-10)

Experimental data are reduced to the same form using the pyridine HDN product distribution figures, which give the number of moles of pyridine or piperidine out of the reactor as a fraction of the number of moles of pyridine fed. The ratio of equation (4-8) thus derives from:

$$\left(\frac{p_{\text{Pip}}}{p_{\text{Pyr}} + p_{\text{Pip}}} \right) = \frac{\left(\frac{\text{moles Pip out}}{\text{moles Pyr in}} \right)}{\left(\frac{\text{moles Pyr out}}{\text{moles Pyr in}} \right) + \left(\frac{\text{moles Pip out}}{\text{moles Pyr in}} \right)} \quad (4-11)$$

For direct comparison of data with equilibrium K_p values, a plot of $\log_{10}(K_p)$ (for both the empirically-determined and thermodynamically-calculated values of K_p) as a function of inverse absolute temperature includes experimental values of the quantity $(p_{\text{Pip}} p_{\text{Pyr}}^{-1} p_{\text{H}_2}^{-3})$. This plot derives from the integrated form of the van't Hoff equation (Denbigh, 1966)

If the reaction were at equilibrium, these points would fall on the K_p line. If, however, the pyridine-feed reaction did not reach equilibrium, the points would fall below the K_p line.

VIII.E. Sample Calculations

VIII.E.1 Sample Calculations - Reduction of Experimental Data

All data reduction calculations were carried out by computer, using an IBM 370/168 or an IBM 1130, and Fortran IV. The printed output for a run is a complete record of all run specifications, experimental data, and calculated values of all types. The output for one run is reproduced in this section and is divided as follows:

- Page 1 - overall run specifications, standards, and flow rates set for the entire run
- Page 2 - summary of all experimental data for each gas chromatograph sample, including both chromatograph and reactor system data
- Page 3 - calculated results covering the entire run: reactor feed rates and feed partial pressures
- Pages 4 and 5 - calculated results for each reaction temperature: reactant conversions, reactor performance parameters, relative molar products, and statistical data quality analysis
- Page 6 - summary of all run parameters for thesis appendix

The results for Run 50 are used to illustrate the method of data reduction employed for all runs. This run was chosen for presentation because its conditions combine aspects found in many other runs. At high pressure (500 psig), it used a mixed thiophene-pyridine feedstock, thus showing both rapid and slow reactant conversions, over the

entire range, and the relative molar analysis for nitrogen compounds. The sample calculations follow a single chromatographic sample and its associated system parameters (sample number 50.21, program sample reference number 19). The properties and conversions of an isothermal set of samples (set number 5, reactor temperature 341°C) are then calculated. Finally, overall run parameters are computed. The following table is a guide to the specifics:

For each GC sample

Standardized reactor flow rate
Normalized gas chromatographic peak area
Area-flow rate product

For each set of isothermal samples

Reactor conditions: flow rate, temperature, pressures
Conversions of reactants
Standard deviations and confidence limits
Relative molar quantities
Reactor performance parameters: residence time, space time, space velocity, LHSV

For overall run

Run average reactor conditions
Hydrogen feed values
Mole fractions, partial pressures, feed ratios

The examples are correlated with the computer output shown. All experimental data used here are from the output summary, and the quantities calculated correspond to those of the program, allowing one to follow completely all steps of the analysis. The rounding of values at each step of the sample calculations sometimes causes the sample results to differ from the computer results in the last

significant figure.

VIII.E.1.a. Calculations for Each GC Sample

VIII.E.1.a.1 Total Reactor Flow Rate at Standard T and P
(0°C, 1 atm)

$$SFLOW = (CFLOW) \left(\frac{PBAR - VPH2O}{760 \text{ torr}} \right) \left(\frac{273.16^\circ\text{C}}{CT + 273.16^\circ\text{C}} \right)$$

$$VPH2O = 3.717 + 0.4958(CT) + 0.000210(CT)^2 + 0.000497(CT)^3$$

where: SFLOW = total exit flow rate corrected to 0°C and 1 atm, std. cc/min

CFLOW = measured soap film column flowmeter flow rate, cc/min

PBAR = barometric pressure, torr

CT = temperature of gaseous stream in soap film column flowmeter, °C

VPH2O = vapor pressure of water at temperature of soap film column, torr

Using data of sample number 50.21 (Program sample reference number 19):

$$VPH2O = 3.717 + (0.4958)(23.6) + (0.000210)(23.6)^2 + (0.000497)(23.6)^3$$

$$= 21.8 \text{ torr}$$

$$SFLOW = (939.9) \left(\frac{747.8 - 21.8}{760} \right) \left(\frac{273.16}{23.6 + 273.16} \right)$$

$$= 826.4 \text{ std cc/min}$$

VIII.E.1.a.2 Normalized Chromatogram Peak Area (for all Components Analyzed in the run)

$$SAREA = (AREA) \left(\frac{GPSTD + 14.696 \text{ psig}}{GPRES + PBAR \left(\frac{14.696 \text{ psig}}{760 \text{ torr}} \right)} \right) \times \left(\frac{GTEMP + 273.16^\circ\text{C}}{GTSTD + 273.16^\circ\text{C}} \right) (GLOOP)$$

$$\text{GLOOP} = \begin{cases} 1.000 & \text{for GSV in position 1} \\ 0.98192 & \text{for GSV in position 2} \end{cases}$$

where: SAREA = area of chromatograph peak corrected to specified standard temperature and pressure, $\mu\text{v-sec}$

AREA = measured area of chromatograph peak, $\mu\text{v-sec}$

GPSTD = specified standard GSV pressure, psig

GTSTD = specified standard GSV temperature, $^{\circ}\text{C}$

GPRES = measured GSV pressure, psig

GTEMP = measured GSV temperature, $^{\circ}\text{C}$

GLOOP = GSV loop equilization factor, cc/cc (dimensionless)

Using the data of sample number 50.21 (program sample reference number 19) for the pyridine peak area:

$$\text{GLOOP} = 0.98192 \text{ (GSV position} = 2)$$

$$\text{SAREA} = 16443. \left(\frac{14.00 + 14.696}{14.03 + 747.8 \left(\frac{14.696}{760} \right)} \right) \times$$

$$\left(\frac{201.5 + 273.16}{200.0 + 273.16} \right) (0.98192)$$

$$= 16314. \mu\text{v-sec}$$

VIII.E.1.a.3 Standardized Area-Flow Rate Product

$$\text{SAFR} = (\text{SAREA}) (\text{SFLOW})$$

where: SAFR = standardized area-times-flow-rate parameter, $\mu\text{v-sec stnd cc/min}$

Using calculated results one gets for pyridine for sample 50.21:

$$\text{SAFR} = (16314) (826.4)$$

$$= 1.348 \times 10^7 \mu\text{v-sec stnd cc/min}$$

VIII.E.1.b Calculations for Each Set of Samples, at one Reaction Temperature

VIII.E.1.b.1 Average Conditions for Set

VIII.E.1.b.1.a Mean Values

The mean values of the standardized flow rate, reactor temperature, reactor pressure, and barometric pressure are calculated. For thiophene and pyridine, the area-flow rate products previously calculated are also averaged.

For those quantities required in subsequent sample calculations:

$$\text{AFLOW} = \frac{1}{n} \sum_{i=1}^n \text{SFLOW}_i$$
$$\text{ASAFR} = \frac{1}{n} \sum_{i=1}^n \text{SAFR}_i$$

where AFLOW = average total flow rate at standard conditions (0°C, 1 atm) for the reaction temperature, stnd cc/min

ASAFR = average standardized area-flow rate product, $\mu\text{v-sec-stnd cc/min}$

n = number of samples at this reaction temperature

for the 341°C data set (samples 50.20 through 50.23), for pyridine areas:

$$\begin{aligned} \text{AFLOW} &= \frac{1}{4}(832.1 + 826.4 + 824.0 + 829.5) \\ &= 828.0 \text{ stnd cc/min} \\ \text{ASAFR} &= \frac{1}{4}(1.425 + 1.348 + 1.508 + 1.375) \times 10^7 \\ &= 1.414 \times 10^7 \mu\text{v-sec-stnd cc/min} \end{aligned}$$

VIII.E.1.b.1.b. Absolute Reactor Pressure

$$\text{APRESA} = \left(\frac{1 \text{ atm}}{14.696 \text{ psi}} \right) (\text{APRESP} + \left(\frac{14.696 \text{ psi}}{760 \text{ torr}} \right) (\text{APBAR}))$$

where APRESA = average absolute reactor pressure for sample set, atm.

APRESP = average guage reactor pressure for sample set, psig

APBAR = average barometric pressure for sample set, torr

For the 341°C data set:

$$APRESA = \left(\frac{1}{14.696} \right) (499.75 + \left(\frac{14.696}{760} \right) (747.9)) = 34.99$$

VIII.E.1.b.2 CONVERSION OF REACTANTS FOR THIOPHENE AND/OR PYRIDINE

$$CONV = (1.0 - Z) (100 \text{ percent})$$

$$Z = \frac{ASAFRT}{ASAFRB}$$

where CONV = conversion of reactant, percent

Z = ratio for computational purposes

ASAFRT = average standardized area-flow rate product at reaction temperature, $\mu\text{v-sec-std cc/min}$

ASAFRB = average standardized area-flow rate product at base (no reaction) temperature. $\mu\text{v-sec-std cc/min}$

For pyridine conversion at 341°C, using ASAFRT from the above calculation and ASAFR analogously calculated at the base temperature;

$$Z = \frac{1.414 \times 10^7}{3.412 \times 10^7} = 0.4144$$

$$CONV = (1.0 - 0.4144) (100.) = 58.6 \text{ percent}$$

VIII.E.1.b.3 Confidence Limits for Conversion Values

VIII.E.1.b.3.a Variance, Standard Deviation, and Relative Standard Deviation

For thiophene, pyridine, and piperidine, when present:

$$\text{VARNC} = \frac{1}{n(n-1)} \left[n \sum_{i=1}^n (\text{SAFR}_i)^2 - \left(\sum_{i=1}^n \text{SAFR}_i \right)^2 \right]$$

$$\text{DEVN} = (\text{VARNC})^{1/2}$$

$$\text{REDVN} = \frac{(\text{DEVN})}{(\text{MEAN})} (100. \text{ percent})$$

where VARNC = variance of the n values of SAFR at this reactor temperature
($\mu\text{v-sec-std cc/min}$)²

DEVN = standard deviation of these values,
 $\mu\text{v-sec-std cc/min}$

RDEVN = relative standard deviation of these values, percent

MEAN = mean (ASAFR) of the n values of SAFR,
 $\mu\text{v-sec-std cc/min}$

i = individual sample of set at this temperature

n = number of samples in this set

For pyridine conversion at 341°C:

$$\text{VARNC} = \frac{1}{4(4-1)} \left[4 \left\{ (1.425 \times 10^7)^2 + (1.348 \times 10^7)^2 + (1.508 \times 10^7)^2 + (1.375 \times 10^7)^2 \right\} - (5.656 \times 10^7)^2 \right]$$

$$= 4.945 \times 10^{11} (\mu\text{v-sec-std cc/min})^2$$

$$\text{DEVN} = (4.945 \times 10^{11})^{1/2} = 7.032 \times 10^5 \mu\text{v-sec-std cc/min}$$

$$\text{RDEVN} = \frac{(7.032 \times 10^5)(100.)}{(1.414 \times 10^7)} = 4.97 \text{ percent}$$

VIII.E.1.b.3.b Confidence Limits

For reactants thiophene and pyridine, for 95 percent confidence limits (68 percent confidence limits are calculated analogously)

$$\text{LIMIT95U} = \text{CONV} + \text{EBAR95}$$

$$\text{LIMIT95L} = \text{CONV} - \text{EBAR95}$$

$$\text{EBAR95} = \frac{(\text{TVALUE})(\text{DEVNZ})}{N^{1/2}}$$

$$\text{TVALUE} = f(\text{NDEGFR}, \text{confidence level})$$

$$\text{NDEGFR} = N - 1$$

$$\text{DEVNZ} = \left(\frac{\text{RDEVNZ}}{100.} \right) (100. \times Z)$$

$$\text{RDEVNZ} = (\text{RDEVNB}^2 + \text{RDEVNT}^2)^{1/2}$$

where $\text{LIMIT95U}, \text{LIMIT95L}$ = upper and lower limits for
the 95 percent confidence
interval, percent conversion

EBAR95 = size of error bar for 95 percent confidence limit, percent conversion

TVALUE = statistical t-value (from tables)
based on the number of degrees of
freedom and the desired confidence
level, dimensionless

NDEGFR = number of degrees of freedom for t-
value determination

N = smaller of: number of base samples or number
of reaction temperature samples, dimensionless

DEVNZ = standard deviation of ratio Z , dimensionless

RDEVNZ, RDEVNB, RDEVNT = relative standard deviations of the ratio Z, base samples, and reaction temperature samples; percent

For Pyridine Conversion at 341°C:

$$RDEVNZ = (1.41^2 + 4.97^2)^{1/2} = 5.17 \text{ percent}$$

$$DEVNZ = (5.17)(0.4144) = 2.14$$

$$NDEGFR = 4 - 1 = 3 \quad (\text{N is smaller of 4 or 6})$$

$$TVALUE \text{ (from table for } NDEGFR = 3, \text{ confidence level} = 95 \text{ percent)} = 3.182$$

$$EBAR95 = \frac{(3.182)(2.14)}{(4)^{1/2}} = 3.4 \text{ percent}$$

$$LIMIT95U = 58.6 + 3.4 = 62.0 \text{ percent}$$

$$LIMIT95L = 58.6 - 3.4 = 55.2 \text{ percent}$$

VIII.E.1.b.4 Relative Molar Quantities

For all nitrogen components analyzed:

$$REL\text{PYR} = \frac{\text{ASAFR (Component at reaction temp.)}}{\text{ASAFR (Pyridine at base temp.)}} \times \text{GCREL (Component)}$$

where RELPYR = moles of component out at reaction temperature per mole of pyridine feed, mole component/mole pyridine

GCREL = calibrated GC response factor for component relative to pyridine, mole component per area component/ mole pyridine per area pyridine

For piperidine analysis at 341°C reaction temperature

$$REL\text{PYR} = \frac{(3.370 \times 10^6)(0.9952)}{(3.412 \times 10^7)} = 0.09829 \frac{\text{mole piperidine out}}{\text{mole pyridine in}}$$

VIII.E.1.b.5.b Space Time and Space Velocity

For each reactor temperature:

$$\text{TAU} = \frac{\text{VBED}}{\text{FFLOW}}$$

$$\text{SPVEL} = (\text{TAU})^{-1}$$

$$\text{FFLOW} = \left(\frac{\text{AFLOW}}{60 \text{ sec/min}} \right) \left(\frac{\text{FTSTD} + 273.16^\circ\text{C}}{273.16^\circ\text{C}} \right) \times \left(\frac{14.696 \text{ psi}}{\text{FPSTD} + 14.696 \text{ psi}} \right)$$

where TAU = space time based on specified standard reactor temperature and pressure and total reactor volume, seconds

FFLOW = total volumetric flow through the reactor at specified standard reactor feed conditions, stnd feed cc/sec

SPVEL = space velocity on same basis as space time, inverse seconds

FTSTD = standard feed temperature specifications, °C

FPSTD = standard feed pressure specification, psig

For the 341°C reactor temperature:

$$\text{FFLOW} = \left(\frac{828.0}{60} \right) \left(\frac{350 + 273.16}{273.16} \right) \left(\frac{14.696}{500 + 14.696} \right)$$

= 0.8989 stnd feed cc/sec

$$\text{TAU} = \frac{2.123}{0.8989} = 2.36 \text{ seconds}$$

$$\text{SPVEL} = (2.36)^{-1} = 0.424 \text{ inverse seconds}$$

VIII.E.1.b.5.c Liquid Hourly Space Velocity

$$\text{LHSV} = \frac{\left(\frac{\text{FEEDT} + \text{FEEDP}}{\text{DENSITY}} \right)}{\text{VBED}}$$

where LHSV = liquid hourly space velocity based on total reactor volume and thiophene plus pyridine liquid feed, inverse hours

FEEDT, FEEDP = feed rates of thiophene and pyridine, gm/hour

DENSITY = density of liquid feed, gm/cc

For the data of the 341°C point (and in this case the entire run):

$$\text{LHSV} = \frac{\left(\frac{0.6771 + 0.6354}{1.0200} \right)}{2.123} = 0.606 \text{ hr}^{-1}$$

VIII.E.1.c Calculations for Overall Run

VIII.1.c.1 Run Average Reactor Conditions

Average values for the entire run for total flow rate at standard conditions, total flow rate at standard feed conditions, total molar flow rate, space velocity, and reactor pressure (all systems of units) are calculated as the mean of the individual isothermal sample set means:

$$\text{AVGRUN} = \frac{1}{m} \sum_1^m \text{AVGSET}_j$$

$$\text{AVGSET}_j = \frac{1}{n} \sum_1^n \text{VALUE}_i$$

where AVGRUN = average value of property for overall run, over all sets j

AVGSET_j = average value of property for set j,
for all values i in set j

For example, the run average total flow rate at standard conditions (TFLOW) is calculated from the average set values (AFLOW, see previous calculation):

$$\text{TFLOW} = \frac{1}{8}(835.5 + 846.6 + \dots + 840.1) = 836.6 \text{ stdnd } \frac{\text{cc}}{\text{min}}$$

VIII.E.1.c.2 Hydrogen Feed Values

Hydrogen values in the feed are determined by difference; for example the run average molar flow rate is calculated:

$$\text{MOLFEEHD} = \text{MOLFEED} - (\text{MOLFEEDT} + \text{MOLFEEDP})$$

where MOLFEEDH = feed rate of hydrogen, moles/hr
 MOLFEED = total feed rate, moles/hr
 MOLFEEDT = thiophene feed rate, moles/hr
 MOLFEEDP = pyridine feed rate, moles/hr

For run 50:

$$\text{MOLFEEHD} = 2.2394 - (0.0080 + 0.0080) = 2.2234 \frac{\text{moles H}_2}{\text{hr}}$$

VIII.E.1.c.3 Mole Fractions, Partial Pressures, Feed Ratios

From the above-determined and otherwise-available values, the following are calculated in a straightforward manner: mole fractions, partial pressures, reactor feed ratios.

VIII.E.2 Sample Calculations for Pyridine-Piperidine Equilibrium

VIII.E.2.a Change in Free Energy for Reaction

$$\Delta G_{\text{rxn}}^{\circ} = \Delta G_{\text{f pip}}^{\circ} - \Delta G_{\text{f pyr}}^{\circ}$$

where $\Delta G_{\text{rxn}}^{\circ}$ = change in free energy for the reaction,
kcal/mole
 $\Delta G_{\text{f pip}}^{\circ}$ = free energy of formation of piperidine,
kcal/mole
 $\Delta G_{\text{f pyr}}^{\circ}$ = free energy of formation of pyridine,
kcal/mole

Using data for 600°K:

$$\Delta G_{\text{rxn}}^{\circ} = 66.85 - 58.77 = + 8.08 \text{ kcal/mole}$$

VIII.E.2.b Equilibrium Constant

$$\log_{10}(K_p) = \frac{-\Delta G_{\text{rxn}}^{\circ}}{2.303 R} \left(\frac{1}{T} \right)$$

where K_p = equilibrium constant, bars⁻³
 R = gas constant, 1.987×10^{-3} kcal/mole°K
 T = temperature, °K

For 600°K data:

$$\log_{10}(K_p) = \frac{-8.08}{(2.303)(1.987 \times 10^{-3})} \left(\frac{1}{600} \right) = -2.94$$

Carrying out the above $\Delta G_{\text{rxn}}^{\circ}$ and $\log_{10}(K_p)$ calculations between 400 and 1000°D yields the plot:

The equation of this line gives the temperature dependence of K_p :

$$\log_{10}(K_p) = 10.36 \left(\frac{1000}{T} \right) = 20.22$$

VIII.E.2.c Equilibrium Pyridine-Piperidine Ratio Values

The equilibrium pip/(pyr + pip) value will be determined for conditions of 500 psig total pressure and 350°C. The thermodynamically-derived equilibrium constant is calculated from the last operation, at 350°C:

$$\log_{10}(K_p) = (10.357) \left(\frac{1000}{350 + 273.16} \right) - 20.221 = -3.60 - 1$$
$$K_p = 2.506 \times 10^{-4}$$

The partial pressure of hydrogen at 500 psig total pressure:

$$PH_2 = (PTOT + 10.65 \text{ psi}) \left(\frac{\text{bar}}{14.504 \text{ psi}} \right)$$

where PH₂ = partial pressure of hydrogen, bars

PTOT = total reactor pressure, psig

$$PH_2 = (500 + 10.65)/14.504 = 35.21 \text{ bars}$$

Equilibrium pip/(pyr + pip) ratio:

$$\left(\frac{p_{\text{pip}}}{p_{\text{pyr}} + p_{\text{pip}}} \right) = \frac{x}{1+x}$$

$$x = \frac{p_{\text{pip}}}{p_{\text{pyr}}} = (K_p) (PH_2)^3$$

where p_{pip} = partial pressure of piperidine, bars

p_{pyr} = partial pressure of pyridine, bars

$$x = (2.506 \times 10^{-4}) (35.21)^3 = 10.94$$

$$\left(\frac{p_{\text{pip}}}{p_{\text{pyr}} + p_{\text{pip}}} \right) = \frac{10.94}{1. + 10.94} = 0.916$$

Using the empirically-determined equilibrium constant temperature dependence (Goudriaan, 1974):

$$\log_{10}(K_p) = 10.21 \left(\frac{1000}{T} \right) - 20.56 = -4.176$$

$$K_p = 6.67 \times 10^{-5}$$

Calculations analogous to those above yield:

$$\left(\frac{p_{\text{pip}}}{p_{\text{pyr}} + p_{\text{pip}}} \right) = 0.744$$

VIII.E.2.d Experimental Pyridine-Piperidine Ratio Values

$$\left(\frac{p_{\text{pip}}}{p_{\text{pyr}} + p_{\text{pip}}} \right) = \frac{\text{RELPIP}}{\text{RELPIR} + \text{RELPIP}}$$

where RELPIP = moles piperidine out of reactor per mole pyridine fed

RELPIR = moles pyridine out of reactor per mole pyridine fed

For pure pyridine feed at 500 psig total pressure and 350°C, using values of curves through data points:

$$\left(\frac{p_{\text{pip}}}{p_{\text{pyr}} + p_{\text{pip}}} \right) = \frac{0.300}{0.230 + 0.300} = 0.566$$

III.E.2.e Experimental Values of Equilibrium Constant Expression

$$\log_{10} \left(\frac{p_{\text{pip}}}{p_{\text{pyr}} \times p_{\text{H}_2}^3} \right) = \log_{10} \left(\frac{\text{RELPIP}}{(\text{RELPYR}) (\text{PH}_2)^3} \right)$$

For pure pyridine feed at 500 psig total pressure and 303.8°C, using values directly from data points:

$$\log_{10} \left(\frac{p_{\text{pip}}}{p_{\text{pyr}} \times p_{\text{H}_2}^3} \right) = \log_{10} \left(\frac{0.3545}{(0.4692) (35.21)^3} \right) = -4.762$$

HDS-HDN EXPERIMENTAL DATA ANALYSIS - RUN 50

PROGRAM HDSDN - JOHN A. WILKENS

RUN SPECIFICATIONS

TOTAL PRESSURE (PSIG) 500.
 PARTIAL PRESSURES (TORR)
 THIOPHENE 93.
 PYRIDINE 93.
 CATALYST NMO/AL2O3, HDS-3A
 RUN DATE 2-13-77

DATA FORM
 INDEPENDENT VARIABLE = TEMPERATURE
 CONSTANT SPACE VELOCITY

EXPERIMENTAL PARAMETERS FOR OVERALL RUN

REACTOR FEED - LIQUID COMPONENTS

COMPONENT	MOL %	FEED RATE (G/HR)
THIOPHENE	84.14	0.6771
PYRIDINE	79.10	0.6354

LIQUID FEED DENSITY (G/CC) 1.0200

CATALYST	TOTAL BED VOLUME (CC)	2.123	SULFIDING TYPE
CATALYST WEIGHT (G)	1.4829		0 - NONE
SULFIDING TYPE	2		1 - FORMAL
			2 - RUN
			3 - SHUTDOWN

GAS SAMPLE VALVE
 STANDARD TEMPERATURE (DEG C) 200.0
 STANDARD PRESSURE (PSIG) 14.00
 LOOP EFFICIENCY FACTOR 0.98192

GAS CHROMATOGRAPH ANALYSES

TOTAL NUMBER OF SAMPLES	31	4	4	4	4	2
NUMBER OF SAMPLE SPTS	4					
NUMBER OF SAMPLES PER SPT	6	4	3	4	4	4

EXTENDED NITROGEN ANALYSIS - YES
 PIE/PYR MOLAR RESPONSE FACTOR 0.9952
 NPA/PYR MOLAR RESPONSE FACTOR 0.6363

EXPERIMENTAL DATA FOR INDIVIDUAL SAMPLES FOR RUN 50

PJM REF NO.	SAMPLE NUMBER	REACTR		GS VLV		GS VLV		COLUMN		COLUMN		BAROM		THIOPHENE		PYRIDINE		PIPERIDINE		NPENTAMINE	
		TEMP DEG.C	PSIG	TEMP DEG.C	PSIG	FLOW CC/MIN	TEMP DEG.C	FLOW CC/MIN	TEMP DEG.C	TORR	INTG AREA UV-SEC										
1	50.01	118.0	500.	200.0	13.89	2	939.9	23.7	747.7	43496.	40559.	0.	0.								
2	50.02	118.0	500.	200.0	13.80	1	934.3	24.0	747.6	44096.	41563.	0.	0.								
3	50.05	118.0	498.	200.5	14.09	2	959.1	23.3	747.5	42660.	40762.	0.	0.								
4	50.06	118.0	498.	200.5	14.09	1	954.9	23.1	747.5	43740.	40070.	0.	0.								
5	50.07	118.0	498.	200.5	14.05	2	954.9	23.0	747.5	43919.	41256.	0.	0.								
6	50.08	118.5	498.	200.5	14.06	1	954.1	23.3	747.5	44263.	40779.	0.	0.								
7	50.09	227.5	500.	201.0	14.14	1	955.1	24.3	747.4	42259.	39239.	1851.	0.								
8	50.10	227.5	500.	201.0	14.11	2	966.0	23.7	747.4	43077.	39389.	1656.	0.								
9	50.11	227.0	500.	201.0	14.10	1	963.4	23.2	747.4	41089.	38126.	1687.	0.								
10	50.12	227.0	500.	201.0	14.09	2	950.0	23.4	747.4	42138.	39331.	1840.	0.								
11	50.13	268.5	500.	201.0	14.10	2	952.6	24.0	747.4	34561.	32414.	2559.	0.								
12	50.14	267.5	499.	201.0	14.00	1	953.2	23.2	747.4	34269.	32892.	2239.	0.								
13	50.15	267.0	501.	201.5	14.08	2	959.1	24.8	747.4	34777.	33384.	2208.	0.								
14	50.16	299.5	500.	202.0	14.20	2	966.0	23.8	747.4	24194.	27827.	5949.	0.								
15	50.17	298.5	500.	202.0	14.20	1	965.1	23.7	747.4	24167.	27244.	6303.	0.								
16	50.18	299.0	500.	201.5	14.20	2	964.2	22.5	747.5	23211.	27929.	7686.	0.								
17	50.19	299.0	499.	201.5	14.20	1	961.7	23.8	747.6	22856.	27230.	8350.	0.								
18	50.20	342.0	500.	202.0	14.10	1	947.4	23.8	747.8	3636.	16971.	3556.	0.								
19	50.21	341.0	500.	201.5	14.03	2	939.9	23.6	747.8	3630.	16443.	3942.	0.								
20	50.22	341.0	500.	201.5	13.98	1	934.2	23.0	747.9	3548.	18083.	4692.	0.								
21	50.23	341.0	499.	202.0	14.18	2	949.0	24.8	748.1	3370.	16778.	4089.	0.								
22	50.25	359.0	499.	202.0	14.21	1	949.0	24.6	748.9	486.	7985.	945.	0.								
23	50.26	358.5	499.	202.0	14.17	2	944.1	23.0	749.2	558.	8952.	1007.	0.								
24	50.27	359.0	499.	202.0	14.18	1	944.1	24.6	749.3	396.	7773.	1523.	0.								
25	50.28	359.0	499.	202.0	14.17	2	943.2	23.7	749.5	437.	8202.	1529.	0.								
26	50.30	368.5	500.	202.0	14.00	1	927.8	24.8	750.3	0.	4246.	390.	0.								
27	50.31	369.0	500.	202.0	14.20	2	944.9	25.5	750.3	0.	4252.	410.	0.								
28	50.32	369.5	500.	201.5	14.21	1	944.9	25.2	750.4	0.	4545.	460.	0.								
29	50.33	368.5	499.	201.5	14.20	2	944.9	25.1	750.5	0.	4248.	467.	0.								
30	50.34	366.5	500.	202.0	14.03	2	952.4	23.4	750.7	0.	470.	0.	0.								
31	50.35	380.5	500.	201.5	14.00	1	948.2	23.3	751.0	0.	520.	0.	0.								

OVERALL RUN PARAMETERS--CALCULATED VALUES OF EXPERIMENTAL RESULTS FOR RUN 50

REACTOR FEED

COMPONENT	MOLF FRACTION	FEED RATE GR. MOLES/HR	FEED RATE GRAMS/HR	FEED RATE STD. CC/MIN	FEED RATE STD. FEED. CC/MIN
HYDROGEN	0.952819	2.223272	4.4821	830.6	54.10
THIOPHENE	0.003594	0.008047	0.6771	3.0	0.20
PYRIDINE	0.003587	0.008033	0.6354	3.0	0.20
TOTAL	1.000	2.239352	5.7946	836.6	54.49

SYSTEM PRESSURES (REACTOR FEED CONDITIONS)

	PSIA	PSI	MM HG	ATM	BARS
TOTAL REACTOR PRESSURE	499.6	--NA--	--NA--	34.98	35.44
PARTIAL PRESSURE OF HYDROGEN	--NA--	510.40	--NA--	34.73	35.19
PARTIAL PRESSURE OF THIOPHENE	--NA--	1.847	95.54	0.1257	0.1274
PARTIAL PRESSURE OF PYRIDINE	--NA--	1.844	95.37	0.1255	0.1271

RATIOS (REACTOR FEED)

(MOLES H2)/(MOLE LIQUID REACTANTS)	138.3
(SCCM H2)/(CC LIQUID/HR)	645.5

NOTES

HYDROGEN VALUES BY DIFFERENCE
 STANDARD CONDITIONS = 0. DEG C AND 1.0 ATMOSPHERE
 STANDARD FEED CONDITIONS = 350. DEG C AND 500. PSIG
 STANDARD FEED CONDITIONS USED FOR STANDARD FEED RATE, SPACE VELOCITY, AND SPACE TIME

CALCULATED VALUES OF EXPERIMENTAL RESULTS FOR INDIVIDUAL DATA POINTS FOR RUN 50

POINT NUMBER	1 (BASE)	2	3	4	5	6	7
REACTOR TEMPERATURE (DEG C)	118.1	227.3	267.7	298.8	341.3	358.9	368.6
REACTOR TEMPERATURE (DEG K)	391.2	500.4	540.8	571.9	614.4	632.0	641.8
THIOPHENE CONVERSION (PERCENT)	0.0	2.6	20.8	45.4	92.0	98.9	100.0
PYRIDINE CONVERSION (PERCENT)	0.0	3.4	19.2	31.8	58.6	80.0	89.6
REACTOR PRESSURE (PSIG)	498.7	500.0	500.0	499.8	499.8	499.0	499.8
REACTOR PRESSURE (ATMOSPHERES)	34.92	35.01	35.01	34.99	34.99	34.94	34.99
REACTOR PRESSURE (BARS)	35.38	35.47	35.47	35.45	35.45	35.40	35.46
TOTAL FLOW RATE (SCCM)	835.5	846.6	840.4	848.1	828.0	831.0	823.2
REACTOR PERFORMANCE PARAMETERS							
SPACE TIME (SECONDS)	2.34	2.31	2.33	2.31	2.36	2.35	2.38
RESIDENCE TIME (SECONDS)	3.717	2.875	2.680	2.510	2.393	2.315	2.305
SPACE VELOCITY (INVERSE SEC)	0.427	0.433	0.430	0.434	0.423	0.425	0.421
LHSV (INVERSE HOURS)	0.606	0.606	0.606	0.606	0.606	0.606	0.606
NUMBER OF SAMPLES	6	4	3	4	4	4	4
THIOPHENE POINT PARAMETERS							
REL STD SMPL DEVI (PCT OF W/FAN)	2.1	1.4	0.4	2.9	4.2	14.7	0.0
63 PCT CONF INVL, UPPER LMT (PCT)	0.0	4.0	22.1	46.6	92.2	99.0	100.0
68 PCT CONF INVL, LOWER LMT (PCT)	0.0	1.1	19.5	44.2	91.7	98.8	100.0
95 PCT CONF INVL, UPPER LMT (PCT)	0.0	0.5	25.0	48.5	92.6	99.2	100.0
95 PCT CONF INVL, LOWER LMT (PCT)	0.0	-1.3	16.6	42.3	91.4	98.7	100.0
PYRIDINE POINT PARAMETERS							
REL STD SMPL DEVI (PCT OF W/FAN)	1.4	1.0	1.6	0.7	5.0	5.3	4.2
68 PCT CONF INVL, UPPER LMT (PCT)	0.0	4.4	20.5	32.4	59.8	80.7	89.9
65 PCT CONF INVL, LOWER LMT (PCT)	0.0	2.4	17.9	31.1	57.3	79.3	89.3
95 PCT CONF INVL, UPPER LMT (PCT)	0.0	6.0	23.5	33.5	62.0	81.9	90.3
95 PCT CONF INVL, LOWER LMT (PCT)	0.0	0.8	15.0	30.1	55.1	78.2	88.9
PIPELINE POINT PARAMETERS							
REL STD SMPL DEVI (PCT OF W/FAN)	0.0	5.7	8.2	16.2	11.6	25.3	8.9
NITROGEN ANALYSIS - RELATIVE PRODUCTS							
MOLES PYR OUT PER MOLE PYR IN	1.0000	0.8660	0.8077	0.6823	0.4145	0.1946	0.1039
MOLES PIP OUT PER MOLE PYR IN	0.0000	0.1333	0.0571	0.1743	0.0983	0.0302	0.0103
MOLES NPA OUT PER MOLE PYR IN	0.0000	0.0000	0.0000	0.0000	0.0000	0.0000	0.0000

TABLE CONTINUED ON FOLLOWING PAGE

CALCULATED VALUES OF EXPERIMENTAL RESULTS FOR INDIVIDUAL DATA POINTS FOR RUN 50

POINT NUMBER:	8
REACTOR TEMPERATURE (DEG C)	386.5
(DEG K)	659.7
THIOPHENE CONVERSION (PERCENT)	100.0
PYRIDINE CONVERSION (PERCENT)	98.8
REACTOR PRESSURE (PSIG)	500.0
(ATMOSPHERS)	35.01
(BAPS)	35.47
TOTAL FLOW RATE (SCCM)	840.1
REACTOR PERFORMANCE PARAMETERS	
SPACE TIME (SECONDS)	2.33
RESIDENCE TIME (SECONDS)	2.198
SPACE VELOCITY (INVERSE SEC)	0.430
WHSV (INVERSE HOURS)	0.606
NUMBER OF SAMPLES	2
THIOPHENE POINT PARAMETERS	
REL STD SMPLE DEVI (PCI OF MEAN)	0.0
68 PCT CONF INTVL, UPPER LMI (PCT)	100.0
68 PCT CONF INTVL, LOWER LMI (PCT)	100.0
95 PCT CONF INTVL, UPPER LMI (PCT)	100.0
95 PCT CONF INTVL, LOWER LMI (PCT)	100.0
PYRIDINE POINT PARAMETERS	
REL STD SMPLE DEVI (PCI OF MEAN)	0.2
68 PCT CONF INTVL, UPPER LMI (PCT)	98.9
68 PCT CONF INTVL, LOWER LMI (PCT)	98.6
95 PCT CONF INTVL, UPPER LMI (PCT)	99.7
95 PCT CONF INTVL, LOWER LMI (PCT)	97.9
PIPERAZINE POINT PARAMETERS	
REL STD SMPLE DEVI (PCI OF MEAN)	0.0
NITROGEN ANALYSIS - RELATIVE PRODUCTS	
MOLES PYR OUT PER MOLE PYR IN	0.0122
MOLES PIP OUT PER MOLE PYR IN	0.0000
MOLES NPA OUT PER MOLE PYR IN	0.0000

DATA SUMMARY - RUN 50

PURPOSE -

OVERALL RUN PARAMETERS
 TOTAL PRESSURE = 499.6 PSIG = 34.98 ATM = 35.44 BARS
 LHSV = 0.600 INVERSE HOURS(1)
 SPACE VELOCITY, AVS = 0.428 INVERSE SECONDS(2)
 MOLES HYDROGEN PER MOLE LIQUID REACTANT(1) = 138.3

REACTION FEED

	GRAMS/HR	G MOL/HR	MOLE FRACTION		PARTIAL PRESSURES	
			BAR	TORR	BAR	PSI
TRIPHENYL	0.6771	0.00805	0.203594	0.1274	95.5	1.85
PYRIDINE	0.6354	0.00803	0.203597	0.1271	95.4	1.84
HYDROGEN (3)	4.4621	2.2233	0.99282	35.19	-NA-	510.4
TOTAL	5.7486	2.2394	1.00000	35.44	-NA-	514.1

ANALYSIS - JMO/AL2O3, HDS-3A

TOTAL BED VOLUME = 2.123 CC
 CATALYST WEIGHT = 1.4929 GRAMS
 SULFIDING TYPE = 2
 SULFIDING TYPE
 0 - NONE
 1 - FORMAL
 2 - RUN
 3 - SHUTDOWN

EXPERIMENTAL RESULTS FOR INDIVIDUAL DATA POINTS

REACTOR	TRIPENYL	CONVRSN	PERCENT	PERCENT	PERCENT	PIP IN	PIP OUT	NPA	OUT/	SPACE	RESIDNC
TIME	TEMP	TEMP	TEMP	TEMP	TEMP	TEMP	TEMP	TEMP	TEMP	TEMP	TEMP
SEC(1)	SEC(2)	SEC(3)	SEC(4)	SEC(5)	SEC(6)	SEC(7)	SEC(8)	SEC(9)	SEC(10)	SEC(11)	SEC(12)
227.3	50.4	2.6	3.4	0.0433	0.0000	2.31	2.88	0.0000	2.31	2.88	2.88
297.7	54.9	20.8	19.2	0.0571	0.0000	2.33	2.68	0.0000	2.33	2.68	2.68
293.3	571.9	45.4	31.3	0.1743	0.0000	2.31	2.51	0.0000	2.31	2.51	2.51
341.3	514.4	52.5	58.6	0.0983	0.0000	2.36	2.39	0.0000	2.36	2.39	2.39
358.9	632.1	98.9	40.0	0.0302	0.0000	2.35	2.31	0.0000	2.35	2.31	2.31
368.6	641.3	160.0	85.6	0.0103	0.0000	2.38	2.30	0.0000	2.38	2.30	2.30
336.5	659.7	100.0	98.6	0.0000	0.0000	2.33	2.20	0.0000	2.33	2.20	2.20

NOTES

- (1) BASED ON TRIPHENYL PLUS PYRIDINE LIQUID FEED
- (2) BASED ON TOTAL BED VOLUME AT 350. DEG C AND 500. PSIG
- (3) BY DIFFERENCE
- (4) BASED ON TOTAL BED VOLUME AT REACTOR CONDITIONS
- (5) PYP = PYRIDINE, PIP = PIPERIDINE, NPA = N-PHENYLAMINE
- (6) DATA FROM -- CONST SPACE VELOCITY, INDEP VARIABLE = TEMP
- (7) 1 :AV = 10**5 PASCAL = 10**5 N/M**2

VIII.F Assessment of Possible Heat and Mass Transfer Limitations

The packed bed catalytic reactor of this study was designed to maximize the dissipation of heat from the highly exothermic hydrogenolysis reactions. The catalyst pellets were ground to a size which would eliminate mass transfer limitations. After the initial set of runs showed the reactant conversion characteristics with temperature and pressure which could be expected, specifications for final runs were drawn up to avoid heat transfer limitations. Specifically, the ability at high reactor pressures to completely convert all reactants imposed a severe limitation on the amount of reactant material which could be fed. It was determined that it was not possible to feed thiophene and pyridine reactants at combined partial pressures greater than 186 torr without much excess heat generation. All further experiments were then subject to this thiophene-plus-pyridine feed limit.

The calculations of this section indicate that for the maximum feed rates used and the complete conversions possible at the higher reaction pressures, the reactor was free of both heat and mass transfer limitations. However, these were indeed the maximum amounts of reactants which could have been properly converted, as interparticle heat transfer would have become significant at any greater molar

conversion rates. Similarly, these rates appeared to be the greatest which could have been used without the onset of mass transfer limitations.

The following analyses of the heat and mass transfer characteristics of the system are based on the results of runs at 1000 psig using equal thiophene and pyridine feed partial pressures of 93 torr (corresponding to feed rates of 0.008 gm moles per hour of each reactant, the maximum permitted under the above limitations). The thiophene and pyridine conversion characteristics indicated that by 370°C both reactants had been completely converted.

The heat transfer analyses use three temperatures: those of the reactor wall, the bulk fluid inside the reactor, and the surface of the catalyst. Although there must be a finite temperature gradient across the bed, these temperatures (in degrees Kelvin) are always used independently in the calculations; differentiating precisely among them is thus not necessary. One temperature will then be used: as measured by the reactor thermocouple, the bulk gas temperature at the entrance to the packed bed.

In the following calculations, the specific criteria for heat or mass transfer are presented first. Where a subsidiary calculation is needed, it will follow the criteria evaluations.

For the heat transfer analyses, the correlations of Mears (1971a,b) were used. These determine (using reactor parameters generally measurable) whether a given conversion of a reactant in a packed bed catalytic reactor will generate enough heat to cause the reaction rate to vary by more than five percent from an isothermal rate. Three different potential gradients were examined: intraparticle, within individual catalyst particles; interphase, between the external surface of the particles and the bulk fluid adjacent to the surface; and interparticle (or intrareactor), across the catalyst bed as a whole.

For heat transfer, the interparticle criterion would usually be the first to become limiting. However, in systems with great excesses of hydrogen, the intraparticle criterion might also be significant (Doraiswamy and Tajbl, 1974). All three heat transfer criteria were evaluated and are presented here.

For mass transfer, diffusion within the catalyst particle becomes limiting before either the interphase or interparticle criteria are violated (Mears, 1971b). Thus, the effectiveness factor for the reaction in the catalyst particle was calculated, using the methods of Satterfield (1970).

For these analyses, it was necessary to determine a value of the activation energies of the pyridine and thio-

phene reactions. Estimates of the activation energies of both the desulfurization and denitrogenation reactions are varied, in large part due to the great variety of catalysts and catalyst activation procedures used by different workers.

For pyridine hydrodenitrogenation, Goudriaan (1974) determined three distinct activation energies using a $\text{CoMo}/\text{Al}_2\text{O}_3$ catalyst: 12.4 kcal/gmole on a sulfided catalyst, in the absence of hydrogen sulfide in the reactant stream; 14.3 kcal/gmole on a sulfided catalyst, with large amounts (4 bars) of hydrogen sulfide in the reactant stream; and 15.8 kcal/gmole over the unsulfided oxidic catalyst, in the absence of hydrogen sulfide. Stengler et al. (1964), using a catalyst containing molybdenum, nickel, and tungsten supported on alumina, found activation energies of 16 kcal/gmole on the unsulfided catalyst, and 23 kcal/gmole on the sulfided catalyst. The higher activation energy on the sulfided catalyst raises questions, as sulfiding has generally been shown to enhance catalyst activity. A higher activation energy of 28 kcal/gmole was reported by Aboul-Gheit and Abdou (1973) over an unsulfided $\text{CoMo}/\text{Al}_2\text{O}_3$ catalyst. In the present study, although a firm value for the activation energy was not determined, it was shown that an average value for the data over the complete range of conversions was approximately 20 kcal/gmole.

For the hydrodesulfurization of thiophene, Owens and Amberg (1961) determined an activation energy of 25 kcal/gmole. Their mathematical treatment, however, was based on the assumption of a zero order reaction, which has been shown in nearly every kinetic study, including their own, to be wholly inadequate for describing the kinetics of the reaction, due to the strong reactant and product adsorption characteristics. In the present study, an average of 20 kcal/gmole was found to hold for a wide range of other kinetic parameter values.

For the purposes of these heat and mass transfer analyses, an average value of 20 kcal/gmole has been chosen as generally representative of the two reactions.

VIII.F.1. Heat Transfer

VIII.F.1.a Interparticle Heat Transfer Criterion

For the absence of interparticle heat transfer limitations, when heat transfer resistance at the wall is significant, the following inequality should hold (Mears, 1971a,b):

$$\frac{qR_o^2}{k_e T_w} < \frac{0.4 R_{id} T_w/E_a}{1 + \left[\frac{8r_p}{R_o (\text{Biot})_w} \right]}$$

where q = absolute value of heat of reaction =
 $|\Delta H_{rxn}|$
= (66,000 cal/gmole thiophene + 84,000 cal/gmole pyridine) (0.5) = 75,000 cal/gmole

$$\begin{aligned} R' &= \text{reaction rate per unit bed volume} \\ &= 0.016 \text{ gmole/hr}/2.123 \text{ cc} = 0.007554 \\ &\quad \text{gmole/hr cc catalyst bed} \end{aligned}$$

$$R_o = \text{reactor radius} = 0.2286 \text{ cm}$$

$$\begin{aligned} k_e &= \text{effective thermal conductivity across} \\ &\quad \text{reactor bed} \\ &= \epsilon k_g + (1 - \epsilon) \lambda = (0.55)(2.65) + \\ &\quad (1 - \epsilon)(2.99) = 2.8 \text{ cal/hr cm}^\circ\text{C} \end{aligned}$$

$$\begin{aligned} \lambda &= \text{thermal conductivity of catalyst particles} \\ &= 2.99 \text{ cal/hr cm}^\circ\text{C} \text{ (Satterfield, 1970)} \end{aligned}$$

$$T_w = \text{reactor wall temperature, } 643^\circ\text{K}$$

$$R_{id} = \text{ideal gas constant} = 1.987 \text{ cal/gmole}^\circ\text{K}$$

$$E_a = \text{activation energy for reaction} = 20,000 \text{ cal/gmole} \text{ (from preceding discussion)}$$

$$r_p = \text{radius of catalyst particle} = 0.0387 \text{ cm}$$

$$\begin{aligned} (\text{Biot})_w &= \text{thermal Biot number at the reactor} \\ &\quad \text{wall} \\ &= h_w d_p / k_e = (51.3)(0.0774)/(2.80) \\ &= 1.42 \end{aligned}$$

$$h_w = \text{wall heat transfer coefficient} = 51.3 \text{ cal/cm}^2\text{hr}^\circ\text{C} \text{ (from separate calculation)}$$

For these values, the above equation gives:

$$\text{L.S.} = \frac{(75,000)(0.007554)(0.2286)^2}{(2.80)(643)} = 0.0164$$

$$\text{R.S.} = \frac{(0.4)(1.987)(643)}{(20,000) \left[1 + \frac{(8)(0.0387)}{(0.2286)(1.42)} \right]} = 0.0131$$

The two terms of the interparticle criterion are of the same magnitude, with the left side greater than the right by 25 percent. This could indicate the onset of a

heat transfer limitation as conversions approach 100 percent for cases of the highest feed rates. However, the inequality is sensitive to several parameters which could, with reasonable variations in values, easily change the sense of the inequality. For example, a higher wall heat transfer coefficient would increase the right-hand term, improving the relative sense of the inequality.

The wall heat transfer coefficient was calculated from an expression which was chosen because of its applicability at Reynolds numbers as low as ten (Beek, 1962). Other correlations which were cited in reviews without Reynolds number restrictions give higher wall heat transfer coefficients, but upon examination of the original sources were found to be derived from data at higher N_{Re} 's. An example of this is the correlation by Calderbank and Pogorski (1957), which gives an h_w several times larger than the one from Beek. Reviews (Perry, 1963; Walas, 1959) give no restrictions on the applicable range of Reynolds numbers, but the original publication shows the correlation to have been well-supported by data as low as $N_{Re} = 100$, and considered a reasonable extrapolation down to at least $N_{Re} = 60$. The applicability at N_{Re} is open to question. The significance of this other calculated value is that it indicates that the h_w used was probably conservative. Thus, within the limits of the accuracy of certain estimated

parameters such as the wall heat transfer coefficient and the activation energy, the criterion essentially yields an equality. This was expected, as the feed rates for the experiments were set at the maximum values which could be used without bringing on heat transfer limitations.

VIII.F.1.b Interphase Heat Transfer Criterion

For the absence of interphase heat transfer limitations, the following inequality should hold (Mears, 1971a,b):

$$\frac{q R r_p}{h T_b} < \frac{0.15 R_{id} T_b}{E_a}$$

where, in addition to previously-defined quantities:

$$\begin{aligned} R &= \text{reaction rate per unit particle volume} = \\ &R' (1 - \epsilon)^{-1} \\ &= 0.01679 \text{ gmole/hr cc catalyst particle} \end{aligned}$$

$$\epsilon = \text{bed void fraction} = 0.55 \text{ (experimentally measured)}$$

$$\begin{aligned} h &= \text{heat transfer coefficient between gas and particle} \\ &= 82.4 \text{ cal/hr cm}^2\text{°C (from separate calculation)} \end{aligned}$$

$$T_b = \text{temperature of the bulk fluid} = 643^\circ\text{K}$$

For these values, the criterion gives:

$$\text{L.S.} = \frac{(75,000)(0.01679)(0.0387)}{(82.4)(643)} = 0.00092$$

$$\text{R.S.} = \frac{(0.15)(1.987)(643)}{(20,000)} = 0.00958$$

Here the left side is an order of magnitude smaller than the right, indicating that interphase heat transfer is not limiting.

VIII.F.1.c Intraparticle Heat Transfer Criterion

For the absence of intraparticle heat transfer limitations, the following inequality must hold (Mears, 1971a,b)

$$\frac{q R (r_p)^2}{\lambda T_s} < \frac{0.75 R_{id} T_s}{E_a}$$

where, in addition to previously-defined quantities:

$$T_s = \text{temperature at outside surface of catalyst pellet} = 643^\circ\text{K}$$

For these values, the above equations yield:

$$\text{L.S.} = \frac{(75,000)(0.01679)(0.0387)^2}{(2.99)(643)} = 0.00098$$

$$\text{R.S.} = \frac{(0.75)(1.987)(643)}{(20,000)} = 0.0479$$

Examination of this criterion inequality indicates that the lack of intraparticle heat transfer limitations is assured by a factor of 50. As this criterion can become limiting for reactions using a great excess of hydrogen, it is interesting to note that the intraparticle heat transfer would have become limiting (other factors constant) if the catalyst particles had had a diameter larger than 0.2 inch. (This is intended to give an idea of the problems of scaling up to a larger reactor. For the specific laboratory equipment used in these studies, it is a moot point, as this size pellet is larger than the inside diameter of the reactor.)

VIII.F.1.d Subsidiary Calculations

VIII.F.1.d.1 Fluid Parameters

VIII.F.1.d.1.a Viscosity

The effect of pressure on the viscosity of the reactant thiophene-pyridine-hydrogen mixture was determined by calculating a pseudocritical temperature and pressure for the mixture. These were used in the correlation of Ross and Brown (Perry, 1963), from which it was determined that the viscosity of the mixture at 1000 psig differed by less than one percent from that at one atmosphere. Thus, no pressure correction was necessary for the viscosities used.

The viscosity of pure hydrogen at $350^{\circ}\text{C} = 0.522$ g/cm-hr (Perry et al., 1963). To estimate the magnitude of the effect on viscosity of adding thiophene and pyridine to hydrogen, the correlation of Willse (1950) was used to calculate the effect of adding benzene (in a molar amount equal to the pyridine and thiophene concentrations which would be present) to hydrogen. The viscosity of the benzene-hydrogen mixture was only two percent greater than that of pure hydrogen. From this it was inferred that the effect of thiophene and pyridine on the viscosity would also be negligible, and the viscosity of pure hydrogen was

used for further calculations.

VIII.F.1.d.1.b Prandtl Number

The Prandtl number for pure hydrogen was used. Using values for hydrogen for the heat capacity ($C_p = 3.44 \text{ cal/g}^\circ\text{K}$), viscosity ($\mu = 0.522 \text{ g/cm-hr}$), and thermal conductivity ($k = 2.65 \text{ cal/cm-hr}^\circ\text{C}$), the Prandtl number at 360°C :

$$N_{Pr} = \frac{C_p \mu}{k} = \frac{(3.44)(0.522)}{(2.65)} = 0.678$$

VIII.F.1.d.2 Reynolds Number for Reaction Stream

For flow through a packed bed:

$$N_{Re} = \frac{d_p G}{\mu}$$

where N_{Re} = Reynolds number based on particle diameter

d_p = diameter of particles in packed bed =
0.0774 cm

μ = viscosity of fluid = 0.522 g/cm-hr

G = mass flow rate of fluid per unit total
cross-sectional area

$$\begin{aligned} &= (8.98 \text{ g H}_2/\text{hr} + 0.68 \text{ g Thi/hr} + 0.64 \text{ g Pyr/} \\ &\quad \text{hr}) / 0.164 \text{ cm}^2 \\ &= 62.8 \text{ g/hr-cm}^2 \end{aligned}$$

Giving:

$$N_{Re} = \frac{(0.0774)(62.8)}{(0.522)} = 9.31$$

VIII.F.1.d.3 Heat Transfer Coefficient Between Gas and Particle

The dimensionless heat and mass transfer quantities j_H and j_D (detailed definitions and discussions of these parameters are found in: Satterfield, 1970) are approximately equal for many catalyst pellet geometries, permitting the heat transfer coefficient between the gas phase and the particle to be calculated. From an empirical correlation for gases with $3 < N_{Re} < 2000$:

$$\begin{aligned} j_D &= \frac{(0.357)}{\epsilon N_{Re}^{0.359}} \\ &= \frac{(0.357)}{(0.55)(9)^{0.359}} = 0.295 \end{aligned}$$

From the approximation $j_H \approx j_D$:

$$j_H = \frac{h N_{Pr}^{2/3}}{C_p G} \approx j_D = 0.295$$

where C_p = heat capacity of gas phase = 3.44 cal/g°C for H_2 (McCabe and Smith, 1967)

Therefore:

$$\begin{aligned} h &= \frac{(0.295) C_p G}{N_{Pr}^{2/3}} = \frac{(0.295)(3.44)(62.8)}{(0.68)^{2/3}} \\ &= 82.4 \end{aligned}$$

VIII.F.1.d.4 Wall Heat Transfer Coefficient

Beek (1962) proposed the use of a relation for determining the wall heat transfer coefficient based upon an analogy to a mass transfer expression developed by Thoenes and Kramers (1958). It is valid for Reynolds numbers as low as the order of ten:

$$h_w = \frac{k_g}{d_p} \left[(0.203) N_{Re}^{1/3} N_{Pr}^{1/3} + (0.220) N_{Re}^{0.8} N_{Pr}^{0.4} \right]$$

All of these quantities have been previously defined, giving:

$$\begin{aligned} h_w &= \frac{(2.65)}{(0.0774)} \left[(0.203) (9.31)^{1/3} (0.68)^{1/3} + \right. \\ &\quad \left. (0.220) (9.31)^{0.8} (0.68)^{0.4} \right] \\ &= 51.3 \text{ cal/cm}^2\text{hr}^\circ\text{C} \end{aligned}$$

VIII.F.2 Mass Transfer

VIII.F.2.a Effectiveness Factor for Catalyst Pellets

The methods of Satterfield (1970) were used to determine the effectiveness factor for the simultaneous thiophene-pyridine reaction considered for the heat transfer criteria. For a spherical pellet geometry, a modulus ϕ is defined as:

$$\phi_s = \frac{R^2}{D_{eff}} \left[- \frac{1}{v_c} \frac{dn}{dt} \right] \frac{1}{C_s}$$

where $R = \text{catalyst pellet radius} = 0.0387 \text{ cm}$

$$D_{\text{eff}} = \text{total effective diffusivity} = 0.001335 \frac{\text{cm}^2}{\text{sec}}$$

(from separate calculation)

$$V_c = \text{volume of catalyst particles} = (\text{bed volume}) \times (1 - \text{void fraction})$$

$$= (2.123)(1 - 0.55) = 0.9554 \text{ cm}^3$$

$$-dn/dt = \text{rate of reaction} = 4.44 \times 10^{-6} \text{ gmole/sec}$$

$$C_s = \text{average reactant concentration (i.e. at 50 percent conversion)}$$

$$= \frac{N}{V} = \frac{P}{RT} = \frac{(0.5)(93 + 93)(1/760)}{(82.06)(643)}$$

$$= 2.319 \times 10^{-6} \text{ gmole/cm}^3$$

Thus:

$$\phi_s = \frac{(0.0387)^2 (4.44 \times 10^{-6})}{(0.00144)(0.9554)(2.319 \times 10^{-6})}$$

$$= 2.08$$

Further evaluation of the effectiveness factor requires the use of graphical correlations presented by Satterfield. Use of generalized correlations for Langmuir-Hinshelwood mechanisms requires detailed adsorption data, which are not available. Charts (Satterfield, 1970, Figures 3.4 and 3.5) for first-order reactions indicate an effectiveness factor of 0.90. (Calculated beta and gamma factors for these charts were 0. and 16, respectively. The effectiveness factor of 0.90 was the same for the beta = 0. line for graphs with gamma = 10 and 20.) The reaction was shown in this study to exhibit behavior between zero

and first order. As a zero order reaction would, for the same modulus, have a greater effectiveness factor, the actual case would give an effectiveness factor greater than 0.90. This implies that the reactor is operating at approximately the 0.95 effectiveness factor level, which is the lower limit for operation free of any significant mass transfer effects. Thus the reactor appears to be operating at the maximum reaction rate permitted by mass transfer considerations.

VIII.F.2.b. Subsidiary Calculations

VIII.F.2.b.1 Binary Diffusion Coefficient

The binary diffusion coefficients for thiophene in hydrogen and for pyridine in hydrogen were calculated using the correlations from Satterfield (1970)

The calculation was based on equation 1.16, p. 12, of the reference:

$$D_{12} = \frac{0.001858 T^{3/2} \left(\frac{m_1 + m_2}{m_1 m_2} \right)^{0.5}}{P \sigma_{12}^2 \Omega_D}$$

Details of the procedure are covered in the reference; only results are presented here. Intermediate calculated values were: $V_{B,Thi} = 88.1$, $V_{B,Pyr} = 89.5$, $\sigma_{Thi} = 5.251$, $\sigma_{Pyr} = 5.278$, $\Omega_{D,Thi-H_2} = 0.8868$, and $\Omega_{D,Pyr-H_2} = 0.8937$.

For thiophene in hydrogen:

$$D_{12} = \frac{(0.001858)(643)^{1.5} \left(\frac{2+84}{2 \times 84} \right)^{0.5}}{(69)(4.039)^2(0.8868)}$$

$$= 0.0217$$

Similarly, for pyridine in hydrogen: $D_{12} = 0.0214$
 An average value of 0.0216 was used for subsequent calculations. The effective bulk diffusivity accounts for the void fraction within the catalyst particle and the tortuosity of the pore structure. For a tortuosity of 4 (Satterfield, 1973); and an assumed particle void fraction, $\epsilon = 0.5$,

$$D_{12\text{eff}} = D_{12}\epsilon/\tau = (0.0214)(0.5)/4 = 0.00268$$

VIII.F.2.b.2 Knudsen Diffusion Coefficient

From Satterfield (1970), the Knudsen diffusion coefficient is determined from:

$$D_K = 9700 r_{\text{pore}} \left(\frac{T}{M} \right)^{0.5}$$

where r_{pore} = mean pore radius = 90 Å = 9.0×10^{-7} cm
 (approximate mean pore radius for used catalyst as presented in Figure 4-2 of this thesis)

T = absolute temperature = 643°K

M = molecular weight = 84 (thiophene),
 79 (pyridine)

Giving:

$$D_{K,\text{Thi}} = (9700)(9.0 \times 10^{-7})(643/84)^{0.5} = 0.02415$$

$$D_{K, Pyr} = 0.02491$$

An average value of 0.02453 was used in subsequent calculations. The effective Knudsen diffusivity is calculated similarly to the effective bulk diffusivity:

$$D_{Keff} = D_K \epsilon / \tau = (0.02453)(0.5) / 4 = 0.00307$$

VIII.F.2.b.3 Total Effective Diffusivity

The total effective diffusivity is determined by:

$$\begin{aligned} \frac{1}{D_{eff}} &= \frac{1}{D_{Keff}} + \frac{1}{D_{12eff}} = \frac{1}{0.00307} + \frac{1}{0.00288} \\ &= 0.00143 \end{aligned}$$

VIII.G. Langmuir-Hinshelwood Kinetic Models

Many references detail the background of and techniques for developing Langmuir-Hinshelwood kinetic models for most proposed reaction mechanisms, for example, those by Thomas and Thomas (1967), Thomson and Webb (1959), Walas (1959), Corrigan (1955a,b), and Satterfield (1977a). The basic assumptions underlying the expressions will be covered here.

Langmuir-Hinshelwood kinetic models are based on the Langmuir adsorption isotherm, which requires three principle assumptions (Thomas and Thomas, 1967):

1. "The adsorbed entities are attached on the surface of the adsorbent at definite, localized sites."
2. "Each site can accommodate one and only one adsorbed entity."
3. "The energy of the adsorbed entity is the same at all sites on the surface, and is independent of the presence or absence of other adsorbed entities at neighboring sites."

Further, the model pictures a "dynamic equilibrium between adsorbate molecules in the gas phase and the adsorbed entities in the surface layer". This led to a rate of adsorption proportional to both the adsorbate pressure in the gas phase and the fraction of uncovered adsorption sites. The rate of desorption was proportional to the number of

covered sites (i.e. those sites occupied by an adsorbate molecule).

For the Langmuir-Hinshelwood kinetic model, further assumptions were made (Satterfield, 1977a):

1. "Adsorption equilibrium is assumed to be established at all times, i.e., the rate of reaction is much less than the rate of adsorption or desorption, so that the concentrations of adsorbed species are determined by adsorption equilibria."

2. "Reaction occurs between adsorbed species on the catalyst...If a reaction takes place between adsorbed A and adsorbed B, these must be adsorbed on neighboring sites in order for reaction to occur, and the probability of reaction is taken to be proportional to the product [of the fractional surface coverages of A and B]."

As the above assumptions state, the rate-controlling step for a Langmuir-Hinshelwood model is the surface reaction between adsorbed species. This was considered to be the best assumption for the thiophene and pyridine models developed. Other assumptions for the rate-controlling step, namely the adsorption of reactants or the desorption or reaction products, can be used, and these are considered under the class of Hougen-Watson kinetic models, as presented by Yang and Hougen (1950) and the other references previously given.

The Langmuir-Hinshelwood type of kinetic model, such as developed in this work for thiophene HDS and pyridine HDN, is comprised of three main parts. First, there is the kinetic term, the surface reaction rate constant together with the adsorption constant. This is included as a product with the concentration driving force term, the second part. For thiophene HDS, this driving force term was simply the partial pressure of the thiophene. For pyridine HDN, however, the driving force was the difference between the pyridine partial pressure and its equilibrium value, as determined by the equilibrium expression. The third part of the model is the adsorption term, comprising the denominator, and accounts for the competitive adsorption of each species present in the gas phase. The power to which the denominator is raised represents the number of active sites involved in the controlling step.

Within these general limits are many variations covering a large number of specific cases. These are covered in detail in the references given.

Figure 8-7 : Performance of Langmuir-Hinshelwood Kinetic Models in Correlating Thiophene HDS Reaction Data

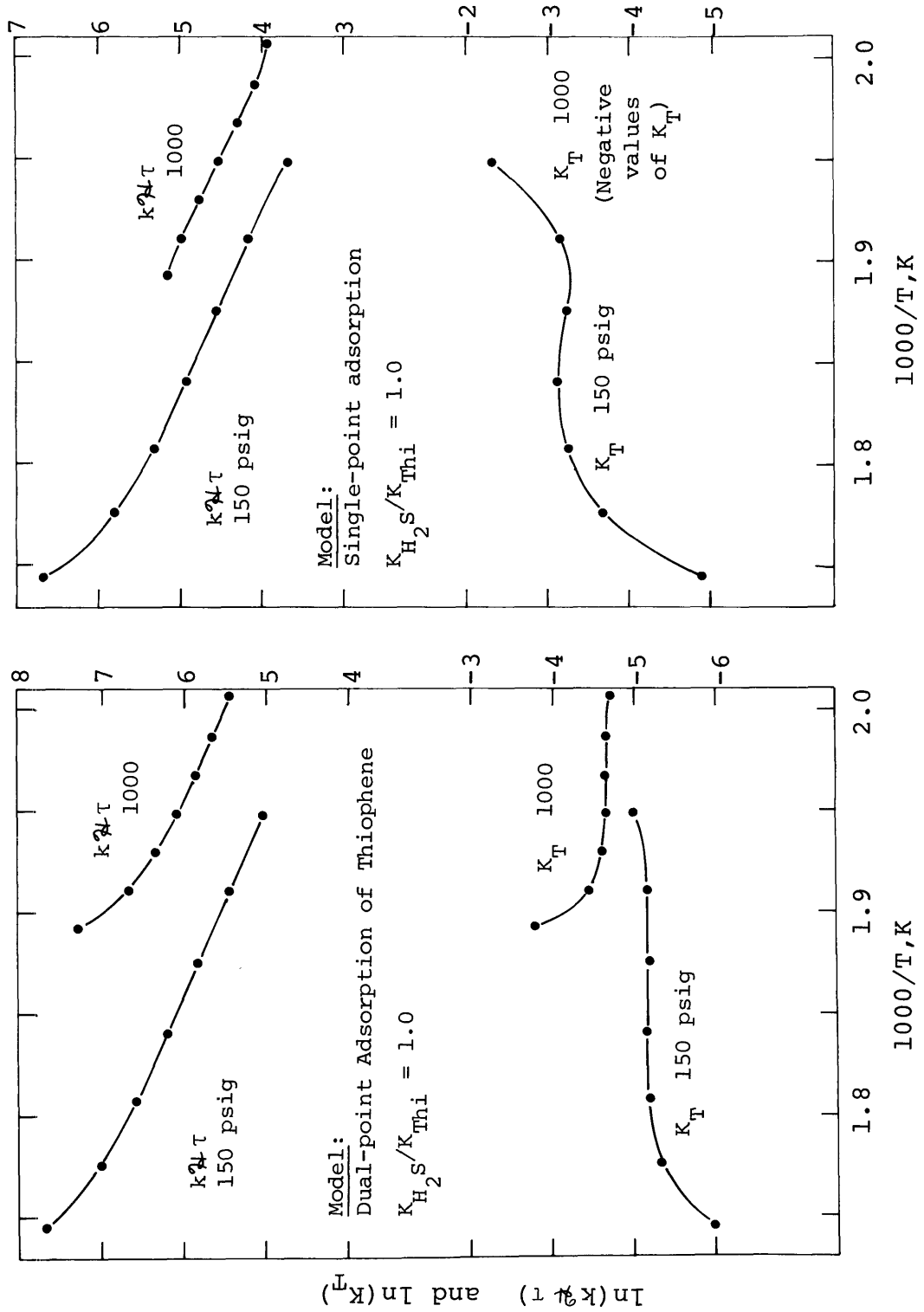
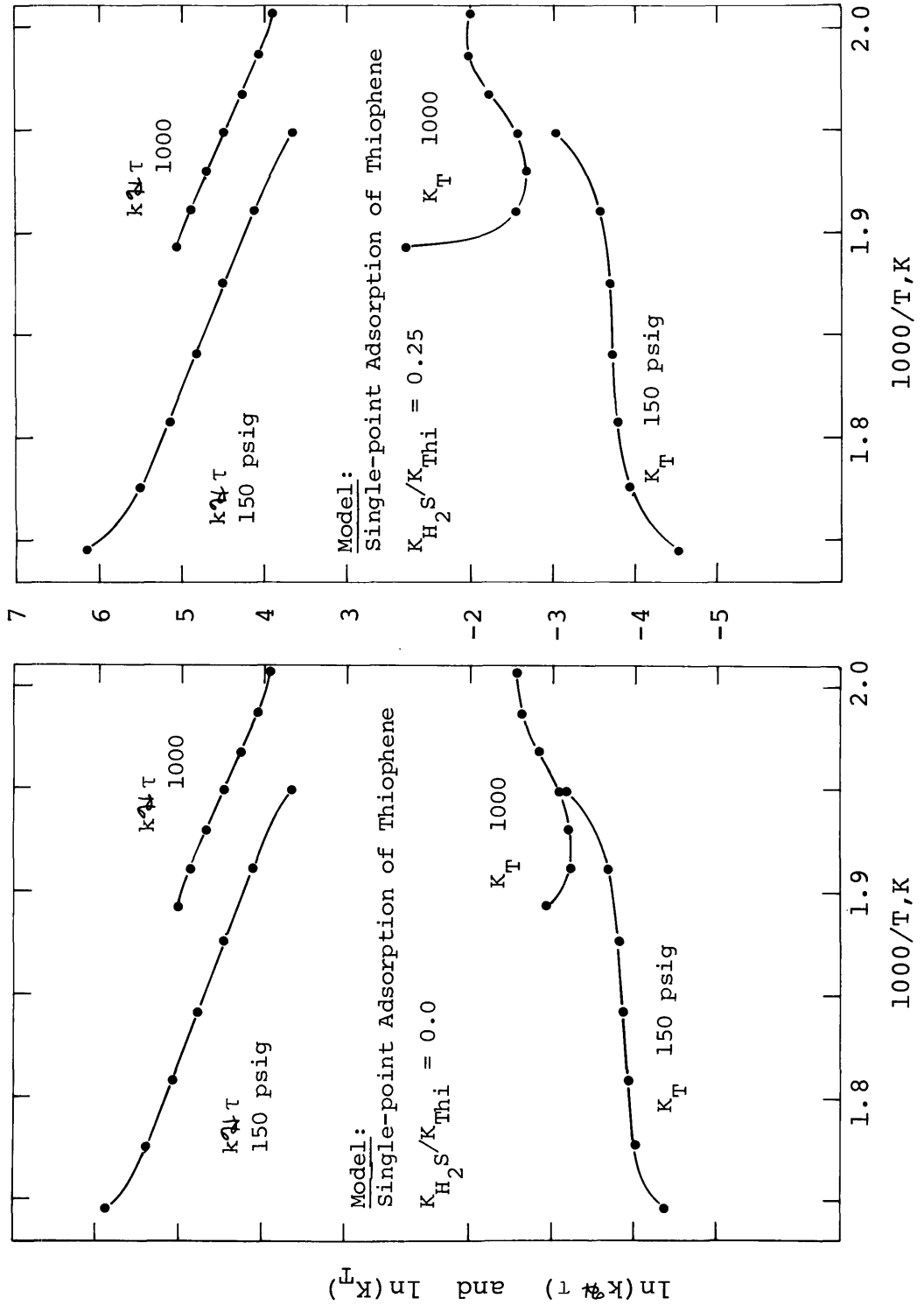


Figure 8-8 : Performance of Langmuir-Hinshelwood Kinetic Models in Correlating Thiophene HDS Reaction Data



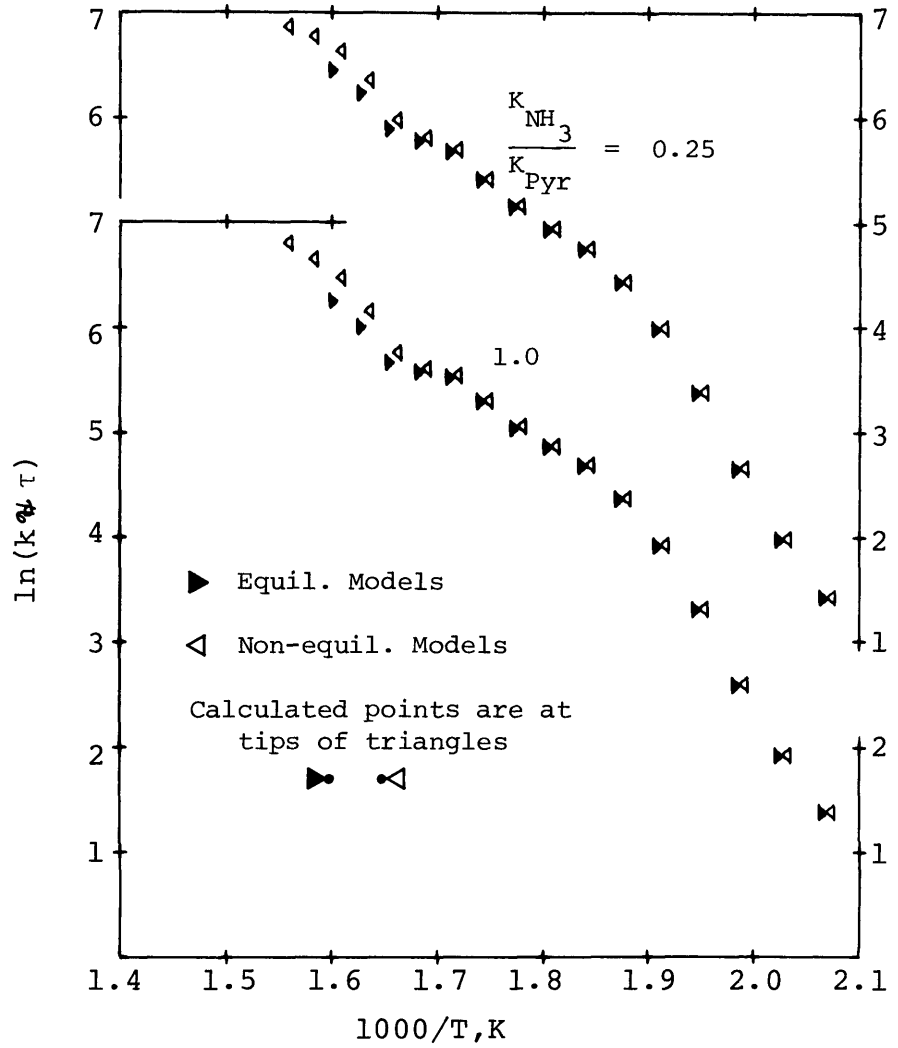


Figure 8-9 : The Relative Performance of Four Langmuir-Hinshelwood Models for Correlating Pyridine Hydrogenation Data at a Total Pressure of 1000 psig for $K_{Pip}/K_{Pyr} = 2.0$

VIII.H. Pyridine-Piperidine Equilibrium Results

Both experimental and calculated values of the equilibrium curves of Figures 5-3, 5-4, and 5-5 are tabulated in the tables of Appendix H.

TABLE 8-10 - VALUES OF PIP-PYR RATIO AT TOTAL PRESS= 1000.PSIG

TEMPERATURE		CALCULATED EQUILIBRIUM		EXPERIMENTAL, PURE PYR FEED	EXPERIMENTAL, PYR + THI FEED
DEG C	DEG K	PIP		PIP	PIP
		PYR + PIP	PYR + PIP	PYR + PIP	PYR + PIP
		(1)	(2)		
190.	463.	1.0000	1.0000	0.0021	0.0000
200.	473.	1.0000	1.0000	0.0283	0.0138
210.	483.	1.0000	1.0000	0.0588	0.0324
220.	493.	1.0000	1.0000	0.0945	0.0527
230.	503.	1.0000	1.0000	0.1366	0.0774
240.	513.	1.0000	1.0000	0.1865	0.1075
250.	523.	1.0000	1.0000	0.2455	0.1410
260.	533.	0.9999	1.0000	0.3177	0.1834
270.	543.	0.9998	1.0000	0.4086	0.2405
280.	553.	0.9996	0.9999	0.5168	0.3252
290.	563.	0.9992	0.9998	0.6366	0.4288
300.	573.	0.9984	0.9996	0.7541	0.5457
310.	583.	0.9967	0.9991	0.8547	0.6407
320.	593.	0.9935	0.9983	0.9123	0.7323
330.	603.	0.9875	0.9967	0.9419	0.8009
340.	613.	0.9766	0.9937	0.9458	0.8302
350.	623.	0.9576	0.9883	0.9415	0.8031
360.	633.	0.9256	0.9789	0.9406	0.7083
370.	643.	0.8747	0.9627	0.9326	0.0000
380.	653.	0.7996	0.9360	0.9265	0.0000
390.	663.	0.6987	0.8940	0.0000	0.0000
400.	673.	0.5780	0.8317	0.0000	0.0000
410.	683.	0.4510	0.7464	0.0000	0.0000
420.	693.	0.3333	0.6401	9.0000	9.0000
430.	703.	0.2359	0.5216	9.0000	9.0000
440.	713.	0.1619	0.4039	9.0000	9.0000
450.	723.	0.1091	0.2991	9.0000	9.0000
460.	733.	0.0729	0.2140	9.0000	9.0000
470.	743.	0.0486	0.1494	9.0000	9.0000
480.	753.	0.0325	0.1029	9.0000	9.0000
490.	763.	0.0218	0.0704	9.0000	9.0000
500.	773.	0.0147	0.0482	9.0000	9.0000
510.	783.	0.0100	0.0330	9.0000	9.0000
520.	793.	0.0069	0.0227	9.0000	9.0000
530.	803.	0.0048	0.0157	9.0000	9.0000
540.	813.	0.0033	0.0110	9.0000	9.0000
550.	823.	0.0024	0.0077	9.0000	9.0000
560.	833.	0.0017	0.0055	9.0000	9.0000
570.	843.	0.0012	0.0039	9.0000	9.0000
580.	853.	0.0009	0.0028	9.0000	9.0000
590.	863.	0.0006	0.0020	9.0000	9.0000
600.	873.	0.0005	0.0015	9.0000	9.0000

(1) EQUILIBRIUM CONSTANT EXPERIMENTALLY DETERMINED (GOUDRIAAN)

(2) EQUILIBRIUM CONSTANT CALCULATED FROM THERMODYNAMIC DATA

9.000 = NO EXPERIMENTAL DATA AT THIS REACTION CONDITION

TABLE 8-11 - VALUES OF PIP-PYR RATIO AT TOTAL PRESS= 500.PSIG

TEMPERATURE		CALCULATED EQUILIBRIUM		EXPERIMENTAL, PURE PYR FEED	EXPERIMENTAL, PYR + THI FEED
DEG C	DEG K	PIP		PIP	PIP
		PYR + PIP	PYR + PIP	PYR + PIP	PYR + PIP
		(1)	(2)		
190.	463.	1.0000	1.0000	9.0000	9.0000
200.	473.	1.0000	1.0000	0.0344	9.0000
210.	483.	1.0000	1.0000	0.0426	9.0000
220.	493.	1.0000	1.0000	0.0573	9.0000
230.	503.	1.0000	1.0000	0.0779	0.0420
240.	513.	0.9999	1.0000	0.1026	0.0457
250.	523.	0.9997	0.9999	0.1325	0.0507
260.	533.	0.9994	0.9999	0.1692	0.0582
270.	543.	0.9987	0.9997	0.2143	0.0760
280.	553.	0.9971	0.9993	0.2693	0.1151
290.	563.	0.9939	0.9985	0.3361	0.1569
300.	573.	0.9874	0.9968	0.4094	0.2042
310.	583.	0.9748	0.9934	0.4823	0.2437
320.	593.	0.9515	0.9870	0.5328	0.2568
330.	603.	0.9105	0.9749	0.5668	0.2322
340.	613.	0.8434	0.9533	0.5789	0.1912
350.	623.	0.7444	0.9163	0.5660	0.1526
360.	633.	0.6161	0.8567	0.5217	0.1145
370.	643.	0.4739	0.7690	0.4204	0.0833
380.	653.	0.3398	0.6536	0.2273	0.0000
390.	663.	0.2303	0.5210	0.1257	0.0000
400.	673.	0.1502	0.3894	0.0970	0.0000
410.	683.	0.0958	0.2752	0.0855	0.0000
420.	693.	0.0606	0.1866	9.0000	9.0000
430.	703.	0.0383	0.1233	9.0000	9.0000
440.	713.	0.0243	0.0804	9.0000	9.0000
450.	723.	0.0155	0.0522	9.0000	9.0000
460.	733.	0.0100	0.0339	9.0000	9.0000
470.	743.	0.0065	0.0222	9.0000	9.0000
480.	753.	0.0043	0.0146	9.0000	9.0000
490.	763.	0.0029	0.0097	9.0000	9.0000
500.	773.	0.0019	0.0065	9.0000	9.0000
510.	783.	0.0013	0.0044	9.0000	9.0000
520.	793.	0.0009	0.0030	9.0000	9.0000
530.	803.	0.0006	0.0021	9.0000	9.0000
540.	813.	0.0004	0.0014	9.0000	9.0000
550.	823.	0.0003	0.0010	9.0000	9.0000
560.	833.	0.0002	0.0007	9.0000	9.0000
570.	843.	0.0002	0.0005	9.0000	9.0000
580.	853.	0.0001	0.0004	9.0000	9.0000
590.	863.	0.0001	0.0003	9.0000	9.0000
600.	873.	0.0001	0.0002	9.0000	9.0000

(1) EQUILIBRIUM CONSTANT EXPERIMENTALLY DETERMINED (GOUDRIAAN)

(2) EQUILIBRIUM CONSTANT CALCULATED FROM THERMODYNAMIC DATA

9.000 = NO EXPERIMENTAL DATA AT THIS REACTION CONDITION

TABLE 8-12 - VALUES OF PIP-PYR RATIO AT TOTAL PRESS= 150.PSIG

TEMPERATURE		CALCULATED EQUILIBRIUM		EXPERIMENTAL, PURE PYR FEED	EXPERIMENTAL, PYR + THI FEED
DEG C	DEG K	PIP		PIP	PIP
		PYR + PIP	PYR + PIP	PYR + PIP	PYR + PIP
		(1)	(2)		
190.	463.	1.0000	1.0000	9.0000	0.0000
200.	473.	0.9999	1.0000	0.0054	0.0000
210.	483.	0.9998	1.0000	0.0077	0.0000
220.	493.	0.9995	0.9999	0.0110	0.0000
230.	503.	0.9986	0.9997	0.0167	0.0031
240.	513.	0.9966	0.9992	0.0235	0.0092
250.	523.	0.9919	0.9981	0.0315	0.0134
260.	533.	0.9814	0.9954	0.0439	0.0166
270.	543.	0.9591	0.9896	0.0617	0.0178
280.	553.	0.9148	0.9774	0.0803	0.0190
290.	563.	0.8346	0.9526	0.0968	0.0203
300.	573.	0.7090	0.9056	0.1085	0.0207
310.	583.	0.5466	0.8246	0.1115	0.0210
320.	593.	0.3793	0.7024	0.1066	0.0159
330.	603.	0.2405	0.5479	0.0944	0.0105
340.	613.	0.1436	0.3887	0.0812	0.0048
350.	623.	0.0831	0.2541	0.0646	0.0000
360.	633.	0.0476	0.1569	0.0491	0.0000
370.	643.	0.0273	0.0939	0.0365	0.0000
380.	653.	0.0158	0.0555	0.0246	0.0000
390.	663.	0.0092	0.0328	0.0137	0.0000
400.	673.	0.0055	0.0195	0.0054	0.0000
410.	683.	0.0033	0.0117	0.0000	0.0000
420.	693.	0.0020	0.0071	9.0000	9.0000
430.	703.	0.0012	0.0044	9.0000	9.0000
440.	713.	0.0008	0.0027	9.0000	9.0000
450.	723.	0.0005	0.0017	9.0000	9.0000
460.	733.	0.0003	0.0011	9.0000	9.0000
470.	743.	0.0002	0.0007	9.0000	9.0000
480.	753.	0.0001	0.0005	9.0000	9.0000
490.	763.	0.0001	0.0003	9.0000	9.0000
500.	773.	0.0001	0.0002	9.0000	9.0000
510.	783.	0.0000	0.0001	9.0000	9.0000
520.	793.	0.0000	0.0001	9.0000	9.0000
530.	803.	0.0000	0.0001	9.0000	9.0000
540.	813.	0.0000	0.0000	9.0000	9.0000
550.	823.	0.0000	0.0000	9.0000	9.0000
560.	833.	0.0000	0.0000	9.0000	9.0000
570.	843.	0.0000	0.0000	9.0000	9.0000
580.	853.	0.0000	0.0000	9.0000	9.0000
590.	863.	0.0000	0.0000	9.0000	9.0000
600.	873.	0.0000	0.0000	9.0000	9.0000

(1) EQUILIBRIUM CONSTANT EXPERIMENTALLY DETERMINED (GOUDRIAAN)

(2) EQUILIBRIUM CONSTANT CALCULATED FROM THERMODYNAMIC DATA

9.0000 = NO EXPERIMENTAL DATA AT THIS REACTION CONDITION

VIII.I. Location of Original Data

The original data are in the possession of the author at E. I. du Pont de Nemours and Company, Inc., Wilmington, Delaware.

BIBLIOGRAPHY

- Aboul-Gheit, A. K., and I. K. Abdou, "The Hydrodenitrogenation of Petroleum-Model-Nitrogen Compounds", Journal of the Institute of Petroleum, 59(568), 188 (1973)
- American Chemical Society, Division of Fuel Chemistry, Symposium of Sulfur and Nitrogen in Coal and Oil Shale, Preprint 20(2), (1975)
- American Cyanamid Company, "Aero HDS Hydrogen Treating Catalysts", Bound Brook, New Jersey (1969)
- Anderson, L. B., "Tests and Estimates on the Statistical Mean", Chem. Eng., 70, 159, Feb. 18 (1963)
- Balandin, A. A., "The Multiplet Theory of Catalysis, Vol. II", Isdatlistava, Moscow Univ. (1964)
- Beek, J., "Design of Packed Bed Catalytic Reactors", Adv. Chem. Eng., 3, 203 (1962)
- Ben-Yaacov, R., and J. T. Richardson, "The Role of Cobalt in Co-Mo Hydrodesulfurization Catalysts", Paper No. 7e, presented at Am. Inst. Chem. Engrs. Nat. Meeting, Los Angeles (1975)
- Beugeling, T., M. Boduszynski, F. Goudriaan, and J. Sonnemans, "Gas-Liquid Chromatographic Analysis of Products Formed by the Hydrogenolysis of Pyridine", Anal. Letters, 4, 727 (1971)
- Calderbank, P. H., and L. A. Pogorski, "Heat-Transfer in Packed Beds", Trans. Instn. Chem. Engrs., 35, 195 (1957)
- Cir, J., and R. Kubicka, "Hydrodesulphurization of Primary and Selectively Repurified Crude Oil Distillation Residues. II. Direct Hydrodesulphurization - Catalysts Used - Concluding Remarks", Erdoel Kohle (Hamburg), 25(4), 181 (1972), English Abstract from U. S. EPA, APTIC Abstract No. 40383
- Cocchetto, J. F., "Thermodynamic Equilibria of Heterocyclic Nitrogen Compounds with their Hydrogenated Derivatives", M.S. Thesis, M.I.T., Cambridge, Mass. (1973)
- Corrigan, T. E., "Chemical Engineering Fundamentals: Catalytic Vapor Phase Reactions - I", Chem. Eng., 62, 199, Jan. (1955)

- Corrigan, T. E., "Chemical Engineering Fundamentals: Catalytic Vapor Phase Reactions - II", Chem. Eng., 62, 195, Feb. (1955)
- Crow, E. L., F. A. Davis, and M. W. Maxfield, "Statistics Manual", Dover Publications, Inc., N.Y., p. 47 (1960)
- de Beer, V. H. J., T. H. M. van Sint Fiet, J. F. Engelen, A. C. van Haandel, M. W. J. Woless, C. H. Amberg, and G. C. A. Schuit, "The $\text{CoO-MoO}_3\text{-Al}_2\text{O}_3$ Catalyst: IV. Pulse and Continuous Flow Experiments and Catalyst Promotion by Cobalt, Nickel, Zinc, and Manganese", J. Catal., 27, 357 (1972)
- de Beer, V. H. J., T. H. M. van Sint Fiet, G. H. A. M. van der Steen, A. C. Zwaga, and G. C. A. Schuit, "The $\text{CoO-MoO}_3\text{-}\gamma\text{-Al}_2\text{O}_3$ Catalyst: V. Sulfide Catalysts Promoted by Cobalt, Nickel, and Zinc", J. Catal., 35, 297 (1974)
- Deichmann, W. B., H. W. Gerarde, Toxicology of Drugs and Chemicals, Academic Press, New York (1969)
- Denbigh, K., The Principles of Chemical Equilibrium, Second Edition, Cambridge, England (1966)
- Department of Chemistry, M.I.T., "Laboratory Techniques Manual", Vol. 1, p.3-1 (1974)
- Desikan, P., and C. H. Amberg, "Catalytic Hydrodesulfurization of Thiophene: IV. The Methylthiophenes", Can. J. Chem., 41, 1966 (1963)
- Desikan, P., and C. H. Amberg, "Catalytic Hydrodesulfurization of Thiophene: V. The Hydrothiophenes. Selective Poisoning and Acidity of the Catalyst Surface", Can. J. Chem., 42, 843 (1964)
- Doraiswamy, L. K., and D. G. Tadjbl, "Laboratory Catalytic Reactors", Cat. Rev. - Sci. Eng., 10(2), 177 (1974)
- El-Sabban, M. Z., and D. W. Scott, "The Chemical Thermodynamic Properties of Hydrocarbons and Related Substances. II Properties of 25 Organic Sulfur Compounds in the Ideal Gas State from 0°K to 1000°K ", U. S. Bureau of Mines, Bulletin 654 (1970)
- Evans, W. H., and D. D. Wagman, J. of Research of the Nat. Bureau of Standards, 49(3), 141 (1952)

- Fairhall, Industrial Toxicology, 2nd Edition, Hafner, New York (1969)
- Fletcher, E. E., and A. R. Elsea, "The Effects of High-Pressure, High-Temperature Hydrogen on Steel", Battelle Memorial Institute DMIC Report 202 (1964)
- Frye, C. G., and J. F. Mosby, "Kinetics of Hydrodesulfurization", Chem. Eng. Progr., 63(9), 66 (1967)
- Goudriaan, F., "Hydrodenitrogenation of Pyridine", Thesis, Technische Hogeschool Twente, the Netherlands (1974)
- Goudriaan, F., H. Gierman, and J. C. Vlugter, "The Effect of Hydrogen Sulfide on the Hydrodenitrogenation of Pyridine", Journal of the Institute of Petroleum, 59(565), 40 (1973)
- Griffith, R. H., J. D. F. Marsh, and W. B. S. Newling, "The Catalytic Decomposition of Simple Heterocyclic Compounds: II. Reaction Kinetics and Mechanism", Proc. Roy. Soc. (London), A197, 194 (1949)
- Gultekin, S., "The Effect of Methyl Substitution on the Catalytic Hydrodesulfurization of Thiophene", M.S. Thesis, M.I.T., Cambridge, Mass. (1977)
- Harper, H. M. Co., "Corrosion Guide", Technical Bulletin No. 101, Morton Grove, Ill. (1968)
- Hottel, H. C., 10.70 Lecture, M.I.T., Cambridge, Mass. (1972)
- Kirsch, F. W., H. Heinemann, D. H. Stevenson, "Selective Hydrodesulfurization of Cracked Gasolines", Ind. Eng. Chem., 49(4), 646 (1957)
- Kirsch, F. W., H. Shalit, H. Heinemann, "Effect of Nitrogen Compounds on...Hydrodesulfurization of Petroleum Fractions", Ind. Eng. Chem., 51(11), 1379 (1959)
- Kline, C. H., and J. Turkevitch, J. Chem. Phys., 12, 300 (1944)
- Kobe, K. A., and H. R. Crawford, "Thermodynamic Data for Petrochemicals", Petroleum Refiner, 37(7), 125 (1958)
- Kolboe, S., "Catalytic Hydrodesulfurization of Thiophene: VII. Comparison Between Thiophene, Tetrahydrothiophene, and n-Butanethiol", Can. J. Chem., 47, 352 (1969)

- Kolboe, S. and C. H. Amberg, "Catalytic Hydrodesulfurization of Thiophene: VI. Comparisons over Molybdenum Disulfide, Cobalt Molybdate, and Chromia Catalysts", Can. J. Chem., 44, 2623 (1966)
- Levenspiel, O., Chemical Reaction Engineering, Second Edition, Wiley, New York (1972)
- Lipka, J., "Graphical and Mechanical Computation", 1st edition, John Wiley, N.Y., p. 159 (1918)
- Lipsch, J. M. J. G., Thesis, Technological University, Eindhoven, The Netherlands (1968)
- Lipsch, J. M. J. G., and G. C. A. Schuit, "The CoO-MoO₃-Al₂O₃ Catalyst I. Cobalt Molybdate and the Cobalt Oxide Molybdenum Oxide System", J. Catal., 15, 163 (1969a)
- Lipsch, J. M. J. G., and G. C. A. Schuit, "The CoO-MoO₃-Al₂O₃ Catalyst II. The Structure of the Catalyst", J. Catal., 15, 174 (1969b)
- Lipsch, J. M. J. G., and G. C. A. Schuit, "The CoO-MoO₃-Al₂O₃ Catalyst: III. Catalytic Properties", J. Catal., 15, 179 (1969c)
- Mayer, J. F., "Interactions Between Hydrodesulfurization and Hydrodenitrogenation Reactions", Sc.D. Thesis, M.I.T., Cambridge, Mass. (1974)
- McCabe, W. L., and J. C. Smith, Unit Operations of Chemical Engineering, 2nd edition, McGraw-Hill, New York (1967)
- McCullough, J. P., D. R. Douslin, J. F. Messerly, et al., "Pyridine: Experimental and Calculated Chemical Thermodynamic Properties between 0 and 1500°K; a Revised Vibrational Assignment", J. ACS, 79, 4289 (1957)
- McIlvried, H. G., "Kinetics of the Hydrodenitrication of Pyridine", Ind. Eng. Chem. Process Des. Develop., 10(1), 125 (1971)
- Mears, D. E., "Diagnostic Criteria for Heat Transport Limitations in Fixed Bed Reactors", J. Catal., 20, 127 (1971a)
- Mears, D. E., "Tests for Transport Limitations in Experimental Catalytic Reactors", Ind. Eng. Chem. Process Des. Develop., 10(4), 541 (1971b)

- Metcalfe, T. B., "Inhibition par le Sulfure d'Hydrogene de la Reaction d'Hydrodesulfuration des Produits Petroliers", Chimie et Industrie - Genie Chimique, 102(9), 1300 (1969)
- Mezey, E. J., S. Singh, D. W. Hissong, "Fuel Contaminants, Volume 1. Chemistry", Battelle-Columbus Laboratories, Columbus, Ohio, Report No. EPA-600/2-76-177a (1976)
- Modell, M., and R. C. Reid, Thermodynamics and Its Applications, Chapter 10, Prentice-Hall, Englewood Cliffs, N.J. (1974)
- Morrison, R. T., and R. N. Boyd, Organic Chemistry, Allyn and Bacon, Boston (1966)
- Nicholson, D. E., "Identification of Adsorbed Species by Infrared Spectrometry: Thiophene--Cobalt Molybdate--Molybdenum Sulfide Systems", Anal. Chem., 34, 370 (1962)
- Owens, P. J., and C. H. Amberg, "Thiophene Desulfurization by a Microreactor Technique", Advan. Chem. Ser., 33, 182 (1961)
- Owens, P. J., and C. H. Amberg, "Hydrodesulphurization of Thiophene: II. Reactions over a Chromia Catalyst", Can. J. Chem., 40, 941 (1962a)
- Owens, P. J., and C. H. Amberg, "Hydrodesulphurization of Thiophene: III. Adsorption of Reactants and Products on Chromia", Can. J. Chem., 40, 947 (1962b)
- Perry, J. H., C. H. Chilton, S. D. Kirkpatrick, Chemical Engineer's Handbook Fourth Edition, McGraw-Hill, New York, Sections 3 and 4 (1963)
- Phillipson, J., "Kinetics of Hydrodesulphurisation of Light and Middle Distillates", Paper No. 31b presented at Am. Inst. Chem. Engrs. Nat. Meeting No. 68, Houston (1971)
- Poulson, R. E., "Nitrogen and Sulfur in Raw and Refined Shale Oils", Am. Chem. Soc., Div. of Fuel Chem. Preprint, 20(2), p. 183 (1975)
- Rihana, D. N., "Thermodynamic Data for n-aminoalkanes", Hydrocarbon Processing, 47(2), 111 (1968)

- Roberts, G. W., "The Kinetics of Thiophene Hydrogenolysis", Sc.D. Thesis, M.I.T., Cambridge, Mass. (1965)
- Rossini, F. D., K. S. Pitzer, R. L. Arnett, R. M. Braun, G. C. Pimentel, "Selected Values of Physical and Thermodynamic Properties of Hydrocarbons and Related Compounds", Carnegie Press, Pittsburgh (1953)
- Satterfield, C. N., Mass Transfer in Heterogeneous Catalysis, Chapters 1, 2, and 3, M.I.T. Press, Cambridge, Mass. (1970)
- Satterfield, C. N., and J. F. Cocchetto, "Pyridine Hydrodenitrogenation: An Equilibrium Limitation on the Formation of Piperidine Intermediate", AIChE J., 21(6), 1107 (1975)
- Satterfield, C. N., M. Modell, and J. F. Mayer, "Interactions Between Catalytic Hydrodesulfurization of Thiophene and Hydrodenitrogenation of Pyridine", AIChE J., 21(6), 1100 (1975)
- Satterfield, C. N., and G. W. Roberts, "Kinetics of Thiophene Hydrogenolysis on a Cobalt Molybdate Catalyst", AIChE J., 14(1), 159 (1968)
- Satterfield, C. N., Heterogeneous Catalysis in Practice, (Class Notes), M.I.T., Cambridge, Mass. (1977a)
- Satterfield, C. N., Personal Communication, M.I.T., Cambridge, Mass. (1977b)
- Sax, N. I., Dangerous Properties of Industrial Materials, 3rd Edition, van Nostrand Reinhold, New York (1968)
- Schuit, G. C. A., and B. C. Gates, "Chemistry and Engineering of Catalytic Hydrodesulfurization", AIChE J., 19(3), 417 (1973)
- Schuman, S. C., and H. Shalit, "Hydrodesulfurization", Catal. Rev., 4(2), 245 (1970)
- Scott, D. W., "Piperidine: Vibrational Assignment, Conformational Analysis, and Chemical Thermodynamic Properties", J. Chem. Thermodynamics, 3, 649 (1971)
- Shoemaker, D. P. and C. W. Garland, "Experiments in Physical Chemistry", McGraw-Hill Book Company, Inc., N.Y., 3rd edition, Chapter 2 (1974)

- Skoog, D. A., and D. M. West, "Fundamentals of Analytical Chemistry", 2nd Edition, Holt, Rinehart and Wilson, Inc., N.Y., Chapter 3, p. 25 (1969)
- Smith, J. M., Chemical Engineering Kinetics, Second Edition, Chapter 3, McGraw-Hill, New York (1970)
- Sonnemans, J., and P. Mars, "The Mechanism of Pyridine Hydrogenolysis on Molybdenum-Containing Catalysts: I. The Monolayer $\text{MoO}_3\text{-Al}_2\text{O}_3$ Catalyst: Preparation and Catalytic Properties", J. Catal., 31, 209 (1973a)
- Sonnemans, J., G. H. van den Berg, P. Mars, "The Mechanism of Pyridine Hydrogenolysis on Molybdenum-Containing Catalysts: II. Hydrogenation of Pyridine to Piperidine", J. Catal., 31, 220 (1973b)
- Sonnemans, J., and P. Mars, "The Mechanism of Pyridine Hydrogenolysis on Molybdenum-Containing Catalysts: III. Cracking, Hydrocracking, Dehydrogenation, and Disproportionation of Pentylamine", J. Catal., 34, 215 (1974)
- Sonnemans, J., W. J. Neyens, and P. Mars, "The Mechanism of Pyridine Hydrogenolysis on Molybdenum-Containing Catalysts: IV. The Conversion of Piperidine", J. Catal., 34, 230 (1974)
- Steere, N. V., CRC Handbook of Laboratory Safety, 2nd Edition, Chemical Rubber, Cleveland (1971)
- Stengler, V. W., J. Welker, and E. Leibnitz, "Behavior of Organic Nitrogen Compounds under Gas Phase, Medium-Pressure Hydrogenation Refining Conditions", Freiberger Forschungshefte, 329A, 51 (1964)
- Thoenes, D., Jr., H. Kramers, "Mass Transfer from Spheres in Various Regular Packings to a Flowing Fluid", Chem. Eng. Sci., 8, 271 (1958)
- Thomas, J. M., and W. J. Thomas, Introduction to the Principles of Heterogeneous Catalysis, Chapter 2, Academic Press, New York (1967)
- Thomson, S. J., and G. Webb, Heterogeneous Catalysis, Chapter 4, Wiley, New York (1968)
- Walas, S. M., Reaction Kinetics for Chemical Engineers, Chapters 7 and 8, McGraw-Hill, New York (1959)

Weast, R. C., Ed., Handbook of Chemistry and Physics,
p. D-106, 47th Edition, Chemical Rubber Co., Cleve-
land (1966)

Weisser, O., and S. Landa, Sulphide Catalysts, Their
Properties and Applications, Pergamon Press, New
York (1973)

Wilke, C. R., "A Viscosity Equation for Gas Mixtures",
J. Chem. Phys., 18(4), 517 (1950)

Yang, K. H., and O. A. Hougen, "Determination of Mechanism
of Catalyzed Gaseous Reactions", Chemical Engineering
Progress, 46, 146 (1950)

BIOGRAPHICAL SKETCH

John Albert Wilkens was born on October 28, 1947 in New York (Manhattan), New York, the son of George A. and Helen P. Wilkens. He attended public schools in West Englewood, New Jersey, and Newark, Delaware, graduating from Newark Senior High School in June, 1965. The author then entered Cornell University, majoring in Chemical Engineering, and earned a B.S. with Distinction in June, 1969 and a Master of Engineering (Chemical) in January, 1971. During the four summers while attending Cornell, he worked at the Du Pont Company, Chevron Research Company, and Atlas Chemical Industries (currently ICI United States).

The author then served as a Commissioned Officer of the U.S. Public Health Service. Assigned to the U.S. Environmental Protection Agency, he worked in technical information retrieval, and as a Project Officer in the Emission Testing Branch.

Entering the Massachusetts Institute of Technology in September, 1972, the author began work toward his Ph.D. in the Department of Chemical Engineering. On April 9, 1977, he married the former Lucie Shanes.

The author was elected to membership in Sigma Xi, Tau Beta Pi, and Phi Kappa Phi.

At the conclusion of his present work, the author will

be employed by E. I. du Pont de Nemours and Company, Inc.,
Wilmington, Delaware.